Contract NAS8-32390
DRD-MA-04

(NASA-CR-161535) SYSTEMS DEFINITION STUDY FOR SHUTTLE DEMONSTRATION FLIGHTS OF LARGE SPACE STRUCTURES, VOLUME 2: TECHNICAL REPORT Final Report (Grumman Aerospace Corp.) 220 p HC A10/MF A01 CSCL 22A G3/12

N80-29377

Unclas
28378

SYSTEMS DEFINITION STUDY FOR SHUTTLE DEMONSTRATION FLIGHTS OF LARGE SPACE STRUCTURES

volume 2
technical

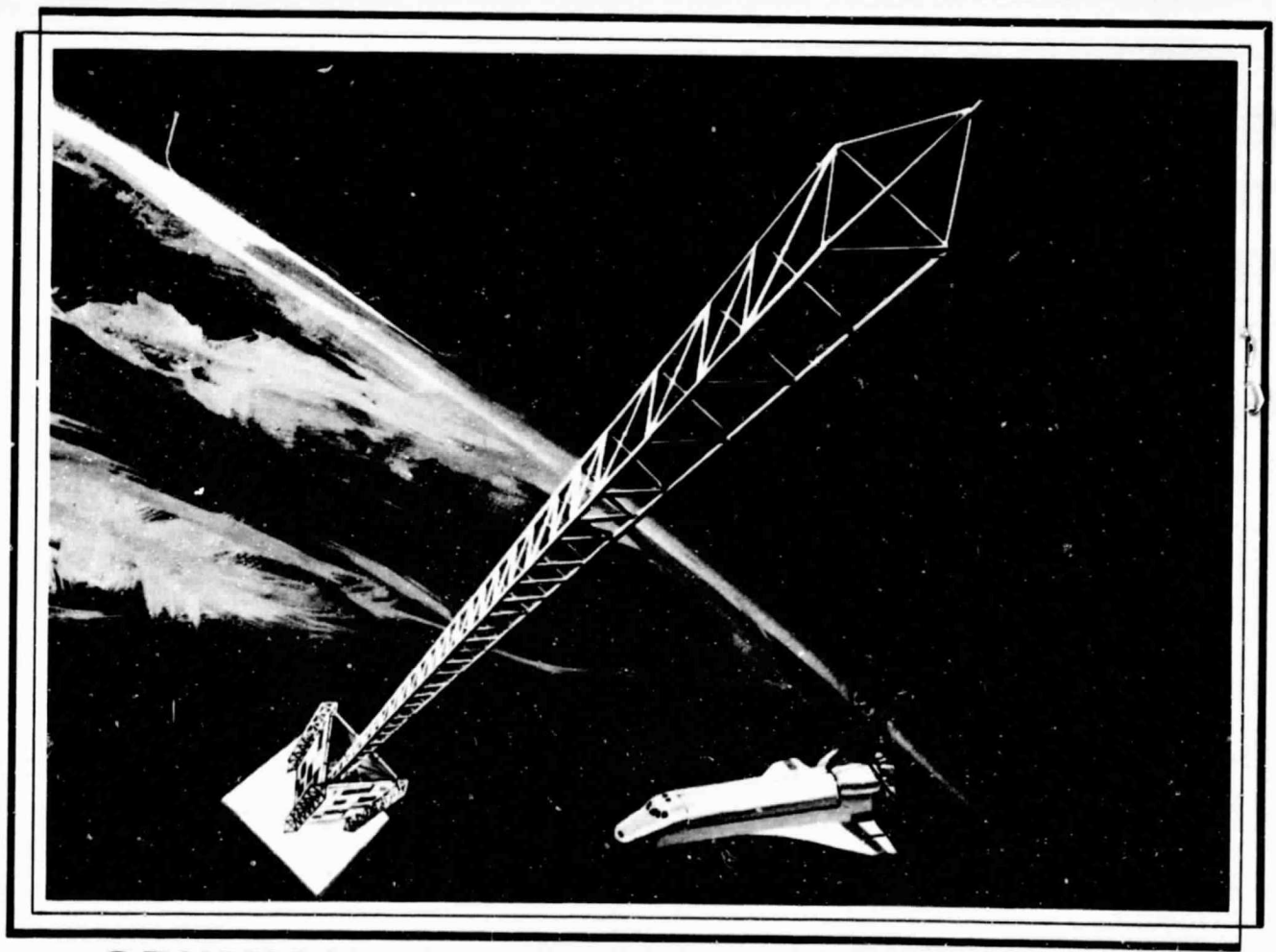

GRUMMAN AEROSPACE CORPORATION

contract NAS8-32390
DRD-MA-04

SYSTEMS DEFINITION STUDY FOR SHUTTLE DEMONSTRATION FLIGHTS OF LARGE SPACE STRUCTURES

volume 2
technical

prepared for
National Aeronautics and Space Administration
George C. Marshall Space Flight Center
Marshall Space Flight Center, Alabama 35812

by
Grumman Aerospace Corporation
Bethpage, N.Y. 11714

July 1979

FOREWORD

This study was conducted for the Marshall Space Flight Center (MSFC) and directed by the Contracting Officer's Representative (COR), Mr. J. Harrison. The Grumman Aerospace Corporation's study manager was John Mockovciak, Jr.

This final report is presented in three volumes:

- Volume 1 - Executive Summary
- Volume 2 - Technical Report
- Volume 3- Thermal Analyses
- Volume 3A - Thermal Analyses Appendix .

2

CONTENTS

2

CONTENTS (contd)

2

CONTENTS (contd)

2

ILLUSTRATIONS

ILLUSTRATIONS (contd)

2

ILLUSTRATIONS (contd)

ILLUSTRATIONS (contd)

2

ILLUSTRATIONS (contd)

2

ILLUSTRATIONS (contd)

2

1 - INTRODUCTION

Future utilization of space will involve new initiatives requiring large space structures (LSS) that can potentially serve a broad range of needs including: communications, Earth resources, radio astronomy, public service and solar electric power systems.

The development of techniques for building large-area, low-density space structures, therefore, represent a new threshold in the continuing evolution and development of space technology. Launch vehicle payload and volume limitations dictate, basically, two approaches:

- Ground fabricated structures, which are packaged and launched into orbit for deployment and assembly
- Space fabricated structures, which are automatically manufactured in space from sheet-strip materials and assembled on-orbit.

Of these alternatives, space fabrication allows structural materials to be packaged in a launch vehicle system with maximum possible density. Further, it allows the fabrication of "building block" structural elements for a wide spectrum of future large space structures.

An essential "stepping stone" in the development of LSS technology is a flight demonstration involving an Automated Beam Builder (ABB) and the Shuttle to establish that on-orbit manufacturing and assembly of large structures is feasible and practical. This study has addressed the definition of this initial LSS demonstration mission.

2

2 - STUDY OBJECTIVES AND SCOPE

A near-term objective of NASA's Large Space Structure Program is to develop the capability to package, transport, fabricate, assemble, and integrate large structures in orbit using the Shuttle Orbiter as a construction platform. In support of that goal, the initial phase of this study:

- Identified desirable LSS demonstration requirements and generated design concepts satisfying those needs, and
- Developed programmatic approaches, using an automated beam builder (ABB) and Shuttle capabilities, to perform an LSS flight demonstration in the 1983-1984 time-period.

The two candidate demonstration options developed during the initial study phase are illustrated in Fig. 2-1.

- Structural Demonstrator - A simple concept which demonstrates a limited degree of on-orbit structural fabrication, and
- LSS Platform - A similar, but larger platform structure which would demonstrate on-orbit fabrication and have user utility.

The free-flyer option of the LSS platform had its major cost associated with subsystem support functions. Hence, it was suggested that an existing or near-term subsystem support module (e.g., the 25 kW Power Module) be investigated as the potential "base" for an LSS platform. As shown in Fig. 2-2, the follow-on phase of this study addressed the development of free-flying platform concepts utilizing a 25 kW Power Module (PM), within which LSS applications were sought to provide a near-term relevance for the LSS demonstration mission. From the LSS applications identified, the latter phase of this study developed an LSS demonstration concept utilizing structural features relevant to space platforms.

In parallel with the concept development activities, supporting analyses related to aspects of LSS and 1-meter beam applications have been investigated. These efforts have enlarged our fundamental understanding of LSS, in general, and have been used

to support the definition of the LSS demonstration mission and to assess the feasibility/ practicability of other candidate LSS concepts, such as the gravity wave interferometer and pinhole camera.

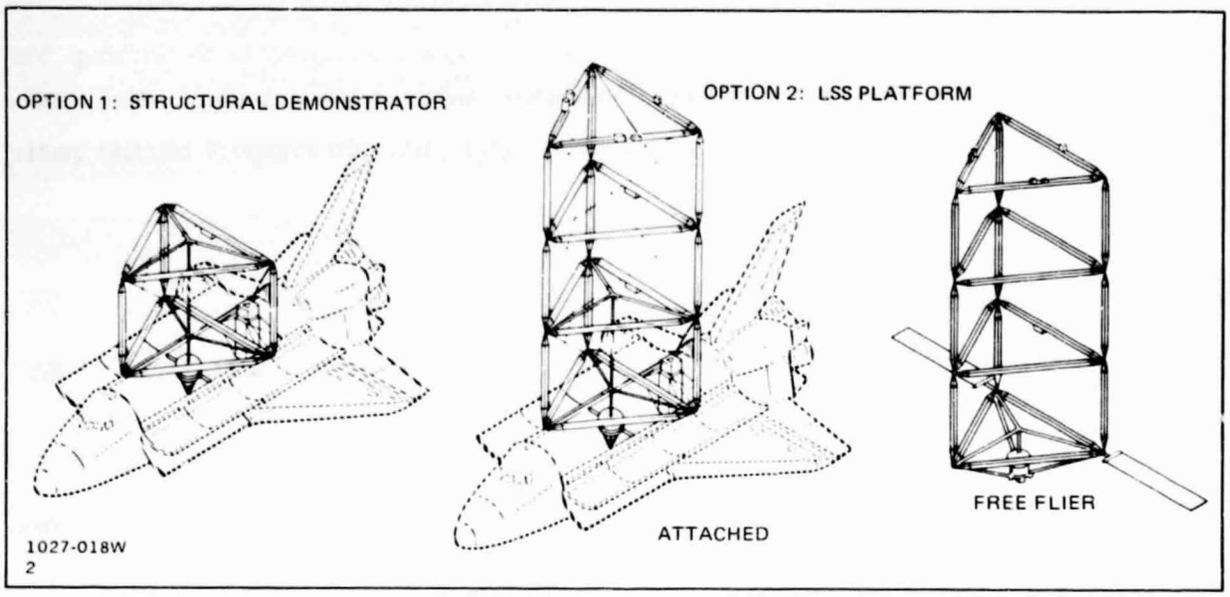

Fig. 2-1 Initial LSS Demonstration Options

PM/PLATFORM CONFIGURATION DEVELOPMENT

- DEVELOP FREE-FLYING LSS CONCEPTS UTILIZING 25 kW POWER MODULE
- IDENTIFY POTENTIAL LSS APPLICATIONS.

LSS DEMONSTRATION CONCEPT DEVELOPMENT

- ADAPT PM/PLATFORM LSS APPLICATIONS TO AN LSS CONCEPT FOR INITIAL STRUCTURAL DEMONSTRATION MISSION
- DEVELOP PROGRAMMATIC APPROACHES, USING AN AUTOMATED BEAM BUILDER AND SHUTTLE CAPABILITIES, TO PERFORM AN LSS DEMONSTRATION IN 1983-84 TIME PERIOD.

SUPPORTING ANALYSES

- STUDY RELATED ASPECTS OF LSS AND 1-METER BEAM APPLICATIONS
  - TRANSIENT THERMAL ANALYSIS OF 1–METER BEAM AND TRIBEAM STRUCTURE
  - CONSTRUCTION LIMITATIONS FROM SHUTTLE

LSS CONCEPTS EVALUATION

- ASSESS ALTERNATE LSS APPLICATIONS
  - GRAVITY WAVE INTERFEROMETER
  - PINHOLE CAMERA.

1027-019W
2

Fig. 2-2 Follow-on Study Scope

3 - SUMMARY

3.1 MAJOR FINDINGS AND CONCLUSIONS

An LSS flight demonstration mission has been identified which will demonstrate on-orbit fabrication, assembly, and integration of a large structure, and also provide a user-oriented satellite platform in the process. As illustrated in Fig. 3-1, the satellite incorporates the two principal large structural elements found in Power Module/Platform concepts developed during this study. Namely, a segment of the Tribeam "strongback" related to an earth viewing platform, and a long stabilizing boom characteristic of the long booms providing inertial symmetry for solar/stellar and materials processing platforms.

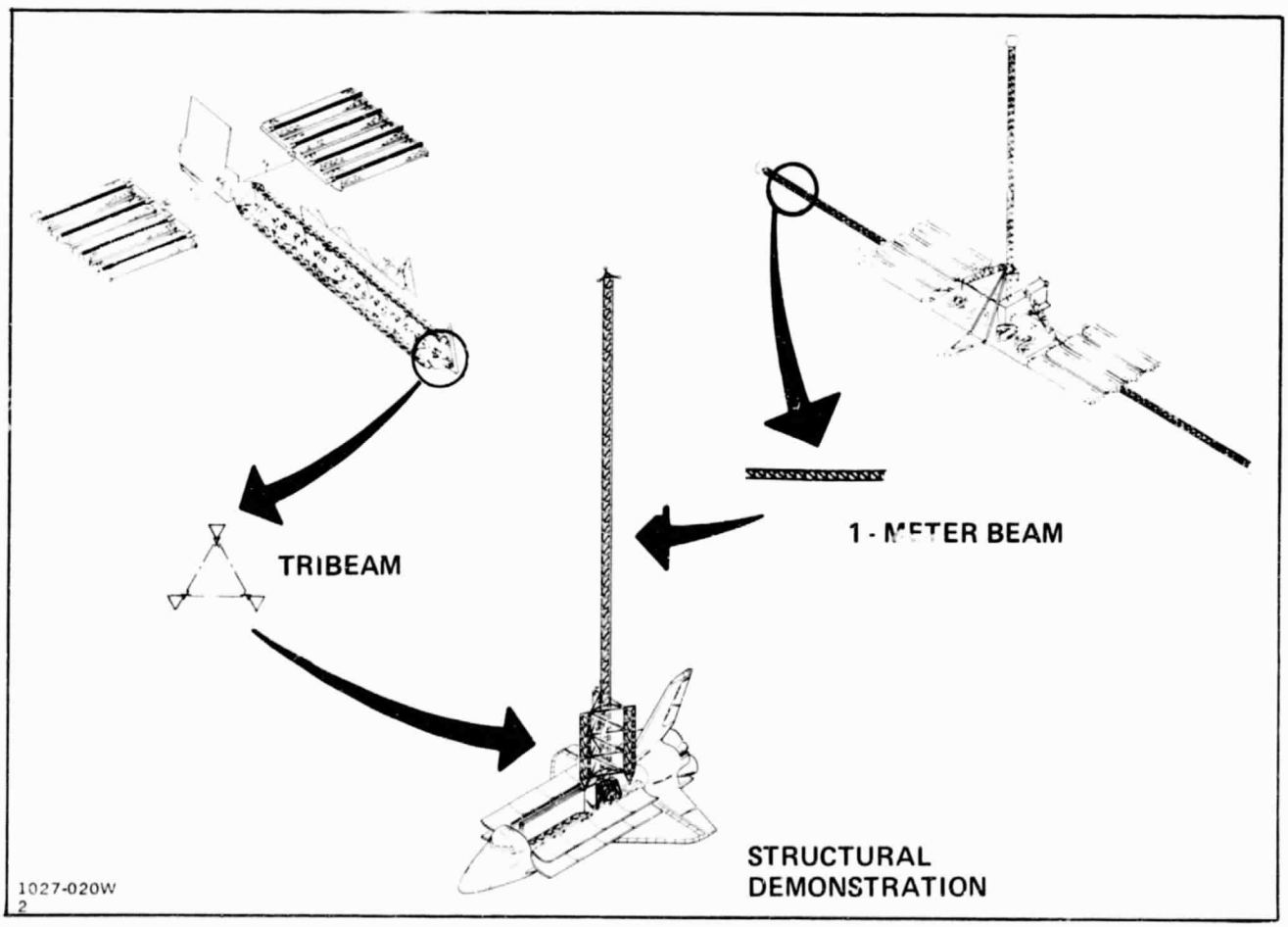

Fig. 3-1 LSS Demo Mission Rationale

2

The LSS Platform, shown in Fig. 3-2, has been configured as a simple, free-flyer satellite capable of supporting low-power payloads as a soil moisture radiometer, and LDEF-type experiments. The long boom provides gravity-gradient stabilization to within ± 3° of the local vertical, and because of the low-power nature of the payloads, allows effective use of a modest era of body-mounted solar cells to provide for a mission duration of five years. A baseline altitude of 500 km and 57° orbit inclination has been selected to provide a flight profile for the soil moisture radiometer with an approximate 3-4 day revisit over a test area located in the central U.S., and to maximize flight times without altitude reboost. The LDEF-type materials exposure experiments would be serviced per experimenter requirements or during Orbiter reboost intervals assumed to occur about once per year.

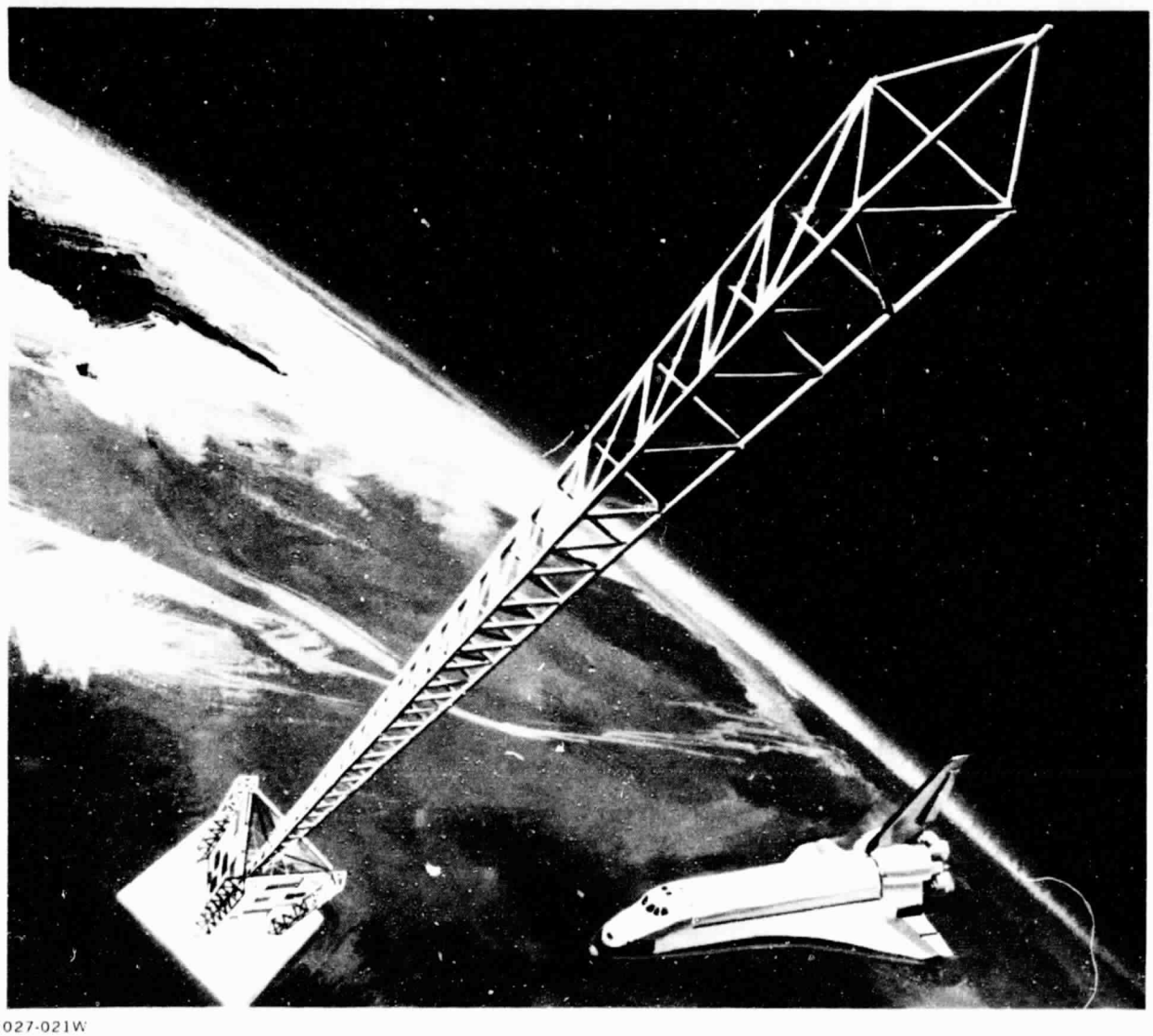

1027-021W
2

Fig. 3-2 LSS Platform Free-Flier

2

Features of the proposed LSS demonstration mission as they relate to Orbiter utilization, Space Platforms, and overall LSS technology development are shown in Fig. 3-3. The mission represents a viable early Shuttle mission candidate with the ability to support useful mission applications in addition to verifying the ability to build space-fabricated large space structures on-orbit. Considerable Orbiter-based construction expertise is acquired, in addition to relevant on-orbit construction, operations, and subsystem/payload integration experience applicable to near-term Space Platforms. Supporting LSS technology development features of the mission cover a broad range of necessary operational and construction-related technology activities relevant to future LSS mission applications. Clearly, this LSS demonstration mission can represent a significant milestone in the development of Large Space Structure capabilities.

This study has concluded that an LSS flight demonstration, using an ABB and the Orbiter as a construction base, could be performed in the 1983-1984 time-period. The estimated cost for a combined ABB verification/LSS demonstration mission is $24 million exclusive of Shuttle launch costs. During this mission, a simple space platform can be constructed in-orbit to accommodate user requirements associated with earth viewing and materials exposure experiment needs.

FEATURES OF INITIAL MISSION	ORBITER UTILIZATION	SPACE PLATFORMS	LSS TECH DEVELOPMENT
• LOW-COST SHUTTLE MISSION	•		
• LOW-WT EARLY 7-DAY SHUTTLE MISSION CANDIDATE	•	•	•
• SOIL MOISTURE RADIOMETER PAYLOAD RESPONDS TO USER NEED		•	
• COUPLES LDEF EXPERIMENTS "EXPANSION" WITH LSS DEMO	•	•	
• CONSTRUCTION FROM THE ORBITER	•	•	•
• USEABLE ORBIT-BUILT SPACECRAFT	•	•	•
• CONSTRUCTION/ASSEMBLY TECHNIQUES	•	•	•
• LIMITED SUBSYSTEM/PAYLOAD INTEGRATION		•	
• PLUME IMPINGEMENT EVALUATION	•	•	
• BERTHING/SERVICING OPERATIONS	•	•	
• TRIBEAM "STRONGBACK" BASELINE		•	•
• BEAM/BOOM APPLICATIONS		•	•
• LIGHTING EVALUATION	•	•	•
• ASTROWORKER/RMS UTILIZATION	•	•	•
• CONCURRENT VALIDATION OF ABB OPERATIONS	•		•
• ABB/ONE-METER BEAM TESTING	•	•	•
• ON-ORBIT TESTING OF LSS		•	•
• PASSIVE PRECISION GRAV-GRADIENT STABLIZATION		•	•
• TIMELINES VALIDATION VIA NEUTRAL BUOYANCY SIMULATION		•	•

1027-022W
2

Fig. 3-3 LSS Platform – Mission Relevance

2

3.2 RECOMMENDATIONS

The Astroworker-erected, space-fabricated, free-flying LSS platform identified in this study is a viable, low-cost, low-risk approach for an early LSS flight demonstration mission with relevance to both near-term Space Platforms and overall LSS technology development. Its consideration as an early Shuttle mission candidate is recommended.

Supporting technology development efforts are recommended relating to a separate "construction control package" for LSS construction missions from the Orbiter, thermal vacuum tests of a 1-meter beam, and further study-development of a clamshell RMS end effector. In addition, the detail design of joints associated with the LSS demo Tribeam should be initiated, and the joint designs evaluated in neutral buoyancy facilities in order to begin the process of establishing relevant construction/assembly timelines. It is also recommended that a neutral buoyancy program be implemented, specifically focused toward this LSS demonstration mission.

Additional simulation efforts are recommended to establish the maximum practical EVA time that can effectively be utilized for an Orbiter-based LSS mission. Although a 6-hour EVA limitation is presently believed to be acceptable, and has been used for mission planning purposes, the reality and effectiveness of this extended EVA duration remains to be verified.

Simulation efforts are also needed to evaluate lighting requirements for darkside construction/assembly operations and Astroworker effectiveness in EVA operations. Both free-floating (tethered and RMU) and restrained (cherry picker/RMS) construction modes should be evaluated, together with the potential area vs task lighting needs associated with these candidate modes of Astroworker construction.

A key output of this study has been the subject of LSS construction limitations both from the Orbiter and future space construction platforms. Limitations concerning maximum length structures, frequency coupling, and construction platform control requirements allowing broad construction latitude have been identified analytically. Verification of these limitations should be a major objective of initial LSS technology flights.

Our present LSS mission planning has baselined a flight adaptation of the ground demonstration ABB machine. This flight version is estimated to weigh about 7250 kg (16,000 lb). Studies of flight weight ABB designs, reflecting ABB ground demonstration experience, are recommended to establish the necessary design characteristics of

these machines and to provide appropriate weight "bogeys" for operational (versus demonstration) ABB hardware. Of critical importance to this LSS demonstration mission is a realistic appraisal of the practicality/cost-effectiveness of flying a modified ground demonstration ABB. This appraisal and its subsequent consequences represent the "long-pole-in-the-tent" vis-a-vis this LSS flight demonstration mission. An early appraisal, therefore, addressing the issue of "what ABB to fly?" is urgently recommended. As expressed previously, the low-cost/low-risk aspects of this proposed LSS mission offer considerable appeal...the ABB issue must be resolved expeditiously.

4 - POWER MODULE/PLATFORM CONCEPT DEVELOPMENT

The purpose of this study phase was to determine if a Large Space Structure (LSS) appeared as an inherent element of space platform adaptations of a 25 kW Power Module (PM). If so, that structure would establish a mission-relevant basis for definition of an LSS flight demonstration mission.

4.1 METHODOLOGY

The process that was employed to develop PM/Platform concepts, and the interrelationship of major configuration-relevant factors, is shown in Fig. 4-1. User considerations are a major driver in evolving PM/Platform concepts, and inputs from OSS, OSTA, and a recent Space Science Platform Conference*, have (to the extent possible at this time) been factored into this initial phase of the configuration development process.

Considerations relating to flight mechanics and momentum implications (in both Orbiter-docked and free-flight modes) have been reflected in evaluations of preferred flight attitudes. Further, the Orbiter's preferred attitude relative to the sun, for heat rejection considerations, has been factored into both Platform servicing and Power Module support phases of flight operations. Initial configurations were developed to establish the extent of "real estate" needed by potential Platform users, and subsequently refined to reflect more detailed user aspects and multi-mission commonality of a Power Module.

4.2 GUIDELINES

Generic concepts of PM/Platforms were developed for the following low earth-orbit applications:

- Dedicated Earth Viewing
- Simultaneous Solar/Earth Viewing
- Simultaneous Solar/Stellar Viewing, and
- Materials Processing.

---

* "UAH/NASA Workshop on Space Science Platform," August 21-25, 1978

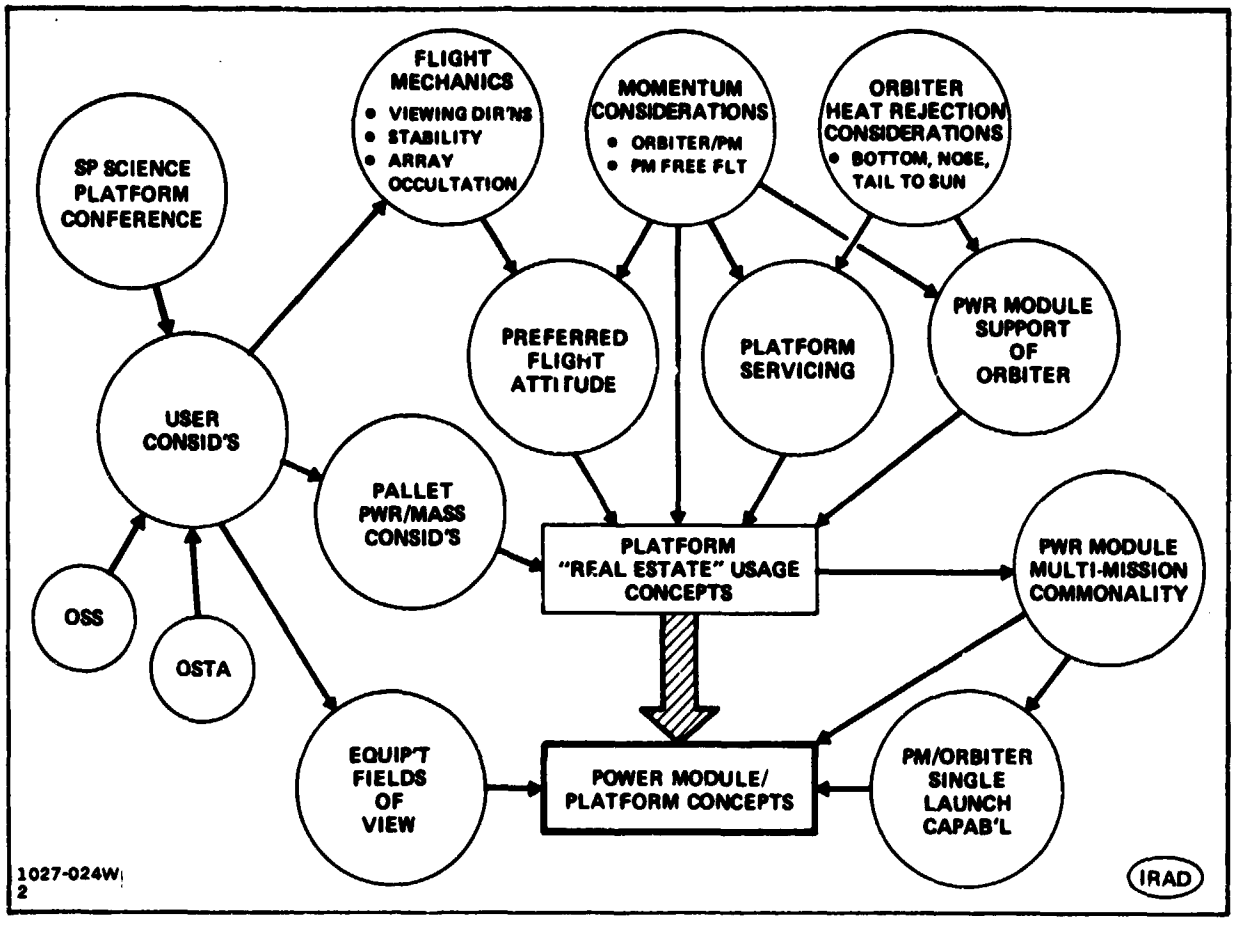

Fig. 4-1 Power Module/Platforms Concept Development Process

As indicated in Fig. 4-2, the stabilization/pointing characteristics associated with these potential users cover a rather broad range, and must be factored into the concept development process. Generic pointing characteristics range from degrees in earth viewing, to-arc-min and arc-sec, for solar/stellar viewing, and also encompass microgravity conditions (10^{-5} to 10^{-8}g) as desired by materials processing.

In addition to "being aware" of the generic stability and pointing needs of potential Platform users, some additional assumptions were made relating to user payloads. A survey of candidate Spacelab missions indicated a demand of about 1 kW/pallet; for platform sizing purposes 2 kW/pallet has been assumed. Thus, allocating about 5 kW for PM/Platform housekeeping, about 8 to 10 pallets (or equivalent) have been assumed for Platform "real estate" sizing. Additionally, provisions have been considered for the ESRO-type (U-shape) Spacelab pallets, and "platform adapters" that are linear "slices" of the Orbiter's payload bay. Further, a design objective is that the Platform/payload interface is intended to be identical to that of the Orbiter/Spacelab to minimize

integration costs. Namely, the Platform would provide the same types of service functions to the payload as the Orbiter vis-a-vis power, heat rejection, attitude control, and data handling.

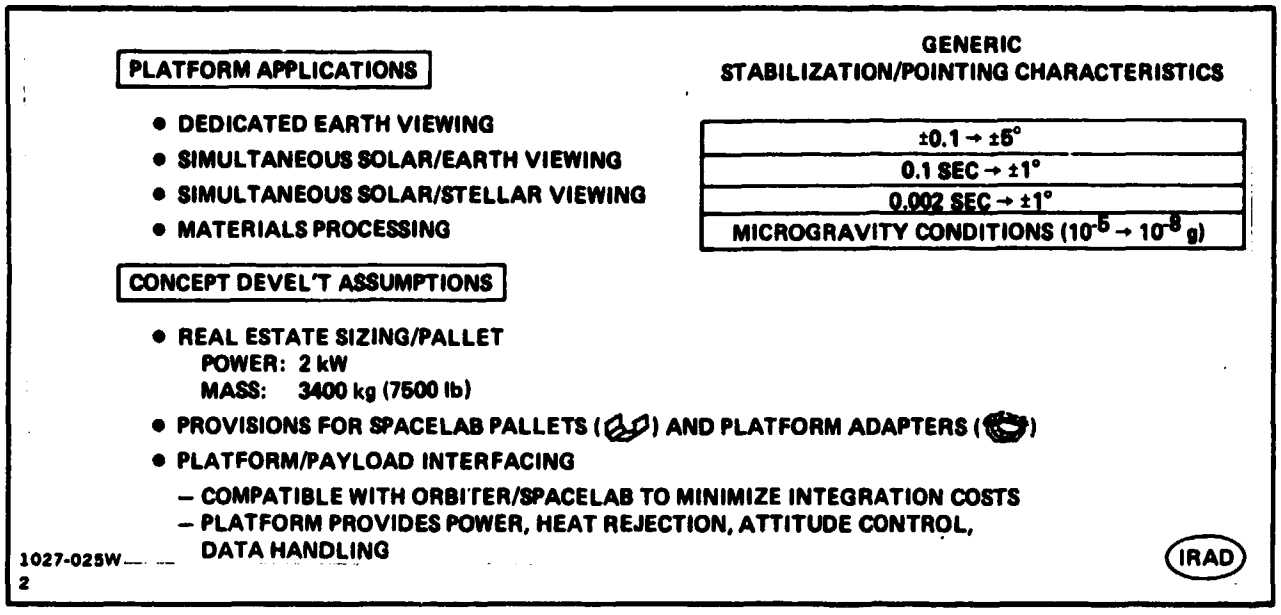

Fig. 4-2 User Considerations

4.3 ORBITER HEAT REJECTION CONSIDERATIONS

Figure 4-3 illustrates desirable Orbiter orientations, relative to the sun, for heat rejection purposes. These considerations are relevant to two phases of PM/Platform operations, namely:

- Power Module support of the Orbiter, and
- Orbiter servicing of the Platform.

These operational considerations have, therefore, been considered in the PM/Platform concept development process and are reflected in the configurations developed herein.

4.4 MOMENTUM CONSIDERATIONS

A representative attitude control capability for a Power Module coupled with an Orbiter is shown in Fig. 4-4. Clearly, minimum control system "muscle" is needed with the coupled Orbiter/PM in local vertical orientations and an X-POP flight mode. Alternative positions of an Orbiter relative to the orbit plane, and their respective momentum implications, are illustrated in Fig. 4-5. These momentum considerations are also relevant to the PM/Platform operational phases mentioned previously (re: Orbiter heat rejection), namely:

2

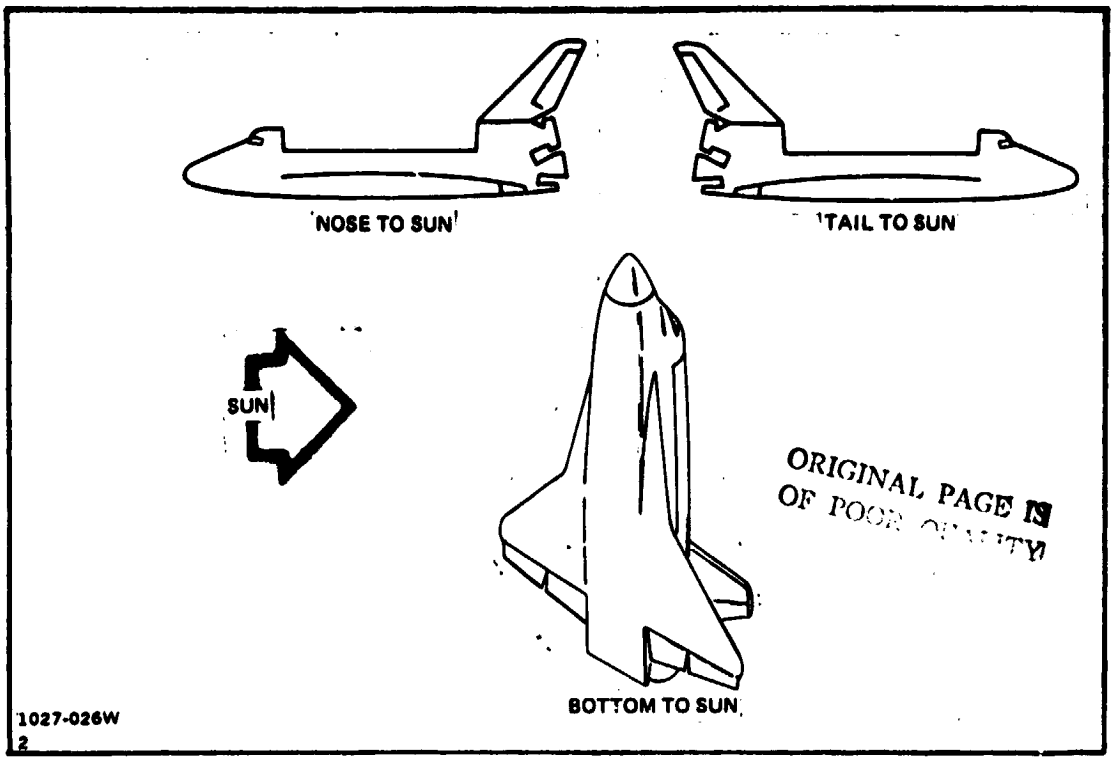

Fig. 4-3 Preferred Orbiter Orientations

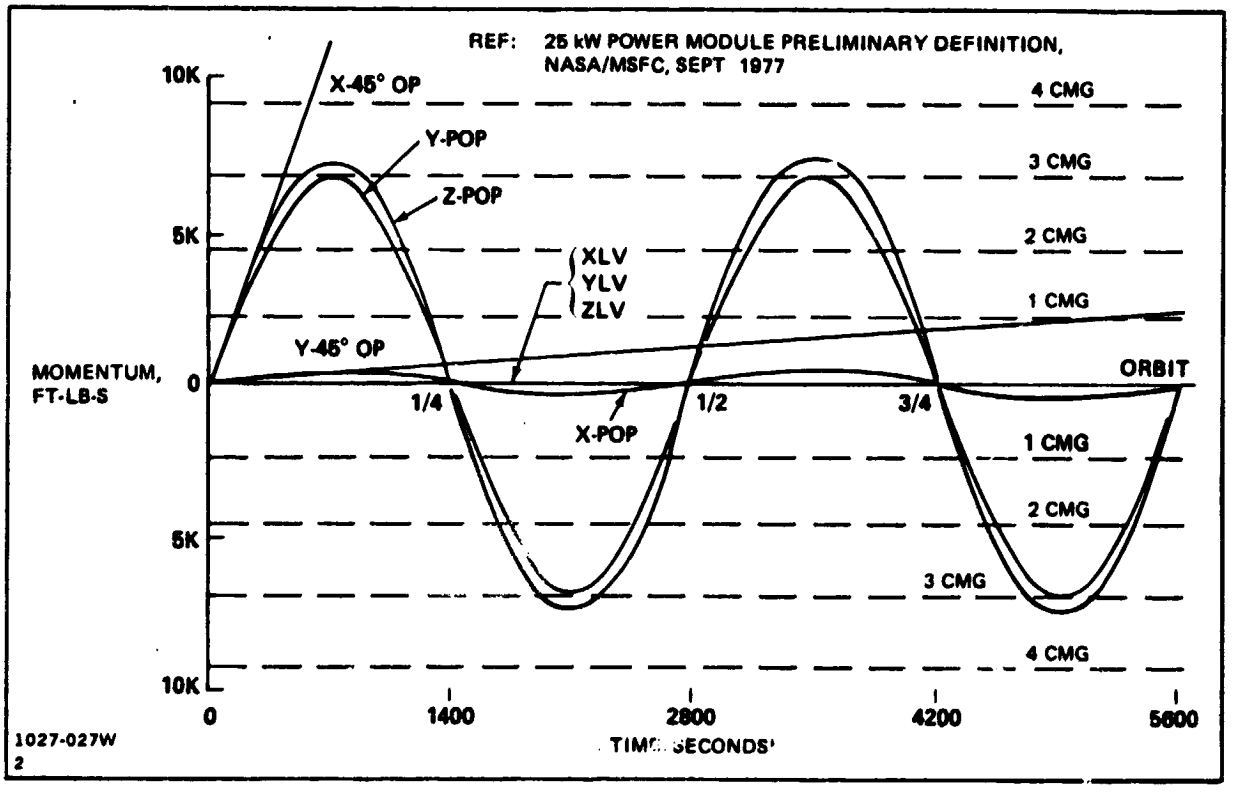

Fig. 4-4 Power Module/Orbiter-Payload Momentum Buildup Profiles

- Power Module support of the Orbiter, and
- Orbiter servicing of the Platform.

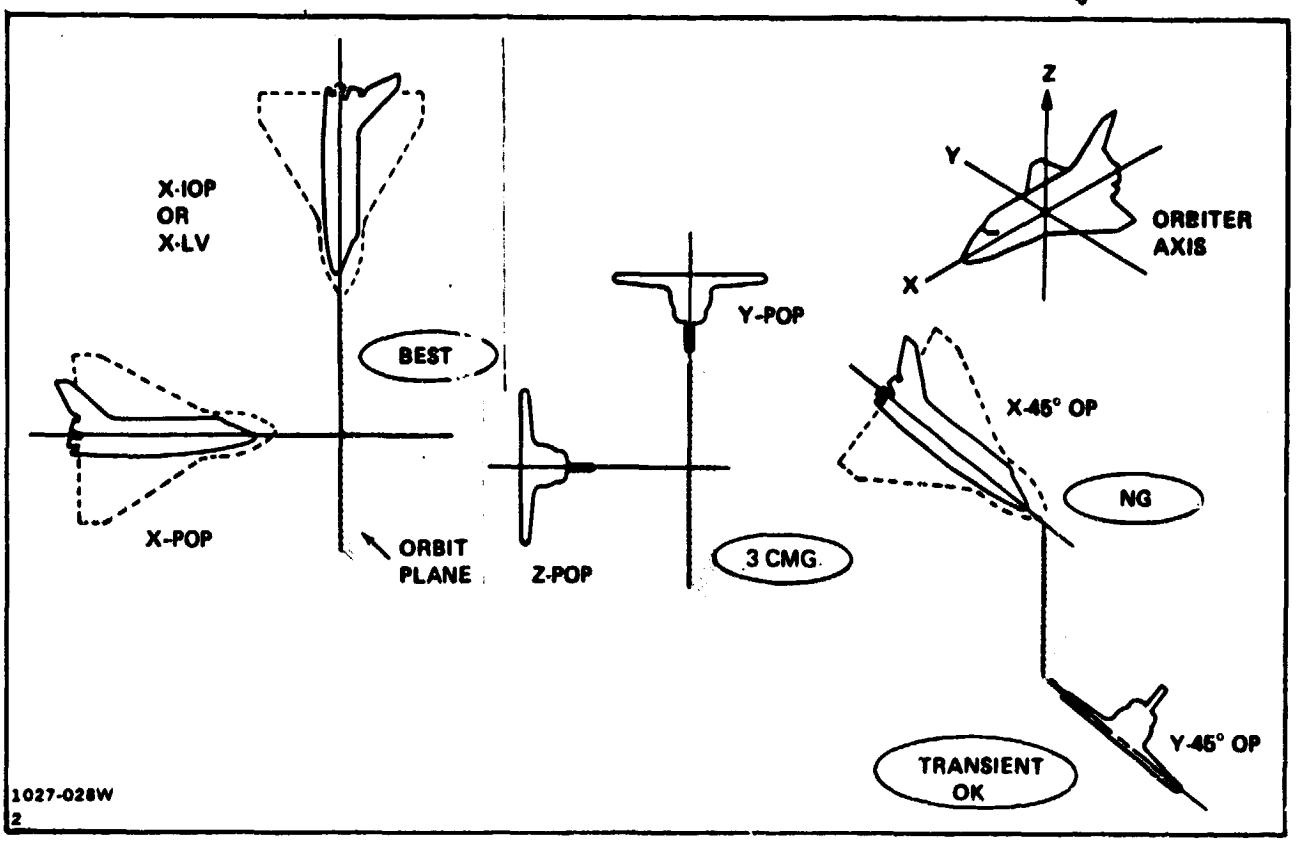

Fig. 4-5 Momentum Considerations

A representative PM attitude control capability in support of free-flight payload operations is shown in Fig. 4-6. As illustrated, POP orientations for a free-flyer are well within the capabilities of a single CMG.

These data, although specific to the PM concept reported by NASA/MSFC on September 1977, suggest that an X-POP PM/Platform flight orientation for both free-flight and Orbiter-docked modes, is favored from a momentum considerations point of view.

4.5 FLIGHT MODE EVALUATIONS

A key consideration relating to the development of appropriate PM/Platform concepts involves the flight mechanics aspects of satellites in low earth orbit. A brief overview of relevant factors follows.

2

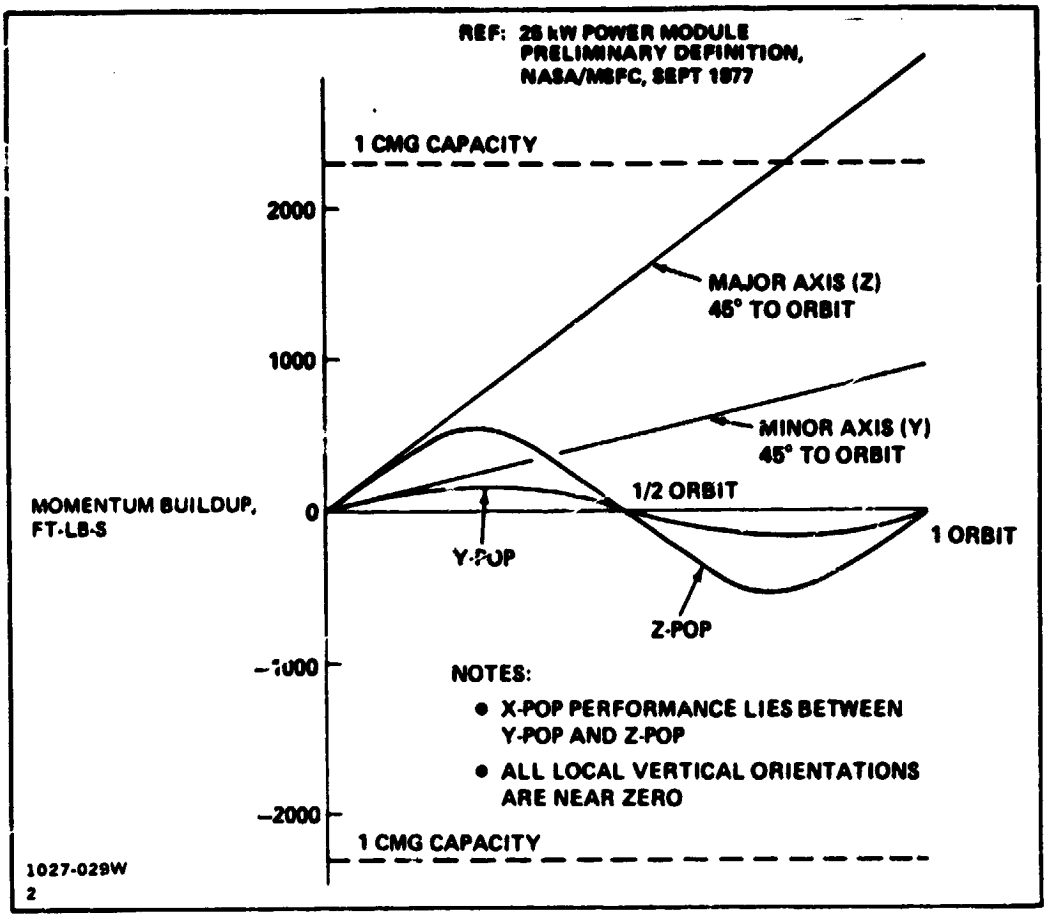

Fig. 4-6 Typical Momentum Buildup on Power Module with Free-Flier Payload

Figure 4-7 illustrates the relationship of an orbit plane to the earth and the ±23-1/2° variation of the solar vector during the year. The orbit plane precesses about the earth's axis of rotation at about 4°/day (i = 57°; altitude = 500 km). Thus the combined effect of seasonal variation of the sun and precession must be considered when describing the position of the sun relative to the orbit plane.

Figure 4-7 also shows the reference axes that are used herein to analyze alternate PM/Platform flight orientations. The axes are:

- X-POP - Perpendicular to the Orbit Plane
- Y-AVV - Along the Velocity Vector
- Z-LV - Local vertical.

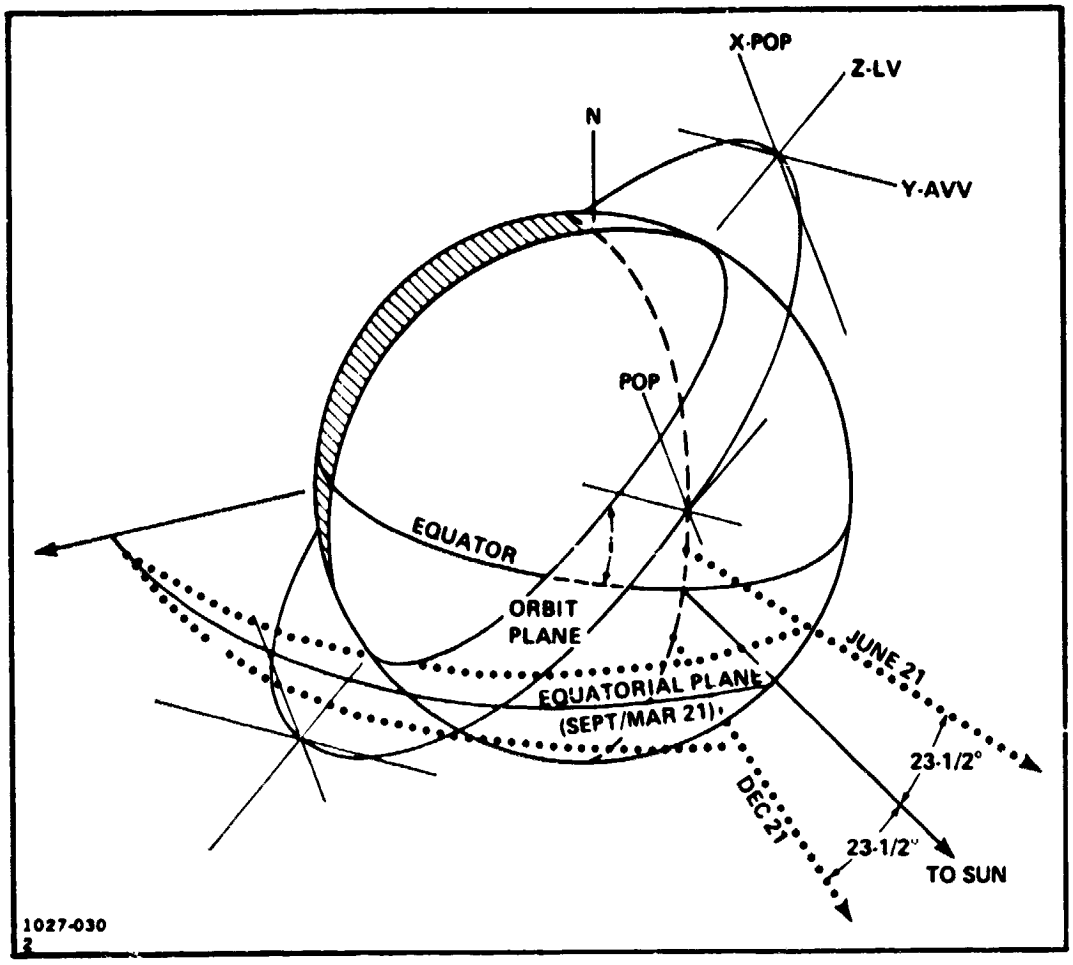

Fig. 4-7 Orientation Diagram – i = 57°

The β angle is defined as the solar incidence angle relative to the orbit plane. As shown in Fig. 4-8, $\beta = 0°$ represents a condition wherein the sun is parallel to the orbit plane. The extreme positive and negative β angle positions are related to orbit inclination and described by the equation:

$$\beta = i \pm 23\text{-}1/2°$$

where i = orbit plane inclination.

The declination angle of the sun relative to the orbit plane ($\beta+$ or $\beta-$) varies as a function of orbit altitude and inclination. A representative time history of the β angle variation, for a high inclination orbit, over a one year period is shown in Fig. 4-9. Note that $\beta = 0°$ conditions occur about every 30 days, and (for this inclination) a complete β cycle is traversed every 60 days.

2

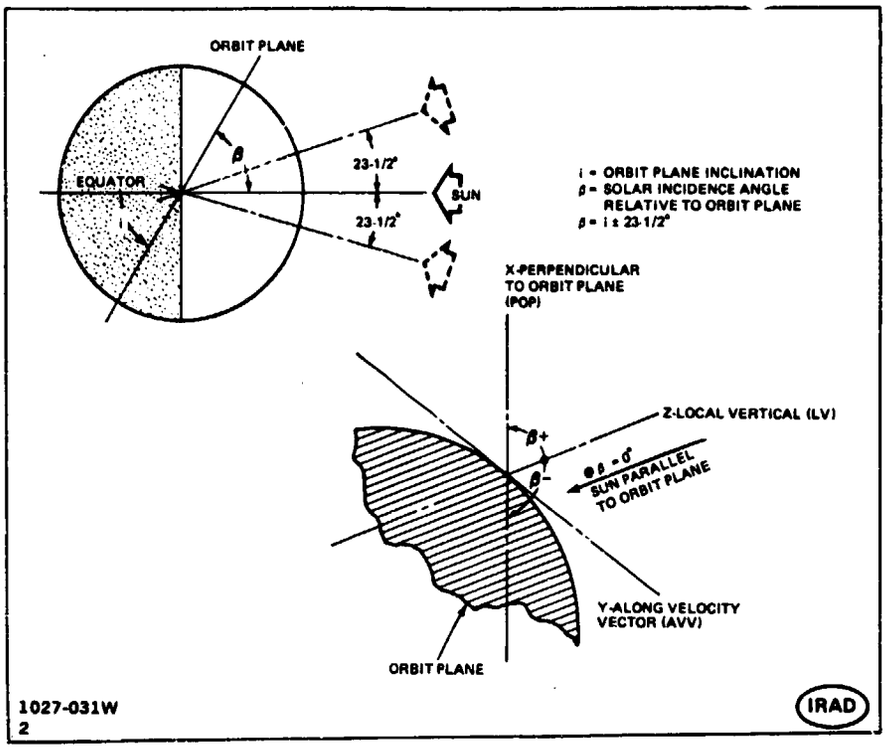

Fig. 4-8 β-Angle

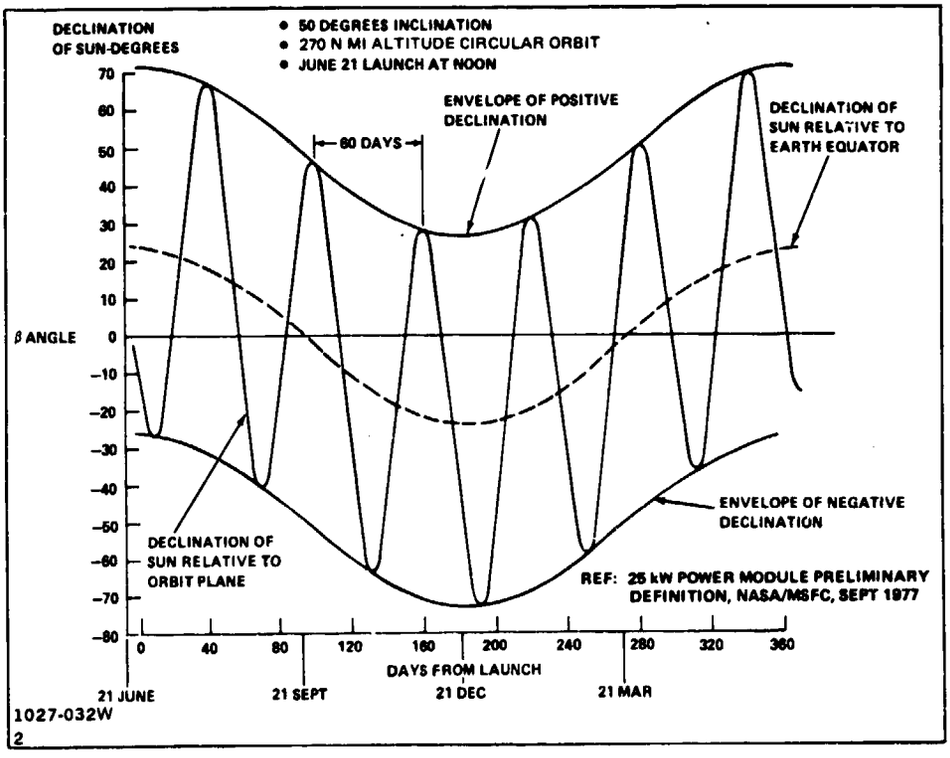

Fig. 4-9 Time History of Sun's Declination Relative to Orbit Plane

2

4.5.1 Alternate Flight Orientations

Figure 4-10 illustrates three fundamental body axis orientations of a PM relative to an orbit plane and the corresponding positions of the earth and sun. The overall goal is to determine which PM body axis flight orientation could readily provide simultaneous earth and solar viewing capabilities for platform operations, while also minimizing or eliminating potential solar array occultation effects during a mission.

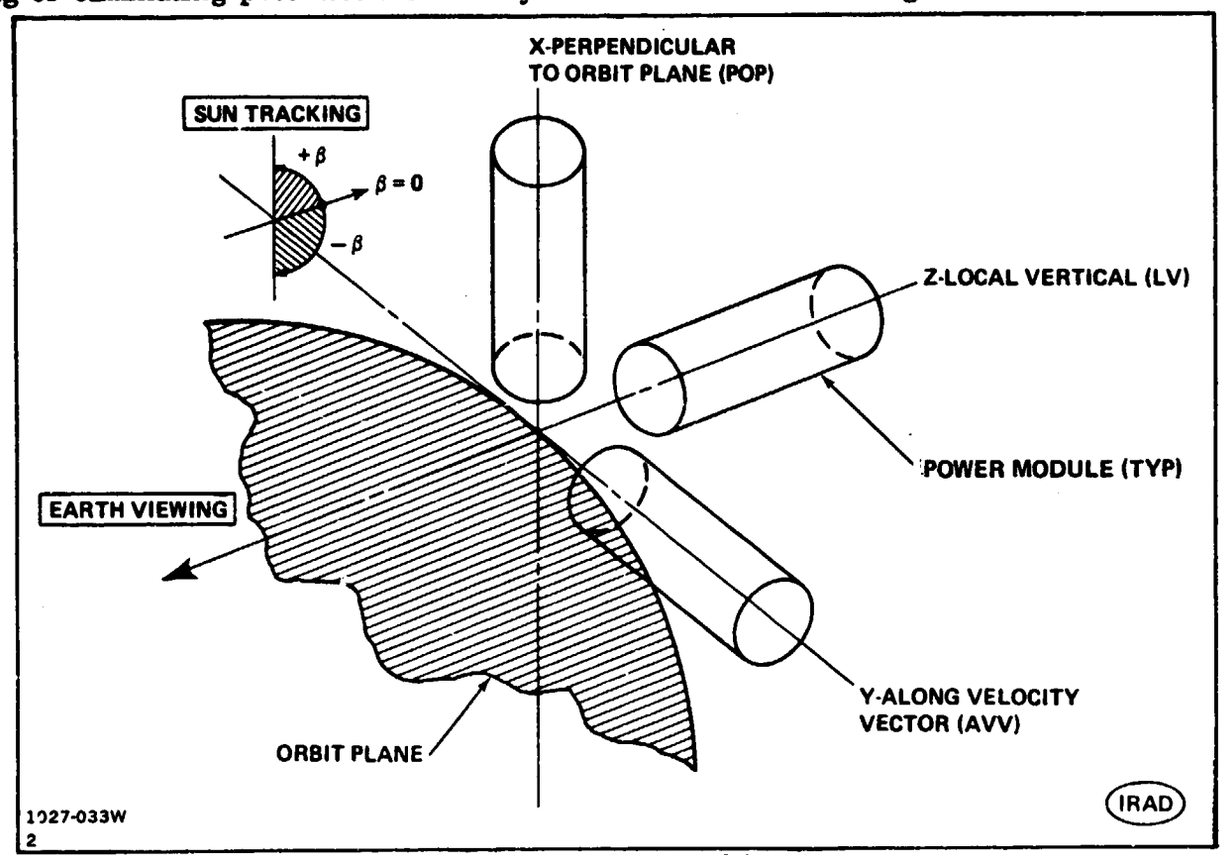

Fig. 4-10 Candidate Body Axis Orientations

The analyses of flight mechanics implications associated with flying a PM in each basic (X, Y, and Z-axis) flight orientation, and the conceptual design of PM/Platforms developed and reported herein, were supported by Grumman's Independent Research and Development (IRAD) Program.

The candidate X, Y, and Z body axis orientations of a PM are shown in Fig. 4-11. Characteristics of these concepts are:

- AVV - PM body axis and earth viewing platform are aligned and maintained along the flight vector (Y-axis). The body axis rotates at orbit rate, relative to the solar array, to maintain earth viewing.
- LV - PM body axis and earth viewing platform are aligned along the local vertical (Z-axis), and simultaneously maintain along-the-velocity-vector (AVV.

2

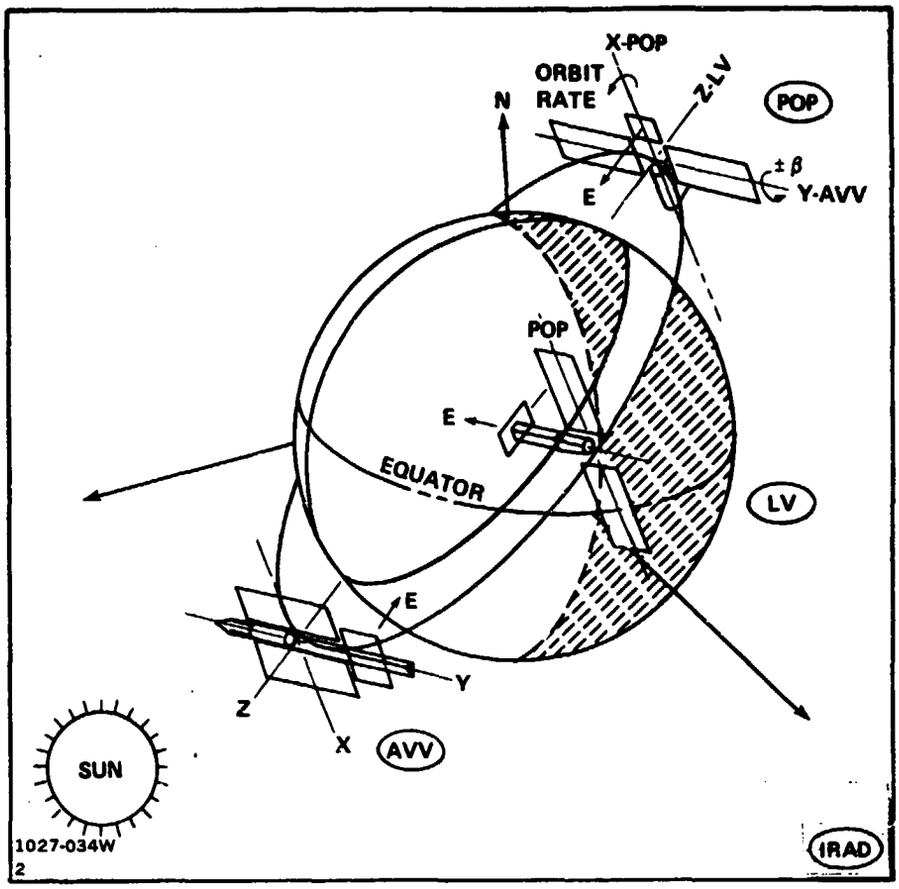

Fig. 4-11 Alternate PM/Platform Flight Orientations

Y-axis) orientation for the earth viewing platform. The body axis rotates at orbit rate relative to the solar array, to maintain earth viewing.

- POP - PM body axis and earth viewing platforms are aligned perpendicular to the orbit plane (X-axis). The earth viewing platform rotates at orbit rate, relative to the solar array, to maintain earth viewing.

The PM/Platform orientations shown in Fig. 4-11 represent $\beta = 0°$ positions of the solar array. The array tracks the sun by rotating about the Y-axis ($\pm \beta$) according to the position of the sun vector relative to the orbit plane.

4.5.2 Power Module AVV

The positions of the principal axis of a Y-AVV PM/Platform relative to the solar array for a $\beta = 0°$ and β + condition, during an orbit, are shown in Fig. 4-12. The body of the PM and the earth viewing platform rotate at orbit rate, relative to the solar array, to maintain an earth viewing capability. Note that the β + condition (or β -)

2

of this flight mode would result in occultation of the array by the body during a complete orbit.

4.5.3 Power Module Z-LV

Figure 4-13 illustrates the positions of the principal axis of a Z-LV PM/Platform relative to the solar array for a $\beta = 0°$ and $\beta +$ condition during an orbit transit, and with the Orbiter docked. The body of the PM maintains an earth-pointing direction, with the earth-viewing platform located at its base. The Orbiter is shown docked to the PM at the other end.

In the $\beta = 0°$ condition, it is assumed that the arrays could span the Orbiter to negate occultation of the arrays. However, as shown, a $\beta +$ condition (or $\beta -$) of this flight mode would result in occultation of the array by the Orbiter during a complete orbit.

4.5.4 Power Module X-POP

The positions of the principal axis of an X-POP PM/Platform relative to the solar array for a $\beta = 0°$ and $\beta +$ condition in free flight mode, are shown in Fig. 4-14. The body of the PM maintains an X-POP attitude, while the earth-viewing platform rotates at orbit rate to track the local vertical. Note that no occultation of the solar array occurs in either $\beta = 0°$ or $\beta \pm$ array attitudes, for this flight orientation.

Figure 4-15 illustrates the effect of an Orbiter-docked-to-PM flight condition for an X-POP PM/Platform concept. $\beta = 0°$ and $\beta +$ conditions are clear of array occultation, but at high negative β angles there could be a possibility of array occultation by the Orbiter...unless the arrays were located outboard to span the Orbiter's wing tips. The effect of this Orbiter occultation is shown in Fig. 4-16. An early "real estate usage" PM/Platform concept was examined, and showed that high negative β positions of the solar array might incur occultation by the Orbiter during three weeks of the year. Clearly, if the Orbiter were not receiving support from a Power Module during these intervals there is "no problem". Further development of the PM/Platform concepts, however, has shown that when a user's potential field-of-view and payload location considerations are reflected in a PM/Platform concept, the solar arrays could be sufficiently outboard to clear the Orbiter wing tips in high negative β attitudes. Thus, there appear to be no operational restrictions, vis-a-vis the Orbiter, with an X-POP PM Platform flight mode.

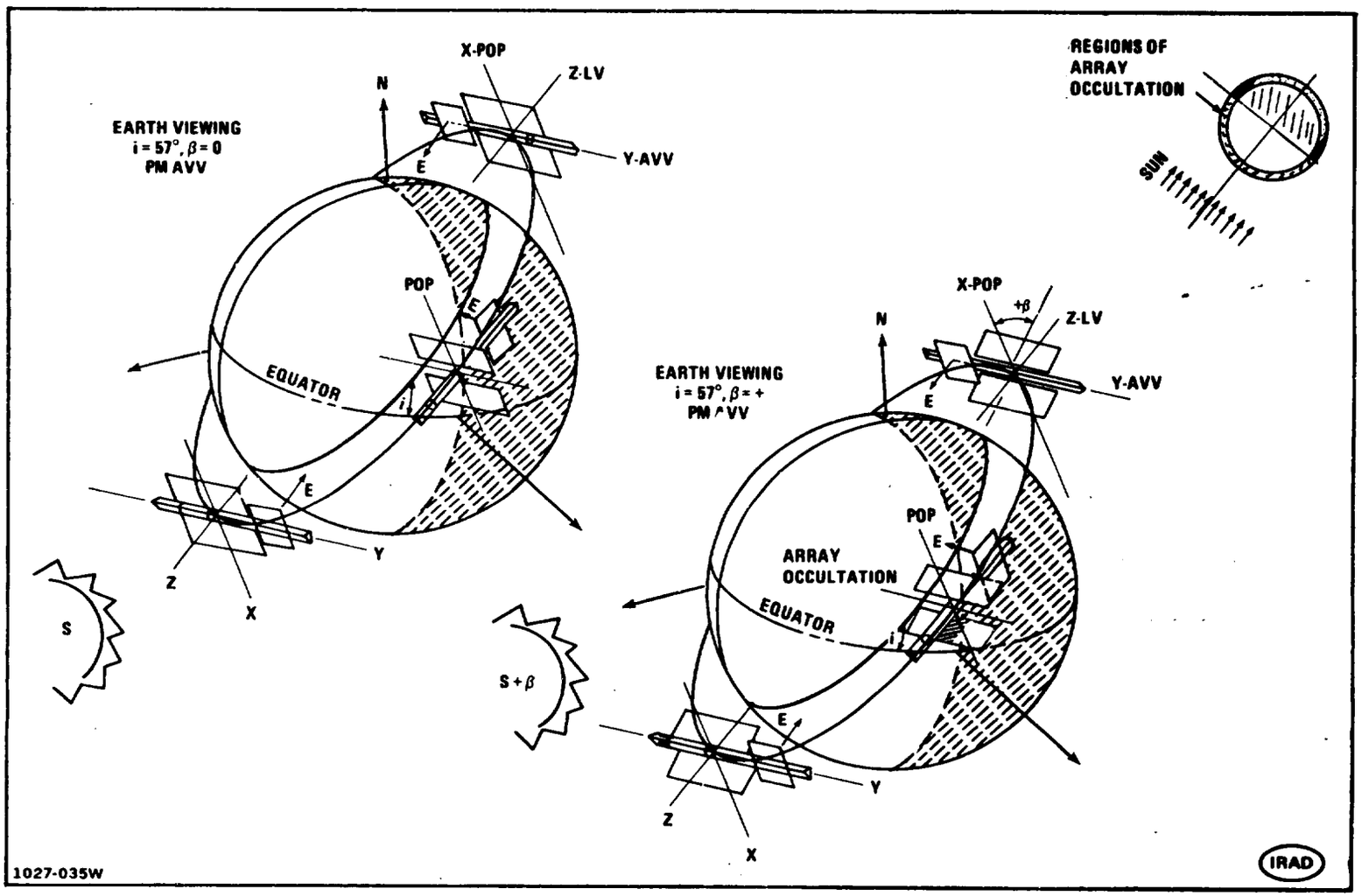

Fig. 4-12 Earth Viewing: Power Module AVV

2

ORIGINAL PAGE IS
OF POOR QUALITY

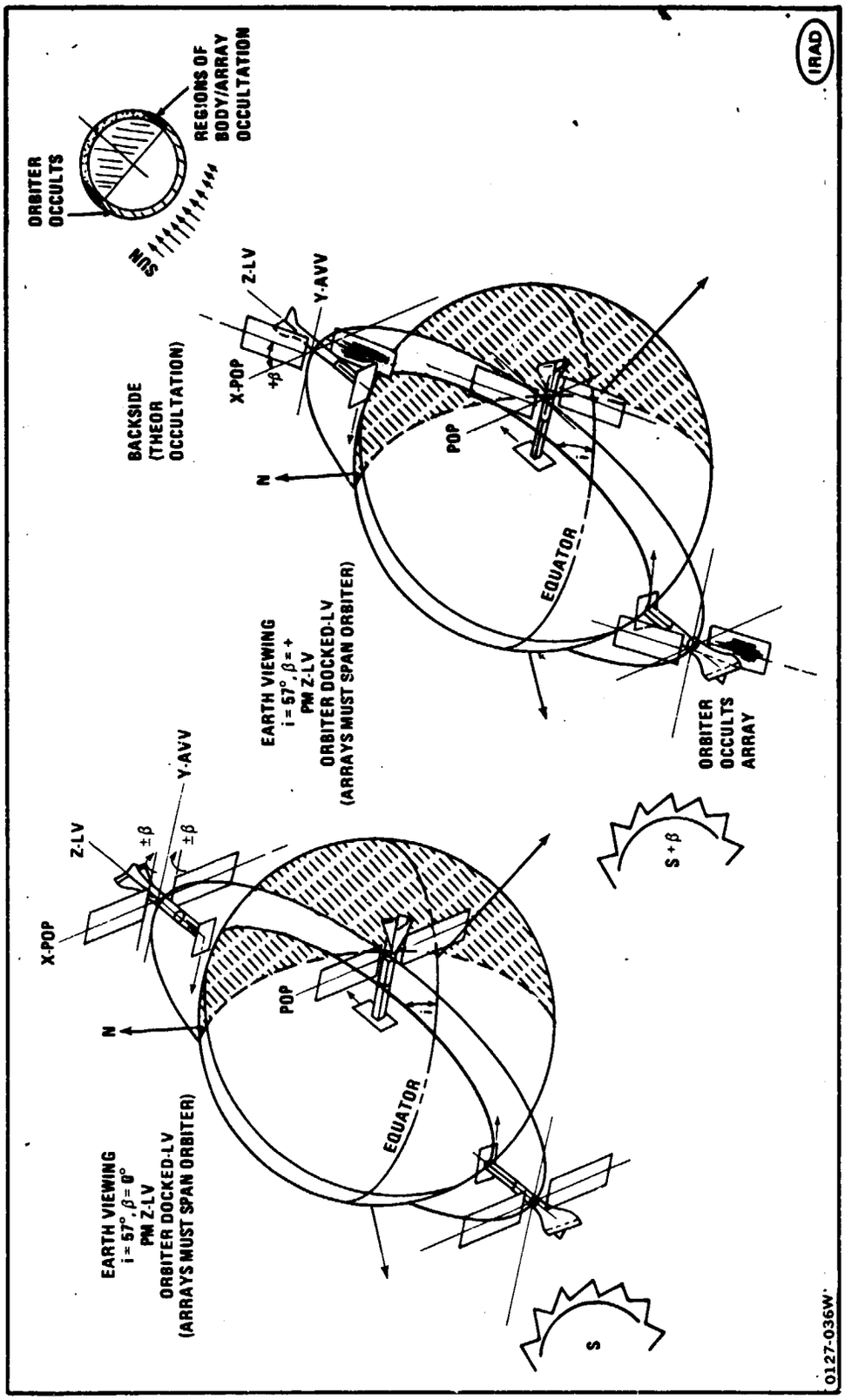

Fig. 4-13 Earth Viewing: Power Module Z-LV

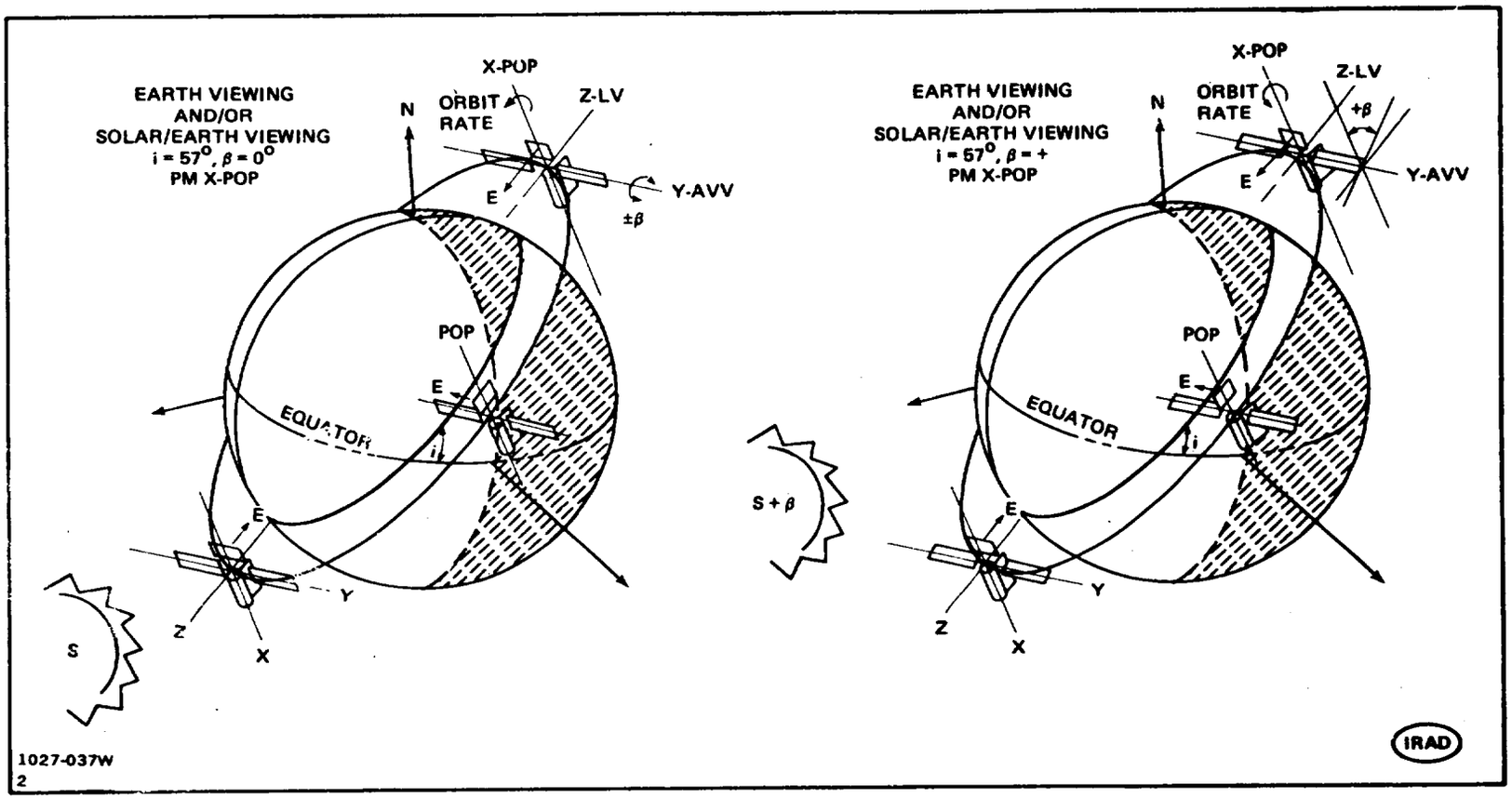

Fig. 4-14 Earth Viewing: Power Module X-POP . . . Free-Flight

2

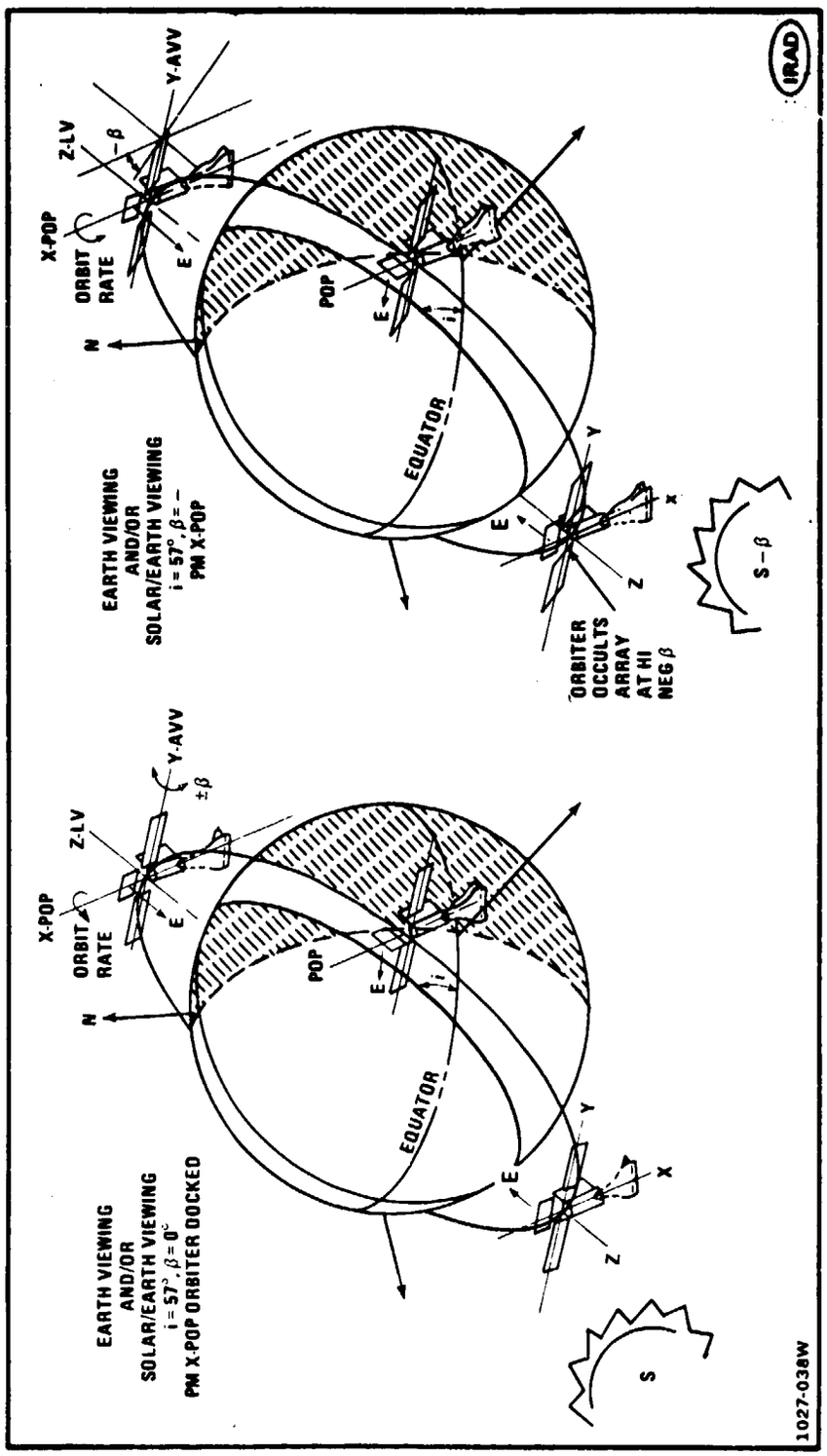

Fig. 4-15 Earth Viewing: Power Module X-Pop . . . Orbiter Docked

2

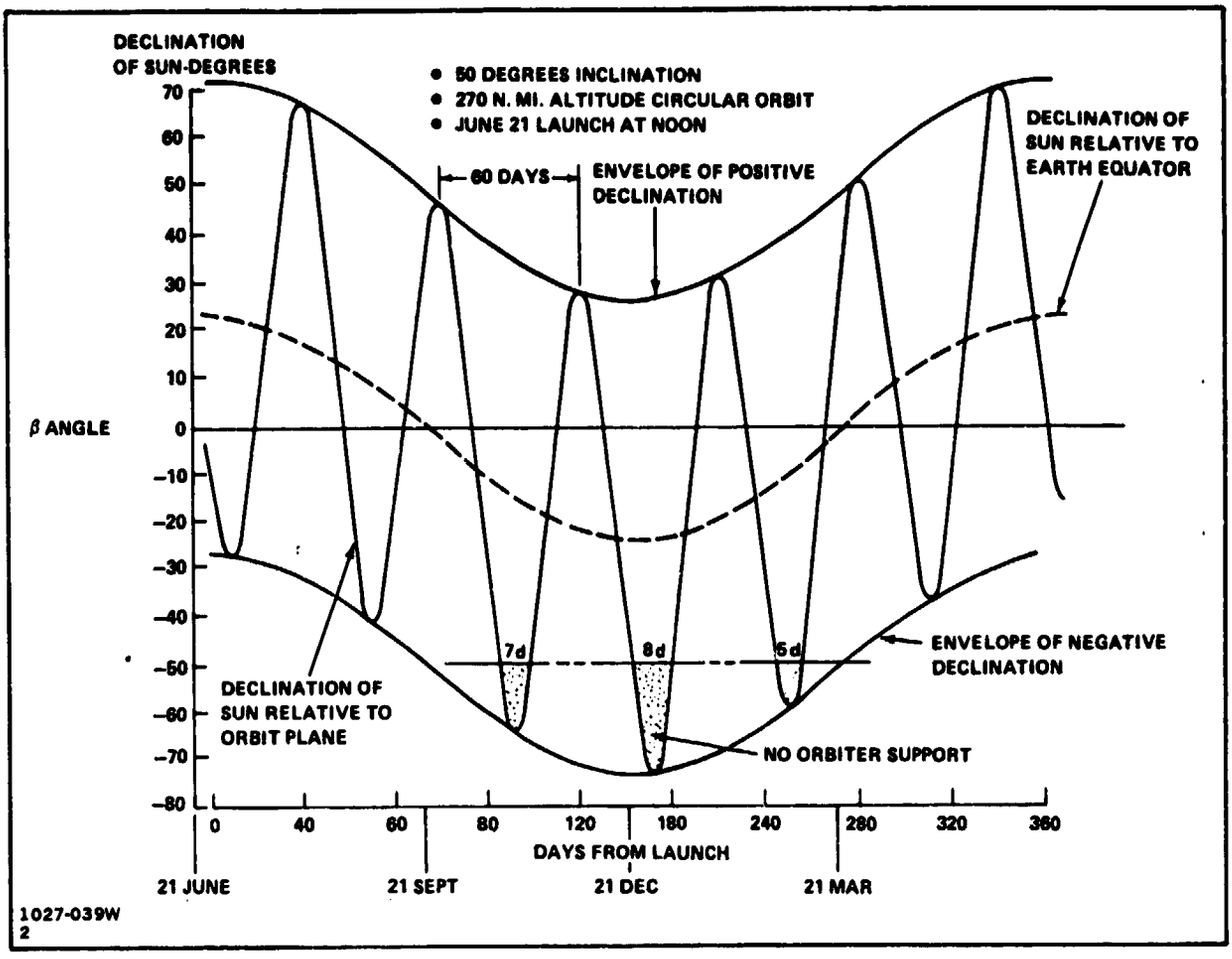

Fig. 4-16 Effect of Orbiter Occultation of Solar Arrays

4.5.5 Summary

Figure 4-17 summarizes the results of the alternate PM/Platform flight orientations evaluated herein.

- AVV - Extensive solar array occultation in both free-flight and Orbiter-docked modes.
- LV - Some occultation in free-flight, but extensive array occultation in the Orbiter-docked mode.
- POP - No occultation in free-flight; minimal-to-none in the Orbiter-docked mode.

2

FLIGHT MODE	SOLAR ARRAY OCCULTATION		
	FREE FLIGHT	ORBITER-DOCKED	
AVV	EXTENSIVE	EXTENSIVE	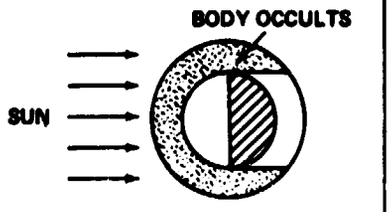
LV	MINOR	EXTENSIVE	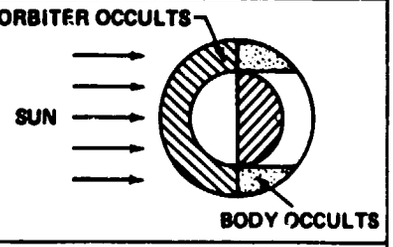
POP 1027-040W	NONE	MINIMAL	TIPS OF ORBITER COULD OCCULT ARRAY @ HIGH β ANGLES

POP FLIGHT MODE FAVORED

IRAD

Fig. 4-17 Summary of Flight Mode Evaluations

Clearly, the X-POP flight mode is favored from a solar array occultation point of view. In addition, as discussed previously, momentum considerations in both free flight and Orbiter-docked modes also favor an X-POP flight orientation. In summary, flight mechanics, momentum implications, and Orbiter heat rejection aspects favor an X-POP PM/Platform flight mode. It has, therefore, been adopted as the baseline for this study.

4.6 "REAL ESTATE" USAGE CONCEPTS

Representative "Real Estate Usage" concepts were developed to assess potential space and area-needs for PM/Platform applications. Figure 4-18a shows a free-flyer concept that provides accommodations for solar and earth-viewing, and, as indicated is oriented X-POP. A total of ten user payloads, vis. pallets/platform adapters (4 solar/6 earth plus a soil moisture radiometer), are depicted on the configuration.

2

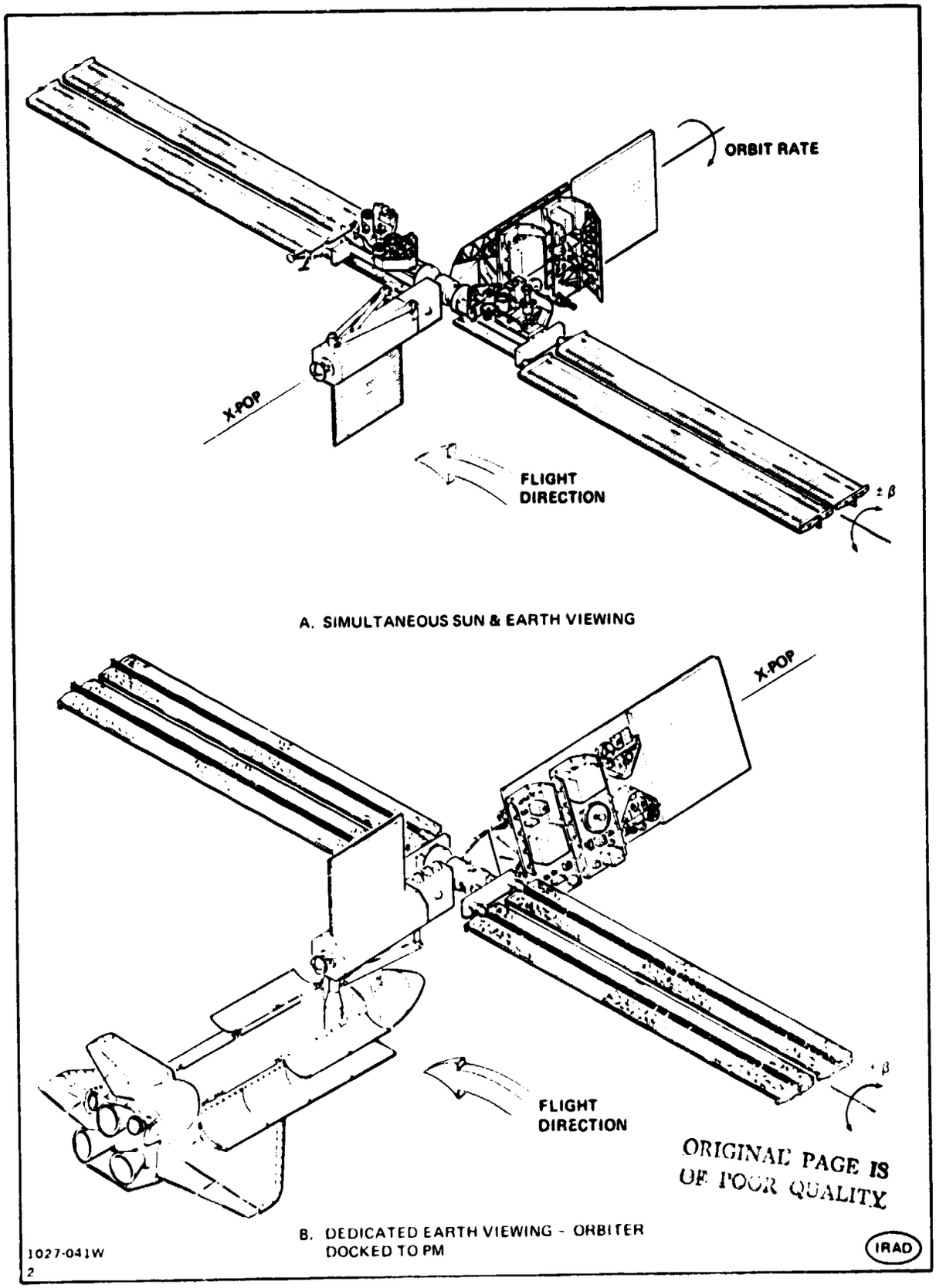

Fig. 4-18 Power Module/Platform Concept – "Real Estate Usage"

2

Solar viewing payloads are mounted on a structure which also supports the solar arrays and tracks the sun vector ($\pm\beta$). Earth-viewing payloads are mounted to a platform which rotates at orbit rate (relative to the PM). The gimbal mechanism assumed for these PM/Platform concepts is the Orientation Drive and Power Transfer System (ODAPT), developed during the early 1970s by NASA.

Figure 4-18b shows a "Real Estate Usage" concept that is similar to the previous one, except that additional earth-viewing payloads are accommodated, and the Orbiter is shown docked in position to derive power from the PM. Note, however, the inboard location of the solar array, which as related previously, would be occulted by the Orbiter at high negative β angles.

Having established the basic flight orientation, user accommodation approaches, and PM commonality potential for PM/Platforms, via these "Real Estate" concepts, our next step was to examine the configuration implications of potential sensor fields-of-view that might be called for by the user community.

4.7 SENSOR FIELDS-OF-VIEW

The significant effects that potential sensor fields-of-view (FOV) could have upon a PM/Platform concept are shown in Fig. 4-19. Typical solar viewing payloads call for a narrow FOV, about ±1°; a 2° clearance has been assumed in the concept shown. Clearly, if payload elements on the earthviewing platform call for long lengths in the direction of the flight vector, (1) the solar viewing platform and arrays must move outboard, or (2) occultation of solar viewing instruments and solar arrays must be accepted. Note, however, that for the configuration shown, the position of the solar payloads results in a location of the solar arrays which spans the Orbiter...thus, in this case, no occultation of the arrays would occur in an Orbiter-docked mode receiving support from the PM.

Of equal significance is the impact of FOV needs of the earth-oriented platform. The concept shows the implication of a ±45° FOV for a representative (early-generation) soil moisture radiometer. As shown, a "quad" solar array concept may be desirable.

It is conceivable that earth oriented users could call for horizon-to-horizon viewing; in this case the FOV requirement could be on the order of ±60° to ±70°, depending upon flight altitude. A longer earth-viewing platform would thus be called for. Conceptually, the earth viewing platform's "real estate" could be configured in terms of FOV "accommodation zones", with large FOV needs located outboard and those with lesser FOV requirements mounted at appropriate locations inboard.

2

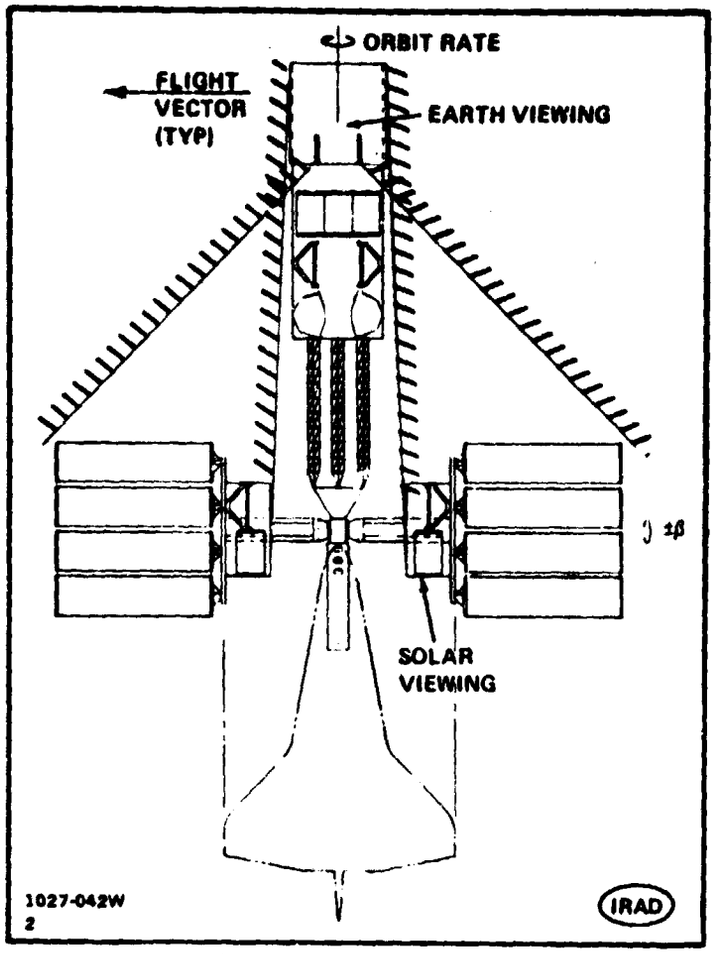

Fig. 4-19 Sensor Fields of View (FOV)

Clearly, the solar and earth-viewing user's FOV, and payload length requirements along the flight vector, are dominant considerations in evolving acceptable PM/Platform concepts. Further, in this early state of configuration development, the application of large space structures does appear necessary.

4.8 POWER MODULE/PLATFORM CONCEPTS

The PM Platform concepts illustrated herein reflect the aforenoted FOV considerations, and show how a common PM could be adapted to a broad spectrum of potential user-oriented platform missions.

4.8.1 Simultaneous Sun and Earth Viewing

Figure 4-20 illustrates free-flight and servicing concepts of a PM/Platform providing simultaneous solar and earth-viewing capability. The platform accommodates four

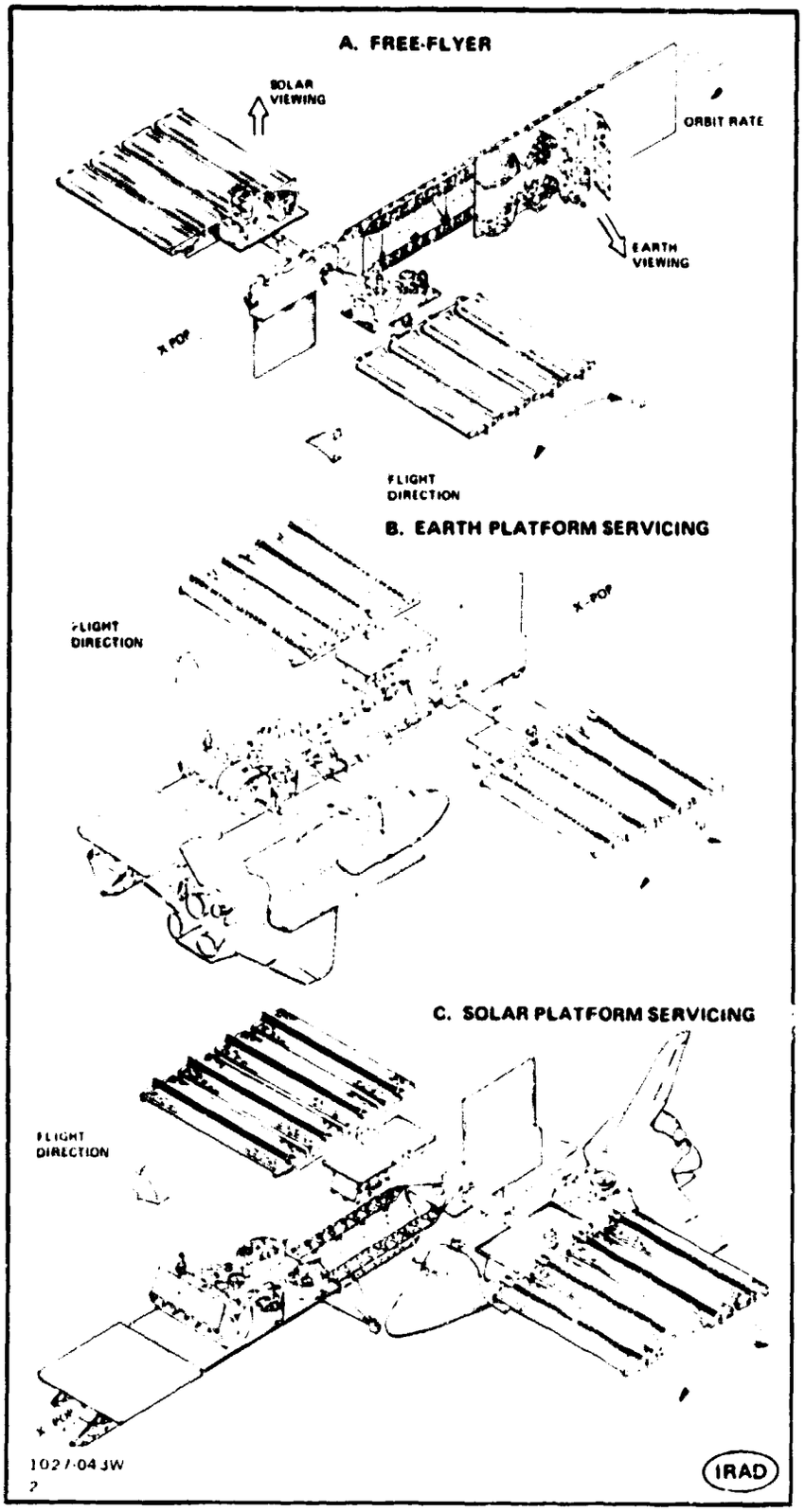

Fig. 4-20 Power Module/Platform Concept – Simultaneous Sun & Earth Viewing

solar-viewing pallet/platform adapter payloads and seven (plus a radiometer) earth-viewing payloads.

Figure 4-20b shows an earth-viewing platform servicing concept. Platform servicing intervals are assumed to occur at the $\beta = 0°$ flight attitudes of the solar array. These intervals occur monthly and could be utilized for payloads installation, servicing, and replacement. During platform servicing, it has been assumed that all necessary Orbiter subsystem support functions are Orbiter-supplied.

The Orbiter is shown berthed for servicing solar-viewing payloads in Fig. 4-20c. The concept shown involves a trapeze-type berthing port...extended for solar platform servicing and retracted to the body of the PM for Orbiter support. The illustrations show the Orbiter berthed, for servicing, in an X-POP orientation due to favorable momentum implications in this coupled flight mode. Additionally, the Orbiter's "belly" faces the sun...a preferred Orbiter orientation for heat dissipation purposes.

4.8.2 Dedicated Earth Viewing

Figure 4-21 illustrates free-flight and Orbiter support concepts of a PM/Platform providing a dedicated earth-viewing capability. This concept is similar to the previous one, except that additional earth-viewing pallets/platform adapter payloads are accommodated.

The Orbiter is shown berthed in support position to the PM in Fig. 4-21a with its "belly" facing the sun. In order to maintain a preferential heat rejection attitude for the Orbiter, it would appear that this type of PM support mode would also favor operations at, or around, the platform's $\beta = 0°$ solar array flight intervals. During this Orbiter-support mode the platform payloads are assumed inoperative, with only standby subsystem functions supplied by the PM/Platform, and the Orbiter receives power and heat rejection support from the PM. The radiator shown is provided for this purpose.

As mentioned previously, the platform provides power, heat rejection and data handling functions for platform payloads, with overall spacecraft stabilization/control provided by the PM. Conceptually, there is no heat rejection interface between the PM and Platform; the interface is limited to power and data transfer only (utilizing the PM's communication antennas).

Figure 4-21b shows the platform "strongback" structure that has been identified within these PM/Platform concept development efforts. The structure utilizes a cross-sectional geometry called an "inverted-apex Tribeam".

2

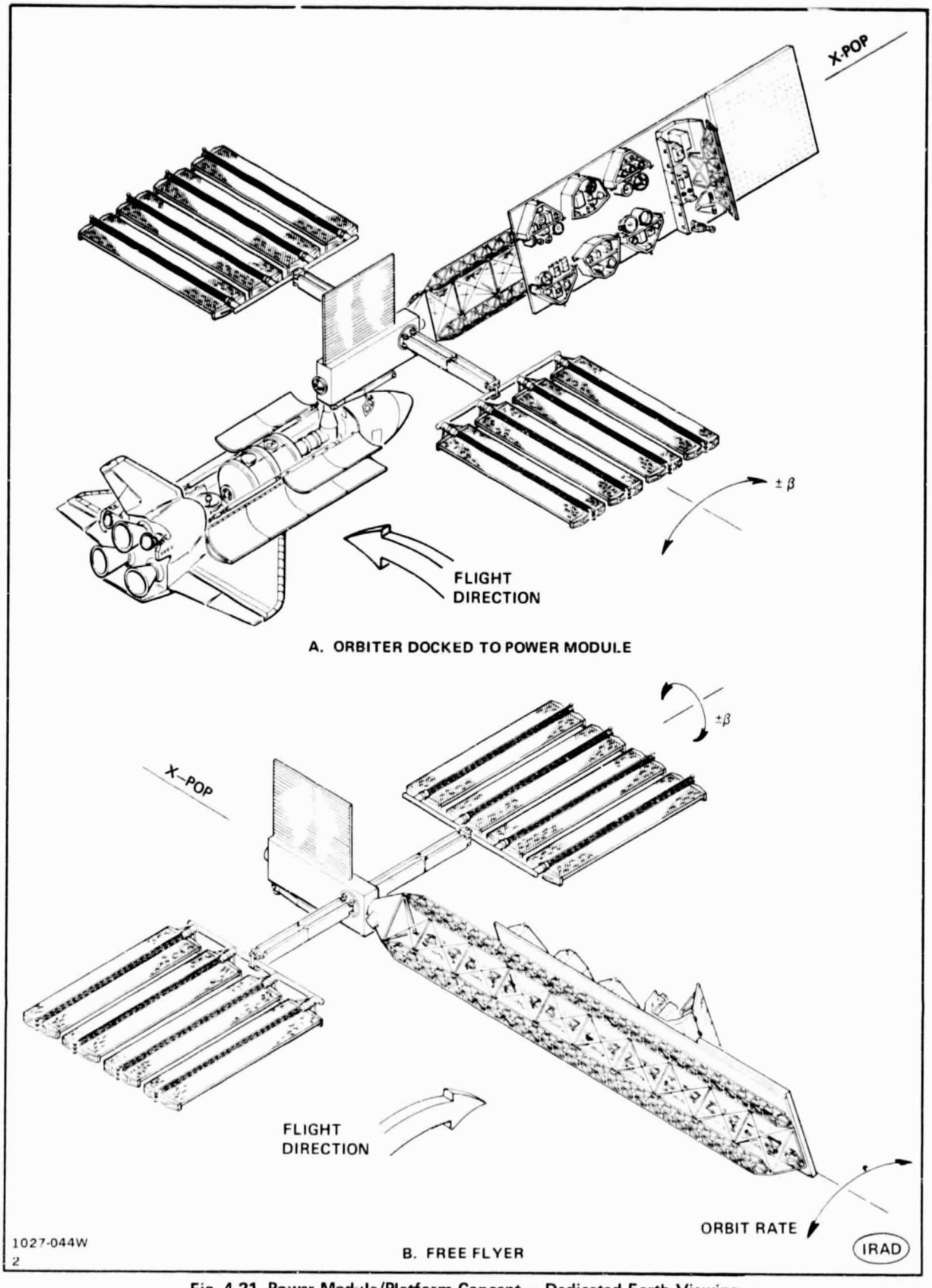

Fig. 4-21 Power Module/Platform Concept – Dedicated Earth Viewing

2

Two types of Tribeam construction adaptable to space fabricated 1-meter beams have been investigated in Grumman's IRAD activity, and are illustrated in Fig. 4-22. The basic cross-sectional geometries are characterized by the apex-position of the 1-meter beam, hence the names:

- Inverted-Apex Tribeam, and
- Upright-Apex Tribeam.

The design approach, in both cases, utilizes fittings attached to the verticals and caps of a 1-meter beam at apex positions. The fittings could be designed to connect either ground- or space-fabricated verticals or diagonals of the Tribeams. For Tribeam depths in excess of 10 meters, space-fabricated verticals/diagonals would be appropriate. For depths less than 10 meters, ground-fabricated Tribeam verticals/diagonals are preferred. Since the Power Module/Platform Tribeam "strongback" is about 5-m deep, the use of ground-fabricated verticals/diagonals has been adopted.

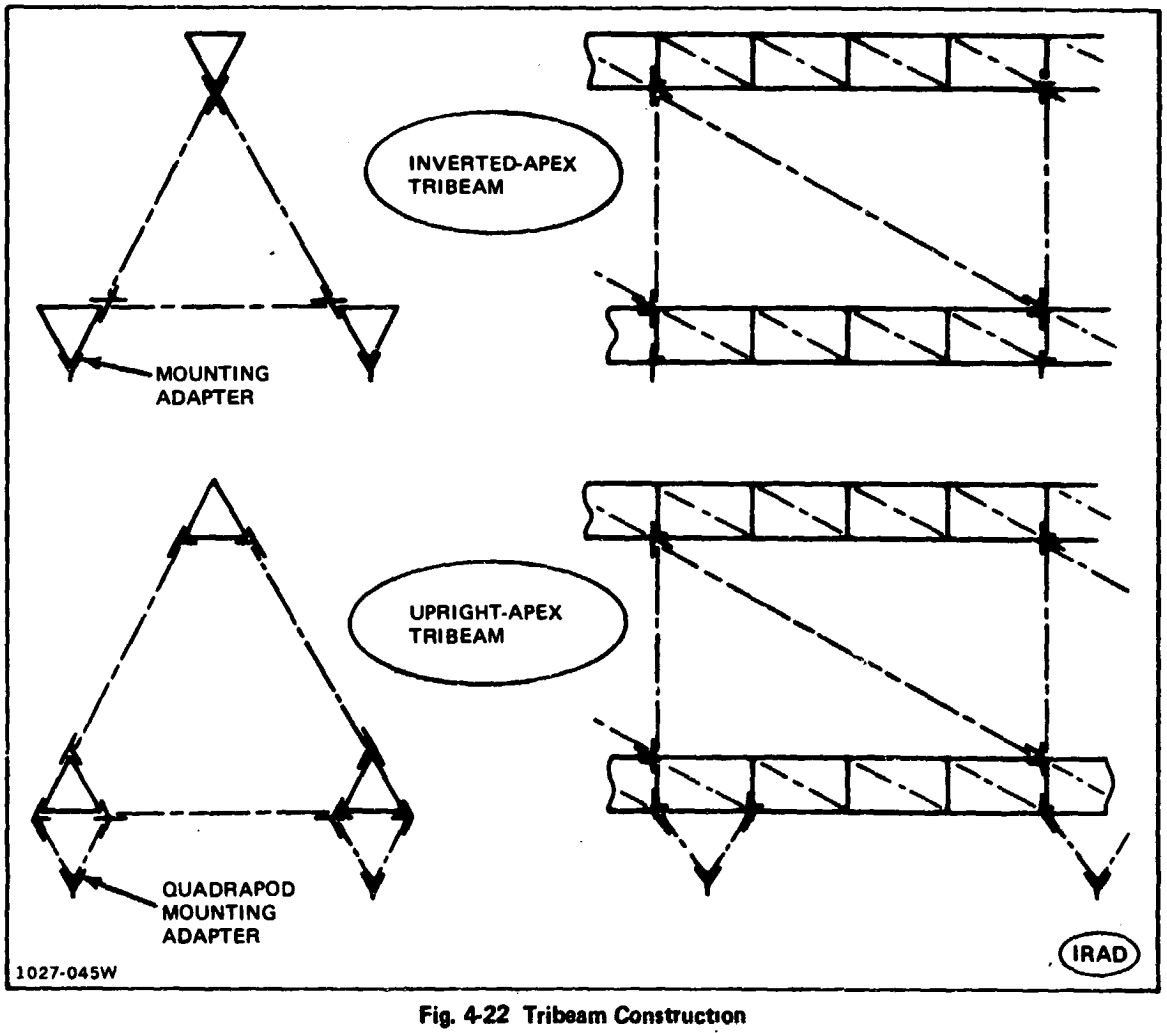

Fig. 4-22 Tribeam Construction

As to the preferred form of Tribeam construction for the Platform application, the figure clearly shows that less fittings are needed to join the verticals of the Tribeam in the Inverted-Apex Tribeam geometry. Additionally, mounting adapters are more readily accommodated directly to the 1-meter beam's apex in this same geometry. The Inverted-Apex Tribeam, therefore, has been selected as the basic design for the Power Module/Platform "strongback".

4.8.3 Simultaneous Solar and Stellar Viewing

Having identified the X-POP flight mode as desirable for a PM/Platform concept with combined solar and earth-viewing, the next step was to adapt the common PM for simultaneous solar and stellar-viewing. Figure 4-23a shows that a $\beta = 0°$ attitude reflects an X-POP condition of the principal axis of the PM. By tilting the body axis of this inertially stabilized spacecraft fore-and-aft, the vehicle could readily track the β angle variation. Further, by providing inertial symmetry about all three axes, through the use of appropriate booms/masses, the effects of gravity-gradient torques can be minimized or negated.

Additionally, a fixed solar array can be accommodated by this flight vehicle concept, which minimizes effects of stabilization disturbances within the spacecraft. This PM/Platform concept, therefore, should be capable of accommodating solar/stellar users and materials processing. (Although further study may indicate that an independent vehicle is needed for the materials processing mission.)

The position of the Orbiter in its PM support mode, and relative to $\beta = 0°$ and β + orientations of the spacecraft, is shown in Fig. 4-23b. To minimize the momentum effect of the coupled Orbiter and PM/Platform, the Orbiter is shown in X-POP orientation during the PM support mode. As assumed for the previous PM/Platform concepts, platform servicing would occur during $\beta = 0°$ intervals with the Orbiter-berthed X-POP.

Figure 4-24 illustrates the common PM adapted for solar/stellar-viewing with fixed solar arrays, incorporating desirable 3-axis inertial symmetry, and Orbiter-berthing accommodations. The Z-axis boom has been located on the sun-facing side of the vehicle to provide clear fields-of-view for instrument slewing generally needed by stellar viewers and is compatible with the narrow-angle viewing needs of solar platform users.

As indicated previously, this same PM/Platform concept is suggested for materials processing missions because of the expected stability of the platform.

2

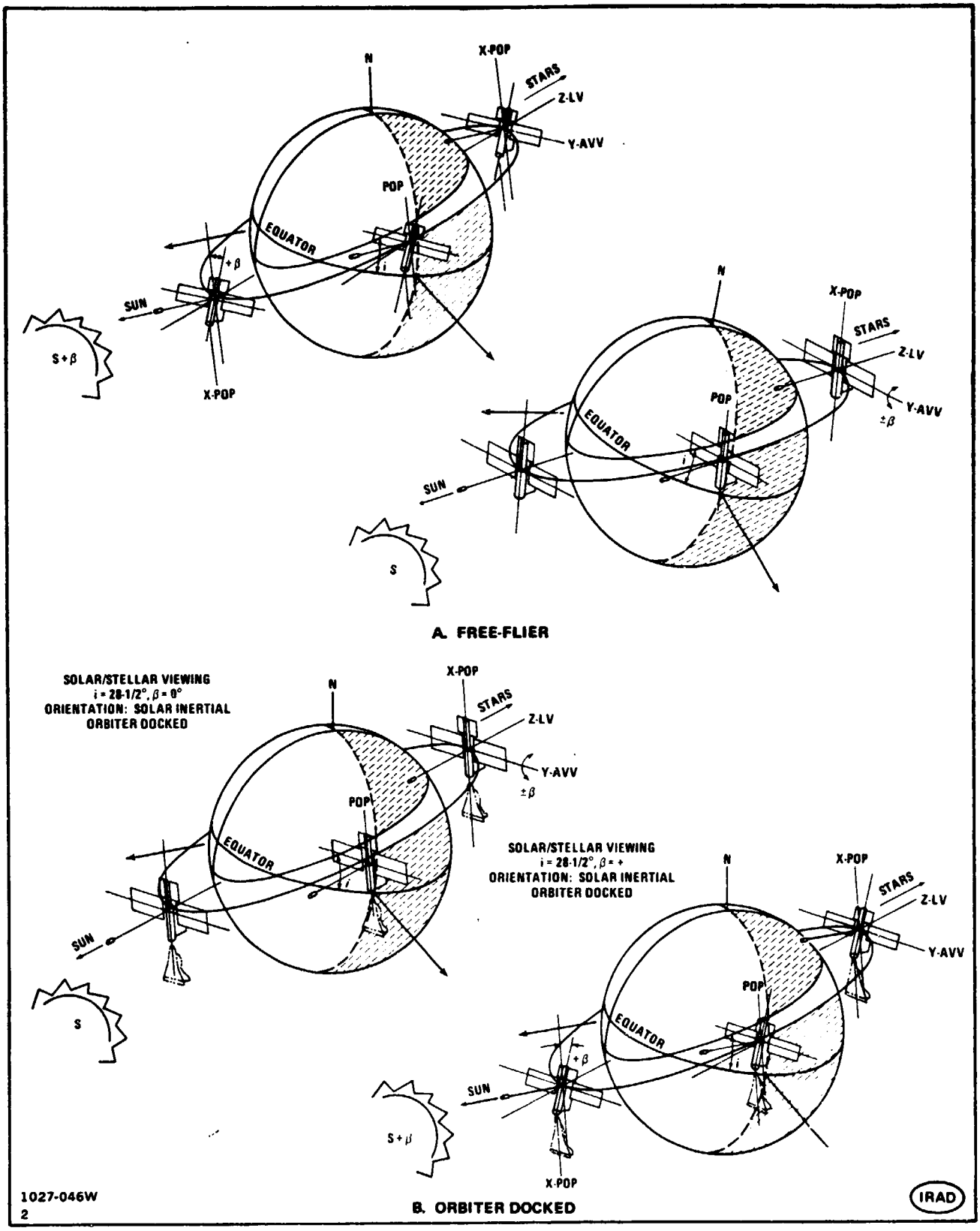

Fig. 4-23 Solar/Stellar Viewing – Orientation: Solar Inertial

2

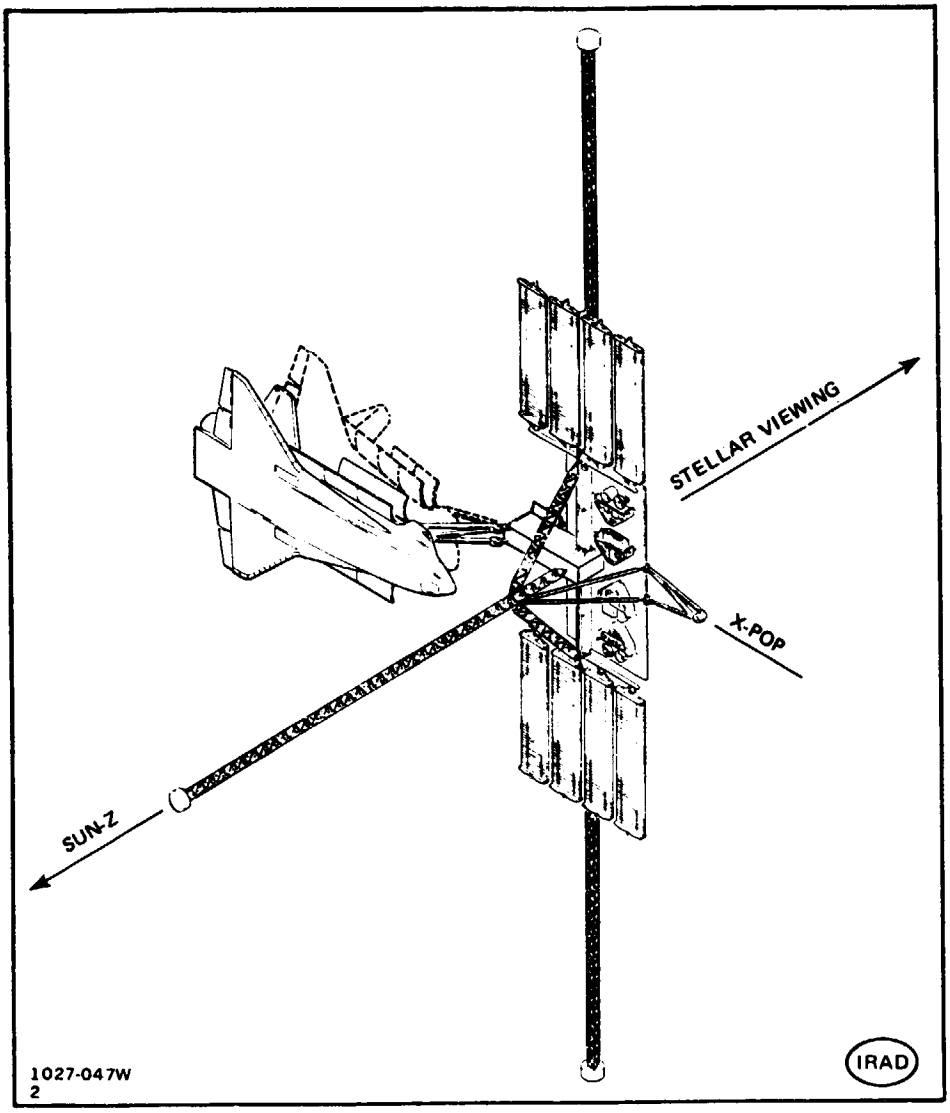

Fig. 4-24 PM/Platform Concept Simultaneous Solar & Stellar Viewing – Orbiter Docked to PM in POP Attitude

4.9 POINTING AND STABILIZATION CAPABILITIES

Figure 4-25 compares the pointing/stability requirements of candidate platform users with an estimate of the PM/Platform's inherent stability. These represent "best judgement" estimates felt to be reasonable at this time, as the platform concepts are in a very early stage of conceptual development. Estimated capabilities for the respective platform concepts are shown in the table, using conventional attitude control concepts. For the more stringent pointing requirements, active payload pointing devices are suggested. Considerable analysis/design effort will be necessary in order to refine these estimates of platform stabilization capability and is recommended for future study.

2

MISSION	REQUIREMENTS		CANDIDATE PLATFORM	CAPABILITIES (4)		CONTROL APPROACH
	ACCURACY	STABILITY		ACCURACY	STABILITY	
EARTH POINTING	±0.1°→±5.° (1)	±36→±360 $\frac{\text{SEC}}{\text{SEC}}$ (±0.01→±0.1 $\frac{\text{DEG}}{\text{SEC}}$) (1)	SOLAR/ EARTH	±0.2°	±72. $\frac{\text{SEC}}{\text{SEC}}$ (±0.02 $\frac{\text{DEG}}{\text{SEC}}$)	CMG'S, MAGNETIC TORQUERS, EARTH SENSOR, GYROS
SUN POINTING	±0.1 SEC→±1.° (2)	±1.→±100. $\frac{\text{SEC}}{\text{SEC}}$ (3)				
STELLAR POINTING	±0.002 SEC→±1.° (2)	±0.1→±10. $\frac{\text{SEC}}{\text{SEC}}$ (2)	SOLAR/ STELLAR	±0.02°	±1.0 $\frac{\text{SEC}}{\text{SEC}}$	CMG'S, MAGNETIC TORQUERS, MMS STAR SENSORS & GYROS, ACTIVE PAYLOAD ALIGNMENT EQUIPMENT (e.g. IPS)
MATERIALS PROCESSING	$10^{-5} \rightarrow 10^{-8}$ g (2)			10^{-6} g		

(1) DATA SOURCE: SYS DEFN STUDY FOR SHUTTLE DEMO FLTS OF LSS, VOL 2A—TECHNICAL APPEND., JULY 78.

(2) DATA SOURCE: UAH/NASA WORKSHOP ON SPACE SCIENCE PLATFORM, AUG 21-25, 1978.

(3) GAC ESTIMATE.

(4) PRELIMINARY ESTIMATES; UPDATE/REFINEMENT REQUIRED.

1027-048W
2

IRAD

Fig. 4-25 Estimated Power Module/Platform Attitude Control Capabilities

4.10 MATERIALS PROCESSING EXPERIMENT IMPLICATIONS

Gravity levels resulting from aerodynamic drag are indicated in Fig. 4-26 as a function of altitude for the LSS Platform free-flyer developed during the initial phase of this study, and a representative PM. These data are based on maximum nominal density values in the solar cycle (Jacchia Model).

A goal of 10^{-8} g has been indicated as a desired g-level for future material processing experiments. For purposes of illustration, the 10^{-8} g line shows where a coupled PM and Materials Experiment Module (MEM) would be in relation to the two curves shown. Considering aerodynamic drag alone, circular orbit altitudes of at least 340 n mi are needed for an LSS Platform free-flyer with 375 n mi needed for the PM/MEM combination. Note that a variation in orbit altitude of about 95 n mi results in an order of magnitude change in g-level.

The acceleration induced on materials processing experiments, associated with a candidate PM/Platform concept, due to attitude control torques has been estimated (Fig. 4-27) based on the characteristics indicated. The accelerations are presented

2

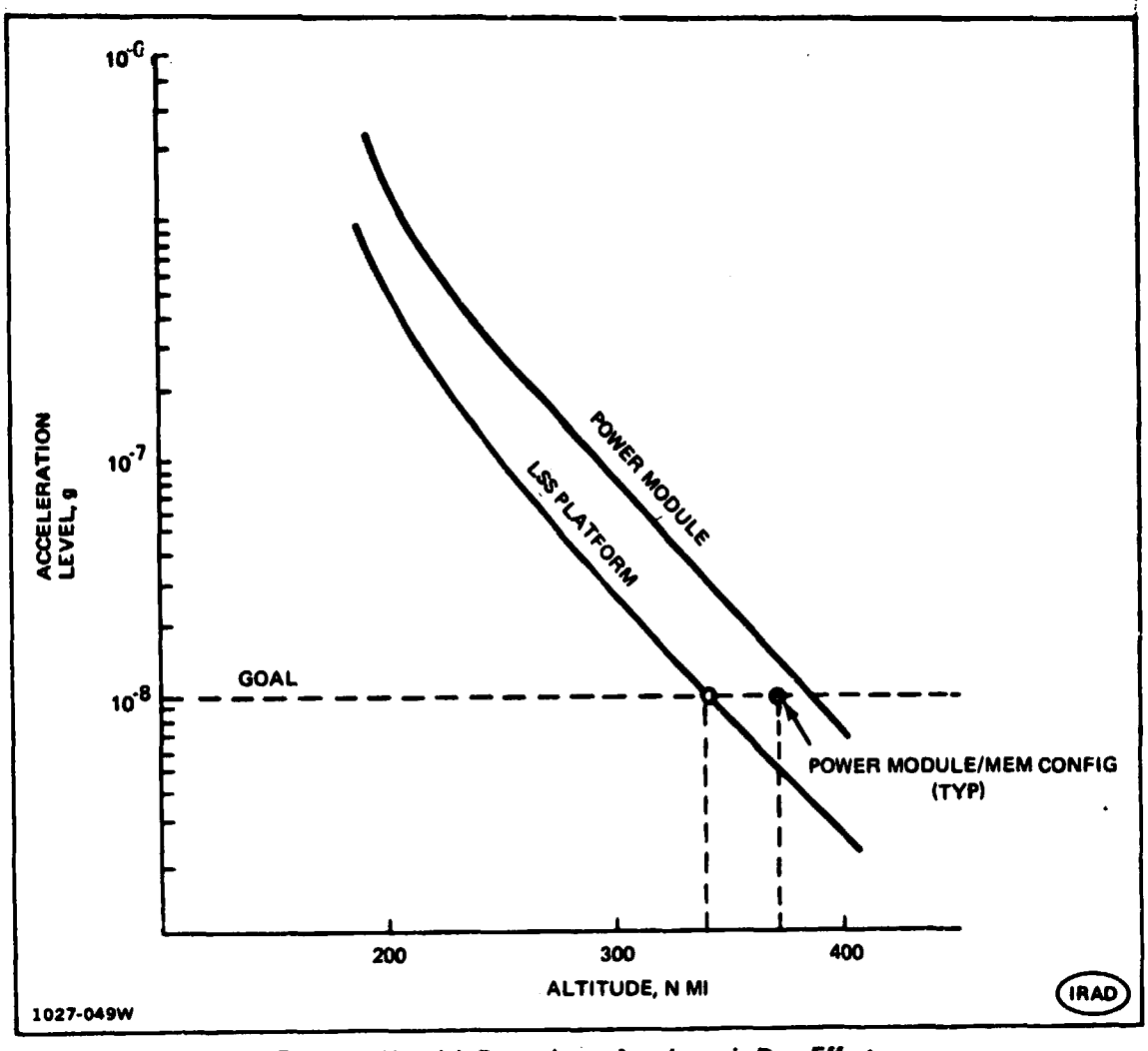

Fig. 4-26 Materials Processing – Aerodynamic Drag Effects

FREE-FLYER

- POWER MODULE/PLATFORM ($1 = 10^7$ kg m^2): MAX MEA DISTANCE FROM C.G. IS 10.5 m
- CMG CONTROL, PEAK TORQUE 160 FT-LB

CMG TORQUE, % OF MAX	ACCELERATION, g
0.1	0.23×10^{-8}
1	2.3×10^{-7}
5	1.2×10^{-6}
10	2.3×10^{-6}
50	1.2×10^{-5}
100	2.2×10^{-5}

1027-050W
2

IRAD

Fig. 4-27 Accelerations Due to Control Torques

as a function of percent of CMG torque capability (Skylab type), assuming the configuration is in a stable mode with CMGs used for damping. A more extensive analysis of the specific PM/Platform configuration and its disturbance torque environment is necessary to refine these estimates. Other types of control actuators, such as reaction wheels, might be considered as a means of further reducing gravity levels induced by control torques.

An additional effect which produces an acceleration on materials processing experiments concerns the orbital dynamics effect, which only produces zero-g at the center of gravity (g) of the configuration. At points displaced from the cg, the pull of gravity is not balanced by the centrifugal acceleration. Conversations with NASA/MSFC personnel have identified the following expressions for the acceleration in g per meter of displacement from the cg due to this effect.

- Max in-plane acceleration = $2\ (\frac{\omega^2}{9.8})$
- Out-of-plane acceleration = $(\frac{\omega^2}{9.8})$

where ω is the orbital rate in rad/sec.

The maximum total acceleration per meter is then $\sqrt{5}\ (\frac{\omega^2}{9.8})$.

For a maximum mounting distance of the experiment from the cg of 10.5M, this expression indicates an orbital altitude of 39,250 km, i.e. near-synchronous orbit altitude, is required to limit the acceleration level to 10^{-8} g. Figure 4-28 illustrates this orbital dynamics effect in terms of attainable gravity levels at altitudes up to synchronous, as a function of the experiment's mounting distance from the cg. At an altitude of 400 km, the experiment would have to be kept within 0.034 m of the cg to meet the 10^{-8} g level. The corresponding acceleration at 10.5 m distance and 400 km altitude is 3.06×10^{-6} g.

In conclusion, control torques and orbital dynamics are as significant as aerodynamic drag in producing undesirable accelerations on materials processing experiments. Great care must be taken in locating these experiments relative to the cg of the configuration. The goal of 10^{-8} g maximum acceleration requires very high altitudes approaching synchronous combined with mounting locations near the cg.

2

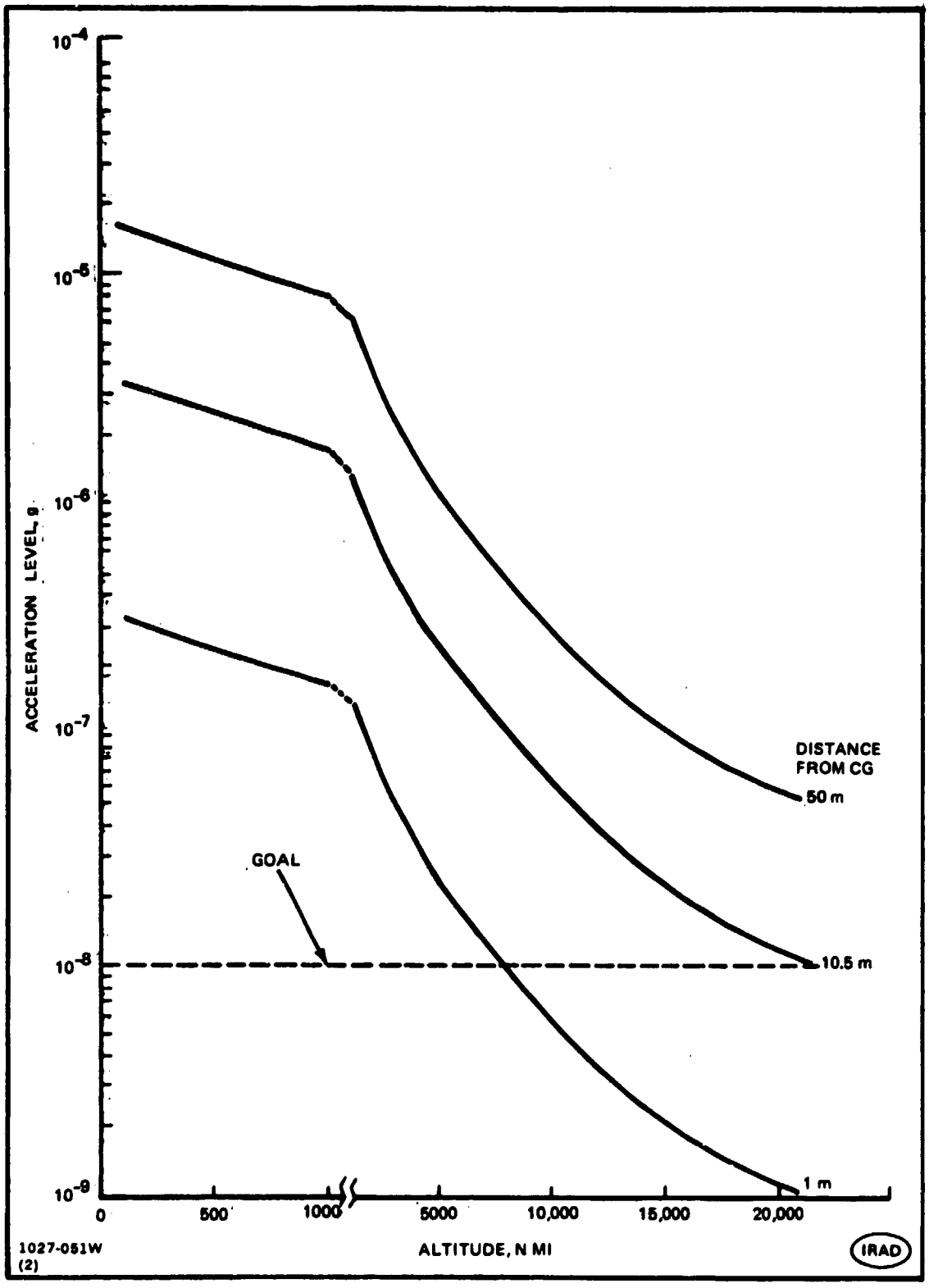

Fig. 4-28 Materials Processing Orbital Dynamics Effects

2

4.11 BERTHING CONSIDERATIONS

A preliminary analysis was performed to determine whether the solar arrays can remain deployed during berthing operations with the Shuttle (Fig. 4-29). A simplified NASTRAN model (Fig. 4-30) of the PM plus Tribeam platform, was developed. The lowest natural frequency was bending of the 52.5-ft long SEPS arrays at 0.2 Hz. Using potential berthing velocities of 0.5 fps in translation and of 0.1°/sec in rotation*, solar array bending moments were calculated using NASTRAN transient response. Figure 4-31 summarizes the maximum bending moments calculated in the 8 arrays (4 per side) for the various berthing conditions. Note that pitch and yaw conditions produce the maximum bending moments.

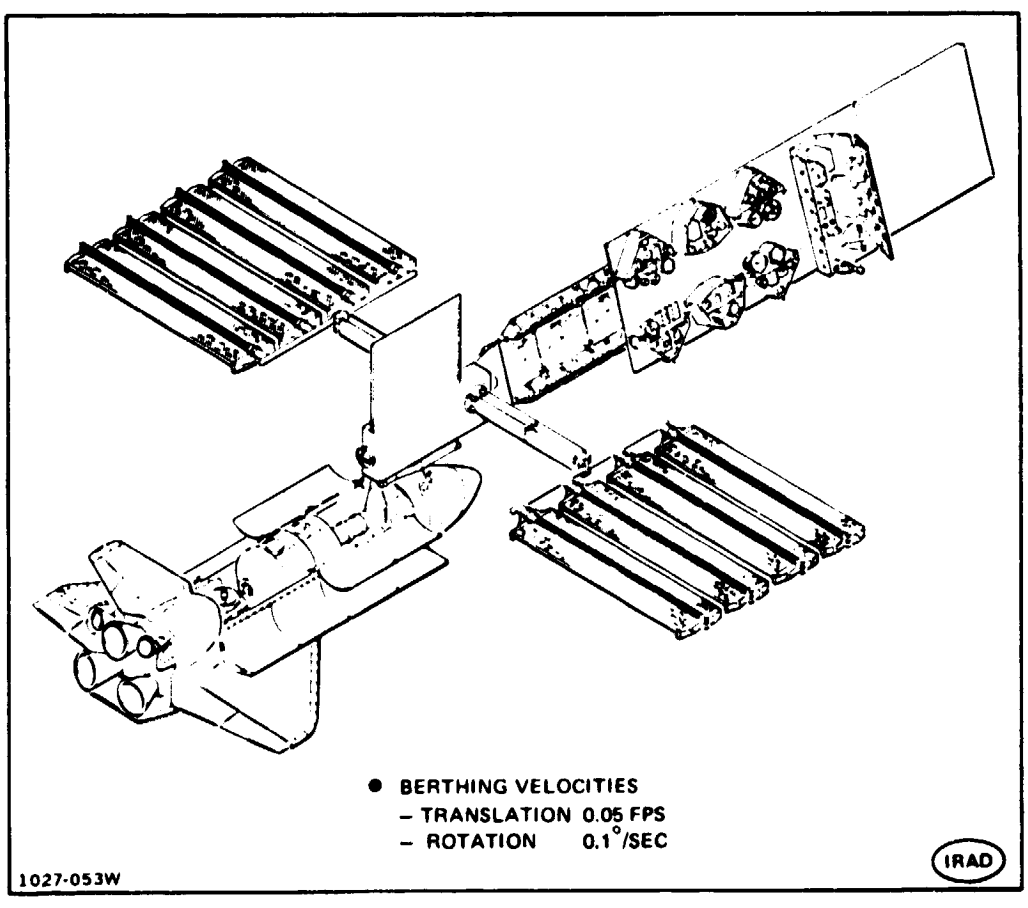

Fig. 4-29 Berthing Considerations

---

* Rockwell Space Division, "Modular Space Station - Phase B Extension - Preliminary System Design, NAS9-9953, Volume V, January 1972

2

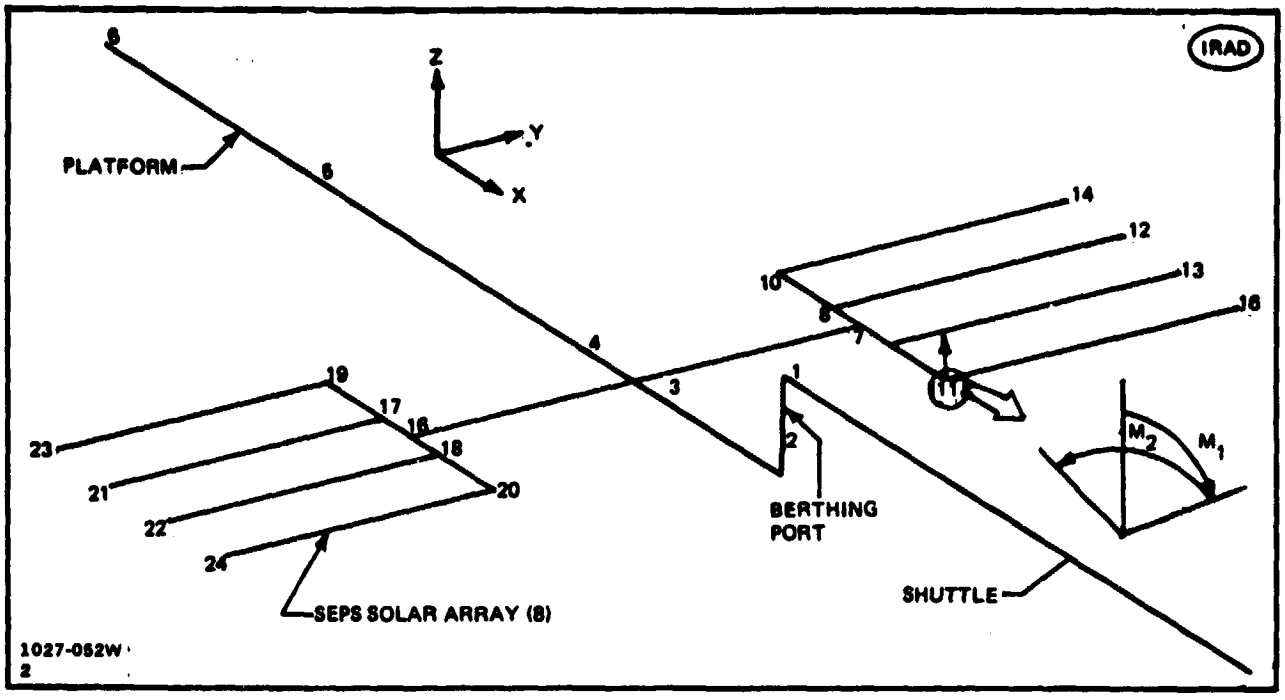

Fig. 4-30 Power Module and Platform Vibration Modes – Undeformed

CONDITION	M_1, IN.-LB	M_2, IN.-LB	M_{TOT}, IN.-LB
TRANSLATION (X) 0.05 FPS	9	118	118
TRANSLATION (Y) 0.05 FPS	26	60	65
TRANSLATION (Z) 0.05 FPS	86	0	86
*ROTATION (ROLL) 0.1°/SEC	116	7	116
ROTATION (PITCH) 0.1°/SEC	395	37	397
ROTATION (YAW) 0.1°/SEC	42	304	307
RSS =	424	334	522

*ROTATION IS ABOUT BERTHING PORT.

1027-054W
2

IRAD

Fig. 4-31 Solar Array Limit Bending Moments

2

A check was made to determine the corresponding rotational velocity if the two vehicles are forced to close at 0.05 fps at the docking port. The analysis follows:

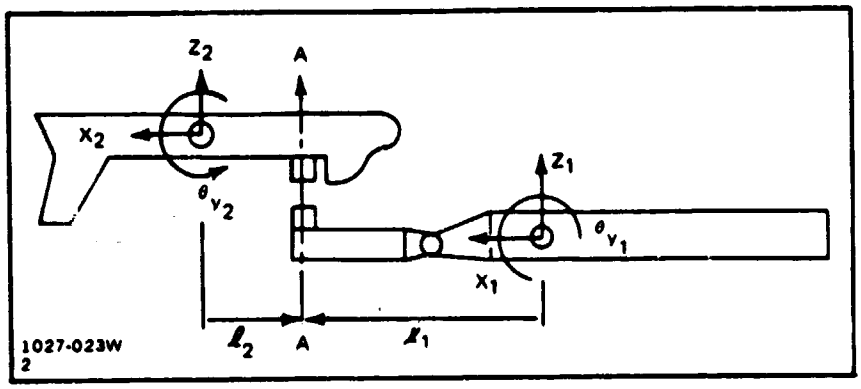

For berthing in Z direction - assume impulse is applied at berthing hatch (A-A)

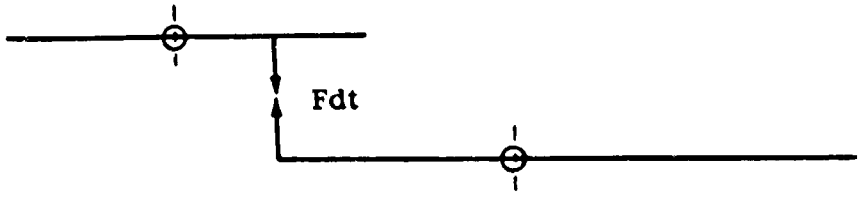

$$M_1 \ddot{Z}_1 = Fdt \quad ; \quad \left(\ddot{Z}_1 - \ddot{Z}_2\right) = \dot{Z}_{REL} = \underbrace{\left(\frac{1}{M_1} + \frac{1}{M_2}\right)}_{\frac{1}{M_e}} Fdt \quad \therefore \ddot{Z}_{REL} = \frac{Fdt}{M_e}$$

$$M_2 Z_2 = - Fdt$$

$$I_1 \dot{\theta}_{Y1} = -\ell_1 Fdt \; ; \left(\dot{\theta}_{Y1} - \dot{\theta}_{Y-2}\right) = \dot{\theta}_{Yrel} = - \left(\frac{\ell_1}{I_1} + \frac{\ell_2}{I_2}\right) Fdt$$

$$I_2 \dot{\theta}_{Y2} = \ell_2 Fdt$$

$$\dot{\theta}_{Yrel} = - \left(\frac{\ell_1}{I_1} + \frac{\ell_2}{I_z}\right) M_e \ddot{Z}_{rel}$$

$$\boxed{\dot{\theta}_{Yrel} = - \left(\frac{M_e \ell_1}{I_1} + \frac{M_e \ell_2}{I_2}\right) \ddot{Z}_{rel}} \quad ; \quad M_e = \frac{M_1 M_2}{M_1 + M_2}$$

2

For:

$M_1 = 371.15$ lb - sec^2 - in.

$I_1 = 2.141 \times 10^8$ - sec^2 - in.

$\ell_1 = 1086.4$ in.

$M_2 = 530.36$ lb - sec^2 - in.

$I_2 = 7.66 \times 10^7$ lb - sec^2 - in.

$\ell_2 = 536.8$ in.

$M_2 = 218.35$ lb - sec^2 - in.

$$\dot{\theta}_{Yrel} = -\left(\frac{218.35\,(1086.4)}{2.141 \times 10^8} + \frac{218.35\,(530.36)}{7.66 \times 10^7}\right) \dot{Z}rel$$

$$= -\,(1.108 \times 10^{-3} + 1.512 \times 10^{-3})\ \dot{Z}rel$$

$$\dot{\theta}_{Yrel} = -\,2.62 \times 10^{-3}\ \dot{Z}rel$$

if:

$\dot{Z}_{rel} = 0.05$ fps $= 0.6$ in./sec

$\dot{\theta}_{Yrel} = -1.57 \times 10^{-3}$ rad/sec

$\dot{\theta}_{Yrel} = -0.09°$/sec; Use $\dot{\theta}_{Yrel} = -0.1°$/sec

The corresponding rotational (0.09°/sec) velocity, therefore, approximates the velocity previously assumed (0.1°/sec.)

Since the peak bending moments do not occur at the same time, the bending moment values shown in Fig. 4-31 were "RSS'd*" to obtain a design limit bending moment of 522 in.-lb. The limit mast bending moment for the 14.6-in. dia mast is 2200 in.-lb.** Thus, for the aforenoted berthing velocities of 0.05 fps and 0.1 deg/sec, the allowable SEPS mast limit bending moment (2200 in.-lb) will not be exceeded. Adequate strength exists within the array support mast to permit Orbiter-Power Module berthing without retracting the solar arrays.

---

* Square (R)oot of the (S)ums of the (S)quares

** Lockheed Missiles & Space Company, "Solar Array Technology Evaluation - SEPS", LMSC, D384250, 1 September 1974

This analysis was performed for berthing at the Power Module port only. Loads induced by berthing at other locations (e.g. the platform) must be determined. It is expected, however, that these loads should be comparable because of the flexibility of the arrays.

4.12 ORBITER PLUME EFFECTS

Orbiter rendezvous, approach and docking/berthing with orbiting satellites has generally been considered with the Orbiter as the active element and the satellite stabilized but passive. The Orbiter Primary Reaction Control System (RCS) provides for translation and rotational control and consists of 38 bipropellant 870 lbf thrusters using monomethylhydrazine (MMH) as the fuel and nitrogen tetroxide (N_2O_4) as the oxidizer. Six 25 lbf vernier RCS thrusters are also available but only for rotational control. The general locations and thrust directions of the thrusters are shown in Fig. 4-32. The thrusters located in the nose are severely scarfed, which could have a significant effect on the plumes. The combustion products include N_2, H_20, $C0_2$ and H_2. Potential contamination mechanisms consist of chemical deposition, mechanical erosion, and heating and pressure effects, as illustrated in Fig. 4-33.

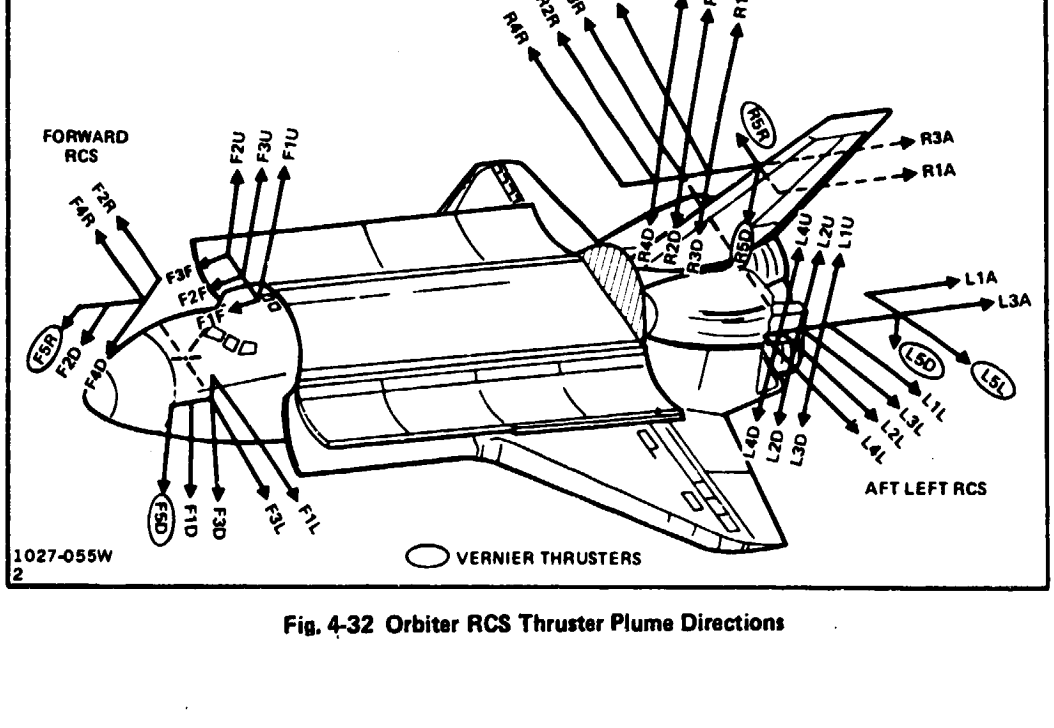

Fig. 4-32 Orbiter RCS Thruster Plume Directions

2

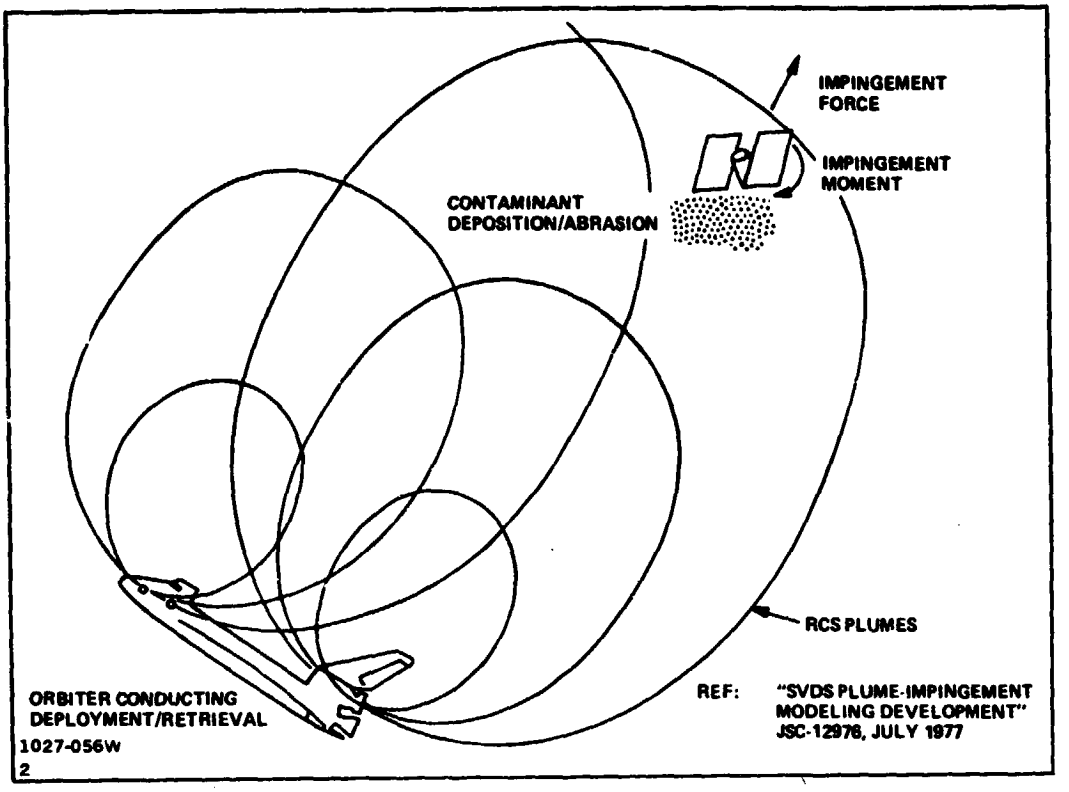

Fig. 4-33 Plume Impingement Problems

The general effects of Orbiter RCS plumes on candidate large space structure configurations were assessed. The results of this investigation are as follows:

- A final selection has not yet been made for approach and stationkeeping prior to grappling payloads by the Remote Manipulator System (RMS).
- Studies have been performed using the NASA Payload Deployment/Retrieval System (PDRS) in the Shuttle Engineering Simulator. This is a man-in-the-loop computer simulation with electronic scene generation.
- The PDRS payload approach simulations have evaluated the effects of Orbiter primary RCS plumes primarily for the Long Duration Exposure Facility (LDEF) although some work was done on a Skylab revisit.
- Primary emphasis has been on evaluating the effects of unwanted moments on the payload being approached due to plume impingement. Contamination effects due to RCS plumes have received very little attention.
- Unwanted moments caused by RCS plumes have a significant effect.

- The current approach to avoid this effect is to program off up-firing (-Z) jets during final approach using simultaneous firing of the plus and minus X jets to produce +Z acceleration. This results in a greatly reduced but acceptable control acceleration with very inefficient fuel utilization.
- Studies of RCS plume effects have been conducted for JSC's Mission Planning & Analysis Division including contamination, overpressurization and impingement effects on LDEF and the Solar Maximum Mission spacecraft.
- Three basic satellite approach techniques have been considered for approach and stationkeeping prior to grappling the payload by the Remote Manipulator System (RMS):
  - v bar - Approach from ahead or behind in the local horizontal plane
  - r bar - Approach from below along the earth radius vector
  - h bar - Approach from out-of-orbit plane.

The r bar approach is favored with a final breaking delta v of about 0.25 fps required.

- RMS constraints prohibit firing of the primary RCS after capture of a payload.
- The MSFC Induced Environmental Contamination Monitor (IECM) will be used on an orbital flight test to make measurements of plumes. The IECM will be positioned at various measurement points above the Orbiter by the RMS. It includes a mass spectrometer to measure the composition of the plumes.

The Orbiter's plume geometry during a typical approach to a PM/Platform is illustrated in Fig. 4-34. The primary thrusters will produce a force of 6×10^{-3} lb/ft^2 at 600 ft on a surface perpendicular to the thrust line. Scaling this according to the square of the distance, a force of 9.6×10^{-2} lb/ft^2 will be produced at 150 ft. A 0.25 fps velocity correction made near the structure will require approximately a one second firing. If the plume effectively intersects 100 ft^2 of solar array at 150 ft, this results in a momentum change of 1440 ft-lb-sec which is about 60% of the capability of one PM control moment gyro. Thus, the disturbance torque effects due to plumes can be significant. During separation from the PM/Platform, thruster firings toward the platform would probably be required. This is a case that has not been addressed because the usual scenario is concerned with retrieval of a satellite, as in the LDEF case, not with visiting an orbital assembly for maintenance and resupply.

2

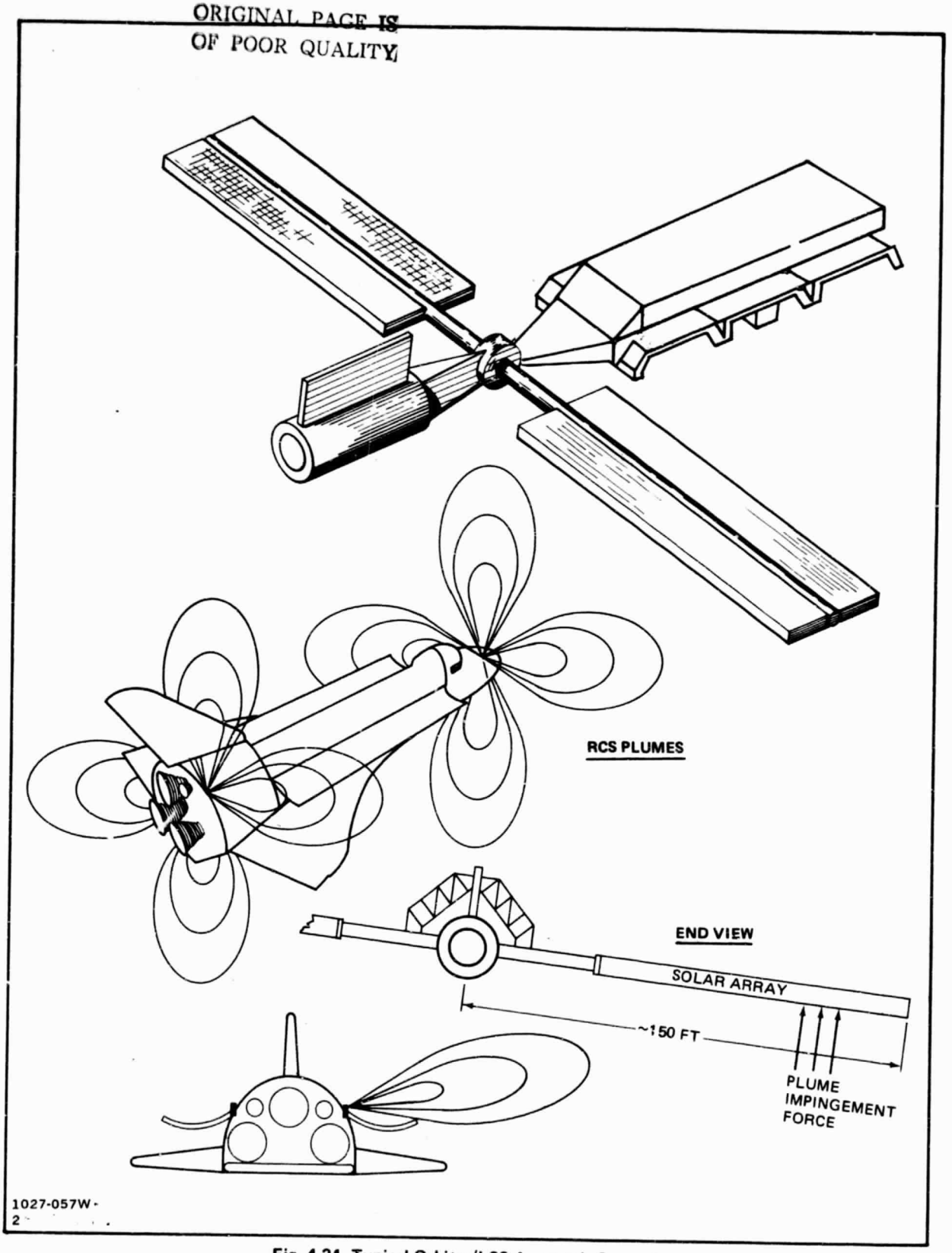

Fig. 4-34 Typical Orbiter/LSS Approach Geometry

The potential contamination due to the plumes from the Orbiter is certainly a real problem but a difficult one to quantify. The solar arrays may be degraded due to deposition of contaminants. Experiments on the pallets and the radiator surfaces could also be very susceptible to contamination. Once again this problem has not received much attention to date because of the emphasis on retrieval of satellites.

The plume effects on Platforms, in general, have not been analyzed. Platform investigations must consider potential contamination mechanisms, techniques for clean departure from an operational platform system, and plume effects during Orbiter-attached attitude and translation maneuvers. The following recommendations are made for future efforts concerning Platform operations:

- Modify and apply existing plume model programs to representative Power Module/Platforms to assess control effects
- Improve contamination models and develop more quantitative definition of contamination classes of experiments
- Define and evaluate Platform concepts which negate undesirable plume effects
- Consider augmenting the Orbiter RCS system, such as, with a payload-bay-mounted auxilliary thruster/torque system to reduce plume problems.

4.13 OBSERVATIONS/RECOMMENDATIONS

Based upon the concept development efforts conducted herein, it is evident that an extensive capability to support the user community can be developed via a PM/Platform approach. Clearly, further definition and development of the PM/Platform concept is warranted.

The PM/Platform concept development efforts have served to identify the potential near-term large space structures for an initial LSS demonstration flight. A Platform Tribeam "strongback" and a long boom have been identified as candidate structures. As illustrated in Fig. 4-35, those structures form the rationale for a relevant LSS spacecraft concept for this LSS demonstration mission.

2

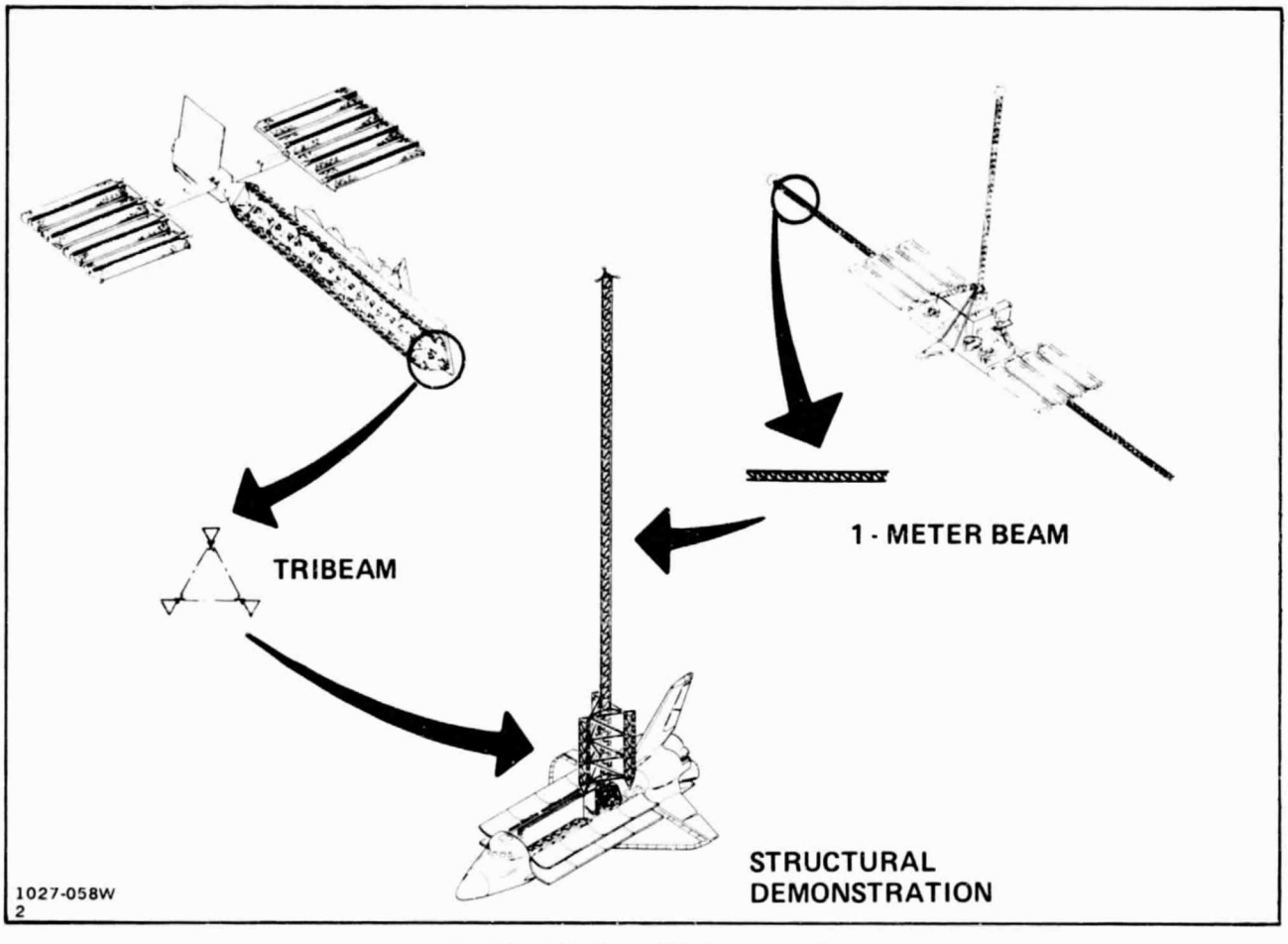

Fig. 4-35 LSS Demo Mission Rationale

5-LSS DEMONSTRATION CONCEPT DEVELOPMENT

During this follow-on phase of the study, efforts were focused toward development and evaluation of LSS demonstration options incorporating large structural elements found in Power Module/Platform adaptations. Technical data and programmatic approaches were developed for fabricating, erecting and operating these large structures in space utilizing an ABB and the Orbiter's capabilities, to accomplish an initial LSS flight demonstration in the 1983-84 time-period.

The goal of this initial flight demonstration has been to accommodate within a single Shuttle mission, both an ABB qualification/verification activity and an LSS demonstration. Specific objectives to be satisfied by this mission are:

- Automated Beam Builder (ABB)
  - Verify by in-orbit test that the ABB meets specification requirements
  - Measure the in-orbit structural properties of typical ABB-built 1-meter beams
- LSS Demonstration
  - Verify that a large space structure can be assembled from the Orbiter cargo bay
  - Measure the in-orbit structural properties of an assembled LSS,
  - Provide a useful in-orbit application, for an LSS demonstration article, in addition to verifying the ability to build large structures in space.

Within these overall goals/objectives, two LSS demonstration concepts were evolved representing varying degrees of structural/construction sophistication. The demonstration concepts are shown in Fig. 5-1. The LSS Platform incorporates the two principal large structural elements found in the PM/Platforms:

- A segment of the Tribeam "strongback" related to the earth-viewing platforms, and
- A long stabilizing boom characteristic of the long booms providing inertial symmetry for the solar/stellar and materials processing platforms.

The LSS Platform has been configured as a simple, free-flyer satellite capable of supporting low-power payloads as a soil moisture radiometer, and LDEF-type experiments.

A Structural Demonstrator version of the LSS Platform has also been investigated. This concept utilizes the Tribeam segment of the LSS Platform and is intended to demonstrate a limited degree of on-orbit structural fabrication.

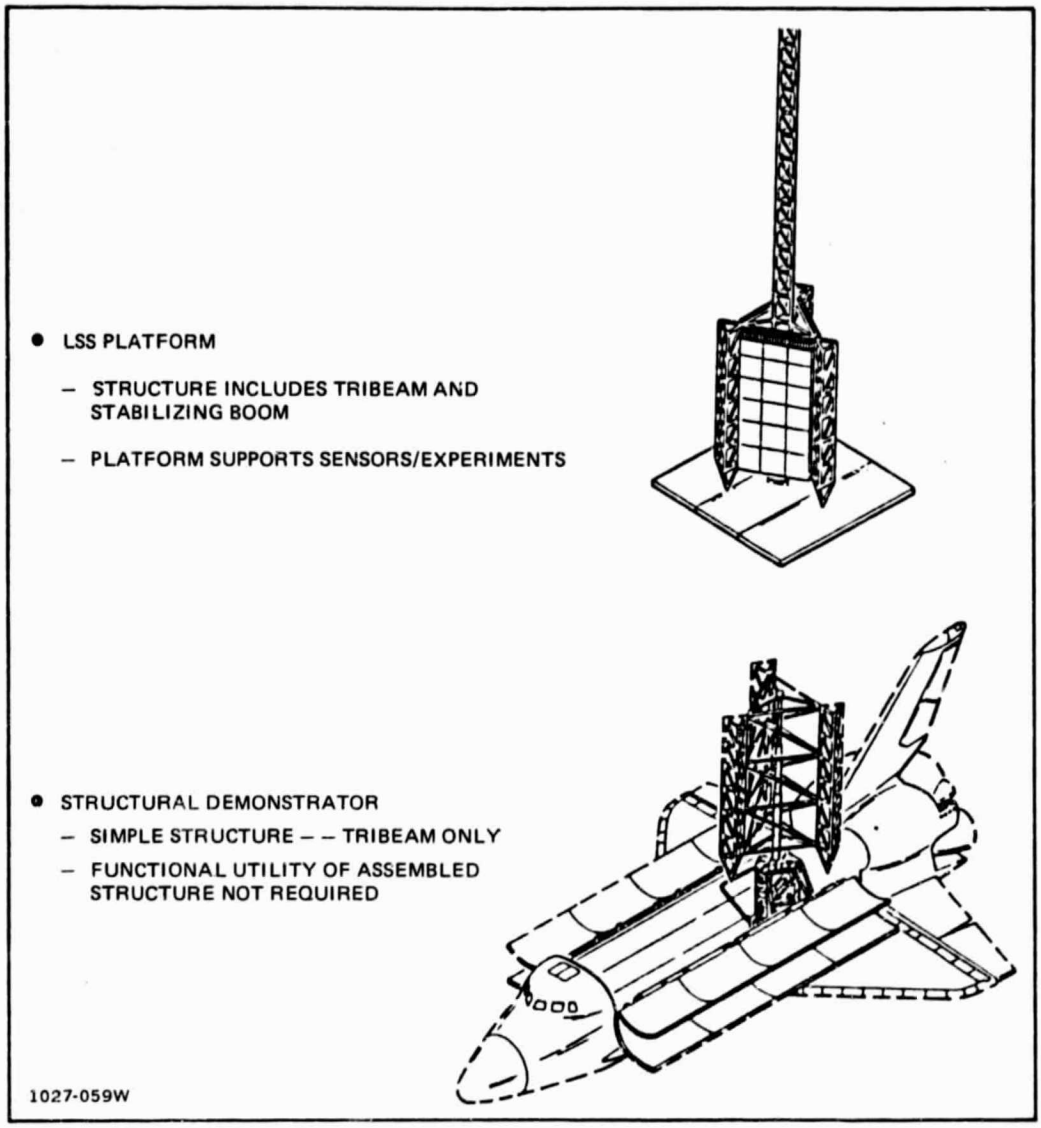

Fig. 5-1 LSS Demo Concept Options

2

5.1 STRUCTURAL DEMONSTRATOR

The Structural Demonstrator option represents a bare-bones approach having limited in-space construction goals. The general arrangement of this concept is shown in Fig. 5-2. The structure is a Tribeam of equilateral cross-section, 4.5 m in height and 10.5 m in length. The three cap members of the Tribeam are one-meter beams fabricated by the ABB; two of the beams are fabricated on-orbit; the third is a specially-instrumented ground fabricated 1-m beam. The cross stiffeners and diagonals are pre-fabricated on the ground and assembled in orbit. This concept differs from the free-flyer in that it does not contain the long central boom, subsystems and payload.

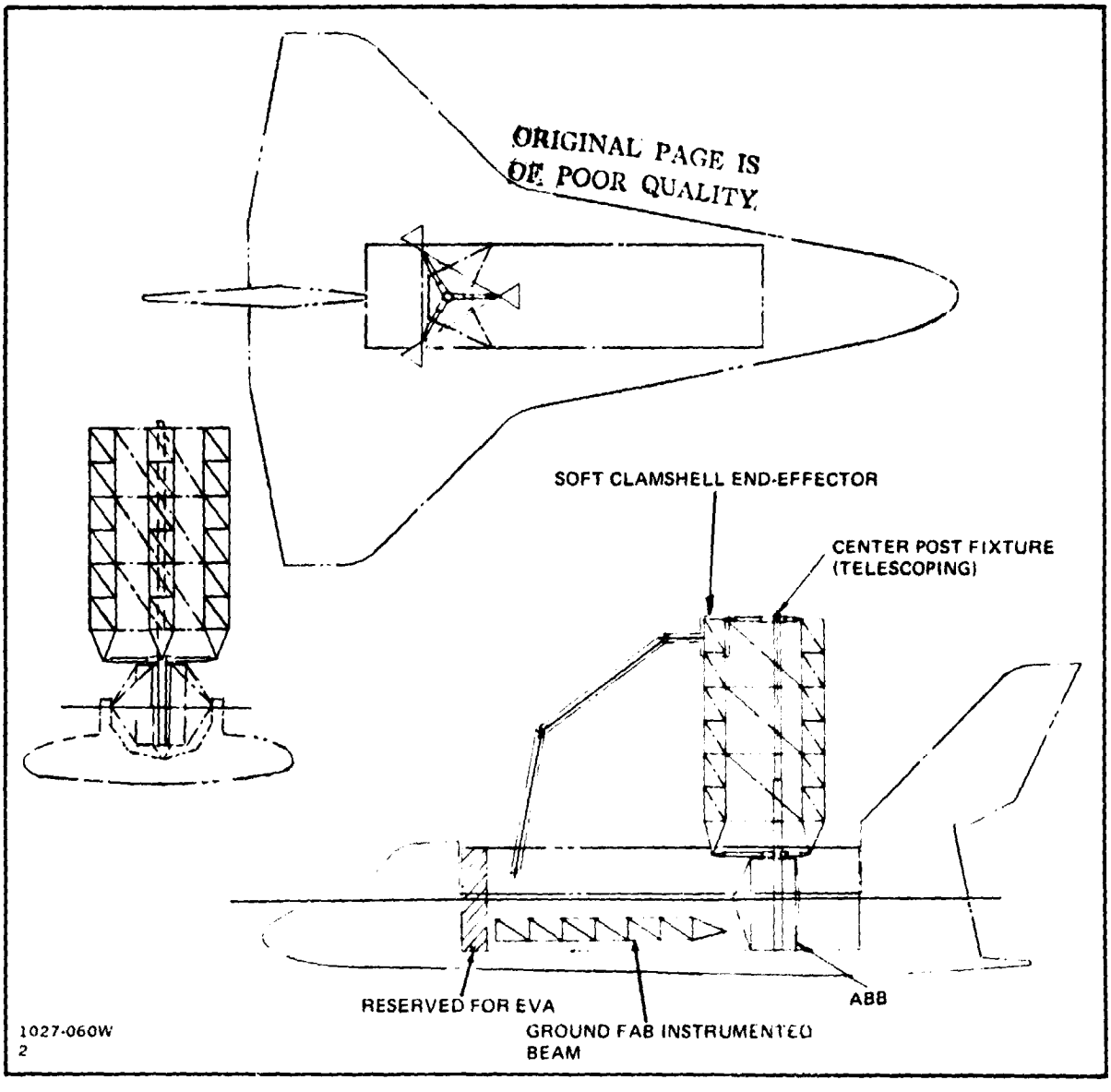

Fig. 5-2 Structural Demonstrator

To assemble this structure, a center fixture consisting of telescoping tubular members, is mounted to the ABB. Three crewmen are involved in the assembly process, two on EVA and one monitoring the activity and operating the RMS, if necessary.

As described in Section 6, the mission objectives relating to ABB test/verification and one-meter beam structural testing have been appropriately modified, as compared to the free-flying LSS option. However, the key timeline activities involving assembly, one-meter beam handling, and related structural testing, are retained. At the conclusion of the mission, the 1-meter beam structure and fixture are disassembled and stowed in the payload bay for the return trip.

A weight summary for the Structural Demonstrator is shown in Fig. 5-3. Launch and landing weights are identical, with an estimated weight of about 8,000 kg. Considerable excess weight capacity is available for other Orbiter payloads. This LSS option, demonstrating limited construction capabilities, therefore, is a potential candidate for a shared-Shuttle flight mission.

5.2 LSS PLATFORM

The free-flyer version of the LSS Platform is illustrated in Fig. 5-4. This platform configuration serves a dual purpose, in that the ability to build a large space structure is demonstrated while providing a useful LEO satellite. Mission objectives intended to be satisfied within a seven day Orbiter flight are:

- Support Development of LSS Technology
  - Automated Beam Builder Operations
  - Validation of analytical techniques
  - On-orbit test approaches
- Evaluate on-orbit techniques applicable to Space Platforms
  - Construction/assembly
  - Astroworker/RMS utilization
  - Limited subsystem/payload integration
  - Orbiter operations (e.g. berthing, servicing)
- Provide a low-cost, useable satellite
  - Minimum subsystem complement/complexity
  - Low-power payloads.

ITEM	WEIGHT, kg LAUNCH & LANDING
BEAM MACHINE	7256
DEMO ARTICLE	190
FIXTURE	546
TEST EQUIPMENT	45
TOTAL	8037 kg (17,713 lb)

CAPABILITY - KSC 28½° SHUTTLE PAYLOAD

200 N MI	29,491 kg - NO OMS KIT	
250 N MI	26,769 kg	ONE OMS KIT
300 N MI	24,500 kg	ONE OMS KIT

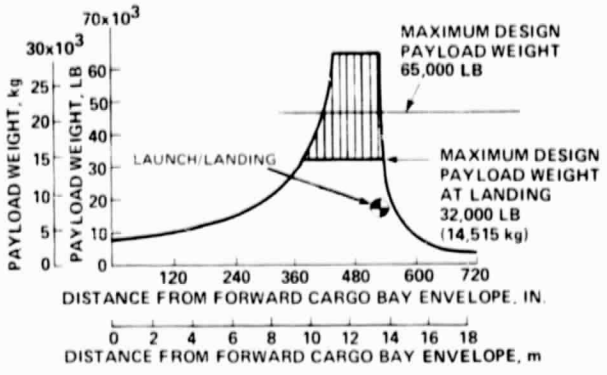

1027-061W
2

Fig. 5-3 Structural Demonstrator Weight Summary; 28½° Inclination, 200 N Mi

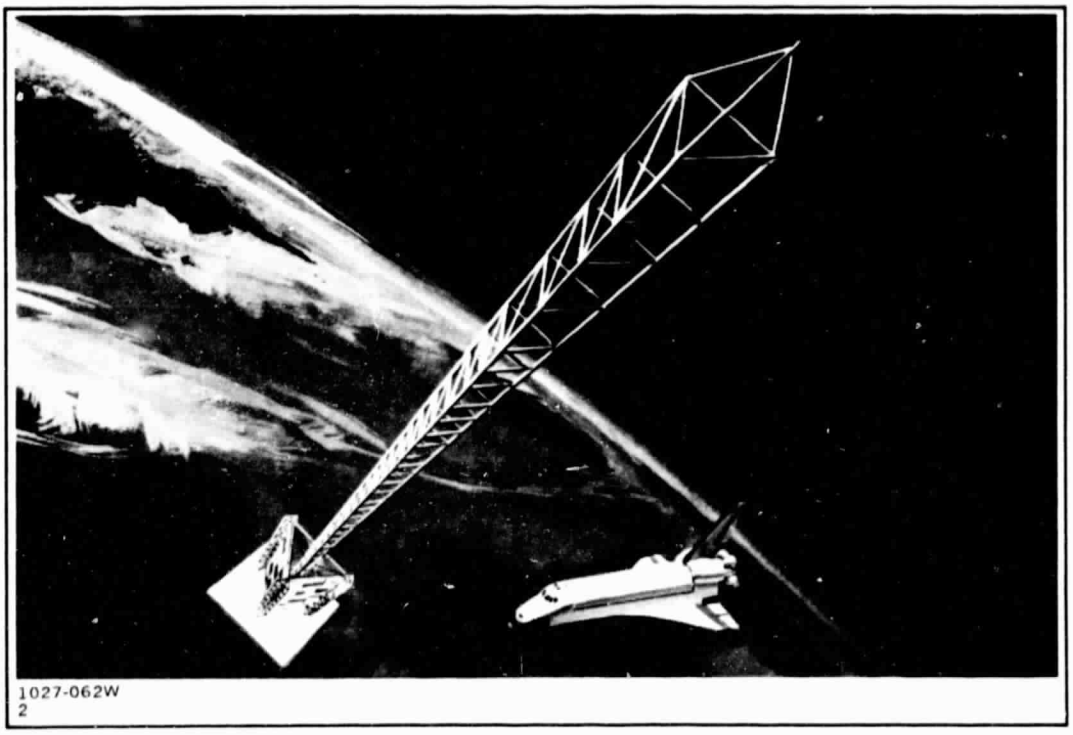

1027-062W
2

Fig. 5-4 LSS Platform Free-Flier

The LSS Platform features gravity-gradient stabilization and a minimal subsystems complement to minimize overall project costs. Low-power payloads (e.g., soil moisture radiometer, LDEF-type experiments) were selected to simplify the power subsystem and enable use of small-area body-mounted solar arrays. The platform structure incorporates the principal large structural elements found in the Power Module/Platforms concepts, the Tribeam "strongback" and a long boom.

5.2.1 Mission Analysis

The desired flight profile for the soil moisture radiometer payload calls for a high inclination orbit with a 3 to 4 day revisit over an assumed test area located in the Great Plains of the U.S., as illustrated in Fig. 5-5. The LDEF-type materials exposure experiments would be serviced per experimenter requirements or during Orbiter reboost intervals assumed to occur about once per year. To provide both a repeating ground track characteristic and a reasonable orbit lifetime, an operating altitude of 500 km and 57° inclination have been selected.

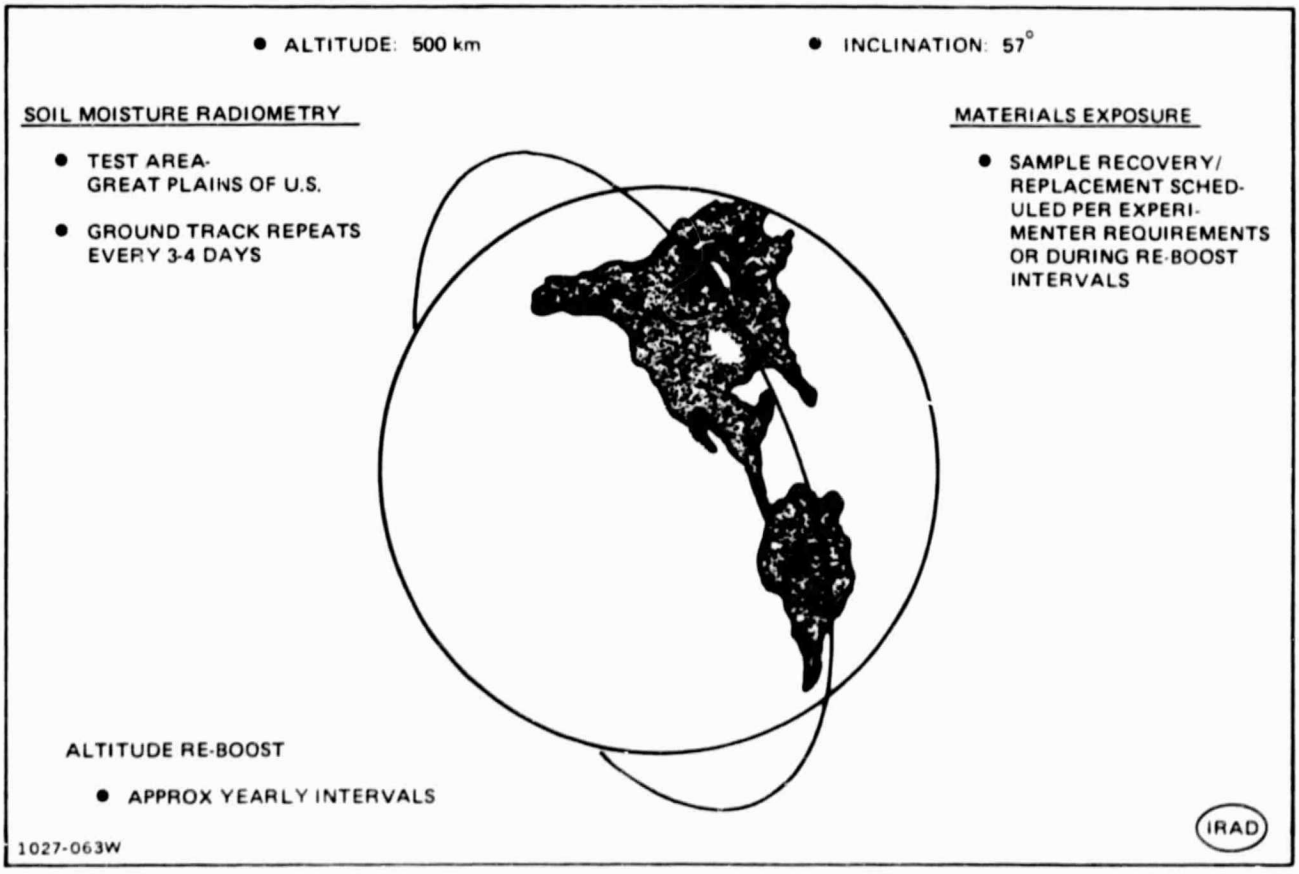

Fig. 5-5 LSS Platform – Operating Profile

2

Parametric data was developed (Appendix B) to identify the orbit altitudes resulting in repeating ground tracks of approximately 3 or 4 day intervals for a range of orbit inclinations. As shown in Fig. 5-6, the data indicates that repeating ground tracks occur within regions of 400 km and 500 km altitudes.

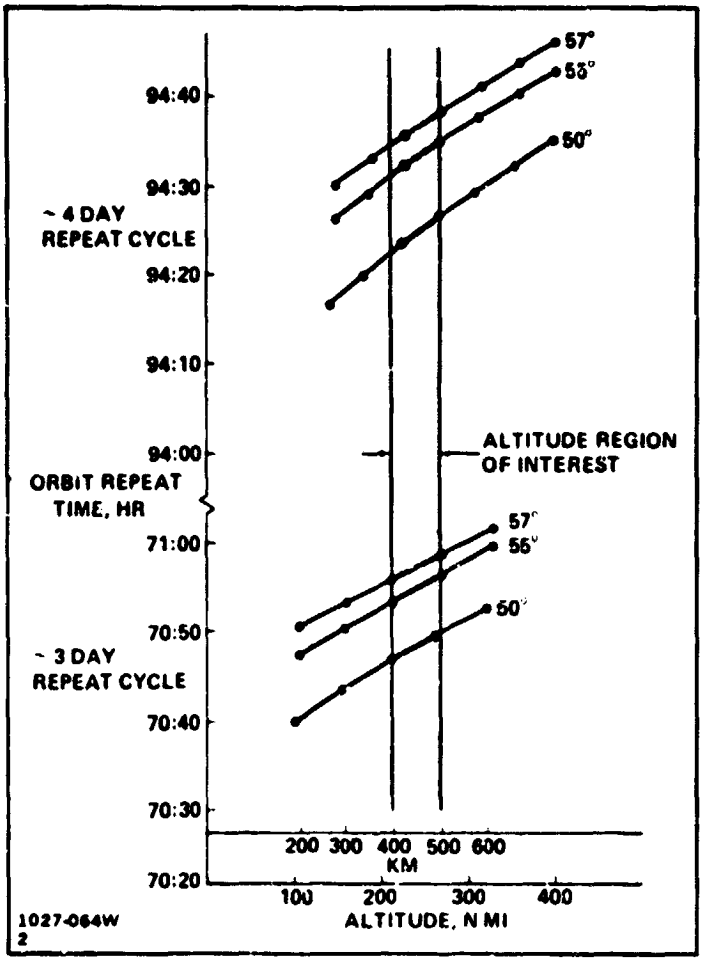

Fig. 5-6 Repeating Ground Tracks

The orbital decay resulting from aerodynamic drag was determined for the LSS Platform using the Jacchia model for aerodynamic density. The configuration frontal area was calculated and the resulting ballistic coefficient (M/C_DA), assuming $C_D = 2$, is then 35.6 kg/m^2. The decay profile is shown in Fig. 5-7 for the average and worst case atmosphere models and the influence of the eleven year solar cycle which peaks in the 1981 to 1982 time-frame. The orbit decay rate would be considerably less in the 1986 time-frame.

2

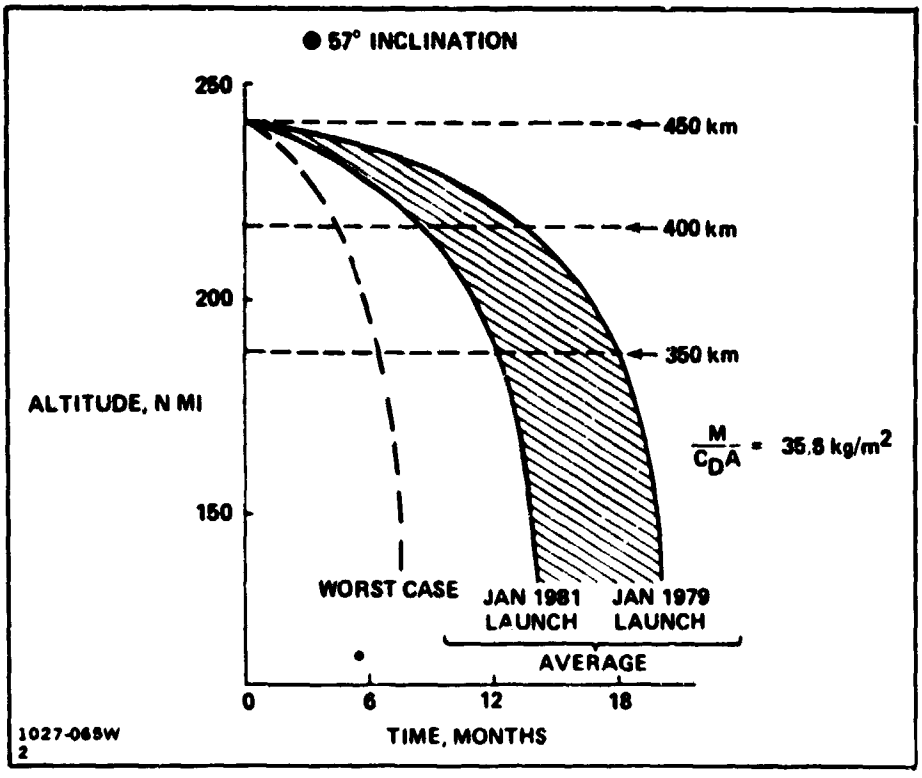

Fig. 5-7 Demonstration Configuration Orbital Decay

An analysis of the demo satellite orbit decay shows that excessive decay rates result from starting altitudes of 400 km or less. Starting altitudes of at least 450 km are desired to assure a 1-year flight duration, without reboost. Since the repeating orbit characteristics occur at specific altitudes/inclinations with 400 or 500 km altitudes acceptable, and orbit decay considerations favor the higher altitude, we have baselined the starting altitude at nominally 57° inclination and 500 km for the LSS demo satellite mission. To attain this desired altitude/inclination, a single Orbiter OMS kit will be required, for which payload bay provisions have been allocated.

5.2.2 Conceptual Design

As shown in Fig. 5-8, the Tribeam portion of the LSS Platform is 4.5 m in depth and 10.5 m in length. The three cap members are 1-meter beams fabricated by the ABB, with the vertical/diagonal members made of ground-fabricated structure. One of the Tribeam's 1-meter beams is a ground-fabricated instrumented test beam utilized for on-orbit thermal/structural testing.

A long gravity-gradient stabilizing boom extends 62 m beyond the Tribeam. During construction of the Tribeam, the long beam serves as the fixture for assembling the complete structure. Figure 5-8 also illustrates the use of a soft Clamshell end-effector for handling 1-m beams and the completed platform.

2

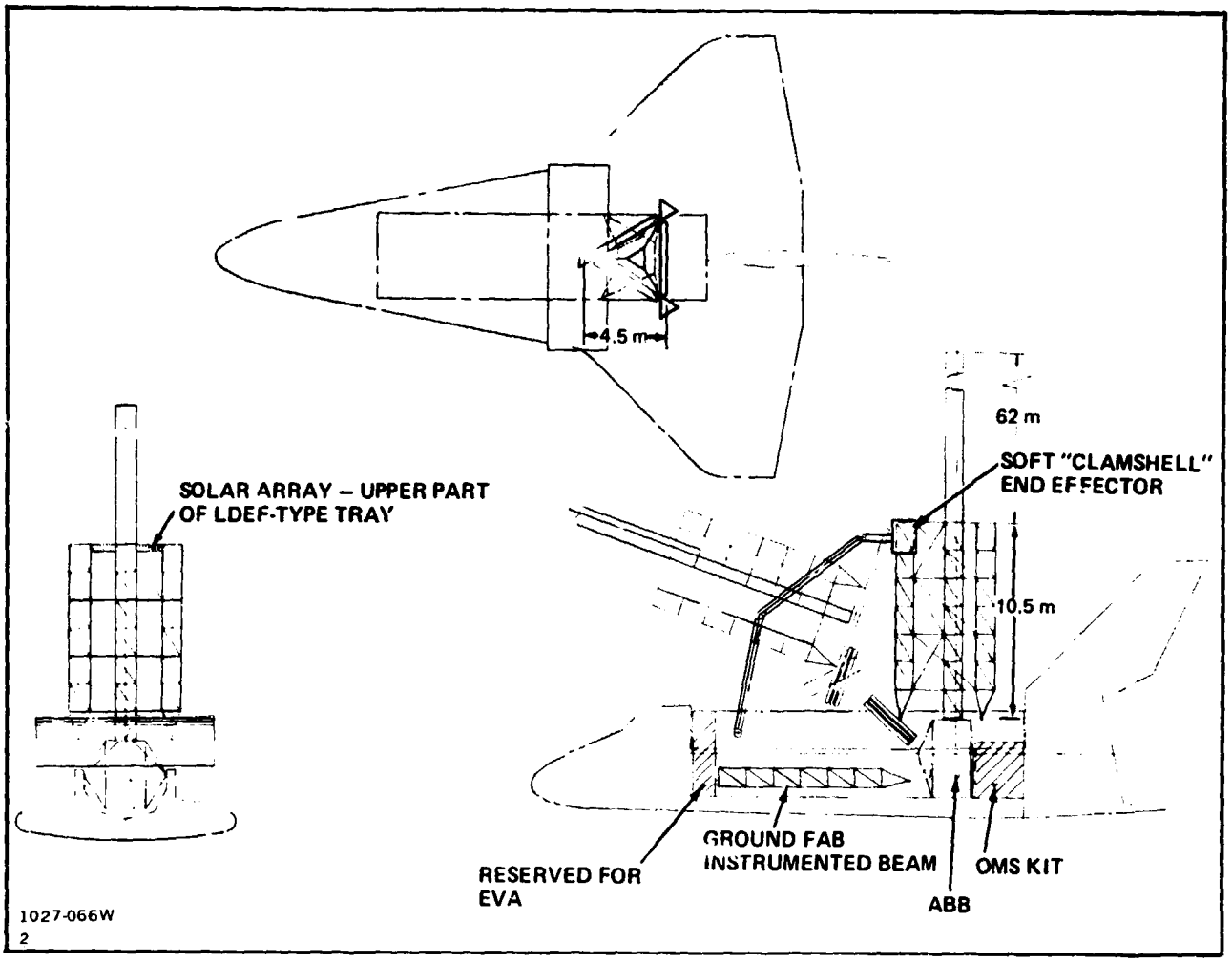

Fig. 5-8 LSS Platform – Structural Arrangement

Construction and handling considerations associated with space-fabricated LSS have surfaced the need for an appropriate RMS end-effector compatible with the "frangible" characteristics of a 1-meter beam. An in-house IRAD effort evaluated alternate end-effector approaches, and has recommended the Clamshell end-effector approach shown in Fig. 5-9. The proposed end-effector is an axial hinged cylinder lined circumferentially with multiple rubber boot elements. The boot assemblies are inflated to a low pressure level (possibly 2 to 5 psi) to capture a segment of the 1-m beam. The "large footprint" of the boot elements engages the 3-cap members of the beam with a low unit area load. The illustration shows RMS motion around the axis of the beam that can be accommodated by a track-carriage/roller assembly driven by a rack-and-pinion drive train. Clamshell open/close and locking cycles would be accomplished by appropriate pneumatic or electromechanical devices.

2

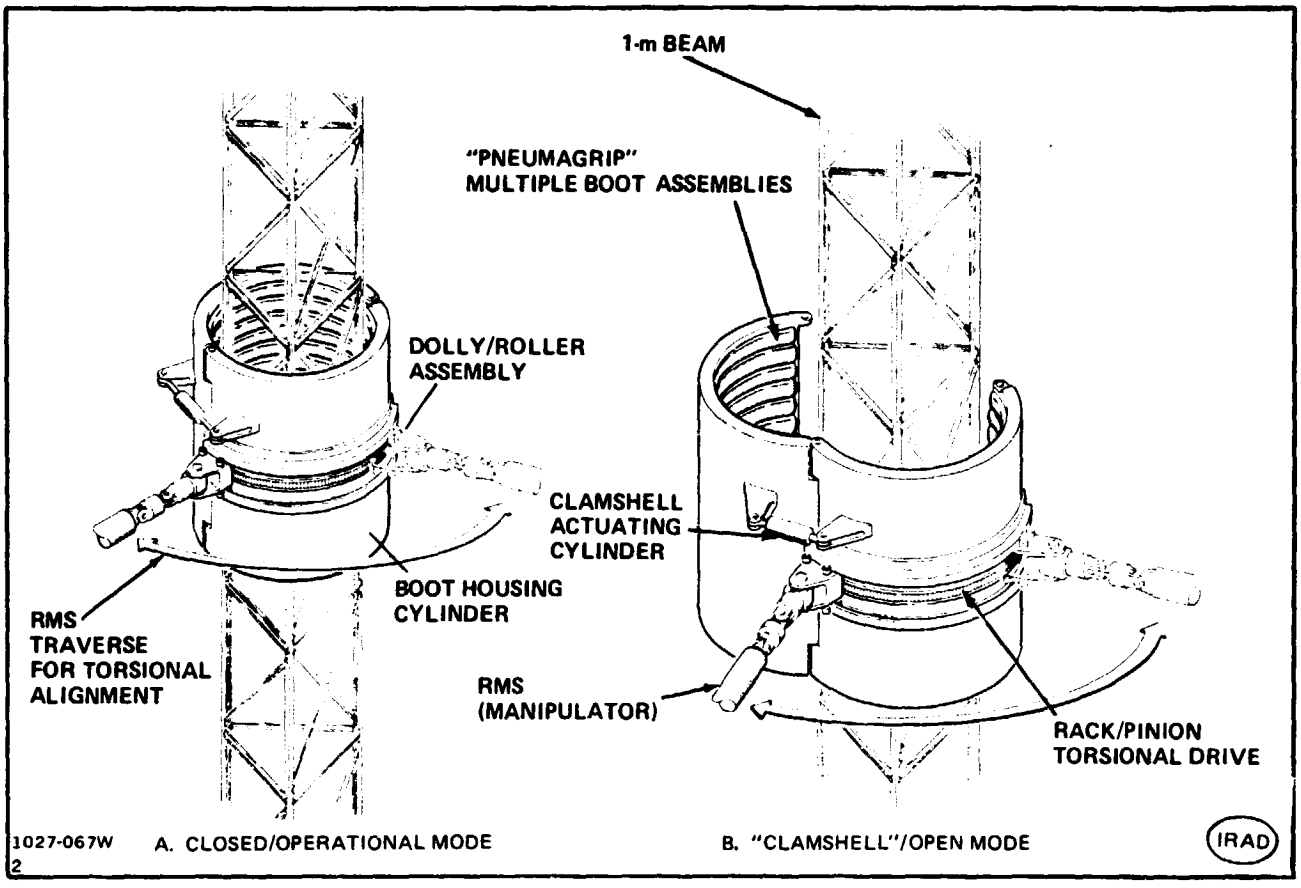

Fig. 5-9 "Clamshell" End Effector

A sequential representation of the platform assembly process is shown in Fig. 5-10. The process begins with construction of two 10.5-m long 1-meter beams, which are then stowed in the payload bay. The next step involves fabrication of the long boom (which serves as the fixture), and installation of the Tribeam verticals connecting the 10.5 meter beams. Following installation of these beams, the ground-fabricated verticals/diagonals are assembled to complete the Tribeam structure.

The equipment racks, supporting the LDEF-type experiments and subsystems, could be installed while the assembly is in vertical position over the ABB, or can be installed after translating the structure into the athwart-ship position. This "table" feature has been incorporated into the mission sequence to permit assembly of the racks to occur in this position and to demonstrate serviceability of the satellite.

Following installation of the radiometer and a final checkout of sensors/subsystems, the satellite would be deployed from the Orbiter, using the Clamshell end-effector/RMS.

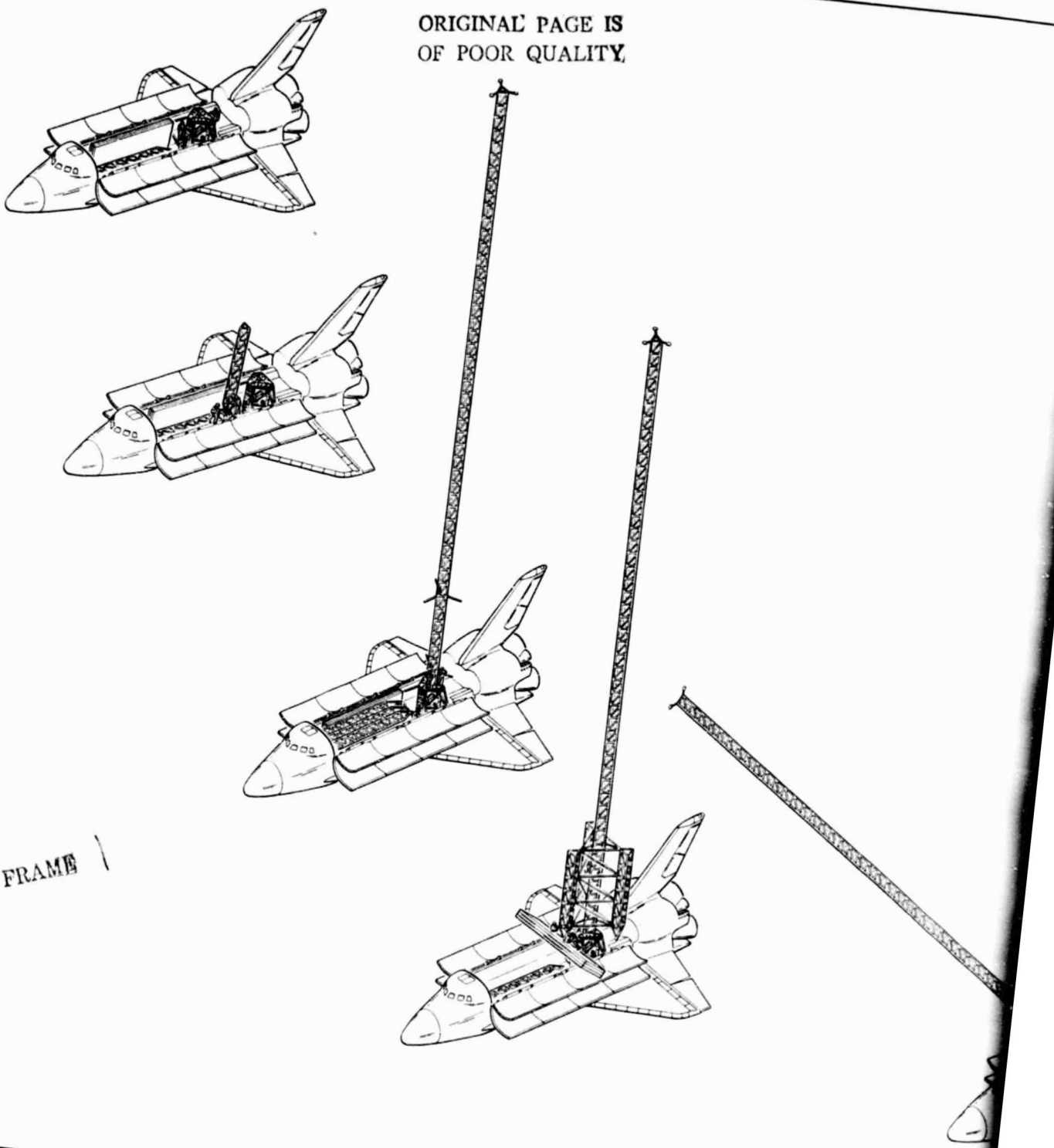

FOLDOUT FRAME 1

FOLDOUT FRAME 2

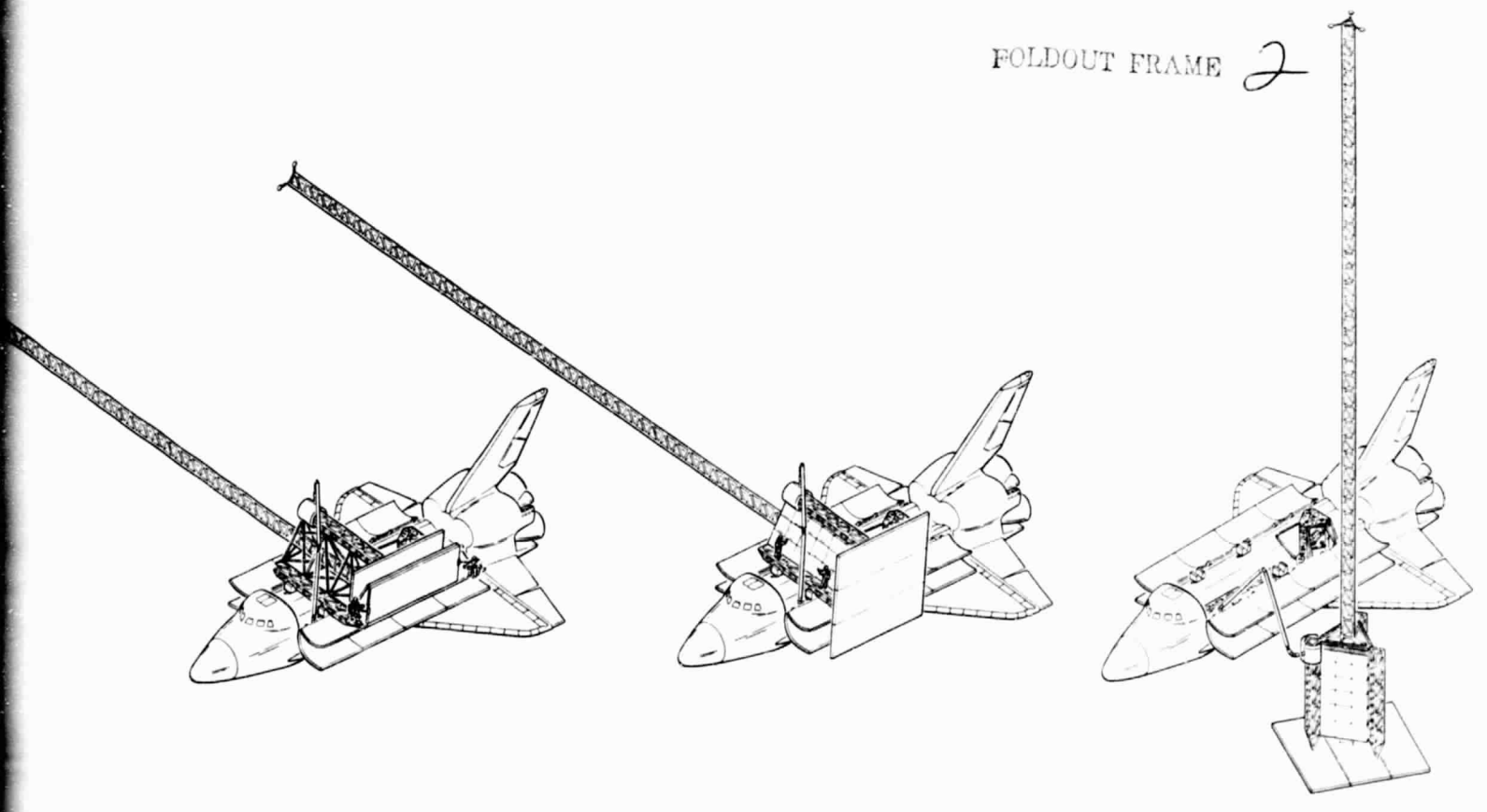

Fig. 5-10 LSS Platform – Assembly Scenario

5.2.3 Preliminary Subsystem Assessment

Preliminary subsystem concepts were generated for the LSS Platform configuration. Inherent guidelines imposed on these efforts have been to minimize subsystem complexity/costs, and to maximize the use of developed space hardware, wherever possible.

5.2.3.1 Attitude Control - The free-flying LSS configuration was analyzed to determine the feasibility of passive gravity-gradient stabilization and an optimum boom length for attitude control. The spacecraft is an earth-oriented free-flyer carrying materials exposure experiments requiring only a mechanical interface with the spacecraft structure and very coarse attitude stabilization. The microwave radiometer requires 15 min of operation every three days with reasonably tight control during these periods.

The steady-state experiment performance requirements are presented in Fig. 5-11. The materials exposure requirements are based on those used for the Long Duration Exposure Facility (LDEF) mission, while the microwave radiometer requirements are based on discussions with NASA/GSFC personnel.

	ROLL, DEG	PITCH, DEG	YAW, DEG
EXPOSURE EXPERIMENTS	± 10	± 10	± 30
MICROWAVE RADIOMETER	± 0.5	± 0.5	± 1.5

1027-069W
2

Fig. 5-11 Steady-State Attitude Pointing Requirements

The overall goal is to provide completely passive control using gravity-gradient techniques to satisfy the above requirements. Gravity-gradient stabilization requires a proper inertia configuration for three-axis passive control; the largest moment of inertia on the pitch axis, the smallest on the yaw axis, and the intermediate on the roll axis. Gravity-gradient torques then provide pitch and roll stabilization with dynamic torques providing yaw axis stabilization.

Configuration Characteristics - The nominal flight attitude selected is with the microwave radiometer facing the earth and one cap member of the Tribeam in the direction of flight as illustrated in Fig. 5-12. The coordinate axes are a conventional orbital coordinate system with X in the velocity direction, Y normal to the orbit plane, and Z along the local vertical towards the earth.

2

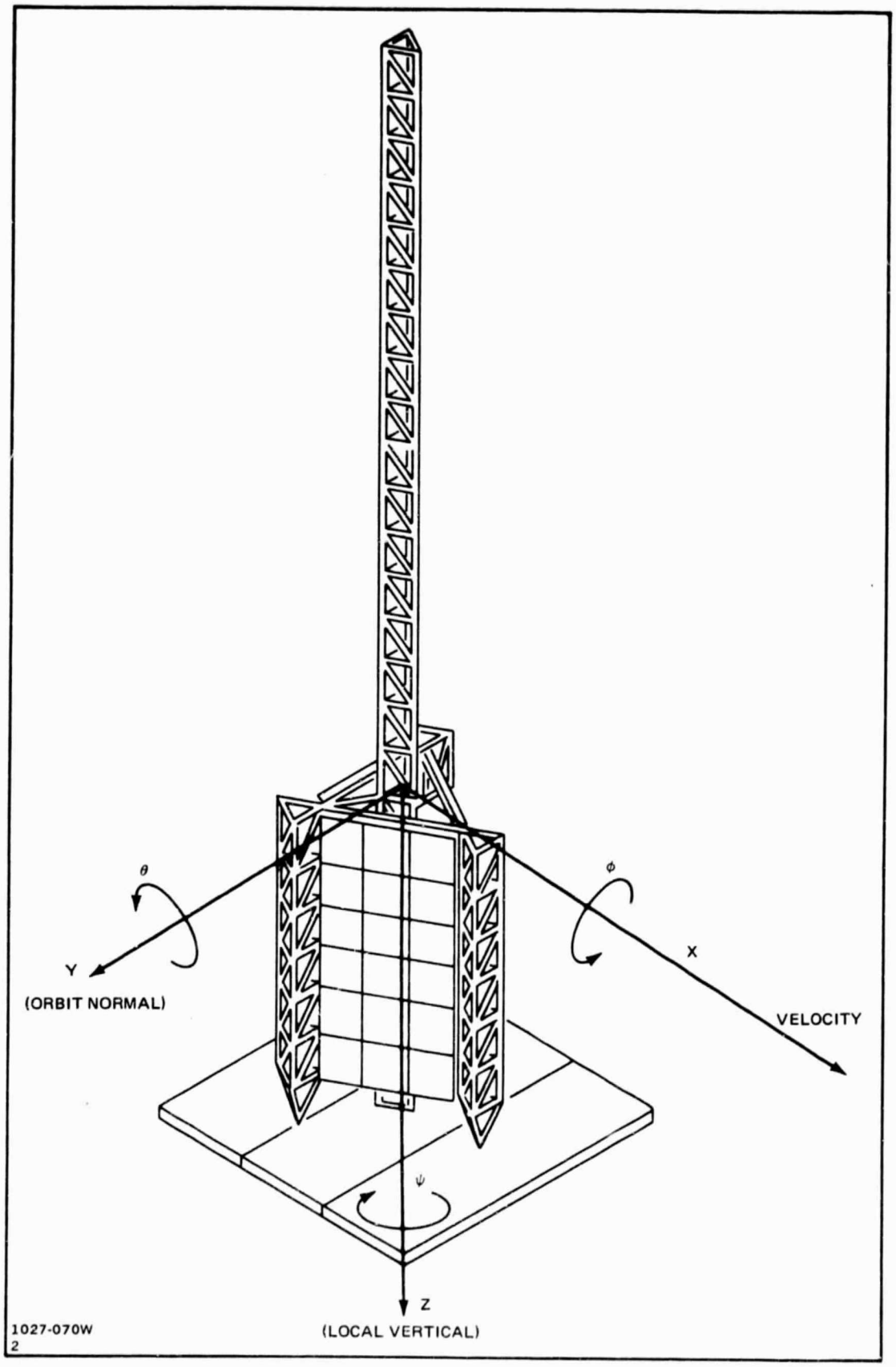

Fig. 5-12 Coordinate System

The variation of the satellite's moments of inertia is presented in Fig. 5-13 as a function of the length of the one-meter beam boom, with and without a tip mass. Although plotted as being equal, the Y-axis inertia is actually slightly larger than the X-axis inertia, which is the condition necessary for three-axis control. The Z-axis moment of inertia is 23,511 kgm^2 for all values of boom length and tip mass.

The variation in the ratio of transverse (Ixx or Iyy) to longitudinal inertia (Izz) as a function of boom length with and without a tip mass is presented in Fig. 5-14. These values were compared with existing gravity-gradient stabilized designs since this parameter is a good measure of the stability of the configuration, higher ratios being better. The ratio for LDEF varies from about 2.8 and 3.3 depending on the particular spacecraft configuration. On the other hand, other sources indicate ratios of from 40 to 100 are preferred for good gravity-gradient stabilization.

Gravity-Gradient Stabilization - Present gravity-gradient stabilization experience indicates that the pointing accuracy which may be expected with passive gravity-gradient techniques is on the order of a couple of degrees for pitch and roll with a higher value for yaw. The pronounced effect of aerodynamic disturbance torques in low orbits makes the prediction of performance with passive control more difficult. Most experience with gravity-gradient stabilization has been at altitudes above 900 km where the aerodynamic drag disturbance torque has been an insignificant effect. LDEF is an exception, aerodynamic drag being the dominant effect with extreme care required to keep the center of pressure within two inches of the center mass.

The subsequent analysis for the LSS demonstration configuration has concentrated on minimizing the attitude excursion in pitch from the combination of aerodynamic drag torque and the gravity-gradient torque. The steady-state attitude angle and stability are primarily addressed; the acquisition and initial settling performance from Orbiter RMS deployment are considered briefly.

It would appear that the microwave radiometer' s pointing requirements cannot be met with passive gravity-gradient stabilization but this approach is suitable for the exposure experiments' requirements. However, long term stabilization via gravity-gradient with active stabilization periodically for the radiometer during overflights over the target area, appears to be an acceptable design approach.

Attitude Control Analysis - Attitude control performance was investigated for the zero tip mass case by modelling the aerodynamic disturbance torque and the gravity-gradient restoring torque as a function of boom length.

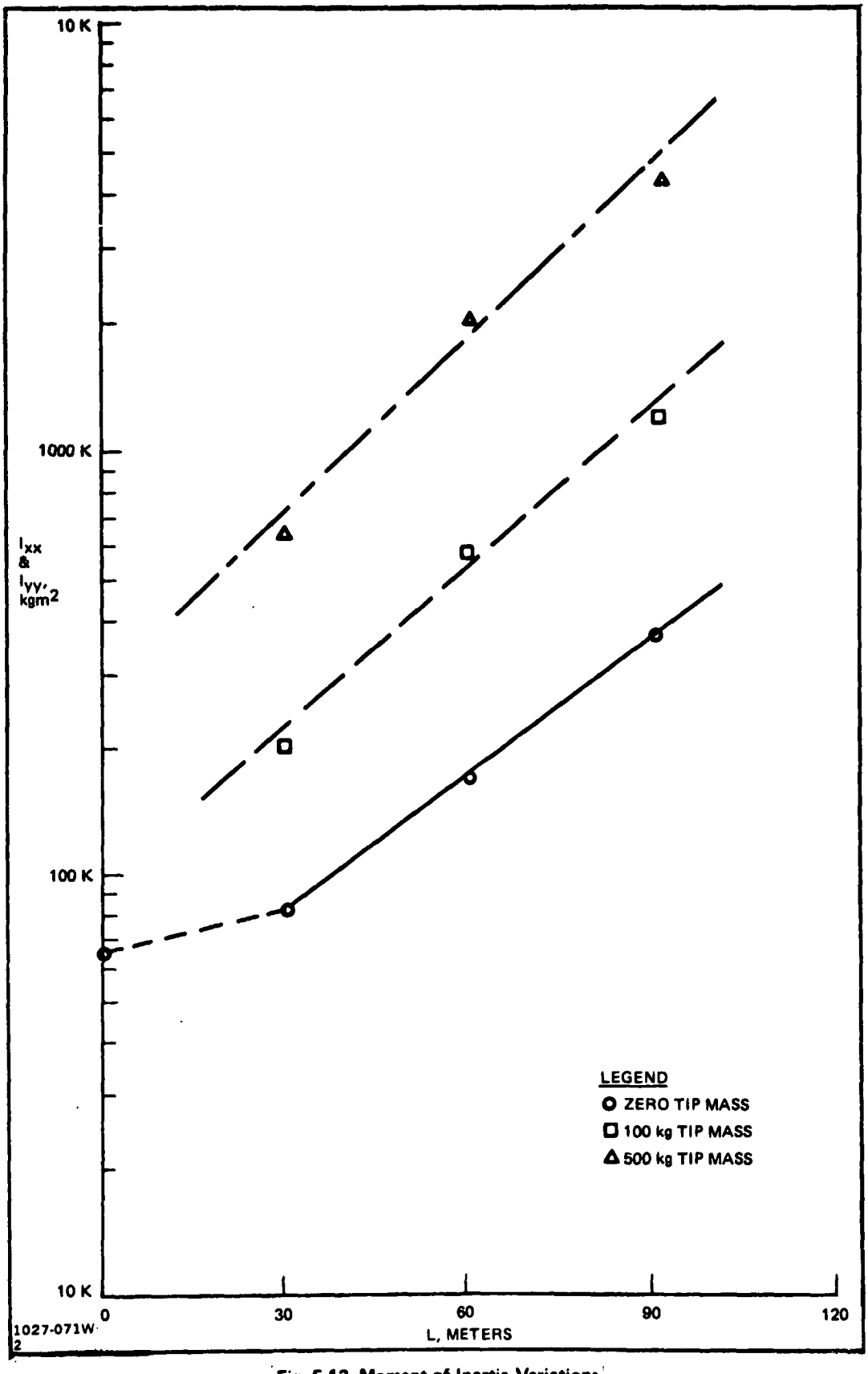

Fig. 5-13 Moment of Inertia Variations

BOOM LENGTH, m	TIP MASS, kgm		
	0	100	500
0	2.8	N/A	N/A
30	3.4	8.7	27.5
60	7.2	24.9	89.3
90	16.6	53.5	189.7

1027-072W
2

Fig. 5-14 Inertia Ratios

The nominal frontal area of the configuration is shown in Fig. 5-15. The Tribeam portion (A_2) is assumed to be a constant area of $10.5 \times 5.2 = 54.6\ m^2$. The boom area ($A_1$) is the projected area of a one-meter beam per unit length times the boom length. The projected area per 1.5 m bay varies from $0.347\ m^2$ to $0.723\ m^2$ depending on the yaw alignment angle and the degree of exposure of hidden elements. An average value of $0.535\ m^2$ was selected resulting in an area of $0.357L\ m^2$ where L is the length of the boom in meters.

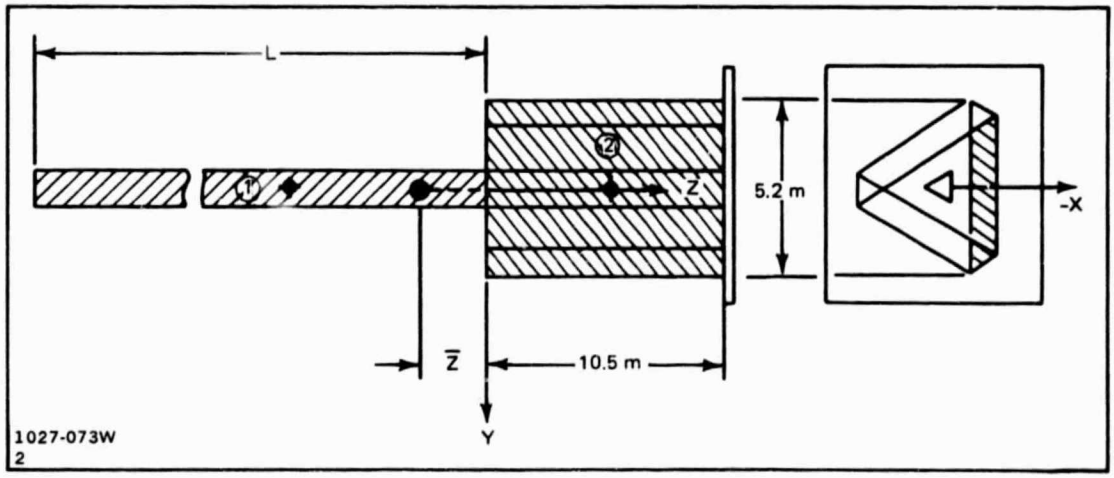

Fig. 5-15 Configuration Dimensions

The net aerodynamic torque acting about the y-axis is then:

$$(T\ aero)_Y = (F\ aero)_1\ (L/2 + Z) - (F\ aero)_2\ (5.25 - Z) \qquad (5\text{-}1)$$

where $(F\ aero)_1$ is the aero force on the boom, $(F\ aero)_2$ is the force on the Tribeam and Z is the center of mass.

The forces are a function of the areas, drag coefficient and the dynamic pressure (q) which varies the altitude. Two altitudes are considered: 400 km (216 n mi), which was the initial design altitude and 450 km (242 n mi) selected based on orbital decay considerations. The corresponding values for q are $q_{400} = 1.15 \times 10^{-4}\ N/m^2$ and $q_{450} = 5.17 \times 10^{-5}\ N/m^2$.

The following equation was developed for the variation of the center of mass location in meters as a function of boom length based on the mass properties analysis:

$$\bar{Z} = -4.76 - (0.00149)L - (0.000106)\,L^2 \qquad (5\text{-}2)$$

Substituting the force and cg expression into Eq. 5-1 results in the following expressions for the aerodynamic disturbance torques in terms of beam length for each attitude.

400 km

$$(T\ \text{aero})_y = -(8.32 \times 10^{-2}) - (2.71 \times 10^{-4})\,L + (2.62 \times 10^{-5})\,L^2 - (5.76 \times 10^{-9})\,L^3 \qquad (5\text{-}3)$$

450 km

$$(T\ \text{aero})_y = -(5.65 \times 10^{-2}) - (1.84 \times 10^{-4})\,L + (1.78 \times 10^{-5})\,L^2 - (3.91 \times 10^{-9})\,L^3 \qquad (5\text{-}4)$$

The variation of frontal area of the one-meter beam results in approximately a ± 35% variation in the coefficients of the L, L^2 and L^3 terms.

Gravity-Gradient Control - The linearized equations of motion for the system including gravity-gradient terms take the form:

$$\left.\begin{aligned} I_x\,\ddot{\phi} + 4\omega_0^2\,(I_y - I_z)\,\phi + W_o\,(I_y - I_x - I_z)\,\dot{\psi} &= T_{dx} \\ I_y\,\ddot{\theta} + 3\omega_o^2\,(I_x - I_z)\,\theta &= T_{dy} \\ I_z\,\ddot{\psi} + \omega_o^2\,(I_y - I_x)\,\psi - W_o\,(I_y - I_x - I_Z)\,\dot{\phi} &= T_{dz} \end{aligned}\right\} \qquad (5\text{-}5)$$

where W_o is the orbital rate and T_{dx}, T_{dy}, and T_{dz} are disturbance torques. Clearly the roll/yaw dynamics are coupled and pitch is uncoupled.

The moments of inertia in kg-m^2 as a function of boom length were approximated from the mass properties as follows:

$$\left.\begin{aligned} I_x &= 65{,}000 + L^{2.82} \\ I_y &= 65{,}300 + L^{2.82} \\ I_z &= 23{,}500 \end{aligned}\right\} \qquad (5\text{-}6)$$

Pitch Performance - The steady-state pitch attitude is the ratio of Td_y and the gravity-gradient term $3\omega_o^2\,(I_x - I_z)$. Using the aerodynamic disturbance as the dominant disturbance torque and substituting the inertia terms (Eq 5-6) results in the following expressions for steady-state pitch attitude (θ_{ss}) in radians as a function of boom length.

2

400 km

$$\theta_{ss} = - \frac{(8.32 \times 10^{-2}) - (2.71 \times 10^{-4})\, L + (2.62 \times 10^{-5})\, L^2 - (5.76 \times 10^{-9})\, L^3}{(.159) + (3.83 \times 10^{-6})\, L^{2.82}} \quad (5\text{-}7)$$

450 km

$$\theta_{ss} = - \frac{(5.65 \times 10^{-2}) - (1.84 \times 10^{-4})\, L + (1.78 \times 10^{-5})\, L^2 - (3.91 \times 10^{-9})\, L^3}{(.159) + (3.83 \times 10^{-6})\, L^{2.82}} \quad (5\text{-}8)$$

Equations 5-7 and 5-8 are plotted in Fig. 5-16 indicating an optimum length of 61.7 m for minimum pitch error in both cases. The effect of the variation of boom frontal area is shown in Fig. 5-17 for the 400 km altitude case indicating a ± 2½° spread about the "optimum" length from yaw attitude excursions.

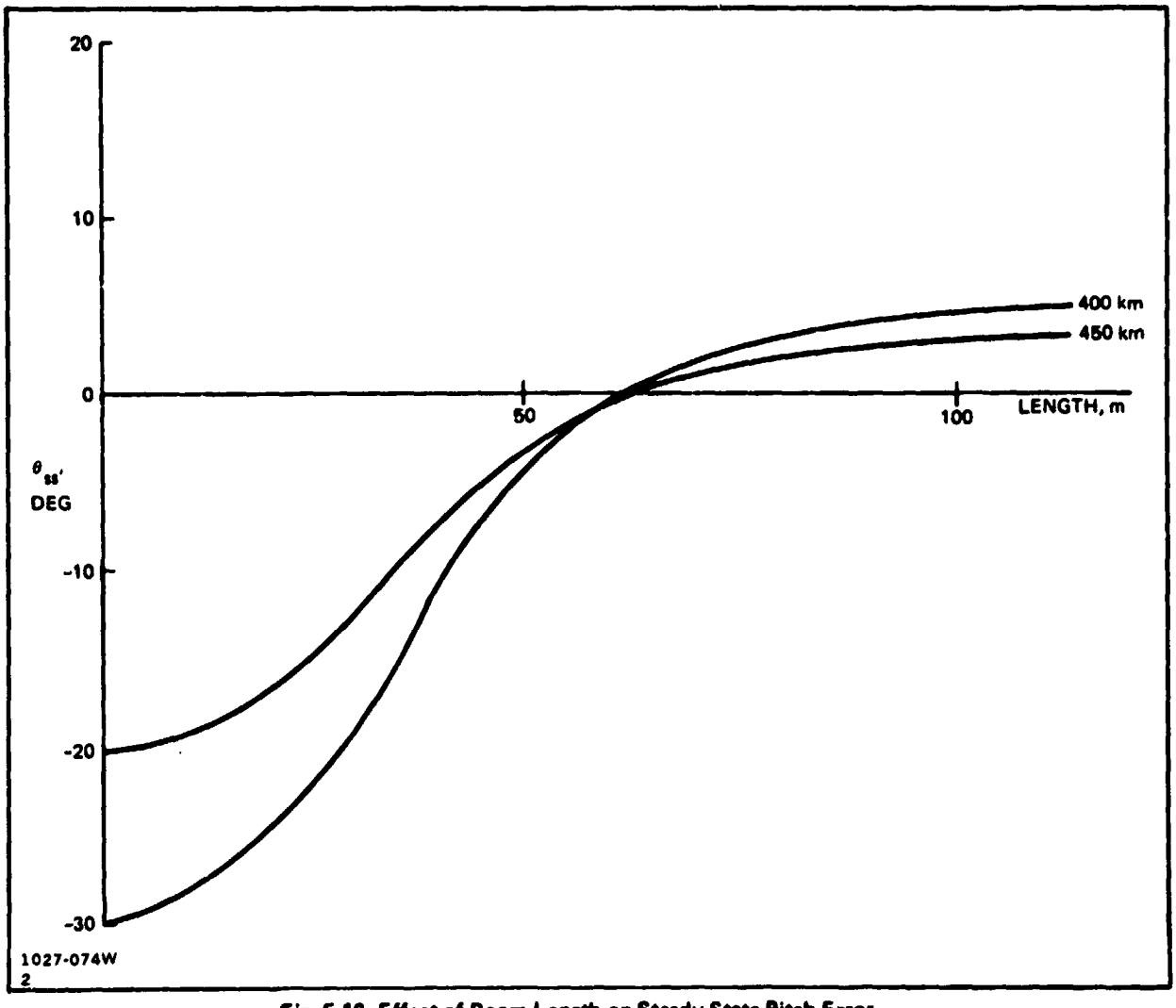

Fig. 5-16 Effect of Boom Length on Steady-State Pitch Error

2

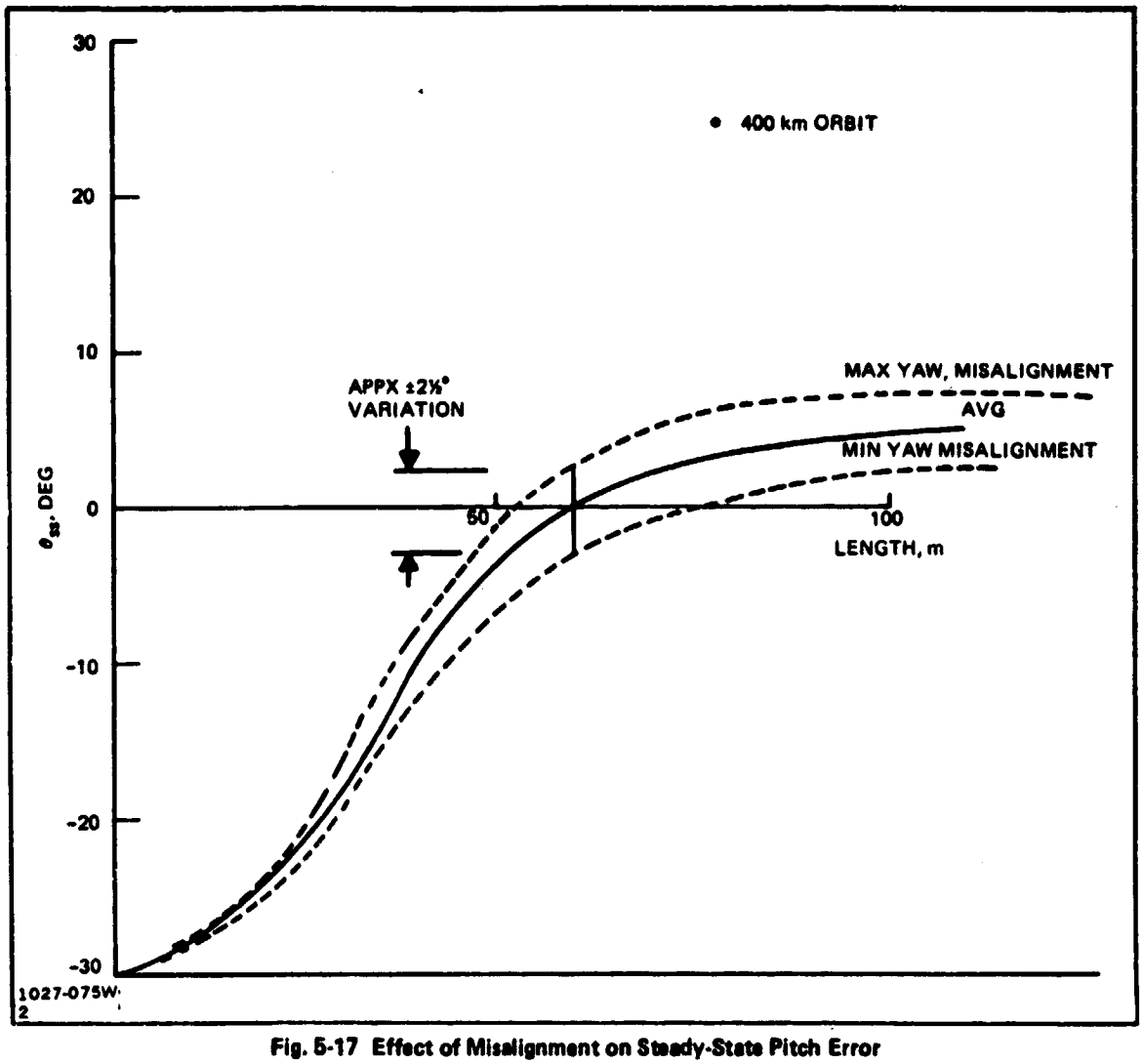

Fig. 5-17 Effect of Misalignment on Steady-State Pitch Error

An estimate of "capture time" for the 400 km case was obtained by adding a damping term (B) to the pitch equation such as would be provided by an LDEF-type passive viscous damper resulting in an equation of the form:

$$I_y \ddot{\theta} + B\dot{\theta} + K_{gg}\,\theta = 0 \qquad (5\text{-}9)$$

where

$$K_{gg} = 0.587\ \frac{N \cdot m}{rad}$$

and

$$I_y = 177{,}140\ kg\text{-}m^2$$

$$(L = 61.7\ m)$$

The natural frequency (ω_n), damping coefficient (ξ) and time constant (τ) are then:

$$\left.\begin{aligned} \omega_n &= \sqrt{\frac{Kgg}{I_y}} = 1.82 \times 10^{-3} \text{ rps} \\ \xi &= \frac{B}{2 I_y \omega_n} = 1.55 \times 10^{-3} B \\ \tau &= \frac{1}{\omega_n} = \frac{3.54 \times 10^5}{B} \end{aligned}\right\} \quad (5\text{-}10)$$

Choosing a realistic value 13.56 N·m/rps for B results in

$$\xi = 0.02$$

and

$$\tau = 4.7 \text{ orbits}$$

This compares to a calculated pitch axis time constant of 3.3 orbits for LDEF which resulted in a 21 orbit time constant based on a three-axis simulation. Applying the same increase factor to the above 4.7 orbits results in a pitch time constant of 30 orbits which may be used as an approximation to estimate capture time for a given initial attitude condition and rates up to 0.1 deg/sec. For example, an initial pitch angle of 20° will be reduced to 5° in 42 orbits.

Roll/Yaw Performance - The unforced roll/yaw equations with an equal damping term (B) added are as follows for the 400 km orbit:

$$\left.\begin{aligned} (1.768 \times 10^5)\,\ddot{\Phi} + B\,\dot{\Phi} = (0.785)\,\Phi - (26.2)\,\dot{\psi} &= 0 \\ (2.35 \times 10^4)\,\ddot{\psi} + B\dot{\psi} + (3.83 \times 10^{-4})\,\psi + (26.2)\,\dot{\Phi} &= 0 \end{aligned}\right\} \quad (5\text{-}11)$$

The resulting characteristic equation of this system is:

$$(4.155 \times 10^9)\,S^4 + (2.0 \times 10^5 B)\,S^3 + (B^2 + 1.92 \times 10^4)\,S^2 + (0.785B)\,S + (3.01 \times 10^{-4}) \quad (5\text{-}12)$$

Neglecting the constant term, the natural frequency (ω_n) is 2.15×10^{-3} rps and with B = 0 the system has a double pole at the origin and a pair of roots on the imaginary axis. Choosing B to provide a damping coefficient of 0.1 results in a realistic value of 8.95 n mi/rps with a roll/yaw time constant of 77.5 min or 0.83 orbits. Again applying an "increase factor" based on LDEF data, the time constant becomes 5.3 orbits indicating shorter capture times than in pitch.

Attitude Control Observations/Recommendations

Passive gravity gradient stabilization of the LSS demonstration satellite is readily capable of meeting the pointing requirements of the materials exposure experiments. An optimum boom length of 61.7 m has been identified for the case with zero tip mass in order to balance the aerodynamic drag and gravity gradient torques. The expected pitch and roll control capability is ± 2.5 deg; yaw axis performance has not been determined but should be well below the ± 30 deg requirement.

A periodically-active stabilization capability appears necessary to meet the pointing requirements of the microwave radiometer during its infrequent periods of operations. Future efforts should include an investigation of the attitude accuracy obtainable with inertia ratios significantly greater than current spacecraft designs which are obtainable by longer boom lengths and the addition of a tip mass.

In order to predict pointing capability more precisely a three-axis simulation is required with additional disturbance sources included. This analysis should include the effect of orbit decay from the selected 500 km to 450 km during the course of the mission.

A tradeoff should be made between active control of the whole spacecraft versus active steering of the radiometer alone. Techniques for "trimming" the configuration parameters in orbit prior to full release from the Orbiter to improve the attitude control performance should also be considered in subsequent analysis; this is a capability available with space fabrication that has not been fully exploited. In the same category is the Orbiter's potential for minimizing the inital attitude angles and rates relative to the orbital axes during deployment, thus reducing capture time. Orbiter plume effects on large space structures should be investigated including potential contamination mechanisms, techniques for clean approach to and departure from an operational platform system, effects of Orbiter-attached attitude and translation maneuvers, and identification of plume-insensitive conceptual approaches.

5.2.3.2 Power Supply

Requirements - The baseline power profile for the Electrical Power System (EPS) is shown in Fig. 5-18. Data acquisition and transmit periods occur for a total of twenty minutes every three days. The 17 watt average standby load includes short housekeeping data record/transmit periods dispersed throughout the mission.

2

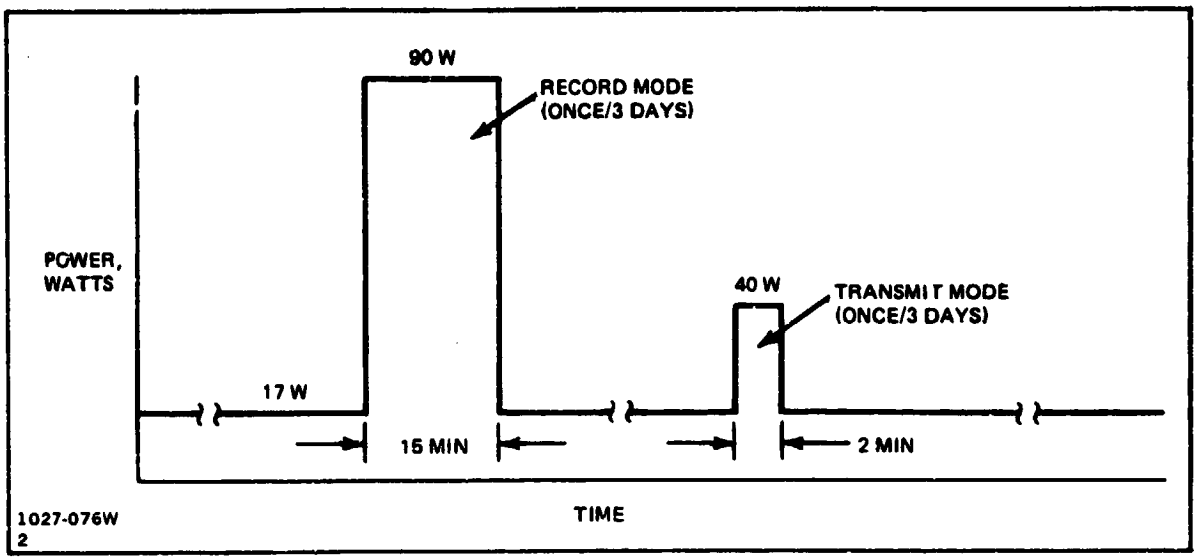

Fig. 5-18 EPS Power Requirements

System operating life is assumed to be one year minimum, with a goal of five years. Total energy requirements resulting from the EPS power profile, including distribution losses, are:

- 1.3 kWh for three days
- 160 kWh for one year
- 800 kWh for five years

EPS Options - Several EPS options were considered, including:

- Batteries - Silver Zinc (AgZn), Nickel Zinc (NiZn) and Nickel Cadmium (NiCd)
- Radioisotope Thermoelectric Generators (RTG) - with and without peaking batteries
- Solar Array/Battery Systems

Characteristics of the various power sources, sized to satisfy the above requirements, are listed in Fig. 5-19. Where possible, these represent state-of-the-art hardware which is space-qualified. Cost comparisons of the respective EPS options are shown in Fig. 5-20. Clearly. the photovoltaic (PV)/Battery option is the preferred approach.

A brief discussion of each of the EPS options considered follows.

2

POWER SOURCE	SIZE, EA	NO. REQD PER S/C	NO. REQD IN 5 YRS	MASS, PER S/C, kg	VOL. PER S/C, m^3	NOTES
BATTERIES						
• AgZn	17.5 kWh	6	60	433	0.136	6 MO LIFE- NEED 2 SETS/YR
• NiZn	10.2 kWh	63/4 YRS 26/5th YR	152	9883/4 YRS 4079/5th YR	5.3/4 YRS 2.2/5th YR	2-3 YR LIFE-NEED 2 RESUPPLIES/5 YRS
• NiCd	1.6 kWh	128	640	6966	4.40	10 YR LIFE- NEED 1 SETUP
RTG(1)						
• NO BATTERIES	90 W	1	1	20	0.050	10 YR RTG LIFE- 20% DEGRADATION/ 5 YRS
• WITH BATTERIES	17 W	1	1	8	0.020	
– NiZn	10.2 kWh	1	2	157	0.084	2-3 YR LIFE- NEED 2 SETS/5 YRS
– NiCd	1.6 kWh	11	11	599	0.380	10 YR LIFE- NEED 1 SET/5 YRS
PV/BATTERY						
• SOLAR ARRAY	20 FT^2	4 PANELS	4 PANELS	10	–	4 SOLAR PANELS– EA ~ 5 FT^2
• NiCd BATTERY	6 a h	2	2	19	0.015	DUAL-REDUNDANT BATTERIES
• PWR ELECTRONICS	50 W-1 kW	1	1	25	0.100	BATTERY CHARGERS & POWER CONTROL UNIT
• TOTAL SYSTEM				54		

(1) BASED ON SNAP 19 TECHNOLOGY

1027-077W
2

Fig. 5-19 EPS Options

OPTION	UNIT COST, $K	COST PER S/C, $K	RESUPPLY HDWRE	COST, $K TRANS	TOTAL SYR COST, $M
• BATTERIES					
– AgZn	20	120	1080	3897	5.097
– NiZn	6	378/4 yrs 156/5th yr	534	13962	14.874
– NiCd	45	5760	23040	27864	56.664
• RTG(1)					
– 90 WATT UNIT	250	1218/411(2)	–	–	1.218/0.411
– 17 WATT UNIT WITH:	100	528/171(2)	–	–	
NiZn	6	6	6	157	0.697/0.340(3)
NiCd	45	495	–	–	1.023/0.666(3)
• PV/BATTERY					
– SOLAR ARRAY	120	120	–	–	0.120
– NiCd BATTERY	25	50	–	–	0.050
– PWR ELECTRONICS	80	80	–	–	0.060
TOTAL SYSTEM		250	–	–	0.250

(1) BASED ON SNAP 19 TECHNOLOGY – ENGRG DEV, SAFETY, ETC; COSTS NOT INCLUDED.
(2) RTG CONVERTER COST INCLUDING 238 P UEL AT $600/$100/THERMAL WATT.
(3) TOTAL RTG SYSTEM COST INCLUDING C ERTER AND BATTERIES.

1027-078W
2

Fig. 5-20 Cost Comparisons – EPS Options

2

Batteries - Batteries, operating as primaries, are the simplest conceivable power source for this application. However, operating life and mass limitations make these the most expensive option.

The largest practical battery size was considered in each case. Sized for a normal 28 vdc system, these are:

- AgZn - 700 AH, 16 cells
- NiZn - 400 AH, 16 cells
- NiCd - 60 AH, 22 cells

Sizing of each battery group also accounts for self-discharge over long service intervals. Charge retention estimates for the three battery types are shown in Fig. 5-21. These characteristics are heavily temperature-dependent, and it is essential that battery temperatures be kept low to provide the service life assume in Fig. 5-19.

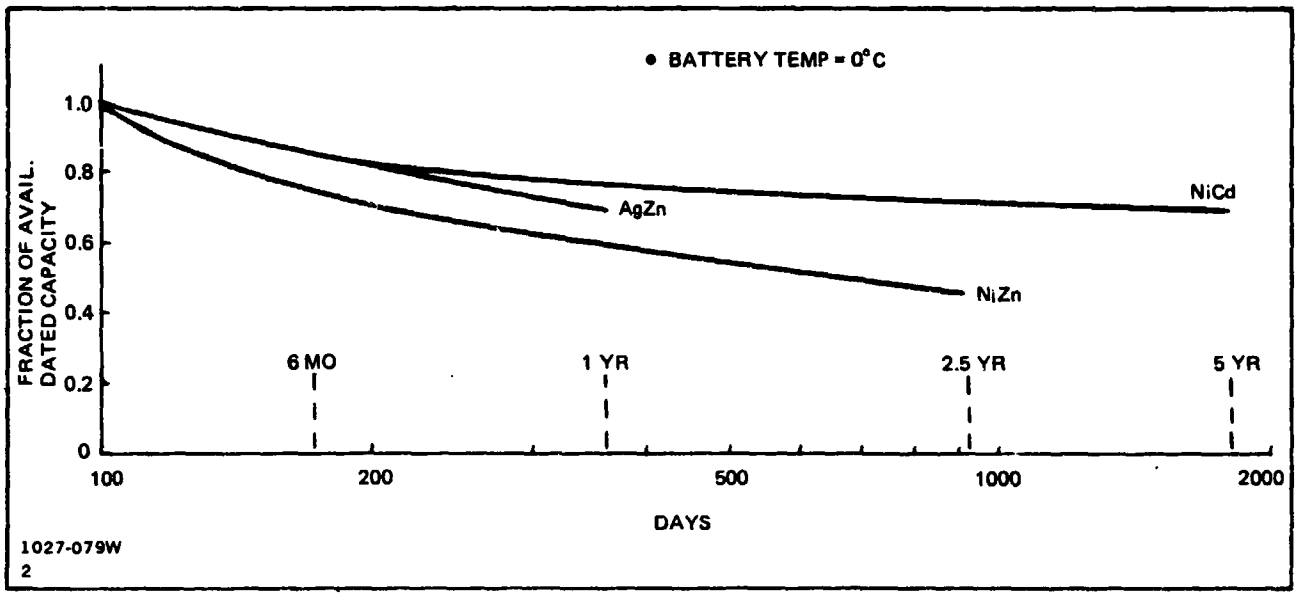

Fig. 5-21 Charge Retention for Candidate Batteries

Operating life of the high energy density AgZn battery is limited to six months. Although only a few of these batteries are required, they would have to be resupplied nine times during a five year mission. For comparison purposes, the resupply costs shown in Fig. 5-20 reflect a $/kg Shuttle transportation charge for the battery system options. Further, a $5K allowance is assumed for silver reclaimation from each AgZn battery. With this assumption, use of AgZn batteries results in the lowest cost among the battery options.

Reliable operation for two to three years is expected with NiZn batteries. Assuming a mass allocation for EPS resupply of 10,000 kg, sufficient NiZn batteries could be installed to support an LSS demo platform mission for two years. About half as many batteries are assumed to be used for the last (fifth) year of operation.

NiCd batteries have the longest operating life, but the lowest energy density. Within a resupply mass limit of 10,000 kg, this option would require four Shuttle visits. This power source is therefore, sized for only one year of operation. As shown in Fig. 5-19 and 5-20, the high weight and cost of these batteries make them unattractive for applications for this type.

AgZn and NiCd batteries have been qualified for DoD space programs. Additional qualification will be required for the NiZn batteries. This cost is estimated at about $30K, and has not been included in the option comparisons.

RTG - The LSS demo mission's almost constant, low power application is ideal for an RTG. Converters such as SNAP 19 are small, light, long-lived and relatively cheap.

Two sizing approaches were considered:

- Size for the peak (90 watt) load
- Size for the continuous (17 watt) load, and use batteries to supply the infrequent peak loads.

Only NiZn and NiCd batteries were considered in the second approach since these are capable of long standby service.

The plutonium (^{238}Pu) fuel is the most expensive component in these systems. Encapsulated fuel elements currently cost about $600/thermal watt. For applications such as this, where the generator can be returned at the end of the mission and the fuel reprocessed, equivalent fuel cost would be about $100/thermal watt. Even with the higher fuel cost, however, RTG systems are substantially cheaper than any of the battery systems.

New SNAP 19 generators could be built today with about seven percent conversion efficiency. The problem, however, is that the fuel capsules are no longer available from the DOE. It is unlikely that the DOE could be convinced to produce the old fuel elements or to develop a new system if alternative power sources are availabe for the mission. Therefore, until new generator development is well underway for other missions, this otherwise attractive option will remain problematic.

Photovoltaic (PV)/Battery System - A conventional PV/NiCd battery system could readily satisfy a five-year mission requirement with no resupply. Several solar array configuration concepts were considered including:

- Fixed panels on four sides of the spacecraft
- Fixed panels and earth albedo reflectors
- Solar-oriented panels

Fixed panels are preferred to minimize system complexity and cost. Total array area requirements of about 20 ft^2 are needed for both of the above fixed panel concepts.

Energy and cycle life requirements could be satisfied with a single four ampere-hour NiCd battery. The proposed baseline system contains two, six ampere-hour NiCd batteries for redundancy.

Several space-qualified, battery charger/power regulators can be considered for this application. The values listed in Figures 5-19 and 5-20 reflect the use of the power regulator unit from the NASA Modular Power System (MPS). A new power control unit must be built to accommodate specific distribution, protection and control requirements of the spacecraft and payload.

A small, low cost photovoltaic/battery system can be readily built and installed, will operate reliably without resupply for mission durations of five years or longer, and can be readily scaled up to accommodate other, higher power payloads. The PV/Battery System is therefore, the preferred EPS option for the LSS demo mission.

EPS Equipment & Block Diagram - A block diagram of the PV/Battery System is shown in Fig. 5-22. Four solar panels feed power through the power control unit (PCU) to the power regulator unit (PRU). The PCU provides power distribution control, protection and monitoring and interconnects the solar panels, PRU, batteries and load buses. The PRU provides maximum power tracking and battery charge control.

The PCU and PRU are sized to accommodate the maximum anticipated loads. The number and/or size of solar panels and batteries can be tailored for each mission as indicated in the diagram. If power requirements for future missions reach the multi-hundred watt level, use of the NASA MPS should be considered. The MPS is a low cost, flexible system with load capabilities from a few hundred watts to more than two kilowatts in low earth orbit.

2

Characteristics and status of equipment for the PV/Battery EPS are given in Fig. 5-23. New solar panels and a PCU can be built with current technology. Use of surplus solar panels from previous NASA or DOD programs may also be possible. Several six ampere hour NiCd batteries have been flown on previous NASA spacecraft, and are readily available. The PRU is identical to the Standard Power Regulator Unit (SPRU) used in the NASA MPS, slightly modified to permit operation at low power levels.

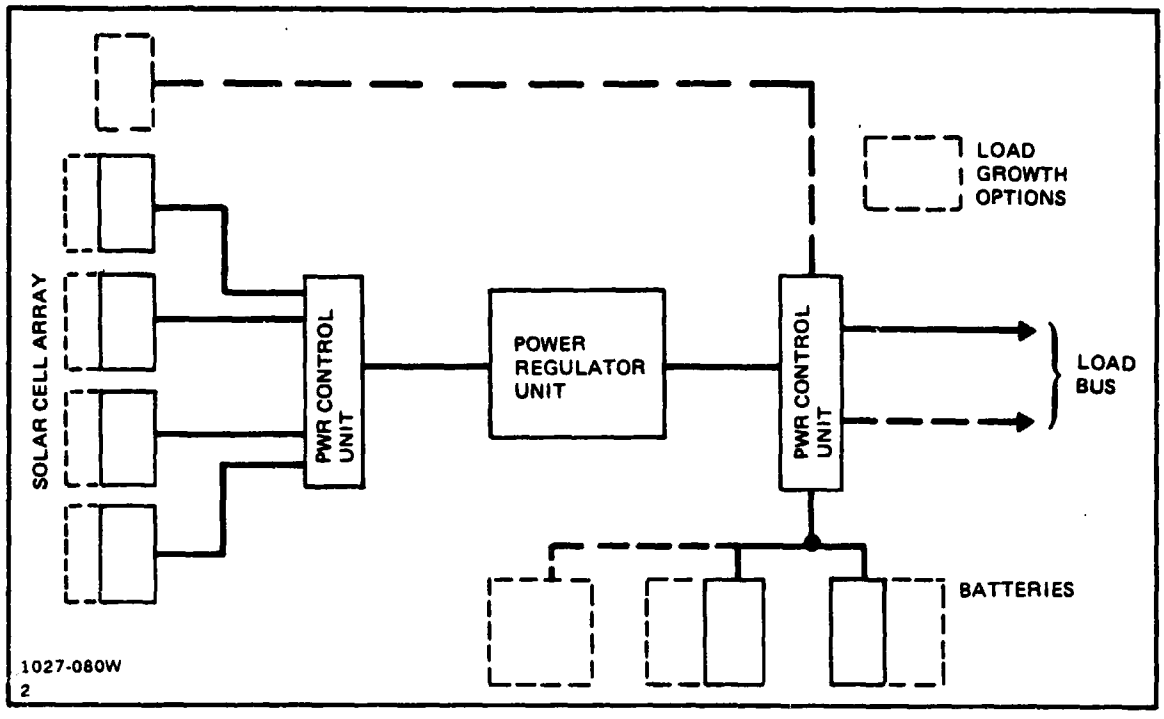

Fig. 5-22 EPS Block Diagram

EQUIPMENT	RATING	SIZE	MASS	STATUS
SOLAR PANELS (4)	55 w/PANEL AT 1 SUN	20 FT^2 TOTAL	10 kg TOTAL	NEW BUILD OR SURPLUS PANELS
NiCd BATTERIES (2)	6ah, 23 CELLS EA	41 x 10 x 11 cm EA	19 kg	QUALIFIED – SKYLAB MISSION
PRU (1)	50 W – 1 kW	25 x 25 x 18 cm	11 kg	NASA STANDARD PRU
PCU (1)	50 W – 1 kW	30 x 30 x 20 cm	14 kg	NEW BUILD – QUAL REQUIRED

1027-081W
2

Fig. 5-23 PV/Battery EPS Equipment

EPS Recommendations - Subsequent efforts should be conducted to refine the design, performance, and cost of the PV/Battery EPS:

- Verify load profiles for all possible subsystems and payloads
- Perform illumination, configuration and sizing analysis for solar arrays
- Verify PRU performance at low power levels
- Compare a simplified, low power baseline system to use of the NASA MPS
- Establish subsystem/payload interface and PCU design requirements
- Develop detailed cost estimates for hardware, system development and testing.

5.2.3.3 Tracking, Telemetry and Command Subsystem - A communications/data handling subsystem has been analyzed and a configuration defined which provides for mission requirements at a minimum prime power investment. The subsystem utilizes STDN-compatible S-Band links to allow downlinking of stored 16 kbps payload/H&S data, real time 500 bps H&S data and provides for uplink payload/housekeeping commands at a 1 kbps rate. Ephermeris determination via SGLS-compatible PRN ranging is also provided. Requirements and capabilities of the TT&C subsystem equipments are summarized in Fig. 5-24. NASA-standard equipments were selected where applicable, and are capable of performing well in excess of mission requirements.

ITEM	REQUIREMENT(1)	CAPABILITY
• L-BAND MICROWAVE RADIOMETER	• 1 kpbs OUTPUT DATA RATE WHILE SCANNING TERRAIN	–
• TAPE RECORDER	• TOTAL CAPACITY 2 Mb (ONE 15 MIN PASS)	• 450 Mb CAPACITY
	• 2 kpbs RECORD RATE	• UP TO 8 Mbps RECORD RATE
	• 15 MIN RECORD TIME	• UP TO 63 HOUR RECORD TIME
	• 16 kpbs PLAYBACK RATE	• UP TO 2.5 Mbps PLAYBACK RATE
• TRANSMITTER	• 16 kpbs DATA RATE	• UP TO 6000 kbps DATA RATE
• RECEIVER/DECODER	• 1 kbps COMMAND RATE	• UP TO 2 kbps COMMAND RATE
(1) REQUIREMENTS DERIVED BY GRUMMAN BASED ON AVAILABLE EXPERIMENT INFORMATION.		

1027-082W
2

Fig. 5-24 TT&C Subsystem Requirements/Capabilities

Groundrules used for sizing the LSS Platform's Tracking, Telemetry and Command Subsystem are:

- The L-band Microwave Radiometer (sensor) is operated once every 3 days for a 15 minute period

2

- H&S data and sensor data are recorded and dumped to a STDN site in the same (or subsequent) orbit - minimum view time of 2 minutes is available
- The sensor output is in digital form and uses 7 bit A/D quantization at a scan rate of 1.64 scans/sec; each scan contains 455 bits (without sync/ID/ parity).
- LSS at 500 km, 57° inclination orbit
- STDN site 30 ft antenna will provide more than 6 db operating margin for received S-Band data transmissions

The recommended TT&C subsystem configuration is shown in Fig. 5-25 and the hardware list is summarized in Fig. 5-26.

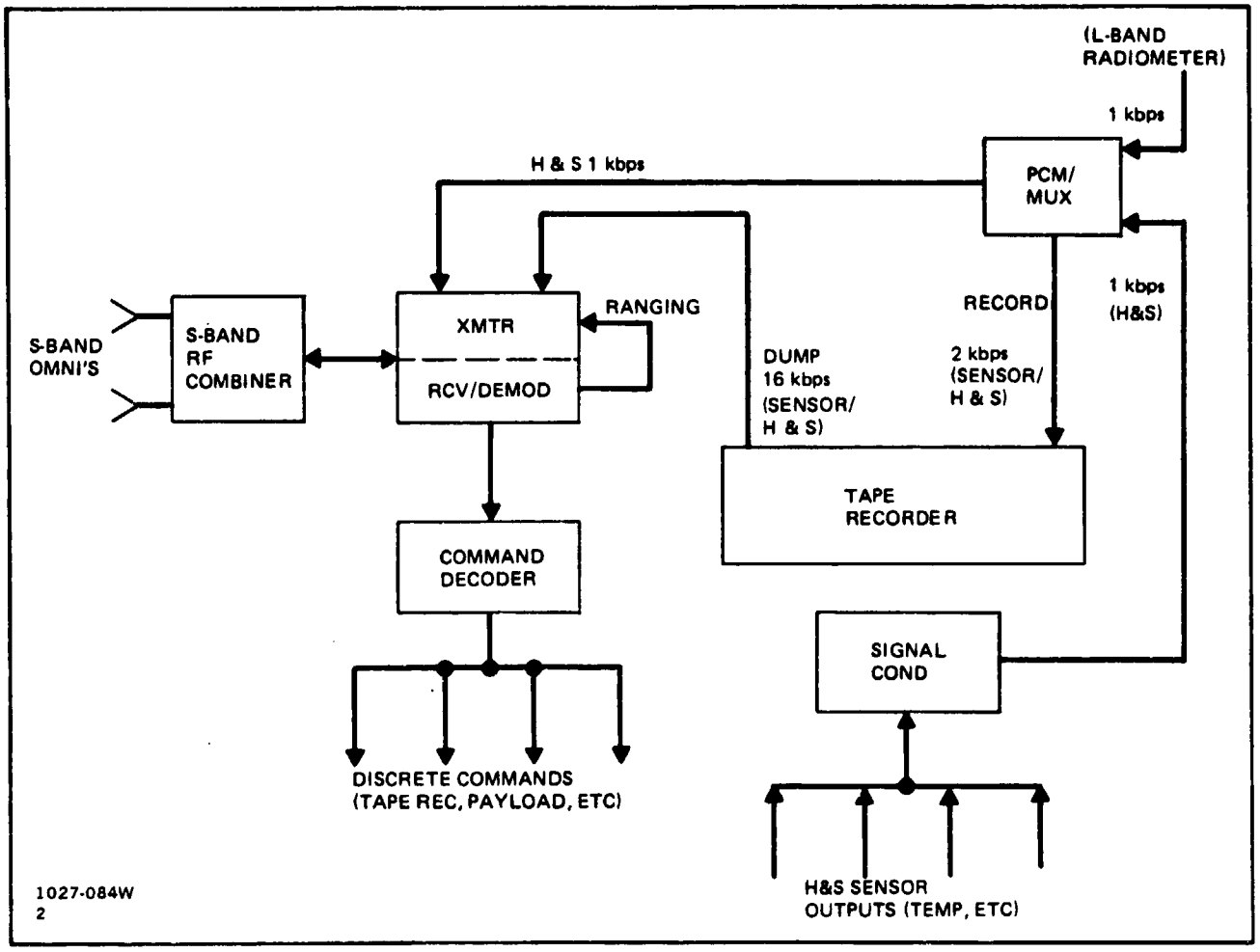

Fig. 5-25 TT&C Subsystem Block Diagram

2

ITEM	NO. PER SYSTEM	DEVEL STATUS	TOTAL WT, LB	POWER, WATTS
TAPE RECORDER	1	NASA STD	15	7 TO 21
TRANSPONDER	2	NASA STD	14	8 (RCV), 12 (XMT)
COMMANDER DECODER	2	TEAL RUBY	10	5
PCM/MULTIPLEXER	1	ELMS	6	12
H&S SENSORS (TEMP, etc)	20	ELMS	5	–
S-BAND OMNI ANTENNAS	2	MMS	2	–
S-BAND RF COMBINER	1	ELMS	1	–
SIGNAL CONDITIONER	1	ELMS	6	5
1027-083W 2		TOTALS	59 LB	(37-55) w

Fig. 5-26 Telemetry Tracking and Command Subsystem Hardware List

5.2.3.4 - Subsystems Summary - A summary of the subsystems complement for the free-flyer LSS platform is shown in Fig. 5-27, maximizing the use of existing hardware available through other space programs. A comparison of requirements vs capabilities indicates that the selected mix of hardware should readily satisfy the needs of this earth-viewing gravity-gradient stabilized platform.

As shown, the power system has been configured to allow for a 5-year life. Since our present estimates of the pointing stability of gravity-gradient stabilization for this configuration is about $\pm 2\frac{1}{2}°$, provisions for a simple vernier control have been included within the attitude control subsystem. The vernier control would narrow-down the pointing stability to the soil moisture radiometer's acceptable range, operating only before and during the 3 to 4 day intervals during which passes over the radiometry test area are made.

The location of experiments and subsystems are illustrated in Fig. 5-28. The soil moisture radiometer is located on the earth-pointing end of the spacecraft, with the LDEF-type materials experiments mounted on pre-assembled racks attached to the faces of the Tribeam. The platform subsystems are also pre-assembled to the racks, together with the fixed solar arrays. The lo-power nature of the satellite permits the use of a modest area (20 - 30 ft^2) of solar cells body-mounted to the spacecraft, thus avoiding the complexity of gimballed arrays tracking the sun.

2

SUBSYSTEM	HARDWARE	SOURCE	REQUIREMENTS	CAPABILITIES
ATTITUDE CONTROL	• MAGNETIC DAMPERS • VERNIER CONTROL (TBD)	LDEF –	ACCURACY (DEG) / STABILITY (°/SEC) ±0.5 / ±0.05	ACCURACY (DEG) / STABILITY (°/SEC) ±0.2 / ±0.02
ELECTRIC POWER	• SOLAR PANELS • BATTERIES • PRU • PCU	NEW OR SURPLUS SKYLAB NASA STD NEW DESIGN	90 w, 17 w, 40 w 160 kWh/YEAR	5–YEAR LIFE
DATA HANDLING	• MUX • STD RECORDER • CSDH	• ELMS • MMS • T'RUBY/ELMS	2 KPBS 2 MBPS 16 KBPS	32 KBPS 450 MBPS 600 KPBS
COMMUNIC'S	• S–BAND ANTENNA	MMS	DIGITAL 1 KBPS	2 KBPS

1027-085W
2

Fig. 5-27 LSS Platform – Subsystems Summary

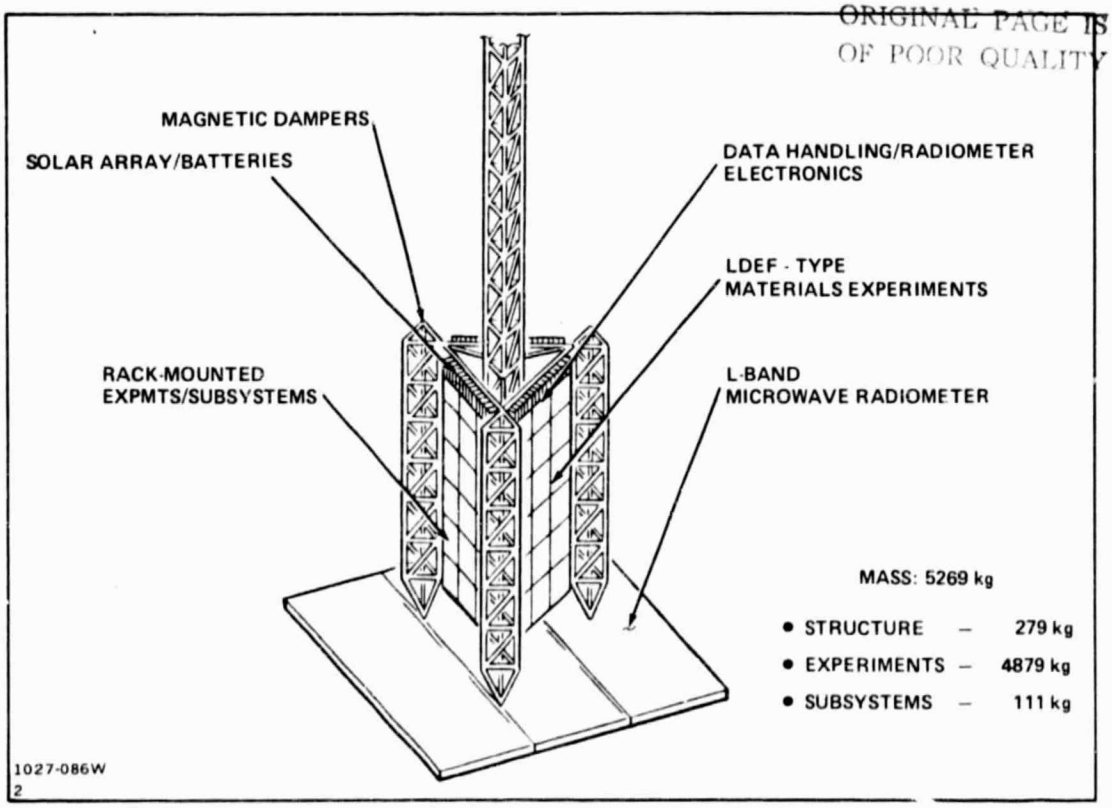

Fig. 5-28 LSS Platform – Equipment Arrangement

5.2.4 LSS Platform - Weight Summary

A weight summary for the free flying platform is shown in Fig. 5-29. The cg locations are based on the Orbiter packaging arrangement illustrated in Fig. 5-30, which accommodates the 10.5 m test beam, soil moisture radiometer, the equipment racks supporting the LDEF-type experiments and subsystems, and the ABB and OMS kit needed for the LSS platform mission.

ITEM	WEIGHT, kg LAUNCH	FREE-FLIER	LANDING
DEMO ARTICLE	279	279	
CONS/MAINT AIDS	136		136
TEST EQUIPMENT	45		45
SUBSYSTEMS	111	111	
BEAM MACHINE	7256		7256
RADIOMETER	479	479	
LDEF-TYPE TRAYS	4400	4400	
SUBTOTAL	12,706 (28,004 lb)	5269	7437
*OMS KIT	5647		
EPS KIT	740		344
TOTAL	19,093 (42,080 lb)	5269	7781 (17,149 lb)

SHUTTLE PAYLOAD CAPABILITY – KSC-57°

200 N MI	24,943 kg	– NO OMS KIT
250 N MI	21,542 kg	ONE OMS KIT
300 N MI	19,274 kg	ONE OMS KIT

OMS KIT ASSUMED TO BE ONE-HALF THE MASS OF ONBOARD OMS FUEL AS PER JSC 07700, VOL XIV, PAGE 3-1

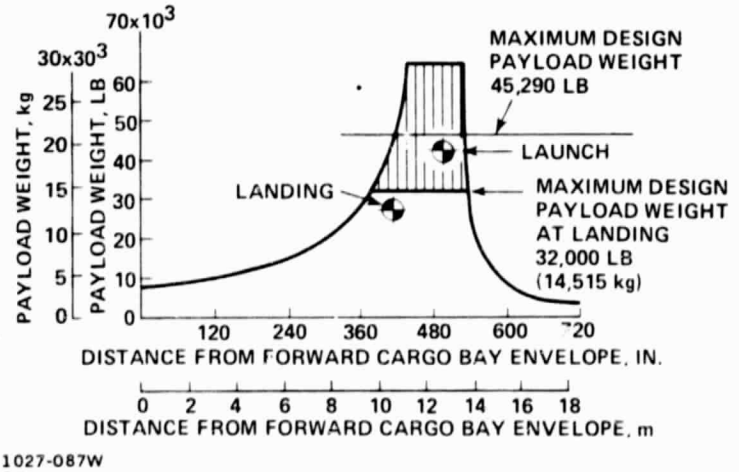

1027-087W
2

Fig. 5-29 LSS Platform Weight Summary: 57° Inclination, 500 km Altitude (270 N Mi)

2

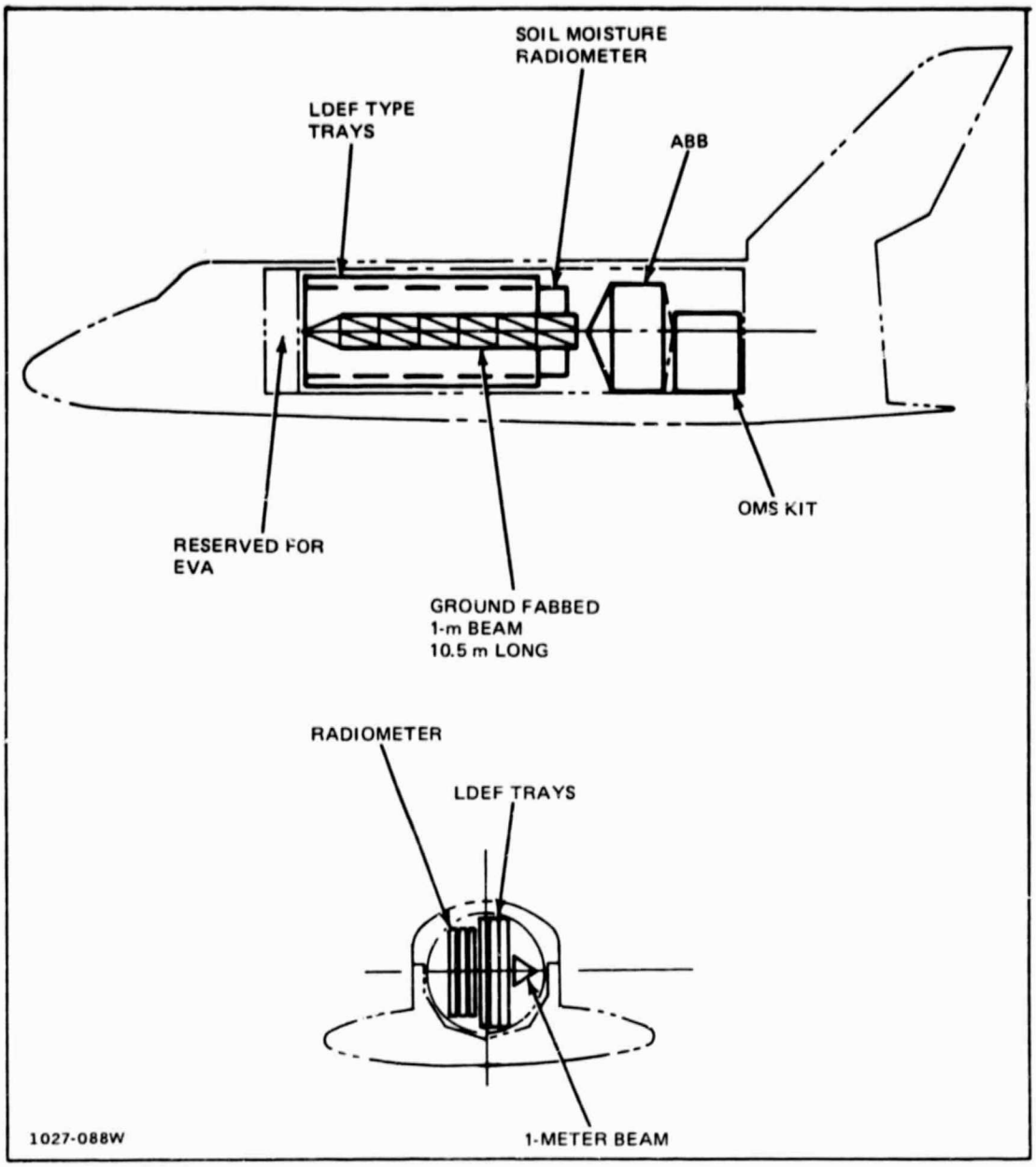

Fig. 5-30 LSS Platform – Launch Configuration

The specified orbit, 57° inclination and 500 km altitude, requires the addition of an OMS kit and results in a reduction of maximum payload capacity (with one OMS kit) to 20,549 kg (45,290 lb). The mass assigned to the OMS kit (5647 kg) is based on the Space Shuttle Payload Accommodation Handbook, JSC Document No. 07700 which determines that each kit will contain 50% of the onboard OMS fuel. As shown, the cg location and gross weight are well within the confines of the cg envelope.

5.2.5 Structural Dynamic Analyses

A structural analysis of the LSS platform has been conducted to verify the integrity of the Tribeam structure and the long central boom. Structural loads in the 1-m beams and cross-bracing were determined for Orbiter vernier RCS firing and steady-state thermal conditions with one vertical blocked. An overall boom length of 100 m was used for preliminary structural calculations.

The structural dynamic effects of configuration flexibility and the load implications of RMS handling and capture were also evaluated.

5.2.5.1 Design Conditions and Strength Verification - The rotational accelerations induced by the Orbiter during RCS thruster firings are shown in Fig. 5-31. Note that the primary RCS accelerations exceed those of the Vernier RCS by factors of 30 to 40 or more.

	ROTATIONAL ACCELERATION, DEG/SEC^2			
REACTION CONTROL SYSTEM	$\pm\ddot{\phi}$	$+\ddot{\theta}$	$-\ddot{\theta}$	$\pm\ddot{\psi}$
PRIMARY SYSTEM	1 2	1.4	1.5	0.8
VERNIER SYSTEM	0.04	0.03	0.02	0.02

- ROLL ϕ, PITCH θ, YAW ψ
- FACTOR OF SAFETY-ULTIMATE = 1.40

REF: PAYLOAD ACCOMMODATION DOCUMENT JSC07700, VOL XIV, REV E

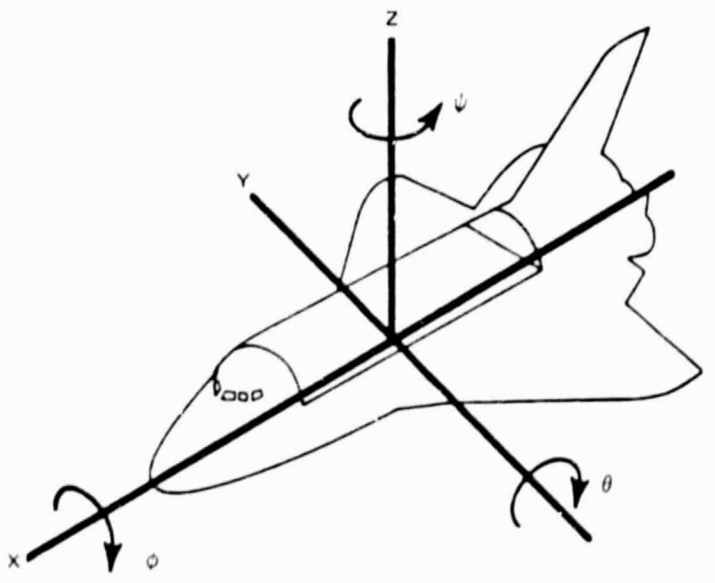

Fig. 5-31 Orbiter RCS Thruster Firing Capability

A summary of maximum loading conditions induced upon 1-m beam elements by Vernier RCS firing is shown in Fig. 5-32. Limit allowable values were obtained using a factor of 1.4 from ultimate allowable values. The chart shows that the maximum bending moment on the central 1-m boom is 63% of the allowable value, while the maximum 1-m beam cap load in the Tribeam is 7% of the allowable value. A load increase of 30 to 40 or more associated with Primary RCS firing is obviously not feasible. Therefore, the use of Vernier RCS is necessary during the assembly process.

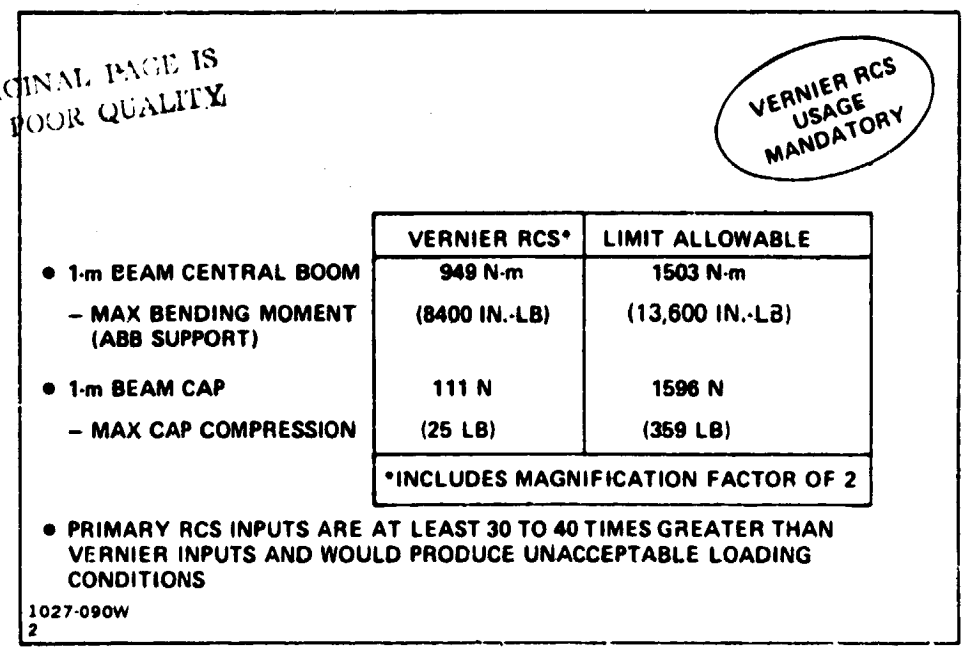

Fig. 5-32 Maximum Limit Loading Conditions Imposed by RCS Firing

5.2.5.2 Solar Blockage - During the previous study phase it was determined that a blockage condition of a 1-m beam by another could occur in flight, although relatively infrequently. Calculations show that a maximum average ΔT of 56°F (31° C) could occur between vertical beams under the "right" set of circumstances. This ΔT is associated with a block anodize coating.

LSS platform loads and deflections are shown in Fig. 5-33 for this blockage condition. Maximum compressive loads in the 1-m verticals are only 55 lb but a significant bending moment (5505 in.-lb) is induced due to the offset load lines of these members. The configuration of the drag bracing (Fig. 5-33) induces a bending moment of 13,200 in.-lb on the central boom. Since the allowable value is 13,600 in.-lb, the structure is only marginally adequate. Figure 5-34, shows loads and deflections for the platform with a revised drag brace configuration. With this configuration, loads

2

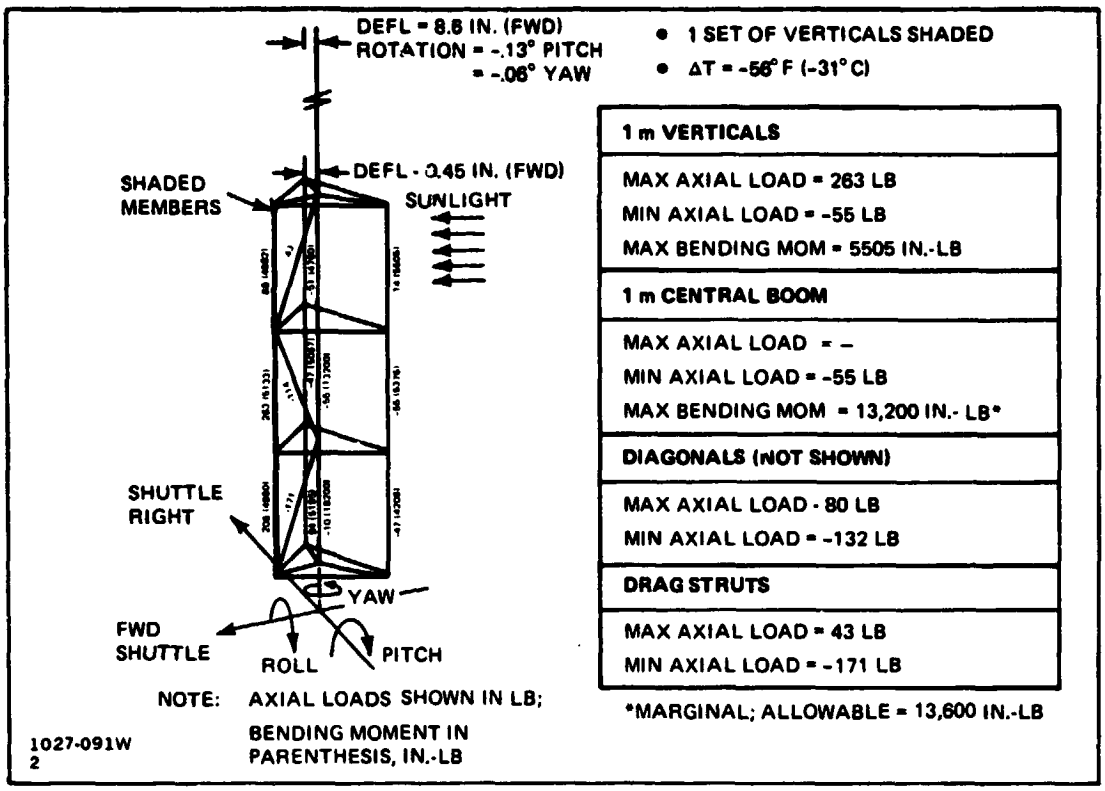

Fig. 5-33 Net Axial Loads Due to Solar Blockage (Original Drag Bracing)

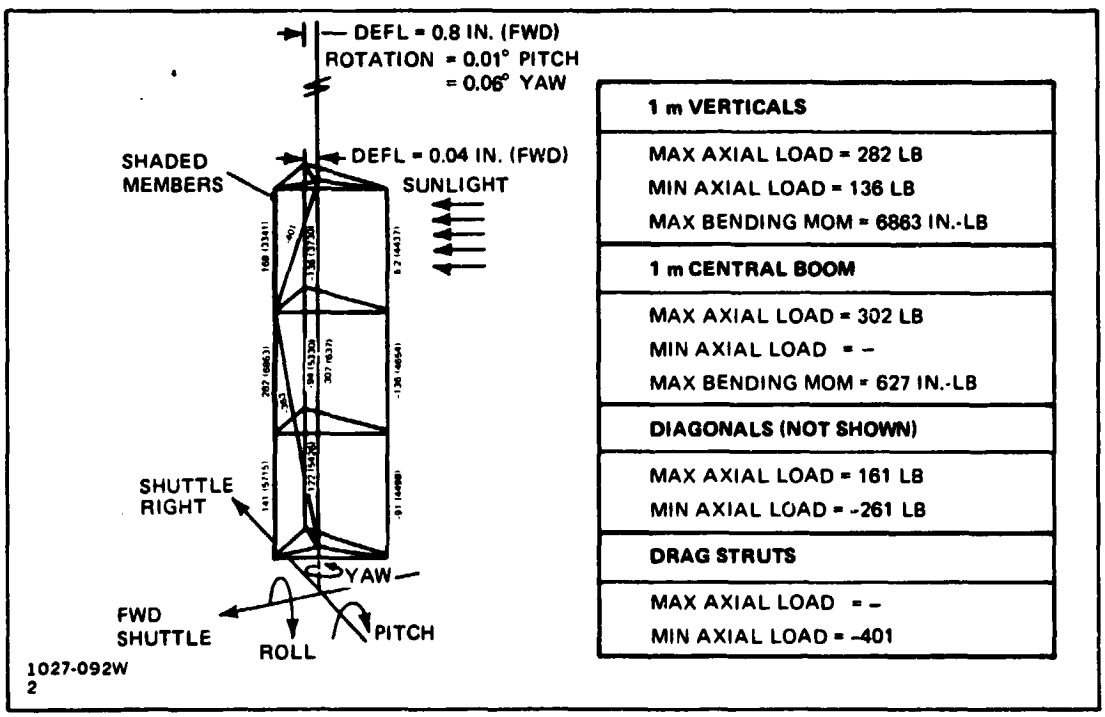

Fig. 5-34 Net Axial Loads Due to Solar Blockage (Revised Drag Bracing)

in the 1-m vertical are increased (-136 lb compression, 6863 in.-lb of bending moment) but the load in the central boom is reduced to a minimal value (627 in.-lb). In addition, boom tip deflections are reduced from 8.6 in. to 0.8 in. with this configuration.

A reduction of ΔT is expected by changing the original configuration coating from black anodize to Z-93 White paint or Alzak, However, the revised drag bracing configuration is still recommended.

5.2.5.3 VRCS Firing - Loads and deflections due to Vernier RCS firing (Fig. 5-35) were calculated for combined pitch, roll, and yaw conditions assuming a steady-state rotational acceleration and a dynamic magnification factor of 2. The increase in overall inertia due to the presence of the LSS platform reduces the nominal Orbiter rotational accelerations of $0.04°/sec^2$ (roll), $0.03°/sec^2$ (+ pitch), $0.02°/sec^2$ (- pitch) and $0.02°/sec^2$ (yaw) to $0.023°/sec^2$, $0.027°/sec^2$, $0.018°/sec^2$ and $0.0198°/sec^2$, respectively.

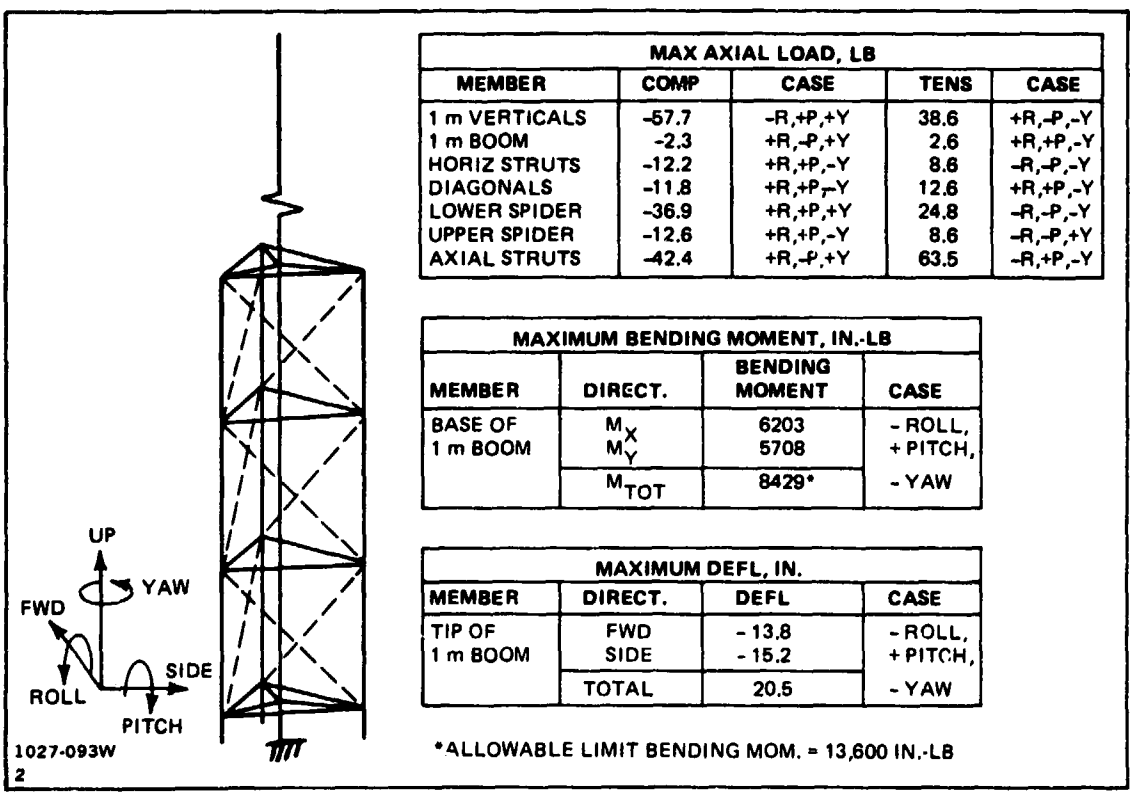

MAX AXIAL LOAD, LB				
MEMBER	COMP	CASE	TENS	CASE
1 m VERTICALS	-57.7	-R,+P,+Y	38.6	+R,-P,-Y
1 m BOOM	-2.3	+R,-P,+Y	2.6	+R,+P,-Y
HORIZ STRUTS	-12.2	+R,+P,-Y	8.6	-R,-P,-Y
DIAGONALS	-11.8	+R,+P,-Y	12.6	+R,+P,-Y
LOWER SPIDER	-36.9	+R,+P,+Y	24.8	-R,-P,-Y
UPPER SPIDER	-12.6	+R,+P,-Y	8.6	-R,-P,+Y
AXIAL STRUTS	-42.4	+R,-P,+Y	63.5	-R,+P,-Y

MAXIMUM BENDING MOMENT, IN.-LB			
MEMBER	DIRECT.	BENDING MOMENT	CASE
BASE OF 1 m BOOM	M_X	6203	- ROLL,
	M_Y	5708	+ PITCH,
	M_{TOT}	8429*	- YAW

MAXIMUM DEFL, IN.			
MEMBER	DIRECT.	DEFL	CASE
TIP OF 1 m BOOM	FWD	- 13.8	- ROLL,
	SIDE	- 15.2	+ PITCH,
	TOTAL	20.5	- YAW

*ALLOWABLE LIMIT BENDING MOM. = 13,600 IN.-LB

Fig. 5-35 Limit Loads and Deflections Due to VRCS Firing

Axial loads in the Tribeam structure are minimal and do not exceed 65 lb. Compressive cap loads in the 1-m beam verticals do not exceed 25 lb vs an allowable of

359 lb. The limit bending moment at the base of the central 1-m boom is 8429 in.-lb vs an allowable value of 13,600 in.-lb. The maximum deflection would occur at the tip of the 1-m boom and is 20.5 in.

5.2.5.4 Frequency Considerations/Orbiter VRCS Coupling - Although platform loading conditions are acceptable for VRCS firing, potential flight control constraints must be considered due to the mass and flexibility of the combined ABB/LSS structure mounted in the Orbiter. Typically, the lowest structural frequency should be 5 to 10 times greater than the control frequency.

With the nominal Orbiter VRCS deadband of 0.1° and an attitude rate of 0.01°/sec the VRCS fires with a control frequency of 0.023 Hz. This control frequency is compared with fundamental vibration modes related to phases of the LSS platform's construction and operations (Fig. 5-36), namely:

- 1-meter beam construction from the ABB -0.096 Hz (rigid base)
- RMS deploy or capture of the LSS -0.028 Hz
- LSS free-flight -0.18 Hz

The construction and RMS usage modes pose potential control interaction problems, since a desirable frequency separation factor of 10 with the Orbiter's VRCS control is not evident.

Previous phases of this study have shown that the stiffness of an LSS structure's support base can significantly affect the structure's frequencies during construction. Figure 5-37a shows the variation in LSS platform fundamental frequency versus base stiffness for platform boom lengths of 100.5 m, 60 m, and 39 m, with the platform structure supported from the ABB. Preliminary estimates of the local base stiffness in this support mode, are in the range of 10^7 to 10^8 in.-lb/rad. The figure indicates that as the overall structural length is decreased from 100.5 m, the fundamental mode changes from bending to torsion and the torsion mode remains relatively insensitive to length. An anti-rotation strut, from a Tribeam apex to the Orbiter would thus be needed to raise the frequency of this mode. With this adaptation, a reduction of the LSS platform's boom length would be necessary (42 m to 58 m) to maintain appropriate frequency separation with nominal Orbiter VRCS control parameters (Fig. 5-37b).

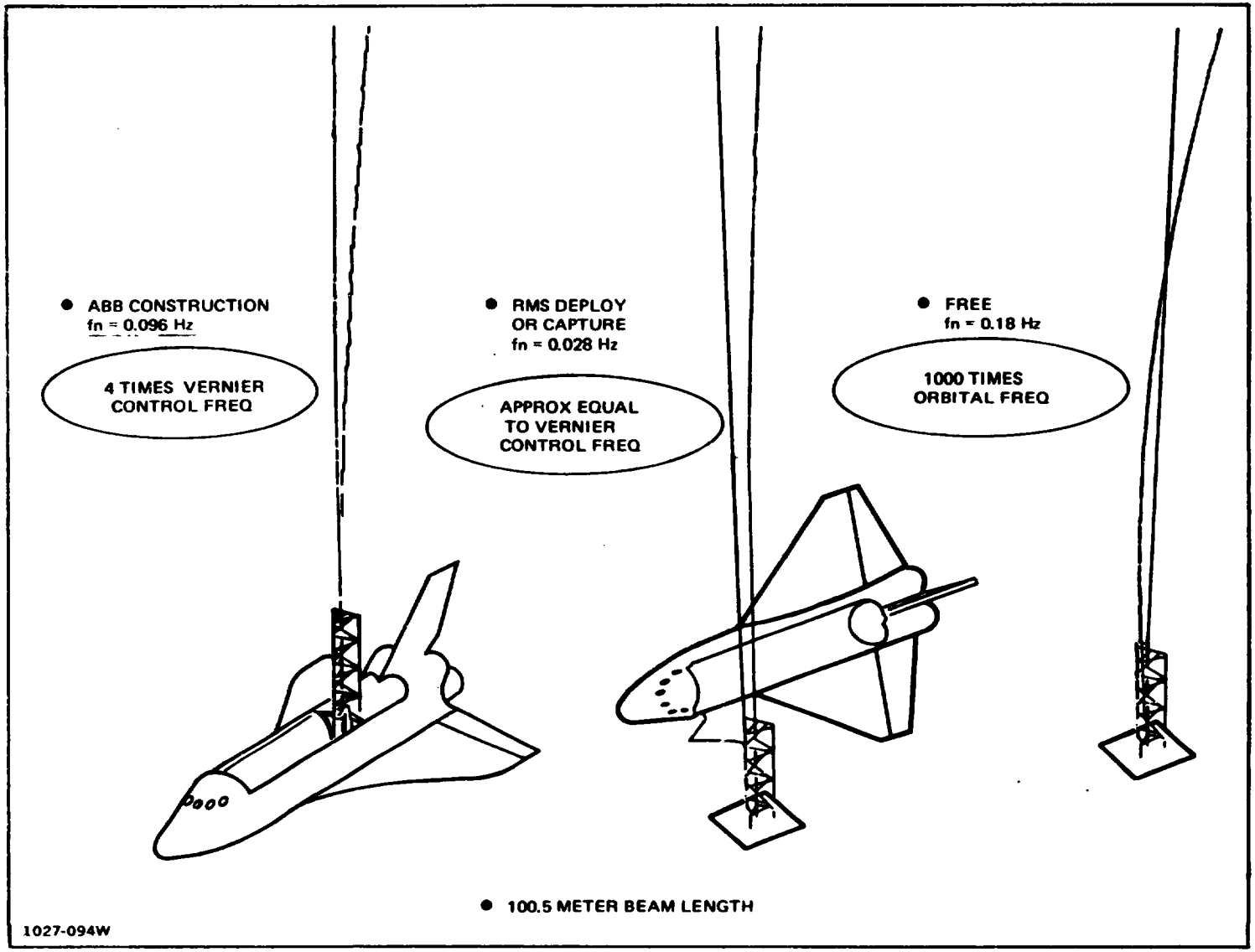

Fig. 5-36 Frequency Considerations – Orbiter VRCS Coupling

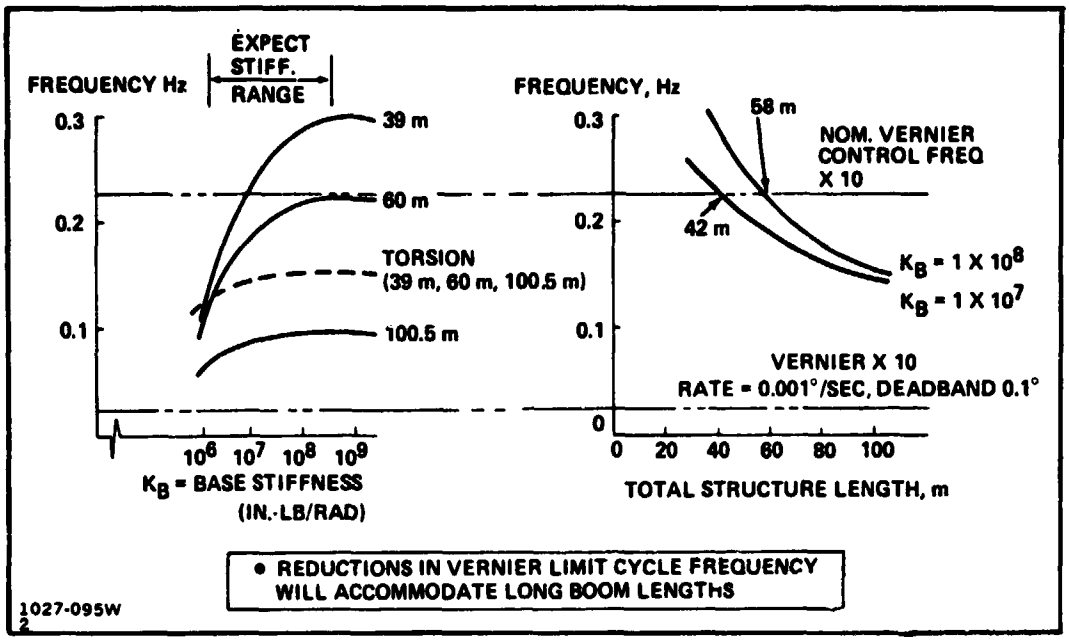

Fig. 5-37 Effect of Base Stiffness on Natural Frequency

However, longer boom lengths can be accommodated by software changes in the Orbiter's VRCS control parameters. To increase the separation of frequencies to a desirable range, the control frequency can be lowered by increasing the deadband or decreasing the limit cycle rate, both of which are selectable parameters in the Orbiter's flight control computer. As shown in Fig. 5-37a, by reducing the Vernier limit cycle rate to 0.001°/sec (an order of magnitude reduction below nominal), the long boom lengths can readily be accommodated.

With a nominal separation distance of 30 ft, a typical RMS configuration produces a frequency of 0.028 Hz (Fig. 5-36). However, during normal RMS operation (in a loaded condition) the VRCS control system is inhibited from firing. If VRCS operations in the RMS-extended position are necessary prior to LSS release, or subsequent to capture, the Orbiter's control frequency should be reduced by implementing software changes in the nominal control parameters as discussed previously.

No major problems are foreseen for the LSS platform in its free-flight mode. The free-flight frequency of 0.18 Hz is almost three orders of magnitude greater than orbital excitation frequencies.

5.2.5.5 RMS Handling - During construction, deployment and berthing of the LSSD vehicle, loads will be induced by the Orbiter's Remote Manipulator System (RMS).

Figure 5-38 shows the RMS and Fig. 5-39 summarizes the maximum forces that can be induced at the end-effector. Figure 5-39 also summarizes maximum torques that can be withstood by the various RMS joints before slippage. The standard RMS end-effector would be replaced by a proposed "soft clamshell" end-effector for the LSSD mission.

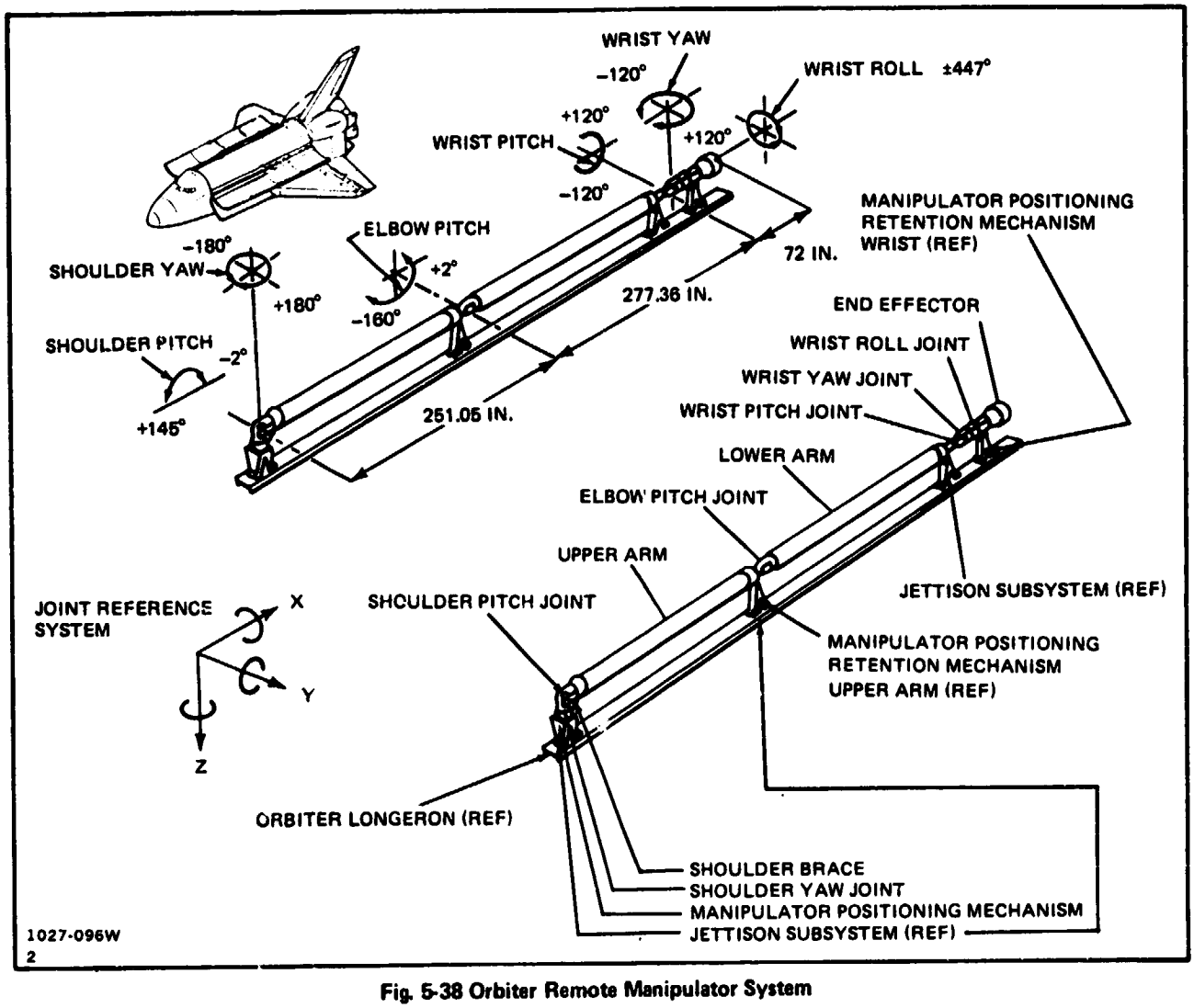

Fig. 5-38 Orbiter Remote Manipulator System

Under pure steady-state translation or rotation of the LSSD vehicle, a bending moment of 36 in.-lb. is induced at the base of the 1-m boom per pound of end effector translation force, while a bending moment of 0.76 in.-lb. is induced for every inch-pound of applied torque. However, the RMS can apply forces as a reverse step. With this type of forcing function a magnification as high as four could result. With a limit

allowable bending moment of 13,600 in.-lb, the maximum allowable translation force is 13,600/(4 x 36) = 94.4 lb; the maximum allowable torque is 13,600/(4 x 0.76) = 4474 in.-lb (373 ft-lb). These loads are greater than the loads that can be applied by the RMS.

	TORQUE RANGE, FT/LB MIN	MAX	FORCE, LB MIN	MAX	CONDITION
SHOULDER YAW	772 –	1158	15.44 –	23.2	STRAIGHT ARM
SHOULDER PITCH	772 –	1158	15.44 –	23.2	STRAIGHT ARM
ELBOW PITCH	528 –	792	18.41 –	27.3	BENT ARM OVERALL LENGTH < 42 FT
WRIST PITCH	231 –	347	37.97 –	57.0	BENT ARM OVERALL LENGTH < 20 FT
WRIST YAW	231 –	347	54.35 –	81.6	BENT ARM OVERALL LENGTH < 14 FT
WRIST ROLL	231 –	347	–		

NOTE: ALL VALUES ARE QUOTES FOR THE ARM UNDER STEADY-STATE RIGID BODY STATIC CONDITION. (e.g., IN PAYLOAD BAY AND SINGLE JOINT DRIVE)

1027-097W
2

Fig. 5-39 Force Torque Capability at End-Effector

If the RMS picks up the Tribeam away from the center of gravity (cg), as shown in Fig. 5-40, the allowable applied force will be limited to the induced moment imposed on the RMS. Figure 5-40 shows the allowable end effector force versus the end effector location on the Tribeam. The force is limited by an allowable RMS wrist joint

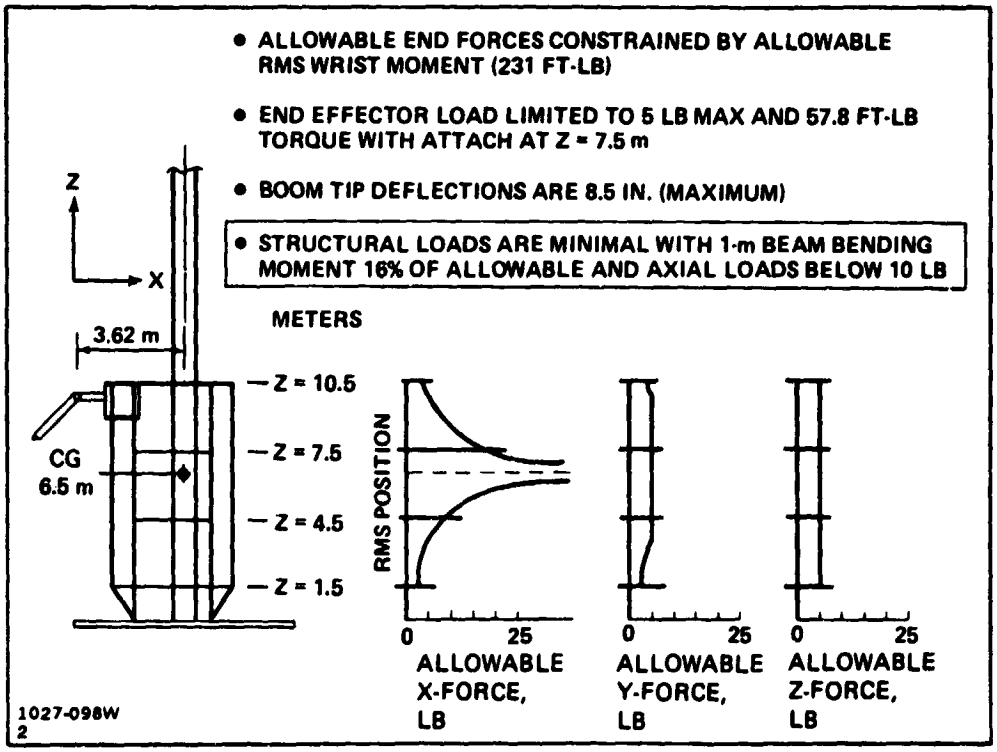

Fig. 5-40 Allowable RMS Forces

moment (231 ft-lb) and decreases with distance from the cg. With a magnification factor of four, the allowable fore and aft force varies from 3 to 17.5 lb while the side force varies from 3 to 5 lb. The vertical force is limited to 5 lb and applied torque is limited to 693 in.-lb (57.8 ft-lb).

Limit loads and deflections on the LSS platform were determined for a 5 lb RMS translation force and a 693 in.-lb torque. The results are summarized in Fig. 5-41. For this calculation, the end effector was moved down one bay to reduce the cg offset and appropriate reacting moments were applied. With a magnification factor of four, the maximum limit bending moment is 2134 in.-lb versus an allowable bending moment of 13,600 in.-lb. The maximum deflection is 8.5 in. at the tip of the boom. Axial members loads are small and are 11.5 lb or less. Thus, RMS handling loads induced into the LSS platform are within "comfortable" limits.

RMS translation and rotation times versus distance are shown in Fig. 5-42 for various end effector forces. The RMS force and wrist torque limitations, discussed previously, establish the conditions applicable to LSS Platform RMS usage. To translate the LSS 20 m (approximately the length of the payload bay) takes about 1.5 to 3.5 min depending on RMS forces. A rotation of 90° takes from 3 to 4 min depending on applied torque. A reverse step force shape was assumed to obtain minimum times and a final velocity of zero.

An estimate of LSS berthing loads was made by calculating the elastic response of the LSS after capture by the RMS. At hard capture by the end-effector, it was assumed the the LSS had residual translation rates of 0.05 ft/sec and rotation rates of 0.1°/sec. It was also assumed that the LSS was 30 ft above (Z-direction) the attachment of the RMS to the Orbiter sill (Fig. 5-43). With pure translation or rotation rates, boom bending moment and RMS joint moments are below allowable. Certain joint moments are marginal, however, as shown in Fig. 5-43. If the conditions are combined, RMS wrist yaw and elbow pitch allowable moments are exceeded. RMS joint slippage could occur under these conditions.

5.2.5.6 Structural/Dynamic Analysis - Conclusions and Recommendations - Analyses of the Orbiter as a construction platform indicate that RCS control usage should be limited to the Vernier system to minimize induced loads in the LSS Platform structure.

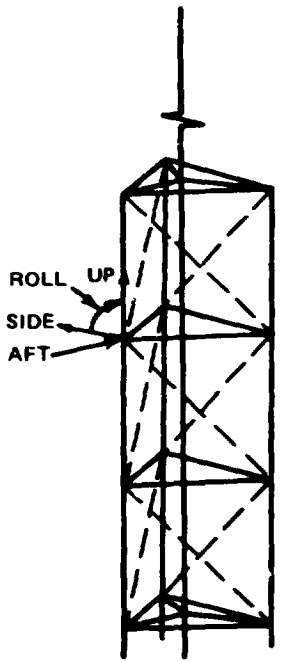

MEMBER	5 LB AFT			5 LB SIDE			5 LB UP			683 IN.-LB ROLL		
	TENS, LB	COMP, LB	B.M., IN.-LB	TENS, LB	COMP, LB	B.M., IN.-LB	TENS, LB	COMP, LB	B.M., IN.-LB	TENS, LB	COMP, LB	B.M., IN.-LB
1 m VERTICALS	2.9	-8.6	488	5.0	-3.0	448/432*	5.8	-3.5	918	8.5	-2.1	1388
1 m BOOM	—	—	720	—	—	720	1.18	-0.1	20.0	—	—	2134
HORIZ STRUTS	2.6	-6.4	10.8	7.4	-3.4	245	5.5	6.3	11.4	11.5	-4.4	8.5
DIAGONALS	4.7	-4.2	4.1	2.3	7.4	154	7.5	-6.1	5.8	3.1	-11.9	5.8
LOWER SPIDER	0.3	-1.16	1.5	2	-2.8	21.2	0.62	—	2.5	3.2	3.1	36.5
UPPER SPIDER	0.12	-.12	10.7	0.2	0.2	25	0.64	—	31.2	0.3	0.2	28.3
AXIAL STRUTS	5.6	-3.6	16.8	3.0	0.2	160	1.8	2.3	8.2	6.5	1.8	77.9
DEFL (IN.) BOOM TIP	2.5 (FWD)			2.8 (SIDE)			0.11 (AFT)			8.5 (SIDE)		

*SECOND NUMBER IS MAX TORSION

1027-099W
2

Fig 5-41 Limit Loads and Deflections Due to RMS Handling Loads – MF = 4

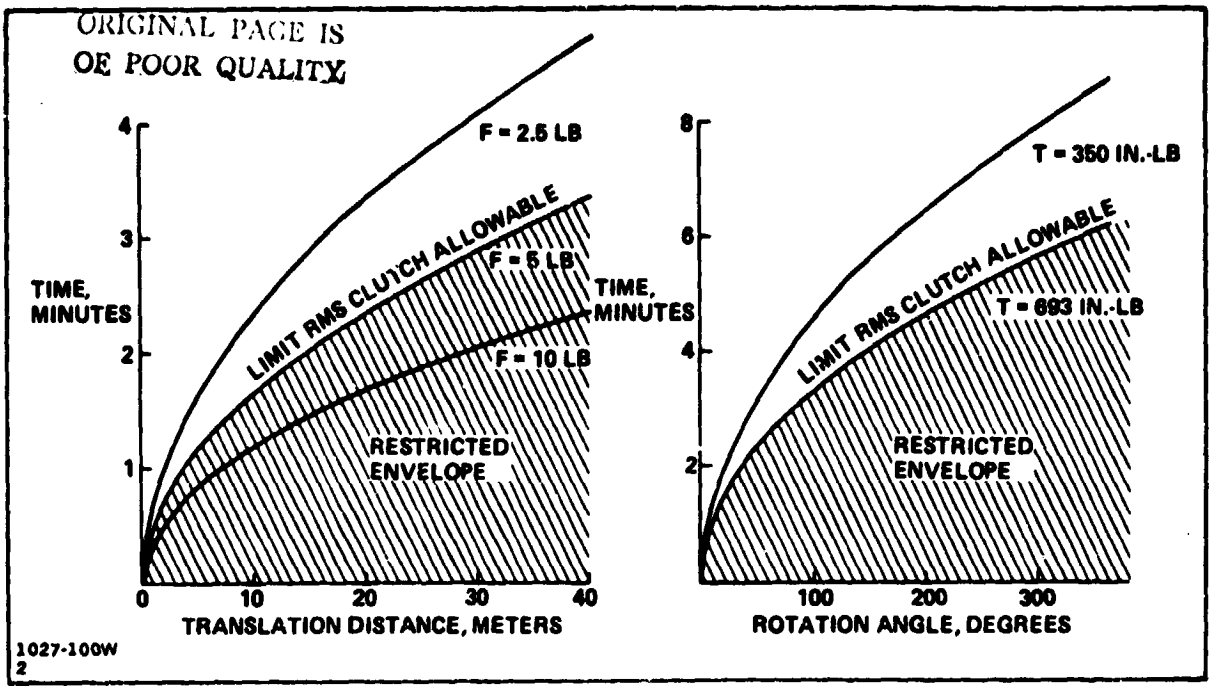

Fig. 5-42 Attainable RMS Motion

		ALLOW. MOM., IN.-LB	X TRANS. MOM., IN.-LB	Y TRANS. MOM., IN.-LB	Z TRANS. MOM., IN.-LB	θ_X ROT. MOM., IN.-LB	θ_Z ROT MOM., IN.-LB	RSS* ALL. CASES
BOOM BASE		13,600	564	2017	1311	2198	1782	3767
RMS	WRIST – ROLL	2772	269	716	575	430	2263	2494
	WRIST – YAW	2772	419	1397	2172	2150	182	3391
	WRIST – PITCH	2772	1951	130	1309	237	306	2384
	ELBOW – PITCH	6336	3029	1635	5182	1506	593	6427
	SHOULDER – PITCH	9264	3363	702	2500	820	590	4334
	SHOULDER – YAW	9264	285	815	662	496	2292	2583

*SQUARE ROOT OF SUMS OF SQUARES

• END–EFFECTOR RATES: TRANSLATION = 0.05 fps, ROTATION = 0.1°/SEC

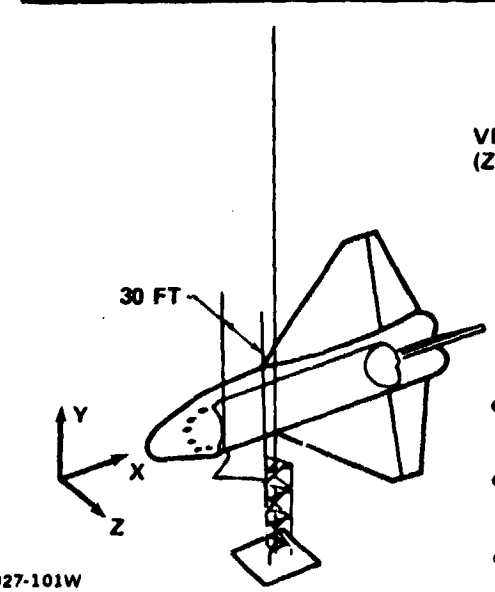

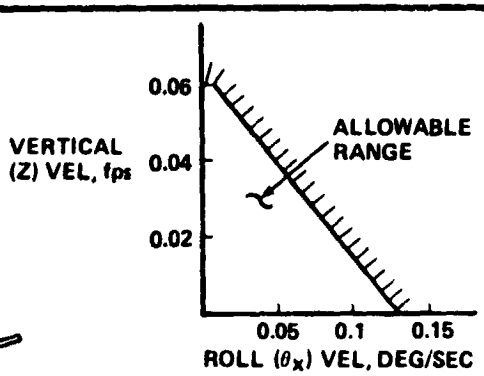

- AT RMS CAPTURE RESIDUAL RATES WILL EXIST BETWEEN THE LSS AND ORBITER
- RMS ALLOWABLE JOINT MOMENTS LIMIT THESE RATES TO THOSE SHOWN
- RMS JOINT SLIPPAGE COULD OCCUR IF ALLOWABLE MOMENTS ARE EXCEEDED

1027-101W
2

Fig. 5-43 RMS Berthing – Capture

With the use of the Vernier system, thermal loading conditions predominate, and as was seen with the drag brace configurations, particular care must be taken to insure that end constraints do not induce unacceptable thermal loadings into the 1-m beam members. Although acceptable, considerable loads are induced in the 1-m verticals, due to their elastic axes offsets. End fittings which distribute the load to the three caps of the 1-m beam would minimize these effects.

To minimize control interaction with the nominal Vernier system, the length of the platform would have to be limited from 40 to 60 m depending on base stiffness. However, longer beam lengths can be accommodated by software changes in the Orbiter's VRCS control parameters.

Handling operations with the RMS are limited by the capability of the RMS rather than the structure. With restricted RMS end forces, operations still, however, can be performed in reasonable times. Relative rates between the Orbiter and LSS Platform must be quite small to affect capture. Translation rates of 0.05 fps and rotation rates of 0.1°/sec appear marginal. Again, the capture capability appears limited by RMS capability rather than Platform strength.

Experimental investigations are recommended relative to the basic 1-meter beam. Certain properties of the 1-meter beam can only be obtained by test. In particular, the potential loss of strength and stiffness for thin wall cap members, due to local buckling, under thermal and dynamic loads, requires experimental investigation. Additionally, manufacturing tolerances as applied to beam straightness and twist as well as the thermal/dynamic response of the beam must be determined experimentally to verify predictions based on analysis, and to refine structural analytical models.

5.2.6 Flight Control Analyses

Orbiter-attached control implications have been analyzed and the results presented herein. The flight control analysis has been supported by a Grumman IRAD-developed three-axis simulation program called SATSIM, described in Appendix C.

The potential interaction of the Orbiter attitude control system with the flexible modes of an attached large space structure is a primary area of concern. Considering rigid body performance on a single axis basis, the basic control technique is described by a position and rate limit cycle system using the vernier thrusters with a minimum impulse bit of 80 milliseconds (the control frequency is the limit cycle frequency). This minimum impulse time corresponds to the flight computer computation time, not

the thruster's minimum impulse which is 30 milliseconds. The variation of limit cycle frequency as a function of deadband and limit cycle rate for the Vernier RCS thruster system is presented in Fig. 5-44 with the nominal operating point indicated (deadband = $0.1°\omega_{LC} = 0.01°$/sec). The trajectory of the limit cycle in the phase plane (attitude rate vs attitude) essentially appears as an unforced response since the control torque is much greater than the disturbance torque and the rate change during the coast due to peak disturbances is small.

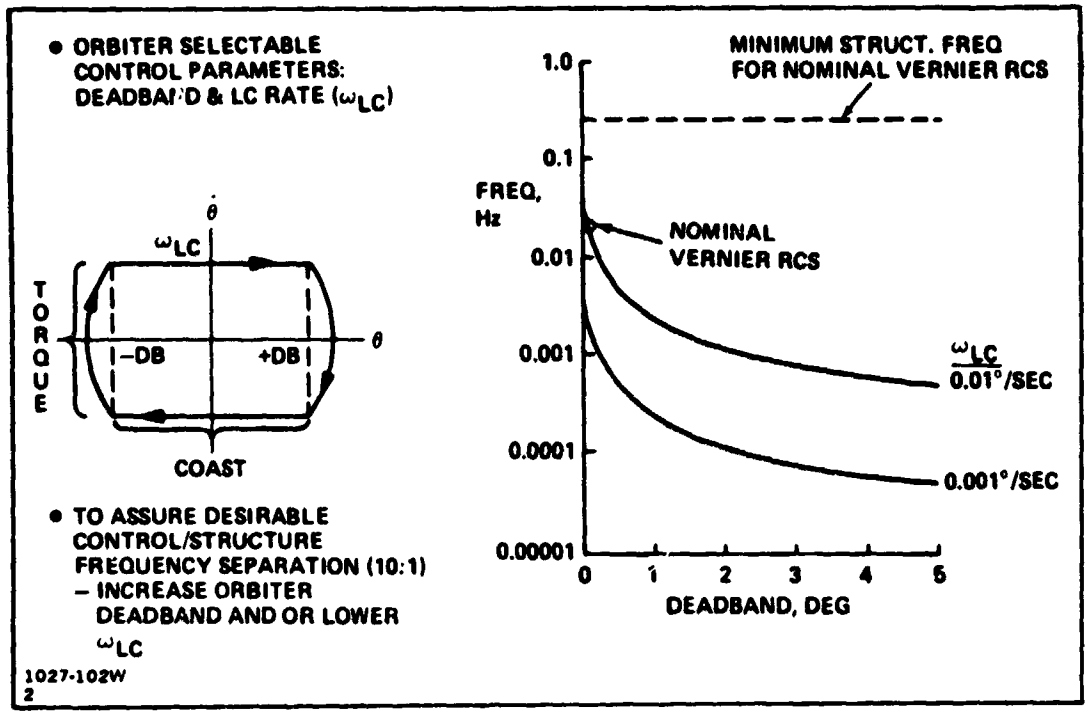

Fig. 5-44 Orbiter Control Capability

The lowest bending mode frequencies for the combined LSS Platform are close to the nominal control frequency, with adverse control/structural interaction possible. To increase the separation of frequencies to a desirable 10:1 range, the control frequency can be lowered by increasing the deadband and/or decreasing the limit cycle rate, both of which are selected parameters in the Orbiter's flight control computer.

The Orbiter's Vernier RCS capability was investigated relative to the needs of a typical seven day LSS construction mission. The VRCS system consists of only six thrusters with no redundancy. Failure logic in the flight computer automatically puts the system into free drift when a VRCS malfunction is sensed. The crew must then decide upon corrective action. Unless the failure can be repaired, control must ultimately be assumed by the primary thrusters. If large space structures are being constructed or assembled, this would require that the structure be jetisoned or disassembled to prevent damage. The lack of vernier thruster redundancy is thus a significant factor in the construction of LSS platform's from the Orbiter.

2

The current flight control capability of the Orbiter provides for a total of six programmed mass property configurations per mission within its onboard computer software. This consists of predetermined moment of inertia values and cg locations which are selectable by the crew as the mission progresses. The selection and evaluation of these steps, for an LSS platform construction mission, is recommended for future flight planning efforts.

Vernier RCS control capability as a function of mission time was investigated relative to two potential limiting factors: gas consumption and thruster duty cycle constraints. Thruster duty cycle constraints include:

- Minimum pulse width of 80 milliseconds
- Unspecified number of pulses per time-period
- TBD seconds cumulative on-time per mission
- Maximum TBD pulses per mission.

The useful life of the thrusters is specified as a minimum of 125,000 sec of operation and 500,000 cycles for 100 missions over 10 years. The operating time and number of cycles per mission have not been determined although typical values of 1500 sec and 10,000 cycles, respectively, are mentioned. These two sets of values were used to determine a range of mission time limits from thruster duty cycle constraints; the actual limit for a single mission should fall somewhere in this range.

The basic limit cycle control technique is illustrated (for one axis) in Fig. 5-45, with and without the presence of a bias disturbance torque. With no disturbance bias, the response is a symmetric limit cycle with equal plus and minus thruster firings. With a bias torque, single-sided operation occurs with only one thruster firing. In the former case, mission time limits are significantly affected by the selected limit cycle rate (ω_{LC}) and deadband (DB), as summarized in Fig. 5-45.

The analysis indicates that the Orbiter's mission time on orbit may be limited to less than seven days by RCS propellant constraints. From a propellant consumption point of view, this would apply for the case with zero bias torque with ω_{LC} = 0.01 deg/sec and DB = 0.1 deg... the Orbiter's nominal VRCS operating conditions. These same nominal VRCS conditions would result in a seven hour mission time limitation if the VRCS operating time is limited to 1500 sec per flight by thruster duty cycle constraints. Although the thrusters are certainly capable of operating beyond 1500 sec per mission, it is not reasonable to expect operation to the limit of their useful life in one flight.

2

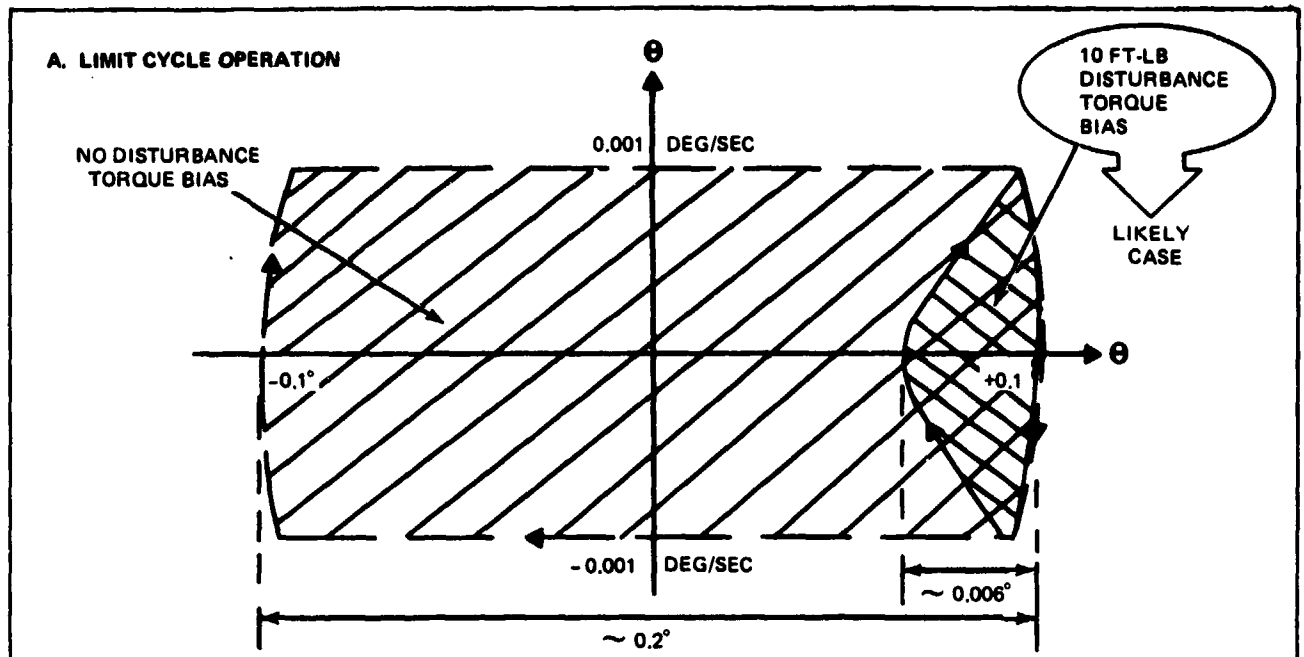

B. MISSION TIME LIMITS, DAYS

	SOURCE OF LIMIT							
	GAS CONSUMPTION*				THRUSTER DUTY CYCLE**			
ω_{LC}, DEG/SEC	0.01		0.001		0.01		0.001	
DB, DEG	1.0	0.1	1.0	0.1	1.0	0.1	1.0	0.1
BIAS TORQUE	102	102	102	102	6/500	6/500	6/500	6/500
ZERO BIAS TORQUE	67	7	5950	667	3/250	7 hr/23	260/59 yr	26/6 yr

RCS CONSTRAINTS MAY LIMIT MISSION DURATION

* 4000 LB PROPELLANT AVAILABLE (ONLY ONE AXIS CONTROL CONSIDERED).
** 1500 SEC/125,000 SEC CUMULATIVE FIRING TIME.

1027-103W
2

Fig. 5-45 Vernier RCS Control Capability

In the light of these potentially serious limitations in flight duration, a prime area for future study is RCS control, with further evaluation of VRCS system limitations and their impact on LSS construction from the Orbiter. Techniques for augmenting the capability of the Orbiter system may prove desirable.

The need for VRCS control relates to the preferred orientation of the Orbiter for LSS construction. From the point of view of construction lighting considerations, it is preferable to have the Orbiter's payload bay oriented relative to the earth so as

to make use of the diffuse reflected sunlight from the earth's atmosphere. With reference to momentum buildup implications, it is preferable to have the Orbiter's X-axis either perpendicular to the orbit plane or aligned with the local vertical. In view of these considerations the preferred Orbiter orientations for LSS construction are either X-POP with Z-LV or Y-POP with X-LV, and are illustrated in Fig. 5-46. VRCS operations will be needed to maintain these flight orientations to overcome the effects of aerodynamic disturbances and mass (cg) changes occurring during the LSS construction phase.

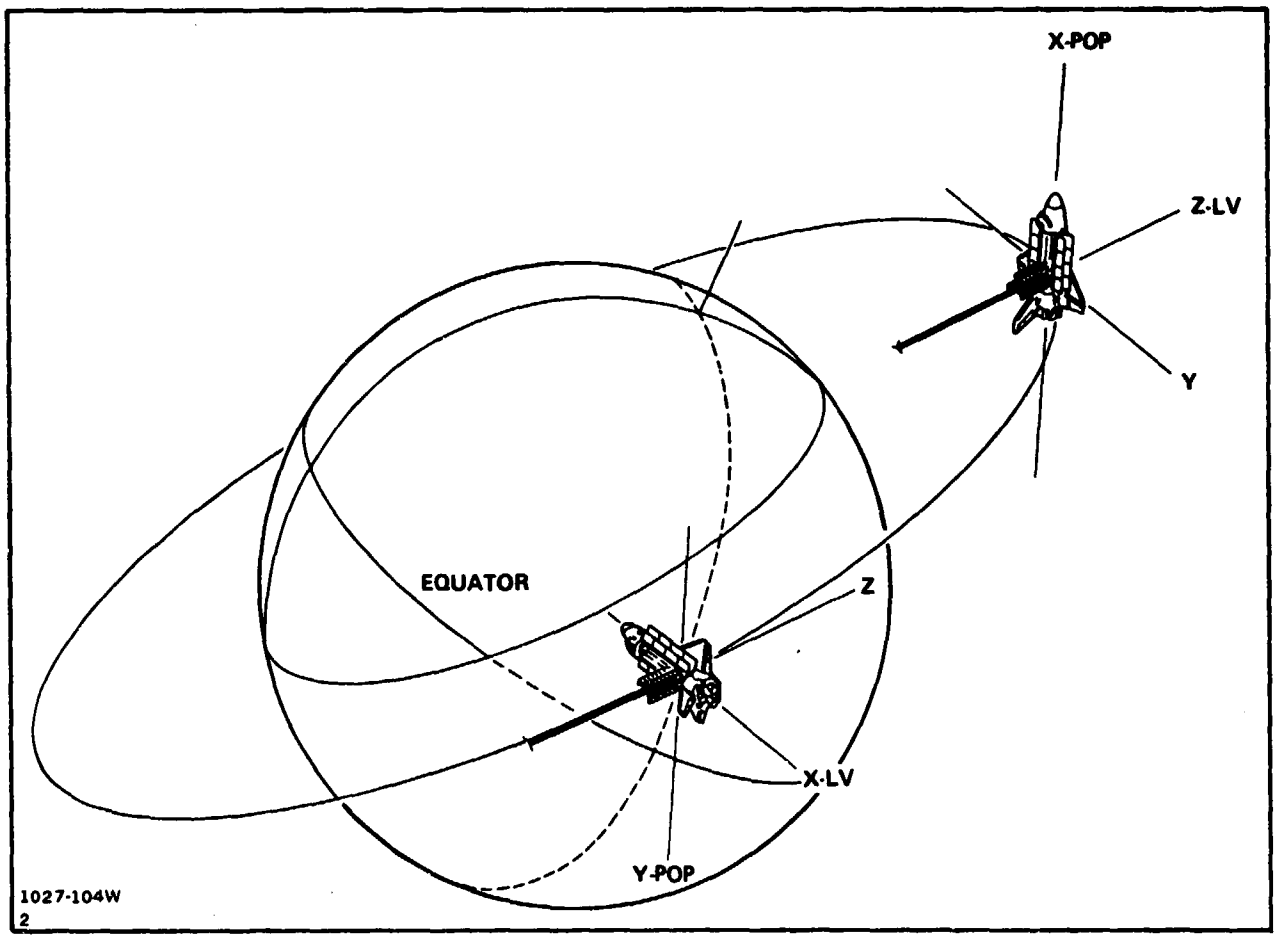

Fig. 5-46 Preferred Orbiter Orientations for LSS Construction

5.3 CONCEPT DEVELOPMENT - OBSERVATIONS AND RECOMMENDATIONS

5.3.1 Observations

Of the LSS demonstration options developed and evaluated during this study, those which appear suitable as LSS Demo "first steps" are the LSS Platform approach and its Structural Demonstrator adaptation. The LSS Platform is particularly appeal-

ing, as both an LSS demonstration can be performed and a useful, simple spacecraft system produced in the process. The simple Platform approach affords the ability to develop Orbiter-based construction expertise, conduct relevant on-orbit construction operations, and acquire subsystem/payload integration experience applicable to near-term Space Platforms. Further, the simplicity and minimal risk associated with the astroworker-erectable space fabrication approach makes it a viable candidate for a near-term Shuttle mission.

Analysis of the Orbiter as a construction base indicates that RCS control usage should be limited to the Vernier System, and that reductions in limit cycle frequency are favored to provide suitable control/structure frequency separation.

5.3.2 Recommendations

It is recommended that the simple, earth-oriented LSS Platform concept be further refined to maximize its user potential. Alternate payloads should be evaluated and larger fixed solar array approaches evaluated to extend the payload support capability of the platform. The platform's potential for growth should be considered, including approaches wherein the initial platform might become an initial element of a larger capability space platform.

A better understanding of the stabilization/pointing capabilities attainable with long booms/tip masses is needed to minimize the need for sophisticated altitude control equipments. Similarly, a better understanding of Orbiter plume impingement effects is needed to assess implications associated with deployment, retrieval, and reboost.

2

6 - DEMONSTRATION MISSION DEFINITION

The LSS Demonstration mission has two major groups of objectives, those related to the Automated Beam Builder (ABB) and those related to the LSS construction phase. The first group addresses ABB checkout and the structural verification of sample beams. LSS-related objectives deal with construction operations, verifying adequacy of analytical structural models and, in the case of the free-flier, the in-orbit construction of a usable spacecraft.

General guidelines applicable to the LSS Demonstration mission are:

- Minimize in-orbit hazards
- No space debris allowed
- Mission to be accomplished within a 7-day flight
- First day of mission is dedicated to space acclimation
- Four crewmen are utilized on a single shift basis
- Two crewmen planned for EVA activity
- Crew is cross-trained for construction tasks
- Adequate illumination is provided for mission activity
- RMS is used to support assembly activities.

6.1 MISSION REQUIREMENTS

6.1.1 ABB Test Requirements/Objectives

A summary of ABB test requirements/objectives is shown in Fig. 6-1. ABB verfication/checkout begins with activation and power-up of the machine. A number of start-ups will be attempted following soaking under varying thermal conditions. Beam fabrication tests are also planned under several solar conditions including the transition from sunlight to eclipse. In addition to ABB operations, the reloading of cannisters and magazines will be demonstrated to verify design suitability.

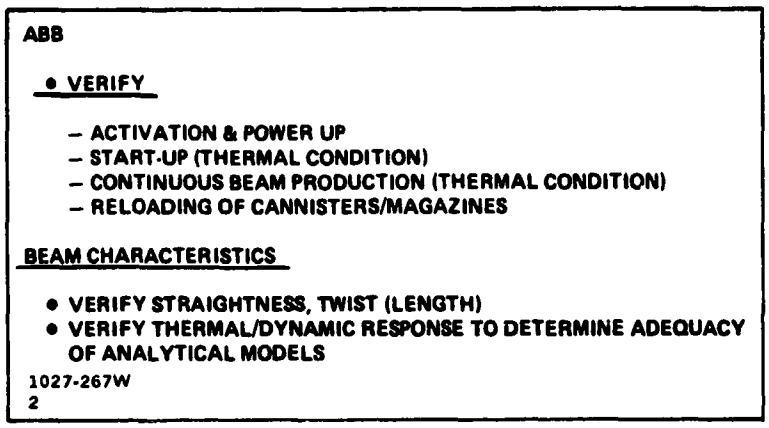

Fig. 6-1 ABB Test Requirements/Objectives

The 1-meter beams produced by the ABB will be checked for straightness and twist as functions of length. Thermal and dynamic response tests will be conducted to verify the adequacy of analytical models. The Space Fabrication Demonstration System Program (SFDS . . .ref: NAS8-32472) previously identified the need for four test beams in this initial flight test; two 9 m, one 39 m and one 90 m. This quantity of beams has been modified, however, as a consequence of this study effort, to accommodate both ABB checkout and LSS demonstration on a single Shuttle flight. The rationale for this change is illustrated in Fig. 6-2.

To accomplish the ABB-desired test operations would call for about 29 hours of EVA time. As the estimated allowable EVA time for a 7-day mission is about 33 hours, the time left for LSS demonstration activity would be on the order of four hours, and is clearly insufficient. Consequently, ABB test requirements were met in a different way from that described in the SFDS program. All beams fabricated by the ABB and used for beam tests are utilized as part of the LSS. This integration of program activity plus a modification of certain tests from EVA to non-EVA status results in an acceptable mission timeline (Refer to Subsection 6.3).

In addition to the planned in-flight tests, post-flight tests will be conducted on a returned beam sample to compare weld quality and overall structural characteristics to beams previously fabricated by the ABB on the ground during qualification testing.

6.1.2 LSS Test Requirements/Objectives

A summary of LSS test requirements/objectives is shown in Fig. 6-3. Testing associated with the LSS demonstration article is intended to investigate/evaluate construction operations, and the adequacy of analytical modeling techniques.

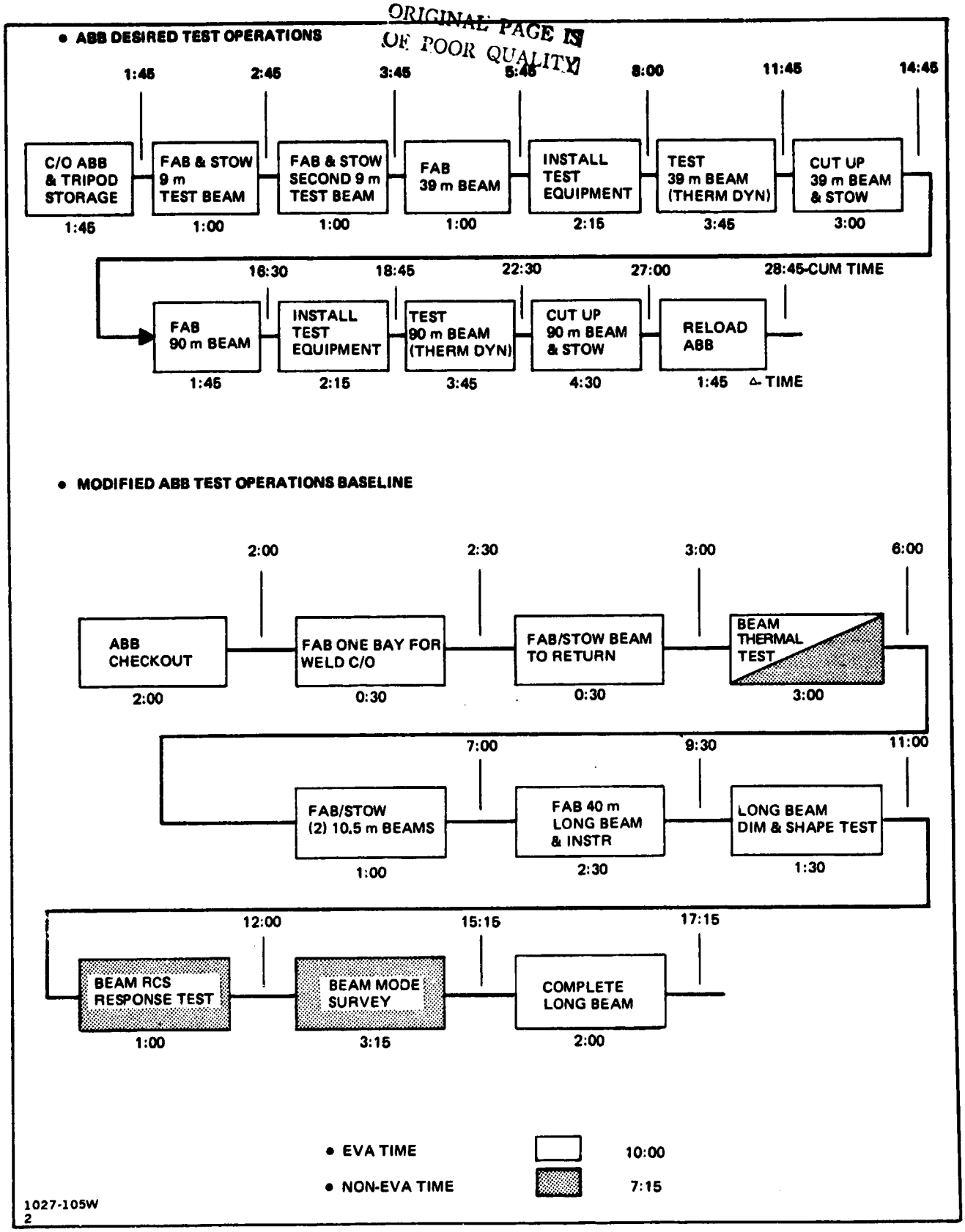

Fig. 6-2 ABB Verification Test Operations

2

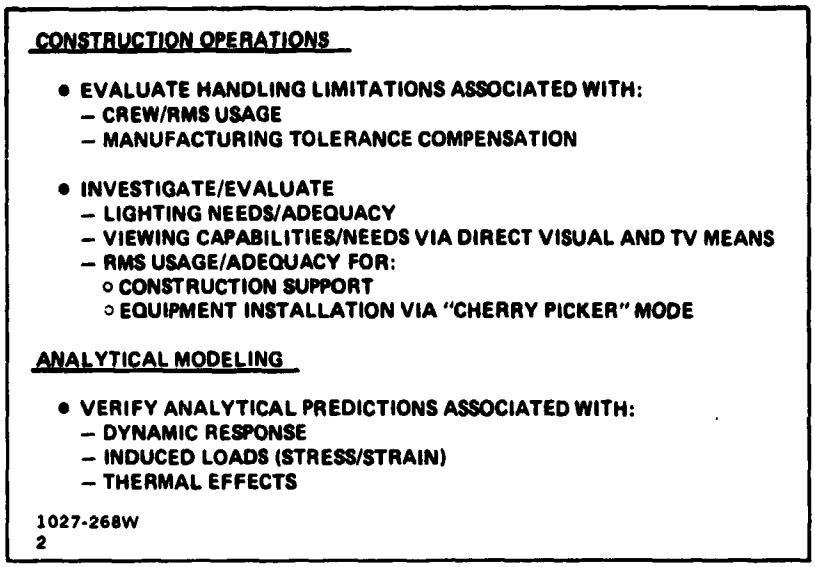

Fig. 6-3 LSS Test Requirements/Objectives

Construction of the LSS provides an opportunity for evaluating RMS usage associated with beam handling and assembly activities under space conditions. This capability will extend the EVA crewman's construction role. As shown in Fig. 6-4 and 6-5, the reach envelope achievable by an astroworker in an EVA suit is rather limited. These limitations must be considered in local situations when establishing an assembly scenario and when evaluating methods for equipment installation.

Lighting of the construction area, and the viewing needs of construction activity through Orbiter payload bay windows and TV monitors, must be evaluated. While these subjects can be studied on Earth via simulations, the actual shading conditions produced in space because of the absence of air and therefore, light diffusion, are difficult to duplicate.

A potential RMS mode of operation that appears useful for assembly activities is its use as a Cherry Picker or remote work station. Equipment installation and construction efforts should benefit from this capability, increasing in-space productivity and reducing astroworker timelines.

In-orbit tests of the LSS assembly will be conducted to verify analytical predictions associated with dynamic response, induced loads, and thermal effects. In addition to verifying analytical predictions associated with the LSS demonstration article, this information is needed to update analytical techniques/models associated with designs for "next generation" LSS missions. The types of thermal/structural data to be acquired are summarized in Fig. 6-6, along with candidate methods of structural excitation and instrumentation. Dynamic excitation is planned to be provided by a shaker, while

2

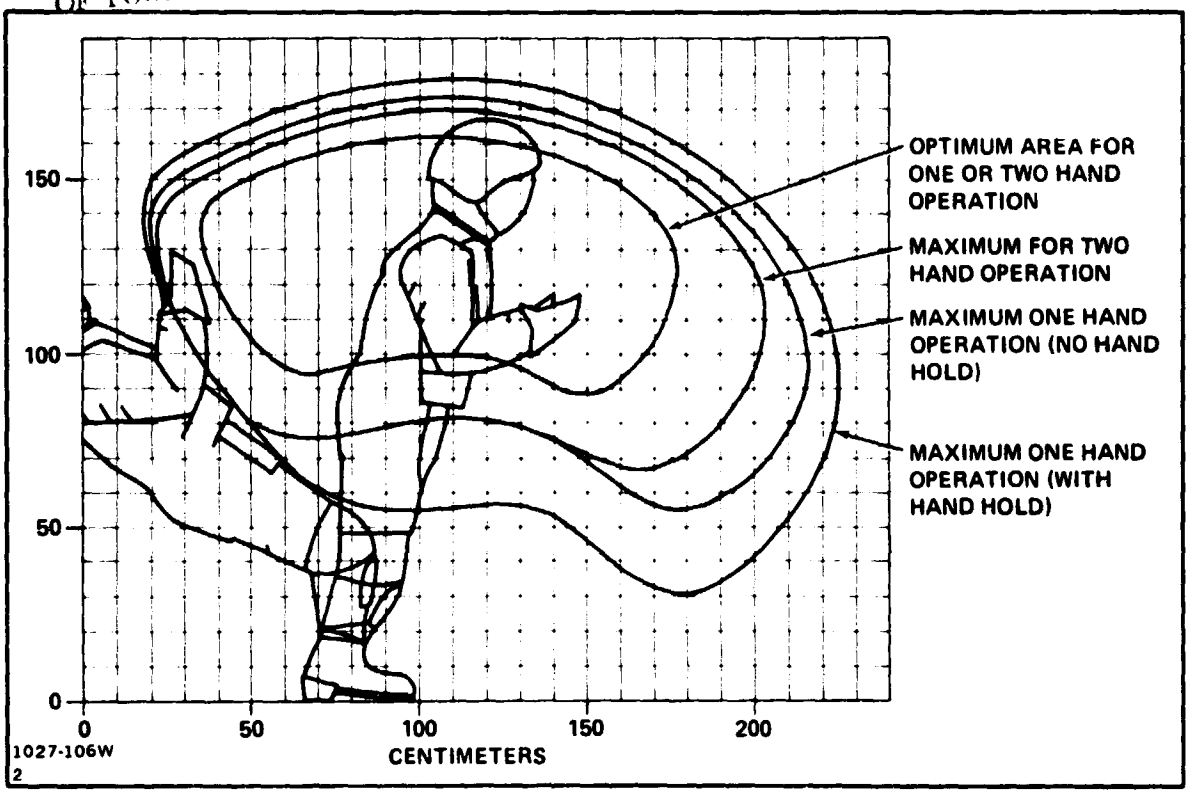

Fig. 6-4 EVA Reach Envelope – Fore & Aft

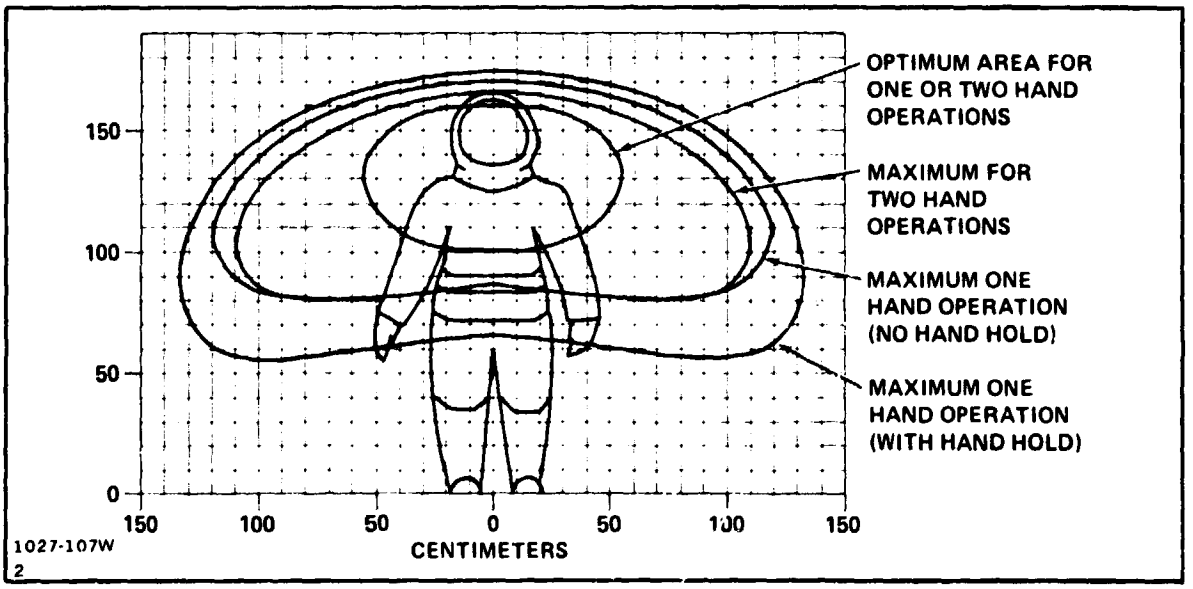

Fig. 6-5 EVA Reach Envelope – Lateral

thermal excitation is achieved by appropriate orientation of the 1-meter beam to the solar vector. It should be noted that the Orbiter's RCS firing will provide data for the demonstration article under load, while the use of the shaker will permit a complete mode survey to be performed under a broad spectrum of forcing frequencies. Instrumentation used, such as accelerometers and thermocouples, requires new installation techniques to minimize the time required for installation, and must be compatible with both the space and construction environment. Strain gage data will be obtained from a 10.5 m-long ground-fabricated/instrumented 1-m beam carried into space on the Orbiter.

	DATA REQUIREMENTS	CANDIDATE TECHNIQUES	
		EXCITATION	INSTRUMENTATION
DYNAMIC	NATURAL FREQUENCIES MODE SHAPES DAMPING COUPLING	SHAKER	ACCELEROMETERS
INDUCED LOADS	THERMALLY INDUCED STRAINS DYNAMICALLY INDUCED STRAINS BEAM HANDLING/ASSY	ORBITER ORIENTATION VRCS NORMAL ASSEMBLY	STRAIN GAGES* THERMOCOUPLES ACCELEROMETERS
THERMAL	GRADIENTS STRUCTURAL DEFLECTIONS	ORBITER ORIENTATION	THERMOCOUPLES OPTICAL

*GROUND FABRICATED/INSTRUMENTED 1-m BEAM

1027-108W
2

Fig. 6-6 In-Orbit Testing

6.2 FLIGHT TEST PROGRAM DEFINITION

Three groups of flight tests are planned for this mission as illustrated in Fig. 6-7. They are:

- Verification of both the ABB's operation and the quality of beam produced
- Determining the structural thermal and dynamic responses of the 1-m beam
- Platform assembly and handling techniques, and determining the Platform's structural response to dynamic and thermal stimuli.

The requirements for 1-meter beam and Tribeam structural testing are provided in Appendix D. These requirements are reflected within the overall flight test program discussed herein.

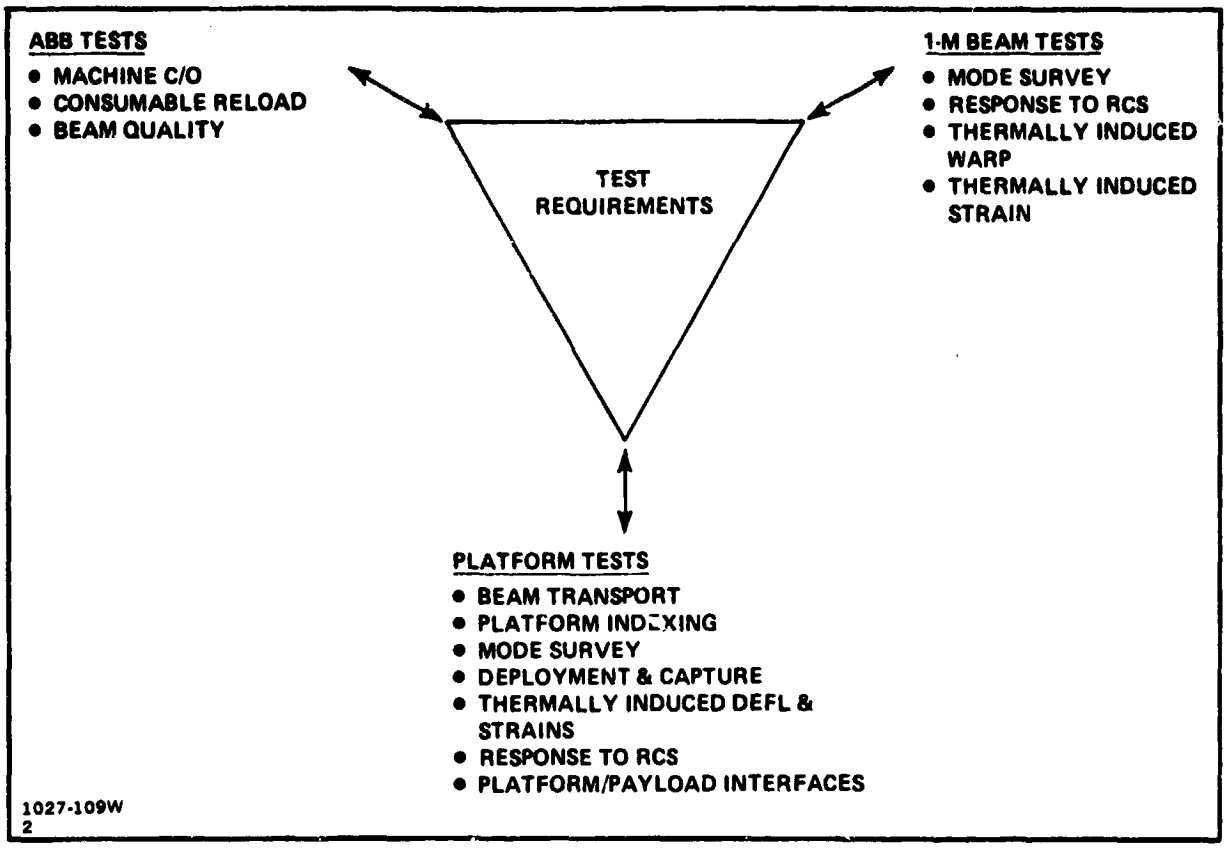

Fig. 6-7 Flight Test Program Definition

6.2.1 One-meter Beam Tests

Flight tests involving 1-m beams will be accomplished using two specimens made by the ABB, one fabricated in space and one on the ground. A ground-fabricated 1-m beam is suggested in order to appropriately instrument the structure with strain gages. The instrumented test beam will be used to determine magnitudes of thermal induced strains associated with various solar orientations. This recommended baseline flight test approach, of fabricating and instrumenting a 1-m test beam on the ground prior to the mission, will yield strain gage data in flight without the program incurring costs for in-space gage installation development. The 1-m beam will be tested both individually and as a member of the LSS platform assembly.

Instrumentation on the ground-fabricated beam is shown in Fig. 6-8 and consists of the following:

- Six accelerometers mounted in three locations to be used in Beam Transport tests as well as Platform Indexing and Deployment/Capture tests
- 36 thermocouples mounted in the end bays and center bay, to be monitored while conducting thermally-induced strain testing

- 30 strain gages mounted in the end and center bays to record thermally induced strain
- An Instrumentation Data Acquisition Package (IDAP) which includes power, signal conditioning, and transmitter with appropriate channels.

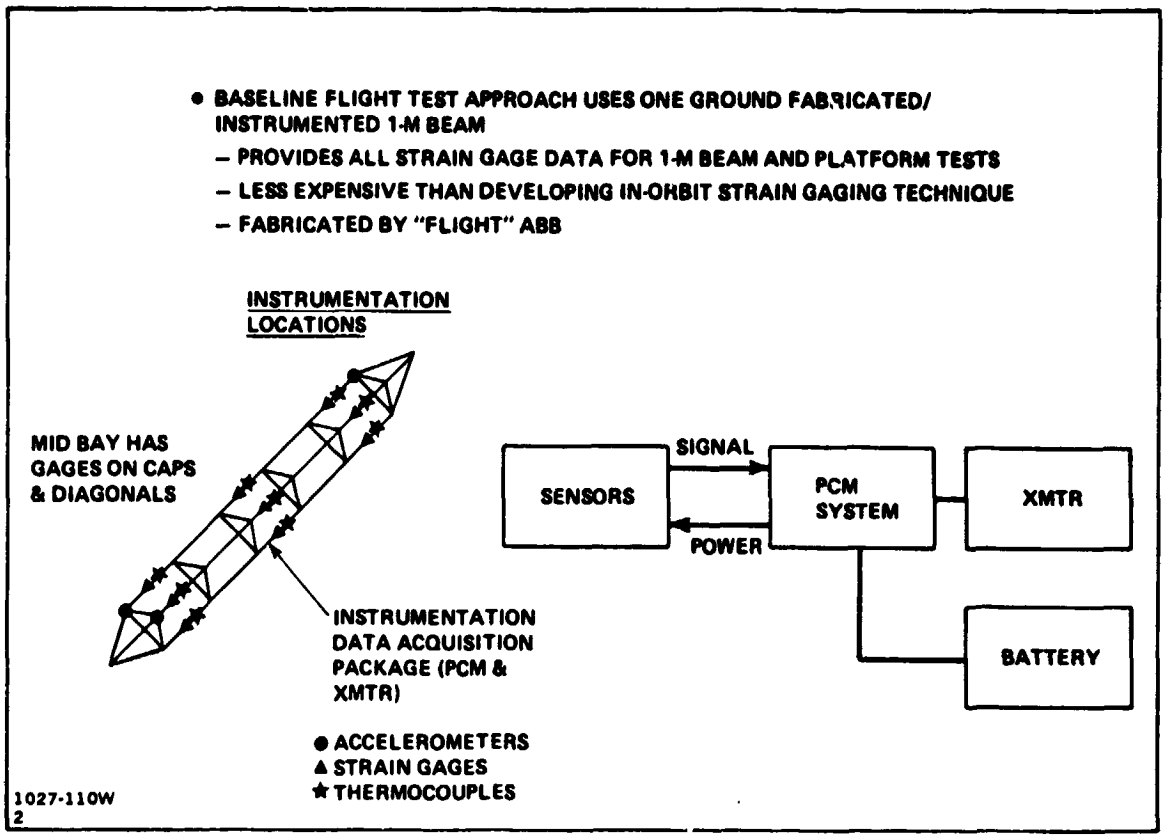

Fig. 6-8 One-Meter Ground Fabricated Beam - Measurement Description/Placement

A space fabricated beam will be tested while attached to the ABB. Tests of beam warp and twist as a function of thermal conditions, will be conducted on this beam. In addition, mode survey data concerning mode shapes, frequencies and structural damping as well as beam response to RCS firing will be gathered from this test specimen.

In-flight testing of the 1-m beams begins with a test to determine the magnitude of strains produced by selected thermal conditioning. The ground fabricated/instrumented beam will be mounted in the payload bay as shown in Fig. 6-9 producing a fixed-free set of end constraints. The Orbiter's orientation will be programmed to produce the following beam test conditions:

2

- Nominal sunlight
- Occulted
- Transition from sunlight to darkness
- One beam cap shading another.

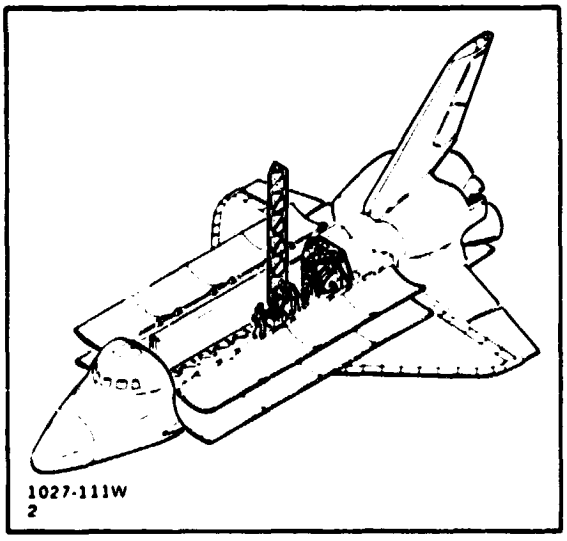

Fig. 6-9 One-Meter Beam Thermal Test

The next series of 1-m beam tests uses a 40-meter space fabricated beam attached to the ABB as shown in Fig. 6-10. This beam is instrumented with accelerometers, thermocouples and optical reflectors for deflection measurements. A dimensional check of the beam will be made using optical instrumentation to determine length, bending and twist changes as functions of thermal conditioning. Tracking theodolites attached to the ABB are planned to be used for these measurements.

This same beam will then be subjected to loads induced by the Orbiter's VRCS. Excitations will be in the following Orbiter reference directions and last for approximately two seconds.

- ± y and + z translation
- ± pitch, roll and yaw rotation.

Data will be recorded from the 25 accelerometers mounted to the beam. A small shaker (2-5 pound force range) will be mounted on the beam to perform the next test which is a model survey. A sinusoidal sweep will be made (0.1 Hz to 10 Hz) to determine resonant response peaks. Modal displacement data will be obtained during resonant dwells and damping will be determined from response decays after shaker cutoff. The Orbiter should be in a drift mode to minimize thruster inputs during the times when data is recorded.

2

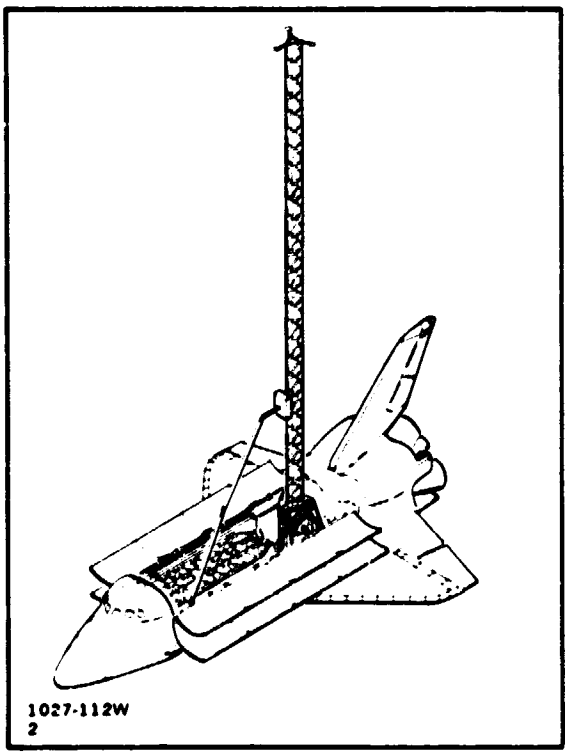

Fig. 6-10 Forty-Meter Beam Structural/Dynamic Test

6.2.2 LSS Platform Tests

LSS-related tests begin with a series designed to determine applied loads induced in the beams during construction activities. Two categories are planned, one using the Remote Manipulator System (RMS) as the beam transporter and the other using crewmen.

As shown in Fig. 6-11, the RMS with appropriate end-effector will capture the ground fabricated/instrumented beam near its center and perform a series of transports. Both coarse and vernier RMS translation/rotation modes will be tested as follows:

- Pure translation (0 - 2.0 ft/sec - coarse)
  (0 - 0.2 ft/sec - vernier)
- Pure rotation (0 - 4.76°/sec - coarse)
  (0 - 0.476°/sec - vernier).

During one transport, the RMS and beam will be stopped and held in an intermediate position. The Vernier RCS will be fired to produce pure roll, pitch and yaw.

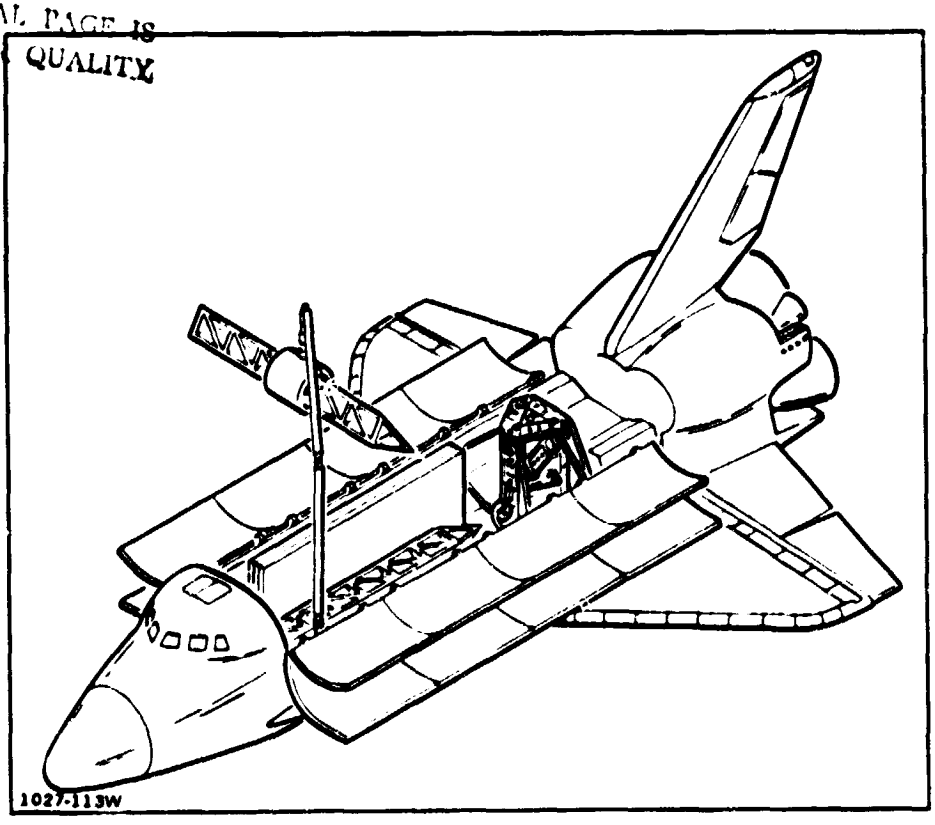

Fig. 6-11 RMS Beam Handling Test

A similar test will be conducted using two crewmen in Manned Maneuvering Units (MMU) for beam transport. Initially, one astronaut will pick up the ground fabricated beam near its center and perform the following maneuvers:

- Pure translation (0.3 ± 0.05 ft/sec^2)
- Pure rotation (10.3 ± 3 °/sec^2)
- Hover (60 sec).

Using two crewmen, one at each end of the beam, the above sequence of events will be repeated. Figure 6-12 illustrates this test.

The next test related to the LSS Platform measures its response to Vernier RCS firings. While still attached to the ABB, the platform assembly will be subjected to:

- ± y and + Z translation
- Pitch, roll and yaw rotation.

The excitations should be applied for approximately two seconds to produce a step input. Data will be gathered from accelerometers mounted at beam joints and on the center boom. Figure 6-13 illustrates the test configuration.

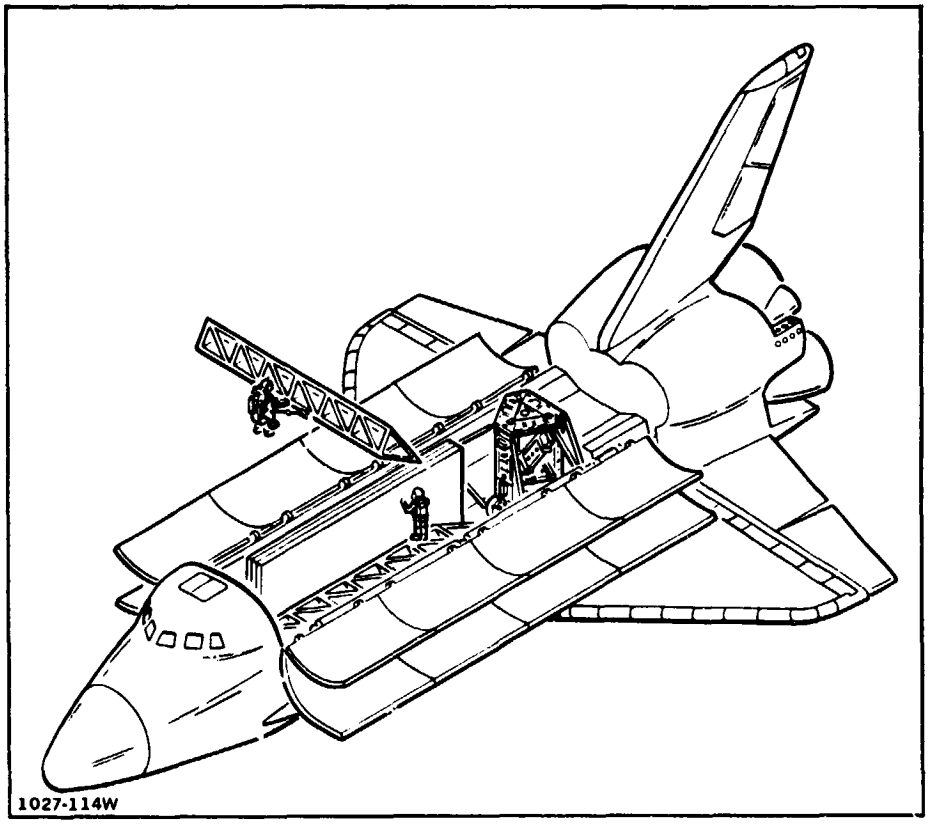

Fig. 6-12 Crewmen Beam Handling Test

A test of the overall LSS is planned to determine thermal response of the one-meter beams in an assembly. The data from this test, as in the case for the single beam thermal test, will be used to verify and update current thermal models. Reactions to predetermined solar orientation will be examined. Sunlight blockage and non-blockage cases will be tested as well as the transient conditions entering and leaving occultation. Data gathered from this series will consist of the following:

- Optical measurements of selected points on the structure
- Strain in the ground fabricated beam as a function of temperatures throughout the assembly.

A modal survey of the LSS Platform will be performed to determine mode shapes, frequencies, and structural damping of the overall assembly. Results of this survey will verify mathematical structural models which are necessary to predict the response of future LSS designs. The same shaker used for the single beam mode survey will be mounted to the LSS platform assembly by the RMS, as shown in Fig. 6-14. Resonant

2

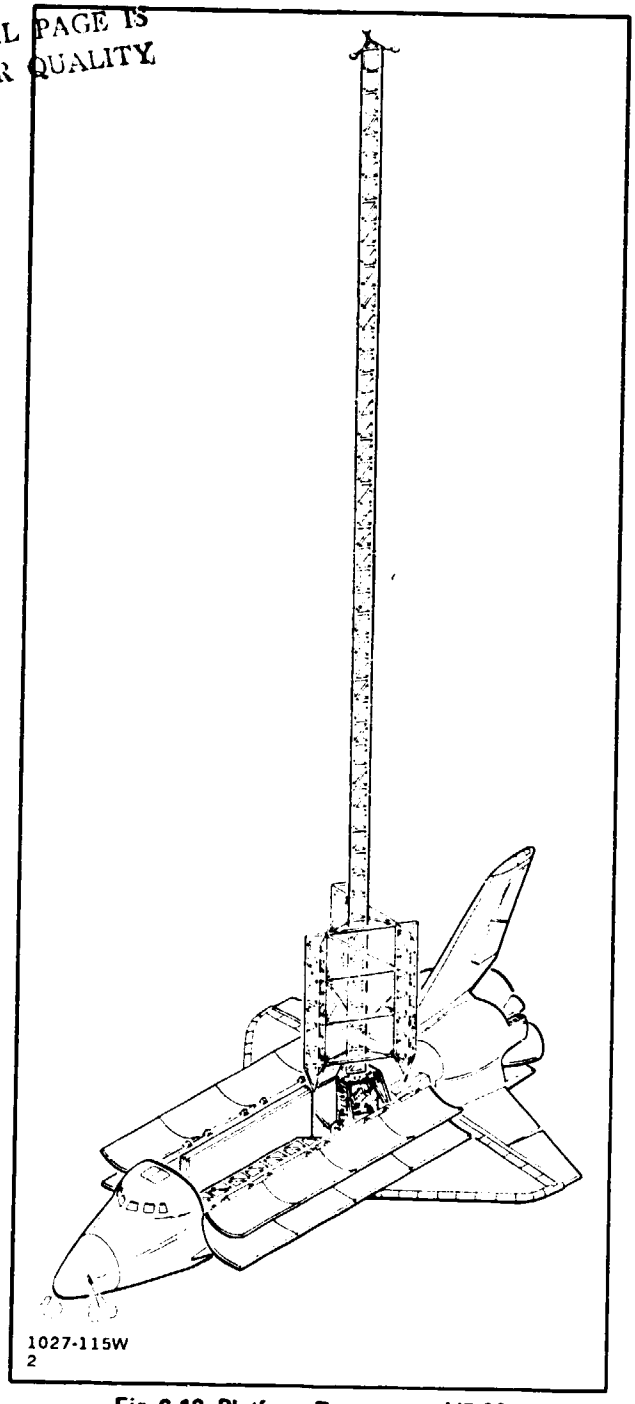

Fig. 6-13 Platform Response to VRCS

2

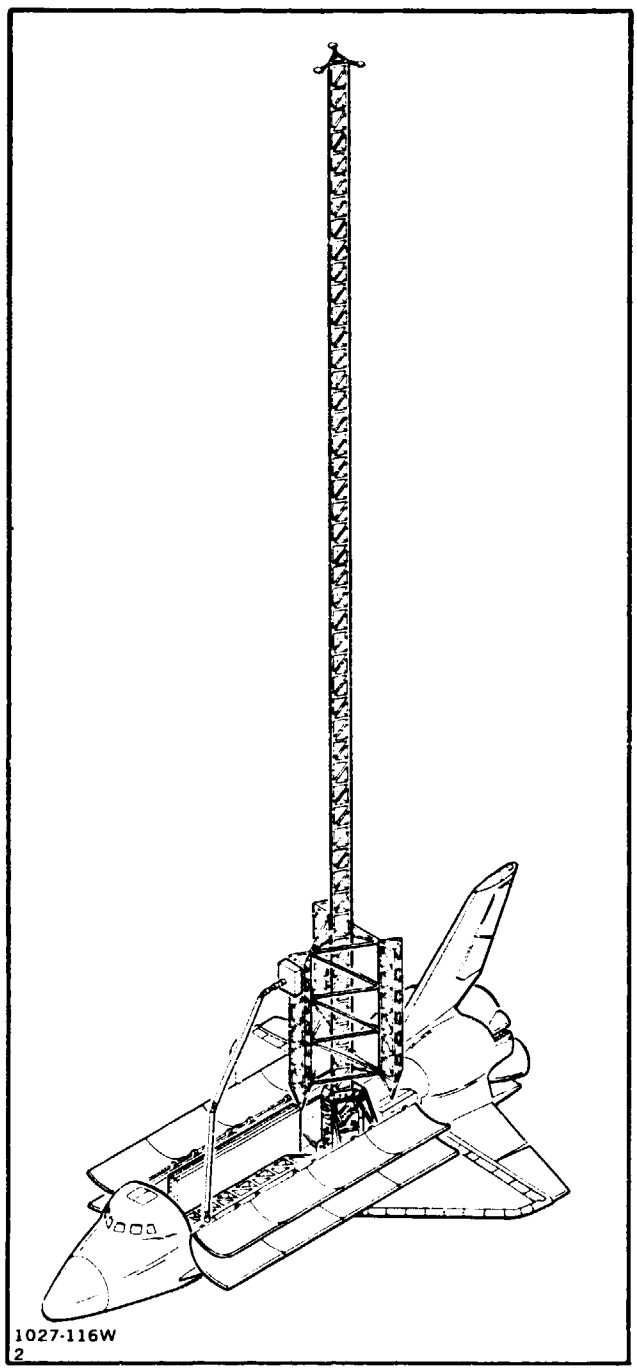

Fig. 6-14 LSS Modal Survey

peaks will be determined by sinusoidal sweeps between 0.05 and 10 Hz. Model displacements will be measured during dwells at resonant frequencies and damping will be determined from response decays after shaker cutoff. As in the single beam mode survey, the Orbiter should be in a free-drift mode to eliminate thruster inputs during times when data is recorded from accelerometers mounted at beam joints and on the center boom. The test will be conducted in both sunlight and darkness to check the effect of temperature transients.

Another test that is planned to determine handling loads induced in the LSS is one which goes through the deployment, capture, and berthing cycle (Fig. 6-15). Accelerometers installed for the previously-conducted dynamic tests will be monitored during this operation, and the data transmitted to the Orbiter. After berthing the platform, a servicing/replacement series of tests will be conducted on the experiments mounted to the LSS. This will verify and help refine operational procedures for revisits.

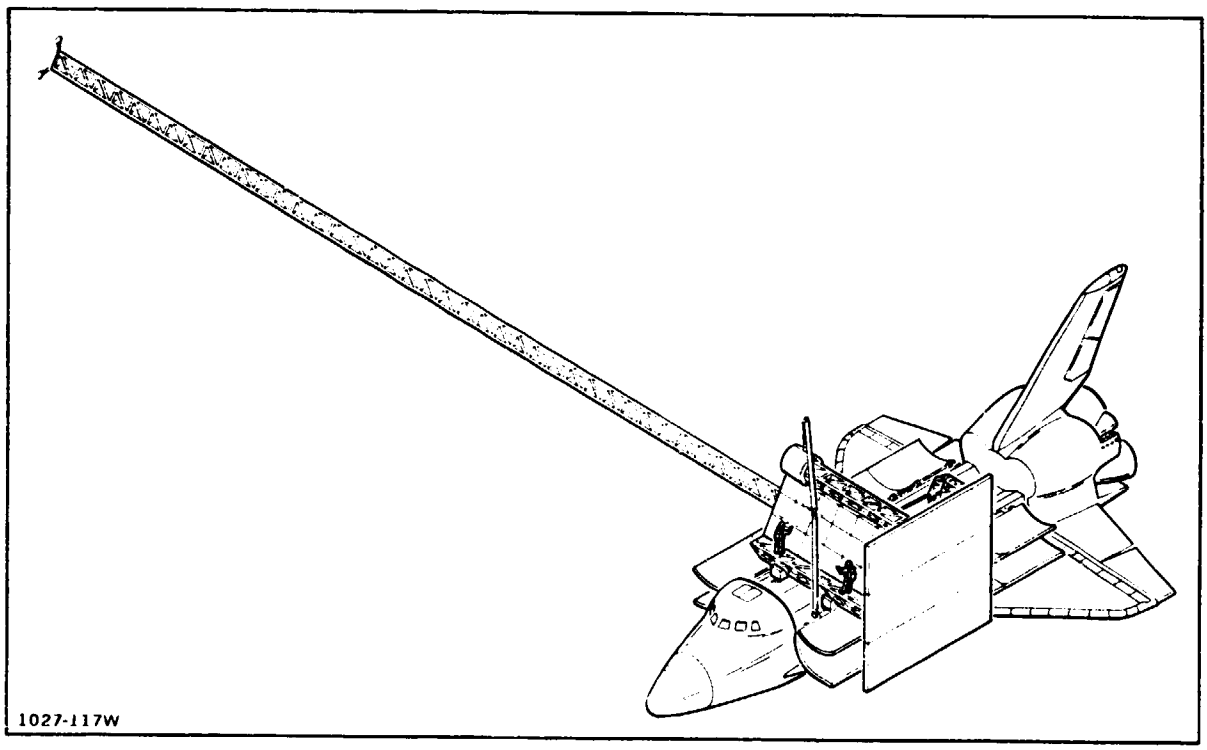

Fig. 6-15 Berthing and Experiment Servicing

6.3 LSS PLATFORM FLIGHT OPERATIONS

The free-flier option of the LSS flight demonstration has the following major goals:

- Verification of both the ABB's operation and the quality of beam produced

- Verification of structural thermal and dynamic responses as well as assembly and handling techniques for both 1-m beams and the LSS
- Assembly and deployment of a usable spacecraft.

These goals were used to define mission tasks which in turn were scheduled to satisfy both test and assembly requirements. The guidelines used in establishing the task sequence are the same as those mentioned in Subsection 6.1, namely:

- Minimize in-orbit hazards
- No space debris allowed
- Mission to be accomplished within a 7-day flight
- First day of mission is dedicated to space acclimation
- Four crewmen are utilized on a single shift basis
- Two crewmen planned for EVA activity
- RMS is used to support assembly activities
- Adequate illumination is provided for mission activity
- Crew is crosstrained for construction tasks.

Figure 6-16 shows a timeline of the task sequence that was developed; Figures 6-17 through 6-19 illustrate the activities conducted during Day 2 through 7. The first day is dedicated to launch activities and space acclimation. Mission activities on day 2 begin with an EVA to checkout the ABB and 1-m beam weld quality. Following this, a beam is fabricated and stored in the payload bay for return to Earth and post-flight testing. The final EVA for the day sets up the ground fabricated/instrumented 1-m beam for a test to determine thermally induced strain levels. This test is conducted after the EVA period. The RMS and 1-m beam transport test concludes activities for the day.

The first task of Day 3 is another handling test, this time with crewmen maneuvering the ground-fabricated 1-m beam. Remaining EVA for that day is dedicated to fabricating beams, two of them 10.5-m long and the last being a 40-m length of the center boom. Two tests are subsequently conducted on the 40-m long beam while still attached to the ABB. These tests are scheduled as non-EVA time.

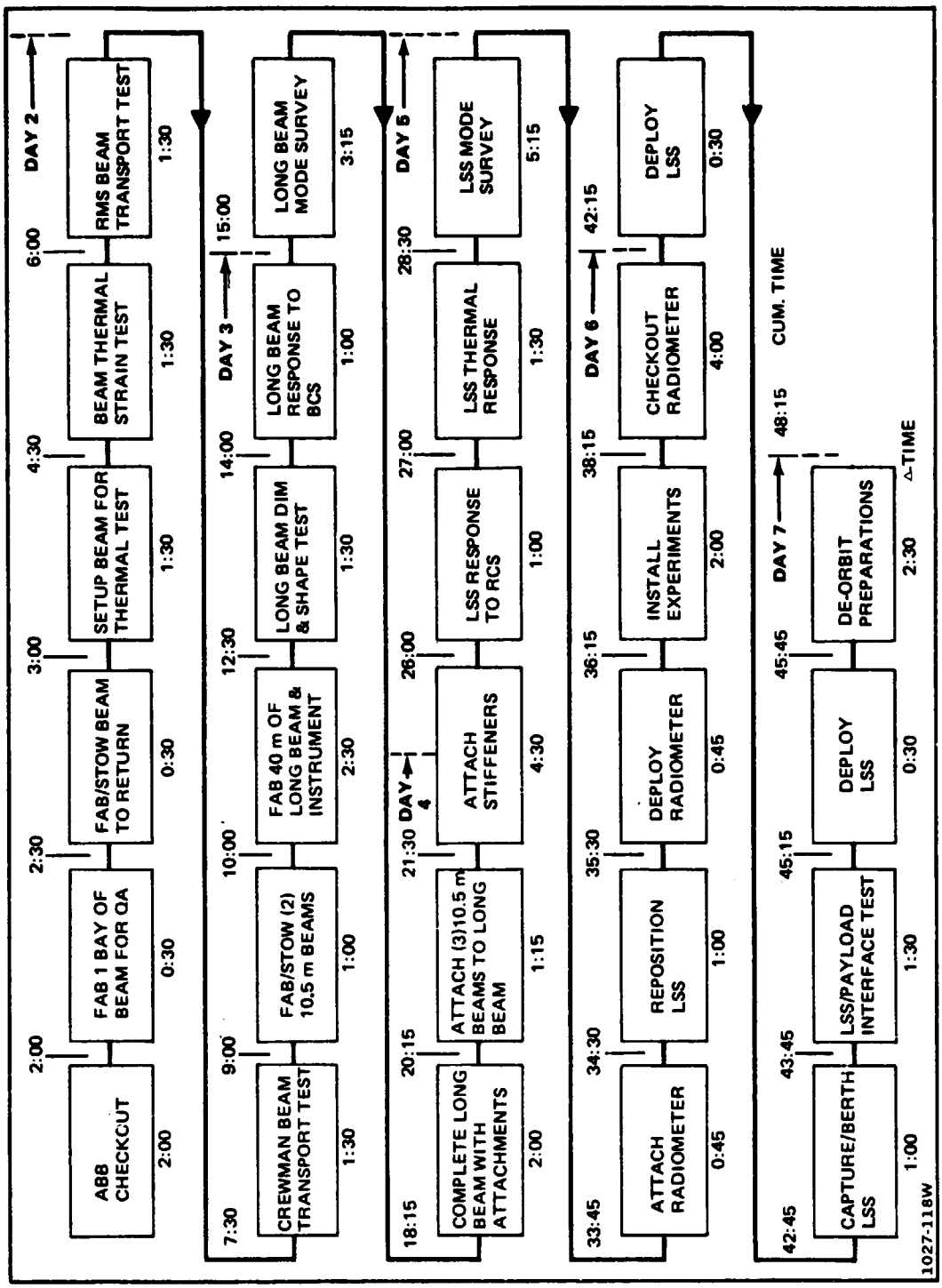

Fig. 6-16 Flight Sequence - Free-Flier Option

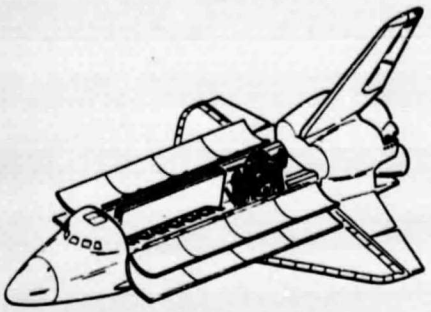

ABB CHECKOUT

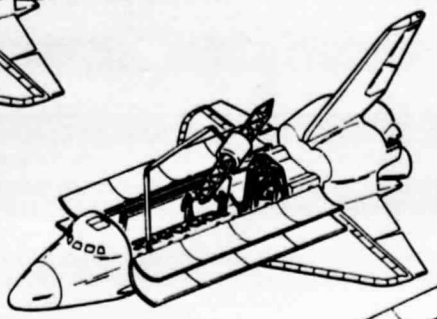

BEAM STOWED
FOR RETURN

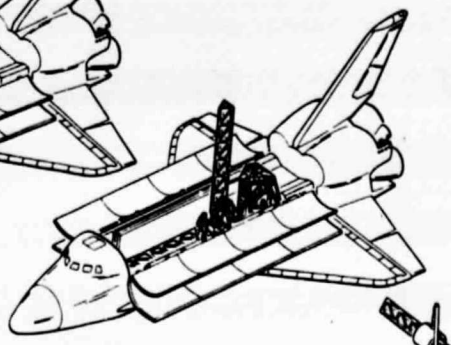

THERMAL TEST
SET-UP

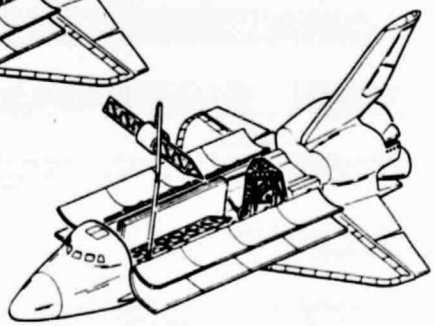

RMS TRANSPORT
TEST

CR
TES

DAY 2

1027-119W
2

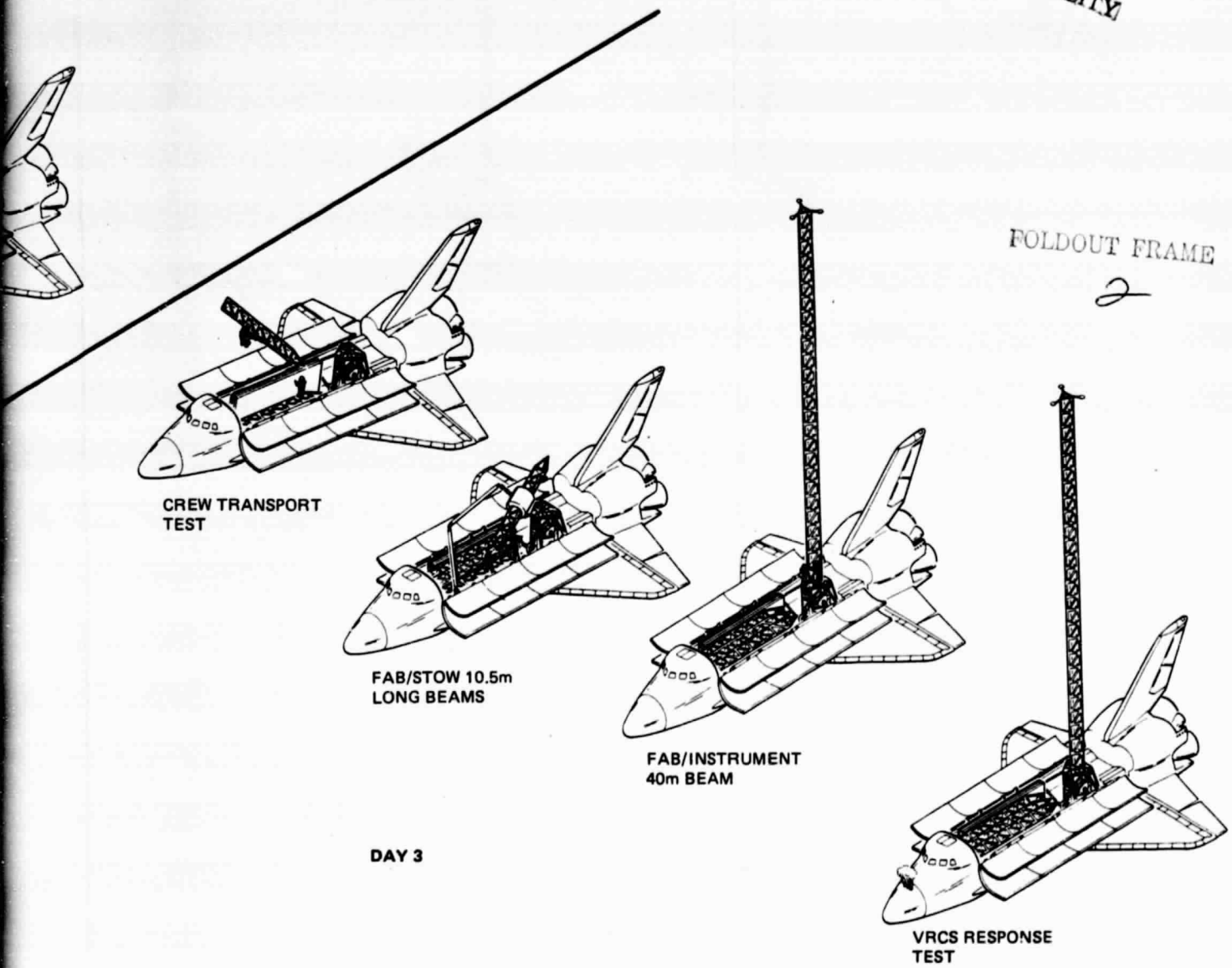

DAY 3

Fig. 3-6 Mission Activity – Day 2 and 3

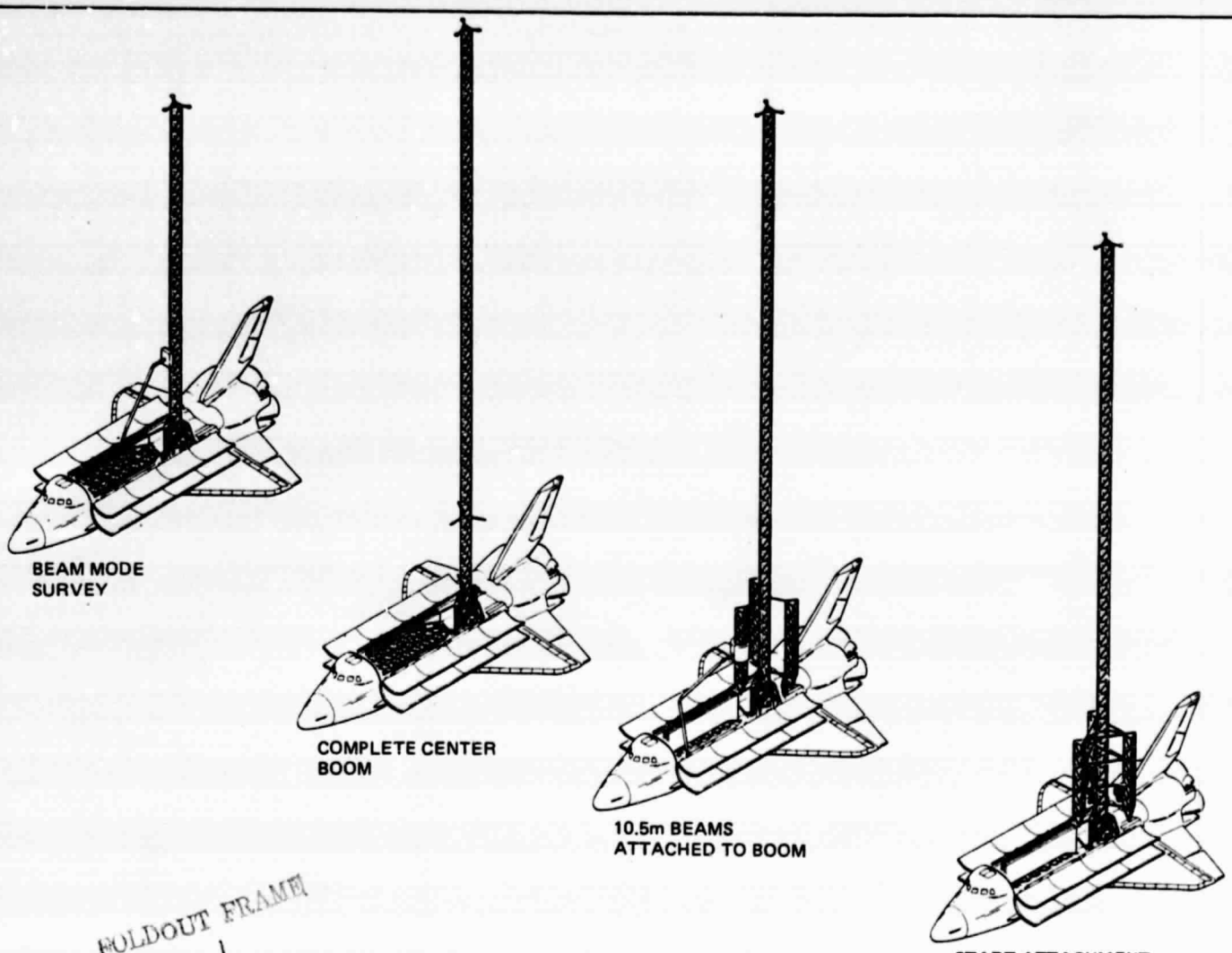

FOLDOUT FRAME

ORIGINAL PAGE IS
OF POOR QUALITY

DAY 4

1027-120W
2

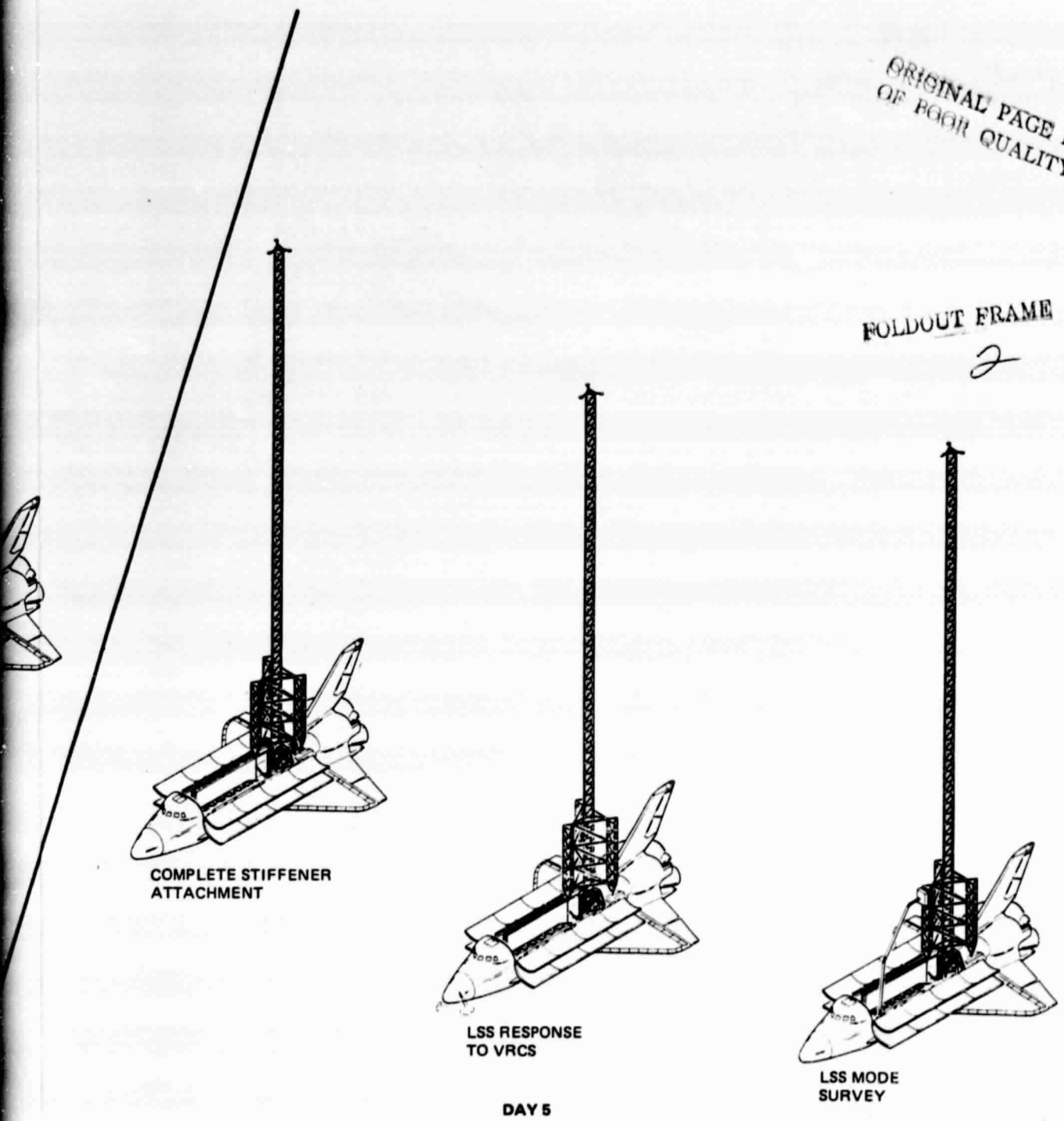

Fig. 3-7 Mission Activity – Day 4 and 5

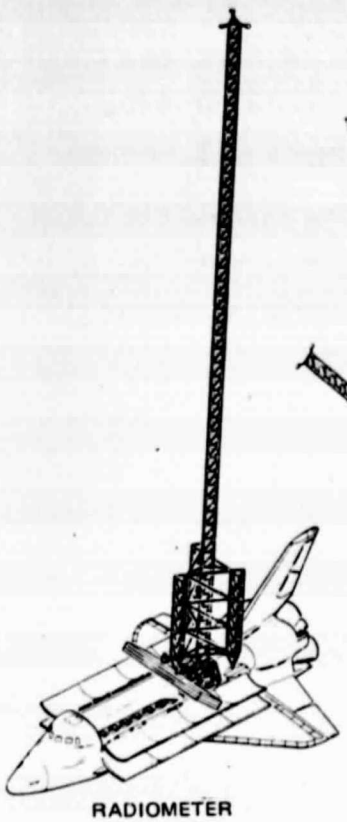

RADIOMETER
ATTACHED

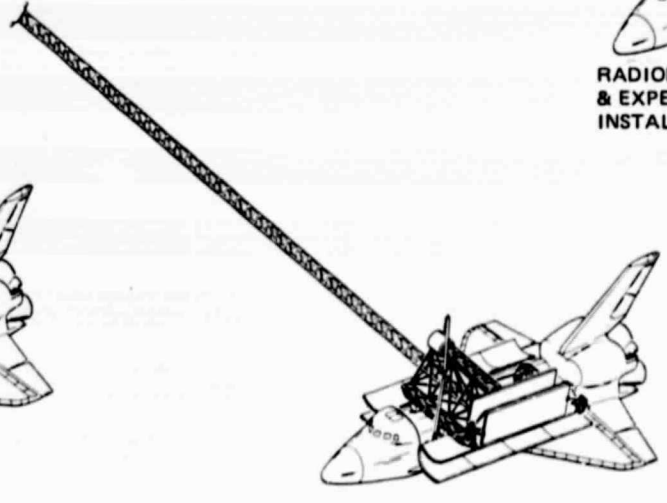

LSS REPOSITIONED

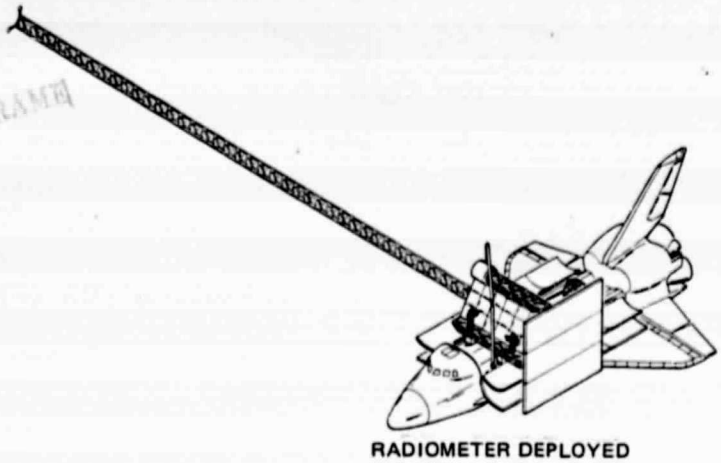

RADIOMETER DEPLOYED
& EXPERIMENT RACKS
INSTALLED

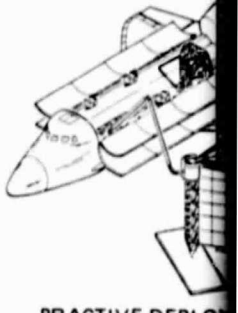

PRACTIVE DEPLO
CAPTURE

DAY 6

1027-121W
2

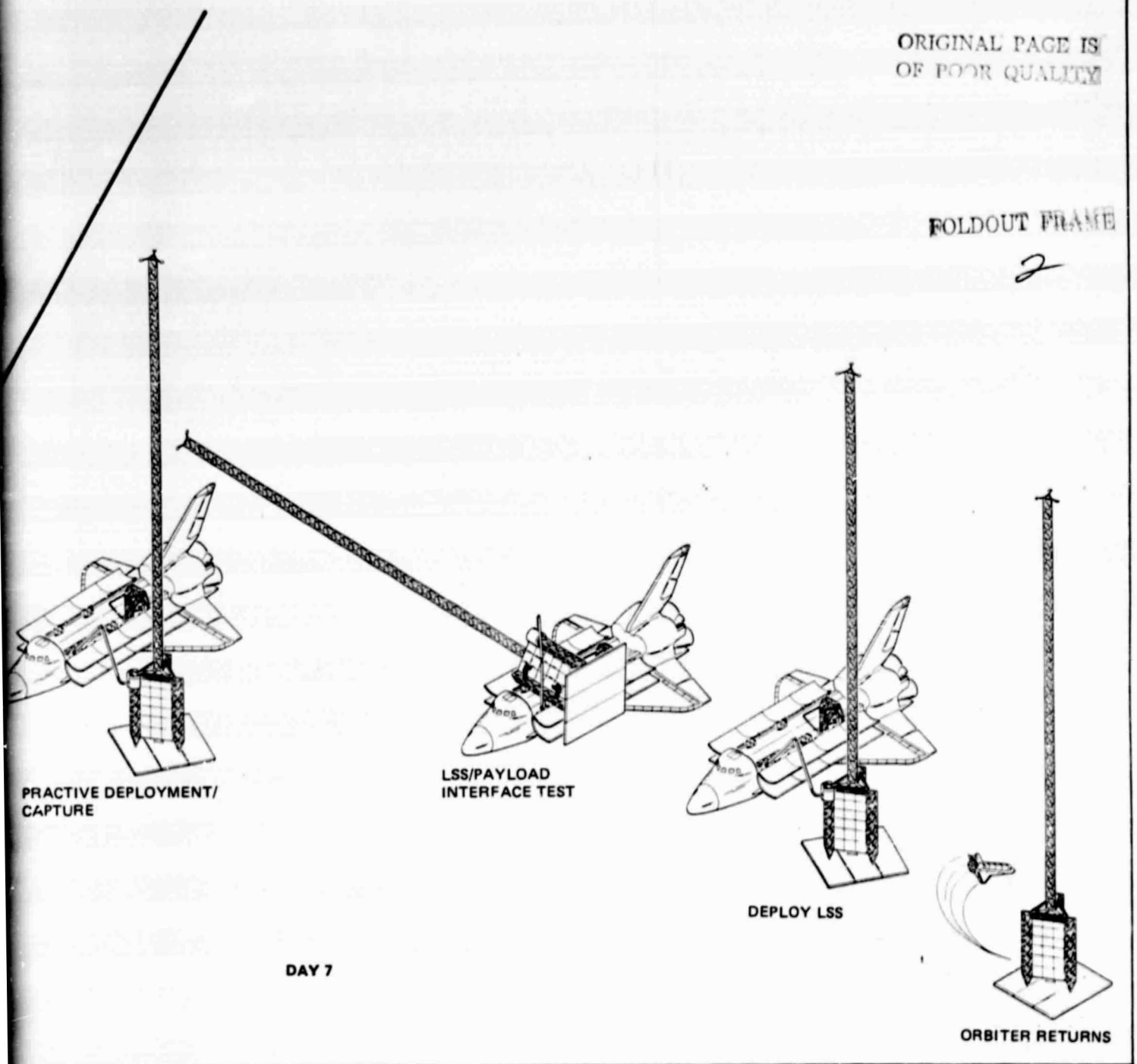

Fig. 6-17 Mission Activity – Day 6 and 7

Day 4 activity begins with a non-EVA mode survey of the 40-m beam. The rest of the day's tasks are all EVA and are involved with assembly of the LSS. All of the Tribeam stiffeners cannot be installed on Day 4, however, because of EVA-duration limitations.

Assembly of the structure is completed on Day 5, followed by three tests of the LSS while it remains attached to the ABB. Day 6 EVA activities involve re-positioning the LSS and attaching both the radiometer and experiments to the basic structure. The radiometer is checked out after the crew returns to the Orbiter cabin.

The final day of the flight starts with a practice deployment, capture, and berthing of the LSS. This is followed by an EVA test verifying satellite servicing procedures. The crew then enter the Orbiter for final LSS deployment and de-orbit.

Figure 6-20 summarizes the EVA and non-EVA hours required to perform the tasks identified in Fig. 6-16. As noted, the maximum EVA duration (5 hr) occurs on Day 3. This level was used as a limit in our planning, although 6 hr is presently considered acceptable, to allow for any contingencies.

DAY	EVA HOURS	NON-EVA HOURS
1	LAUNCH & SPACE ACCLIMATION	
2	4.5	3
3	5	2.5
4	4.25	3.25
5	3.5	7.75
6	4.5	4
7	2.5	3.5
TOTAL	24.25	24.0
1027-122W 2		

Fig. 6-20 Summary of Daily EVA & Non-EVA Hours Required for LSS Free-Flier Option

The daily crew timelines for the free-flier option are shown in Fig. 6-21. The EVA crew have about 11 hours between scheduled meals, which is a very undesirable situation. Previous space experience has demonstrated that one cannot go as long in zero-g without eating as compared to 1-g, particularly during the early part of the mission. One becomes hungry faster and feels the effects of hunger quicker (i.e., fatigue, irritability and overall inefficiency). It is assumed that bite-size snacks would be made available in the air lock prior to EVA, and that an in-suit drink is provided.

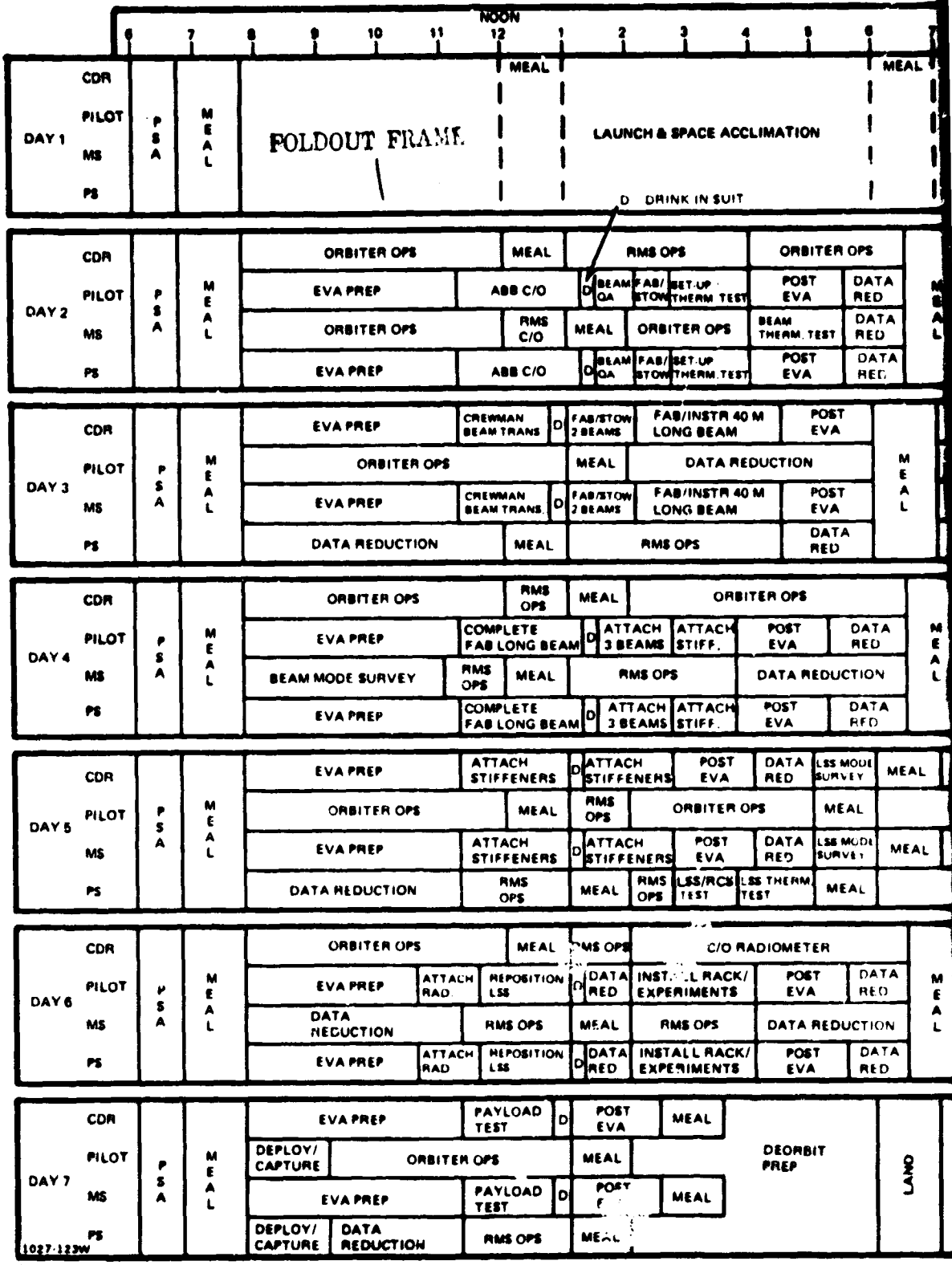

1027-123W

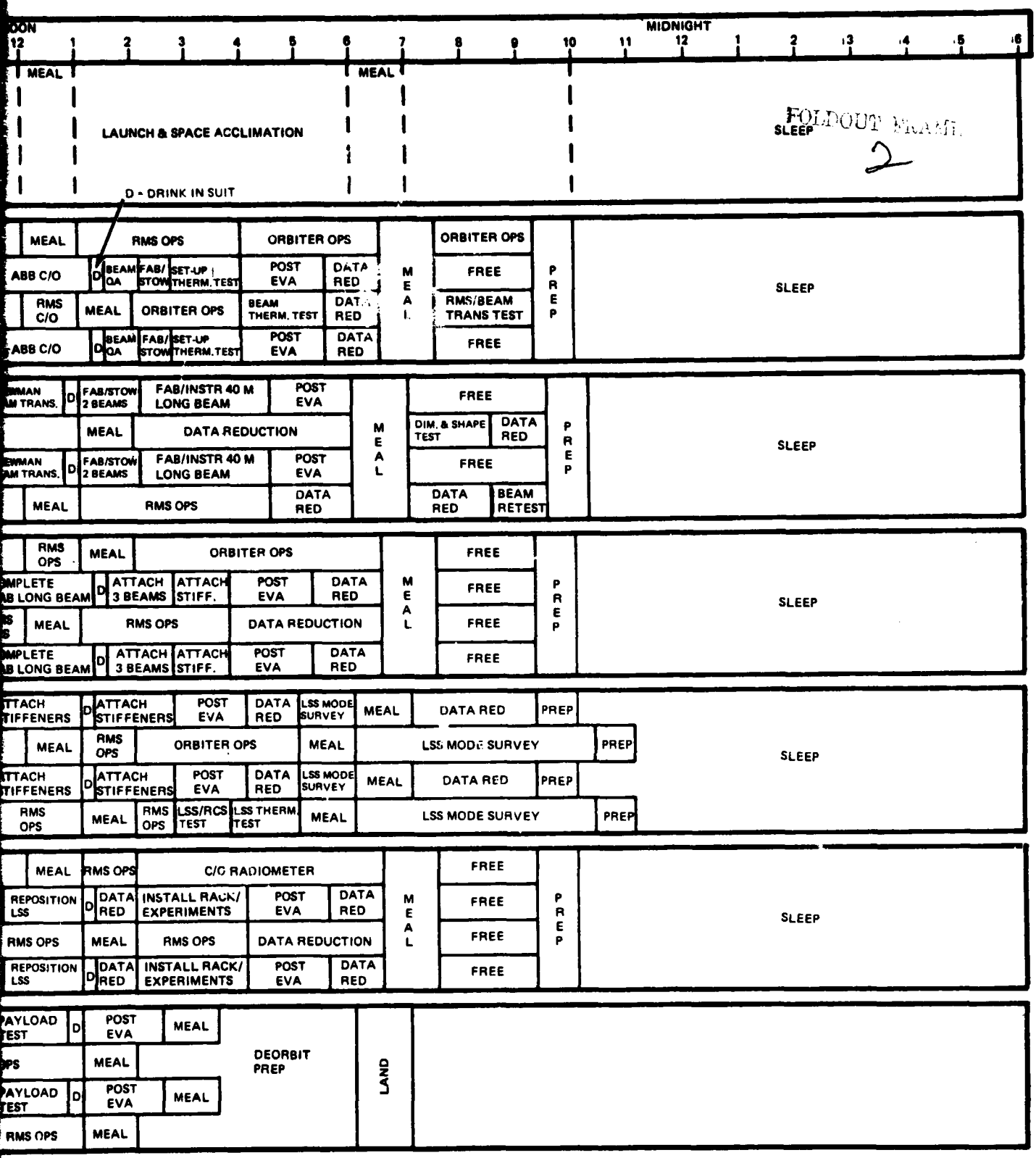

Fig. 6-21 Daily Timeline – Free-Flier Option

The workload and complexity of tasks early in the mission are intended to start out at a low level and gradually increase. The timeline should assure that the crew easily attain each day's short term goals with time to spare. A shopping list of non-critical tasks should be provided to fill spare time, if it exists. The present mission plan allows time for space acclimation of the crew, since all astronauts have experienced some initial discomfort in the zero-g environment. However, the next day's activity is a full schedule that continues throughout the remainder of the flight, with no slack time.

Based upon the activity levels anticipated within the timeline, including daily EVA times ranging from 2.5 to 5.0 hours, the mission appears realizable within the 7-day flight duration.

6.4 STRUCTURAL DEMONSTRATOR FLIGHT OPERATIONS

The free-flier satellite of the basic LSSD mission has been modified for a low-cost Structural Demonstration option in the following ways:

- L-Band radiometer eliminated
- LDEF-type experiments eliminated
- No free-flying capability
- Center boom eliminated
- LSS assembly is taken apart and returned to Earth.

These changes to the basic LSS flight demonstration satellite were factored into the mission task sequence for the free-flier. The resulting flight plan is illustrated in Fig. 6-22.

The first day of the flight is used for launch activities and space acclimation. No LSS tasks are planned. Day 2 begins with an EVA to check out the ABB and verify the quality of beam welds. A 1-m beam, fabricated/instrumented on the ground, is then set up for a test to determine levels of thermally induced strains. This test is conducted after the EVA period and is followed by an RMS and beam transport test used to establish beam handling loads.

A similar beam handling test using crewmen rather than the RMS starts activities on Day 3. Subsequent to this, two 10.5-m beams are fabricated; one is stowed and the other is left in the ABB. After the EVA period, tests are conducted on this beam to determine its response to solar soaks and firing of the Orbiter RCS.

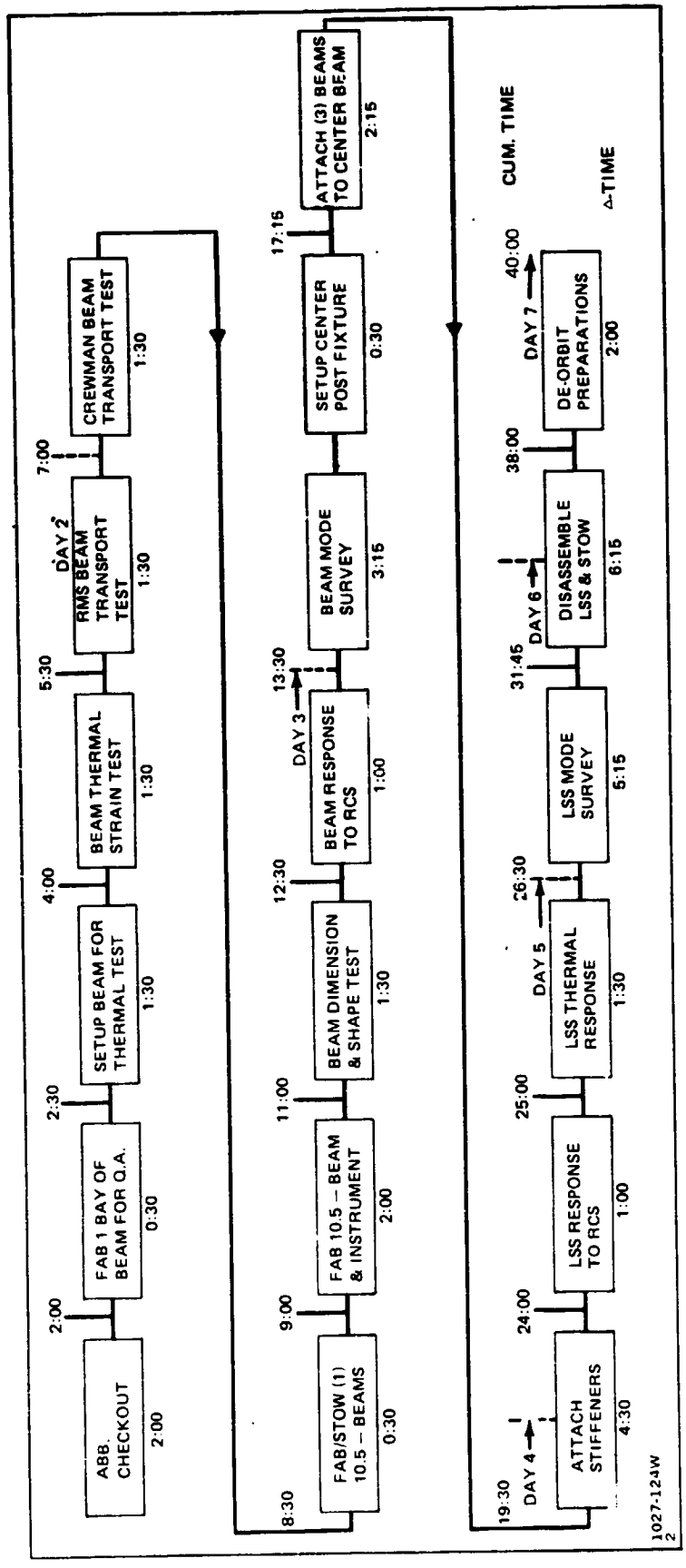

Fig. 6-22 Flight Sequence – Structural Demonstrator Option

Day 4 activity begins with a non-EVA mode survey of the beam attached to the ABB. The remainder of LSS activity for the day is EVA and is used to assemble the Tribeam structure. All of the Tribeam stiffeners cannot be installed on Day 4, however, because of EVA-duration limitations.

Assembly of the structure is completed on Day 5 followed by two tests of the LSS while it is attached to the ABB. Day 6 activities begin with a non-EVA mode survey of the LSS assembly. Disassembly of the structure starts after the test and is completed on Day 7 because of EVA time limitations. The remaining mission activity for day 7 is dedicated to de-orbit preparations.

Figure 6-23 summarizes EVA and non-EVA hours required for the tasks identified in Figure 6-22 and compares these totals to the LSS free-flier option. Maximum EVA time is 4.75 hr which is well below the limit of 6 hr available. The total hours of task time required for either the LSS Platform or Structural Demonstrator option are reasonably close considering the relative complexity of the missions. In the case of the Structural Demonstrator, this is primarily due to the time required to disassemble and stow LSS components for return to Earth.

The daily crew timelines for the Structural Demonstrator Option are shown in Fig. 6-24, indicating that the mission can readily be accomplished within a 7-day Orbiter flight.

DAY	EVA HOURS	NON-EVA HOURS
1	LAUNCH & SPACE ACCLIMATION	
2	4.0	3.0
3	4.0	2.5
4	4.75	3.25
5	2.5	2.75
6	3.0	5.0
7	3.25	2.0
TOTAL FOR STR DEMONSTRATOR	21.5	18.5
TOTAL FOR FREE-FLIER	24.25	24.0
1027-125W 2		

Fig. 6-23 Summary of Daily EVA and Non-EVA Hours Required for Structural Demonstrator Option

FOLDOUT FRAME

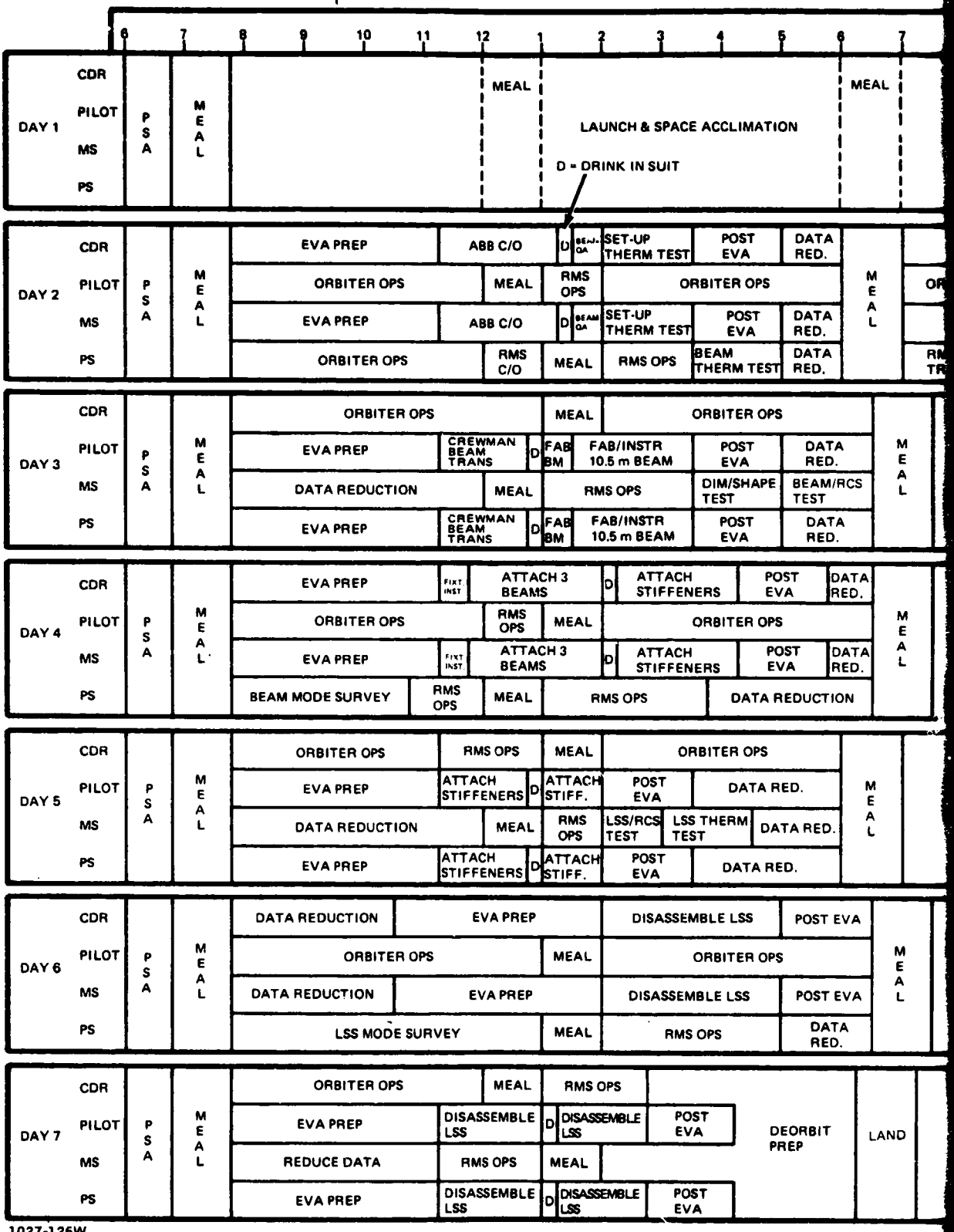

1027-126W
2

FOLDOUT FRAME 2

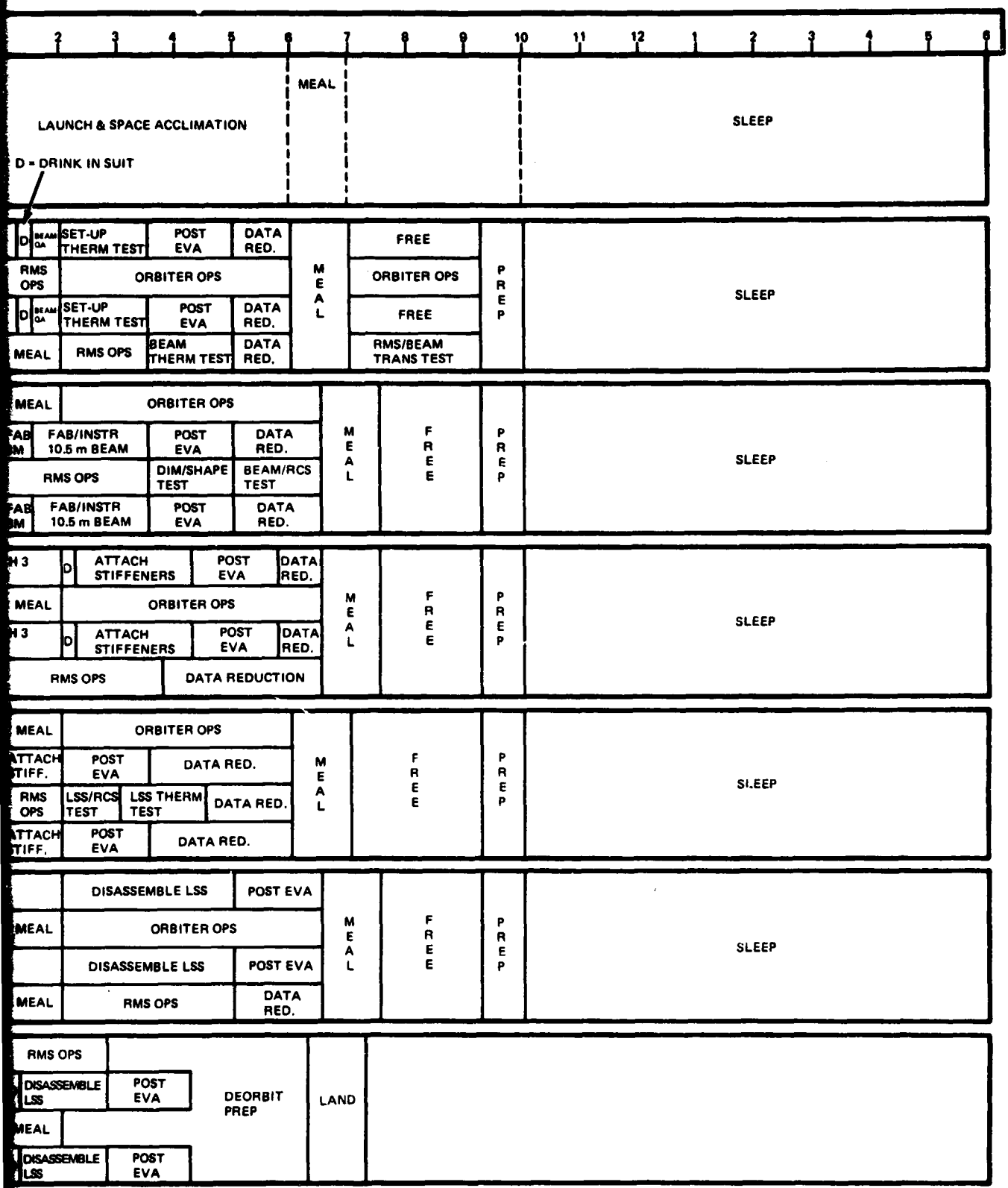

Fig. 6-24 Daily Timeline – Structural Demonstrator Option

6.5 ORBITER SUPPORT

Integration of the LSS demonstration article to the Shuttle requires an examination of structural, power, and avionics interfaces. The ABB, and LSS flight support equipment, will be supported in the payload bay at standard payload attachment points. Preliminary analyses have indicated that structural loads applied to these attachment points are well within their respective capabilities. Power required for ABB operations (excluding welding) will be obtained from the aft cargo bay primary power interface.

6.5.1 ABB Power Requirements

The electrical requirements of the ABB are separated into two systems: the weld system, supplying power to the electrodes for spot welding; and the control system, including the rolling mills, positioning devices, etc.

In the recommended approach, shown in Fig. 6-25, a regulated power supply is interfaced directly with the Orbiter fuel cells. The input side will have the proper impedence match and protection circuits for the Orbiter fuel cells. The voltage regulation and output voltage divider network will provide the dc voltages required by the CPU, computer peripherals, and motors.

The weld system, requiring 63 kVA, 0.017 sec. pulses for each spot weld, is separated from the control system to simplify EMC, and to provide the pulse energy storage source (silver-zinc non-rechargeable batteries) at a high enough voltage to keep peak inverter output currents at a reasonable level.

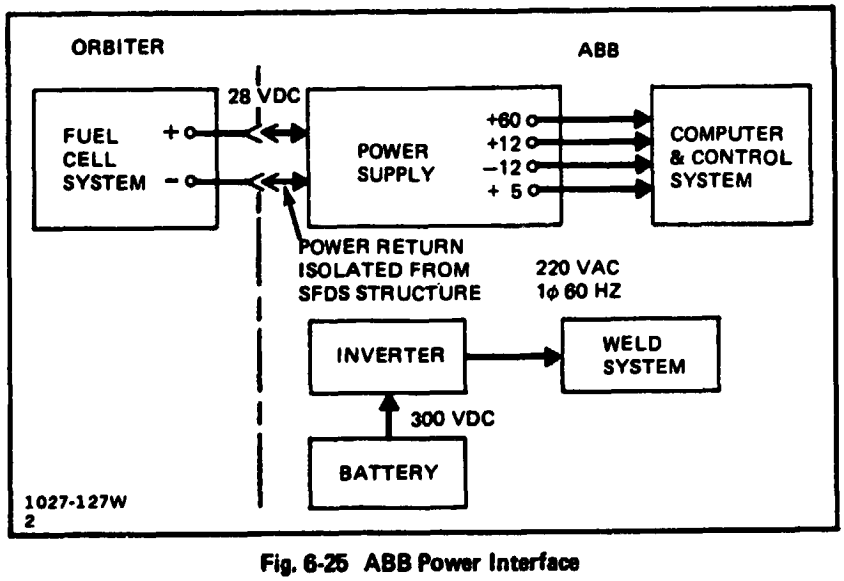

Fig. 6-25 ABB Power Interface

2

6.5.2 Ambient Light Availability

Suitable illumination levels for LSS mission activities are a concern for both light and dark orbital periods. Dark side lighting is expected to be provided by a combination of existing Orbiter lamps and by an added auxiliary lighting system. Natural illumination is available at varying times with combinations of lighting sources including the Sun, Earth, Moon and stars. Figure 6-26 illustrates the maximum illumination levels realizable at the Orbiter payload bay under natural lighting conditions and, with a helmet sun visor. The major light sources are direct sunlight and earth reflectance.

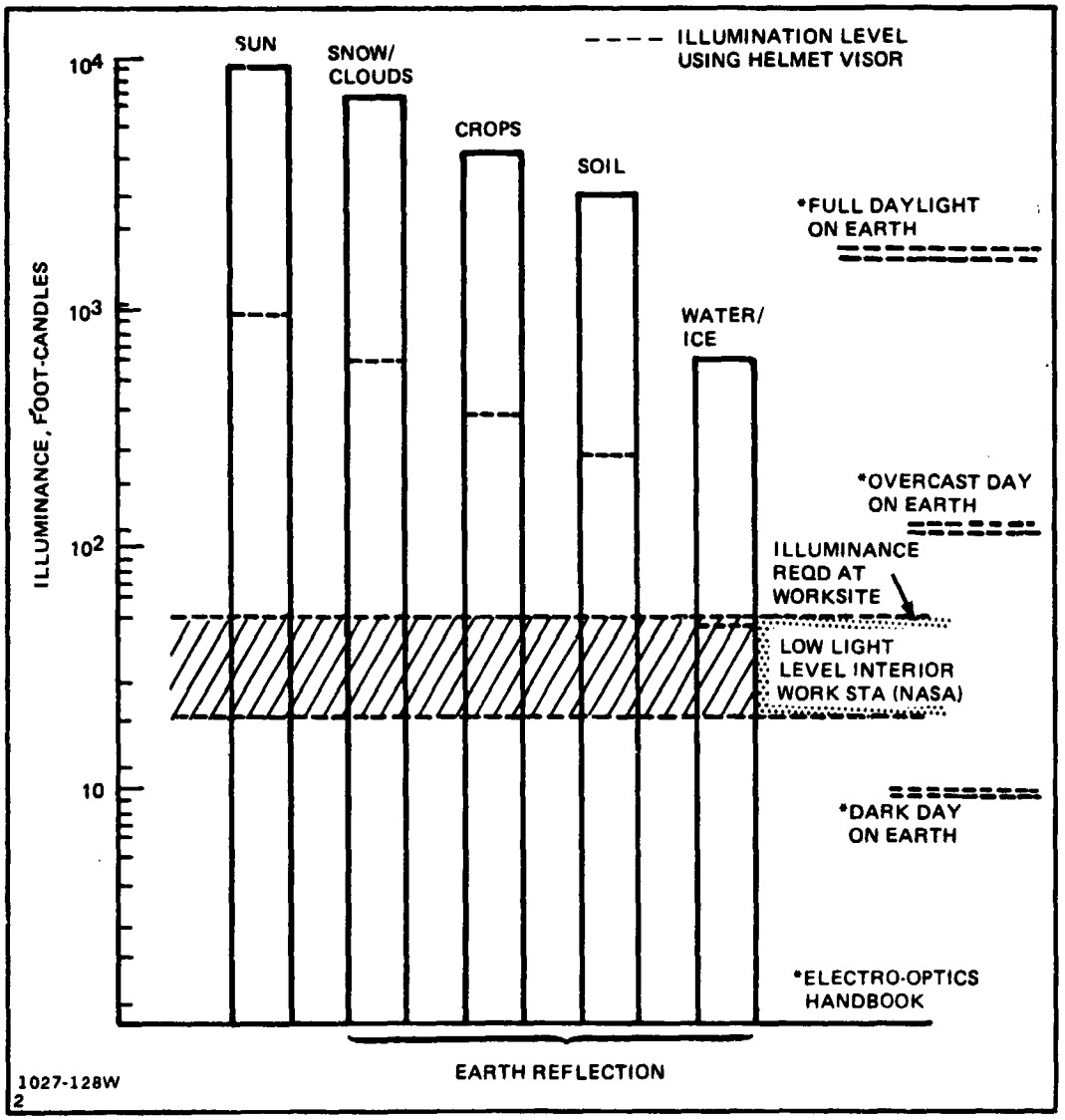

Fig. 6-26 Maximum Ambient Illumination - 400 km; 57° Orbit

The earthshine values shown assume a single reflecting medium for the entire visible surface. Note that the earth-reflected conditions, with sun visor, generally fall within the types of daytime lighting found on the earth's surface during favorable weather conditions.

The quality of light available in space is also of concern. Intense illumination and extreme contrasts are more prevalent than exist for on-earth activities. The sun visors on the EVA crewman's helmet will modify the intensity by limiting light transmissibility to 8% of that available. Shadow conditions can also be reduced by orienting the Orbiter so the payload bay is facing Earth, thereby taking advantage of the diffused light from the Earth's atmosphere. Thus, from a lighting point of view, a flight orientation favoring use of reflected earthshine is desirable.

Illuminating LSS construction activities with natural light obviously would eliminate the need for auxiliary darkside lighting. A technique available to the LSS program is to plan the mission for a time when the high inclination (57°) orbit, called for by the LSS platform approach, can provide 100% sunlight conditions. As discussed in Appendix E of this report, these periods are approximately one week in length at a 300 n mi altitude occuring four times a year. However, since the LSS demonstration flight has requirements for "dark side" activities associated with structural testing, only a portion of a fully sunlit period could be used. Additional mission analysis would be necessary to identify the extent of power savings, but, if these light periods were considered, the launch date and time would have to be tightly controlled to accomplish the necessary "lightside" and "darkside" tasks called for by the LSS mission.

6.5.3 Auxiliary Payload Bay Lighting

The LSS flight demonstration has two major objectives related to lighting:

- Gather engineering data relative to the ABB, the 1-m beam, and the resulting assembly of these beams, and
- Produce a spacecraft with user capability.

Some data requirements of the first objective must be satisfied by flight tests and operations conducted in the dark part of the orbit. This section of the report addresses the lighting that is needed to perform these mission tasks and the resulting power drain on the Orbiter.

6.5.3.1 Requirements for Dark Side Orbital Operations - The mission activities that require light and darkside orbit conditions are:

2

- The LSS mode survey needs to be performed in sunlight and darkness to assess the effect of thermal conditioning on structural damping.
- One part of the test to determine 1-meter beam shape as a function of thermal gradients is planned for a dark period. This will establish baseline beam dimensions at a uniform beam temperature.
- LSS fabrication and assembly techniques should be verified in light, dark and transitional orbit periods. This will provide operational data for use on future LSS programs.

6.5.3.2 Illumination Requirements - Auxiliary lighting will be required for mission activities in the dark part of the orbit to bring illumination levels to acceptable values. It may also be needed in the sunlit portion of the orbit to reduce shadow effects, but dark side operation is assumed to be the major requirement.

Previous studies indicate that 20 to 50 foot-candles is a suitable illumination range for beam fabrication, assembly and other LSS activities. The 50 foot-candle level is also specified by NASA as a design level for interior work stations when performing a good contrast task.

The extent of existing Orbiter payload bay lighting available is identified in Fig. 6-27. The side-mounted payload bay lights have not been factored in this analysis since it is assumed they will be required to be aimed (on the ground) into the payload bay below the level where a significant amount of LSS assembly activity will take place.

STATION	LAMP TYPE	CHROMATICITY AND TEMPERATURE	CONE OF RADIATION	INTENSITY BRIGHTNESS RATIO	FIXTURE	CONTROLS	LOCATION	NO.
PAYLOAD BAY	WIDE ANGLE FLOOD METAL HALIDE	WHITE 3400°K	120°	5 FT-CD CENT LN 10:1	GROUND ADJUST-MENT	INDEP. FROM D AND C	3 EACH SIDE OF BAY	6
RMS LIGHT	NARROW ANGLE FLOOD INCANDESCENT	WHITE 2800°K	40° CONE	3 FT-CD AT 30 FT	PAN/TILT WITH CAMERA	INDEPT. FROM D AND C	ABOVE CAMERA ON RMS ROLL JOINT	1
PAYLOAD BAY FOR-WARD BULKHEAD	WIDE ANGLE FLOOD METAL HALIDE	WHITE 3400°K	120°	5 FT-CD AT 30 FT	GROUND ADJUST-MENT	INDEP. FROM D AND C	576 BULKHEAD BETWEEN AFT WINDOWS	1
1027-129W 2								

Fig. 6-27 Orbiter Payload Bay Lighting

The payload bay light located on the Orbiter's forward bulkhead is in a position to illuminate many of the mission tasks and has been accounted for in this analysis. The RMS-mounted light will be useful for some activities but will not be effective for assembly work. This is because the manipulator is used to grasp and position beams while crewmen make structural connections at the beam ends. The light therefore will not be aimed at the area where crewmen are working and, for this reason, the RMS light contribution was eliminated.

The analysis assumed placement of lamps based on the current LSS assembly and test plan in order to get a "first cut" at lighting power requirements. Specific details of locations, attachments, luminaire design and lamp selection and control (azimuth and elevation) can be determined only after sufficient design and simulation.

6.5.3.3 Lighting Analysis - A total of six auxiliary lamp locations are used for this analysis as shown in Fig. 6-28 and 6-29. The lamps are assumed to be controllable in azimuth and elevation. A point-to-point method of calculation is used where the relationship of illumination, lamp output and distance is expressed by:

$$E = \frac{I}{D^2}$$

where E is desired illumination (ft-candles)
I is lamp output (lumens)
D is distance between lamp and subject (ft)

Lamps 1 and 2

Illuminating the aft beams of the LSS assembly while mounted on the ABB (Fig. 6-28) is the most stringent design condition for Lamps 1 and 2. The existing forward bulkhead mounted lamp produces 5 ft-candles illumination at 30 ft (see Fig. 6-27)

$$I = E\,D^2 = 5\,(30)^2 = 4500 \text{ lumens}$$

Illumination is to be provided by Lamps 1 and 2 equals:

$$E = 50 - 1.2 = 48.8 \text{ ft-candles}$$
$$\approx 49 \text{ ft-candles}$$

Output of Lamps 1 and 2

$$D = 65 \text{ ft}$$
$$I_{1,\,2} = 49\,(65)^2 = 207{,}025 \text{ lumens}$$

2

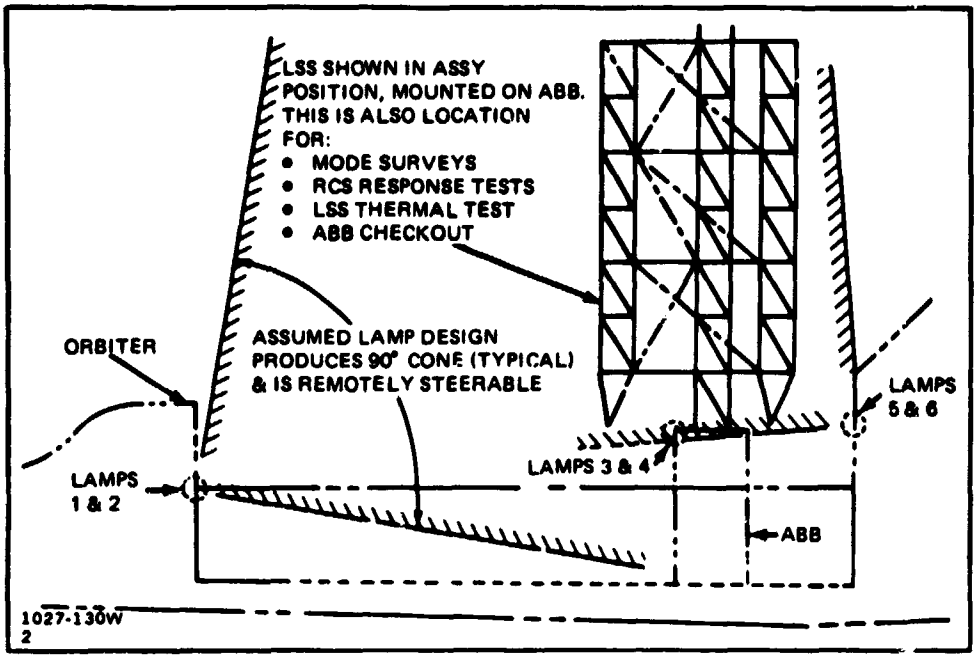

Fig. 6-28 Auxiliary Lighting - Side View - LSS on ABB

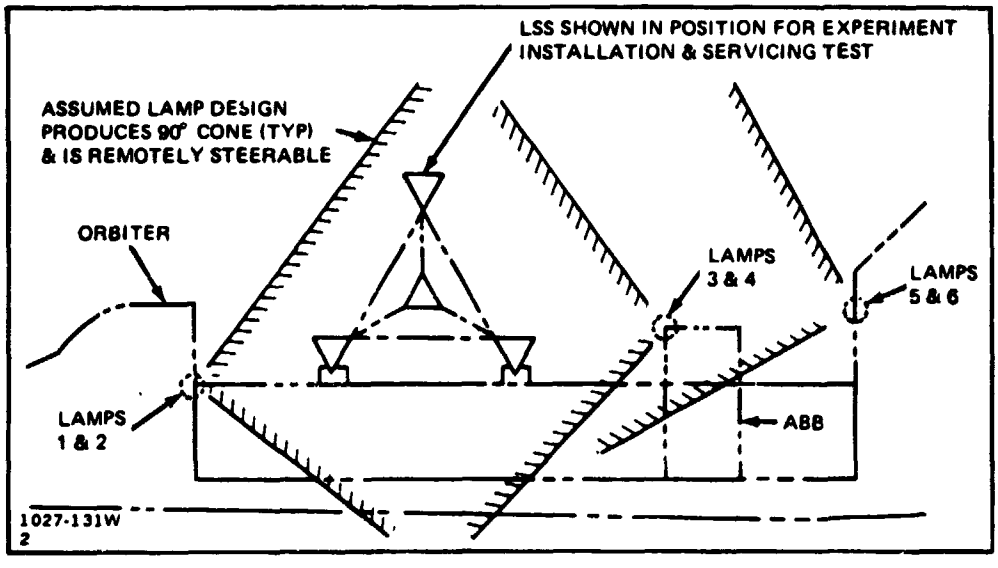

Fig. 6-29 Auxiliary Lighting - Side View - LSS in Berthing Location

Output/lamp

$$I = \frac{207,205}{2} = 103,603 \text{ lumens}$$

Lamps 5 and 6

Illuminating the forward beam of the LSS assembly while it's mounted on the ABB (Fig. 6-28) is the design case for these lamps.

Output of lamps 5 and 6

$$D = 40 \text{ ft} \quad E = 50 \text{ ft candles}$$
$$I = 50\,(40)^2 = 80,000 \text{ lumens}$$
$$\text{Output/lamp} = \frac{80,000}{2} = 40,000 \text{ lumens}$$

Lamps 3 and 4

Illuminating the forward beam of the LSS assembly while mounted across the payload bay (Fig. 6-30) is the design case for these lamps.

Output of lamps 3 and 4

$$D = 40 \text{ ft} \qquad E = 50 \text{ ft-candles (same as lamps 5 and 6)}$$

Output/lamp = 40,000 lumens

Figure 6-31 shows the required output of each lamp as a function of illumination levels for the specific design cases. Figure 6-32 identifies the lamp size required to supply the desired lumen level. Lumen/watt efficiencies used in the calculations are those for high pressure sodium lamps and the sizes selected are all commercially available. For both 30 and 40 foot-candle levels, lumen requirements are more efficiently met by using two smaller lamps at each of locations 1 and 2 rather than a single large one. This is due to the reduced availability of lamps in the range between 400 and 1000 watts.

Figure 6-33 lists total power and energy requirements for auxiliary lighting as a function of illumination levels. Energy usage is based on the current assembly/test mission scenario which identifies approximately 14 dark-side flight hours during which auxiliary lighting would be needed.

Figure 6-34 shows the energy available from the Orbiter for a 7-day mission (50 kWh) as a function of illumination level provided for the 14 dark-side hours of the mission. Subtracting the energy used by the ABB (35.5 kWh), the figure shows that only about 30 ft-candles of illumination could be provided for the mission. The adequacy of this light level should be substantiated by ground simulation. In the absence of this

2

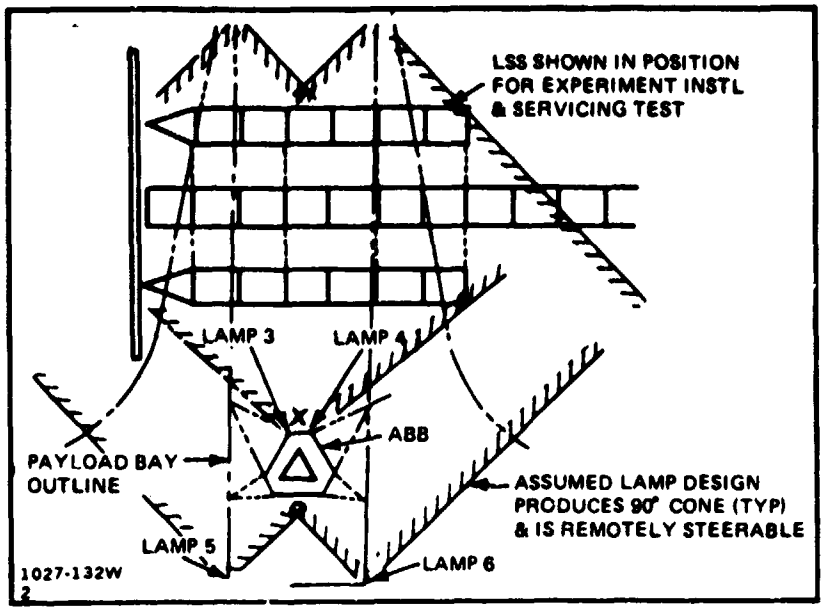

Fig. 6-30 Auxiliary Lighting - Plan View - LSS in Berthing Position

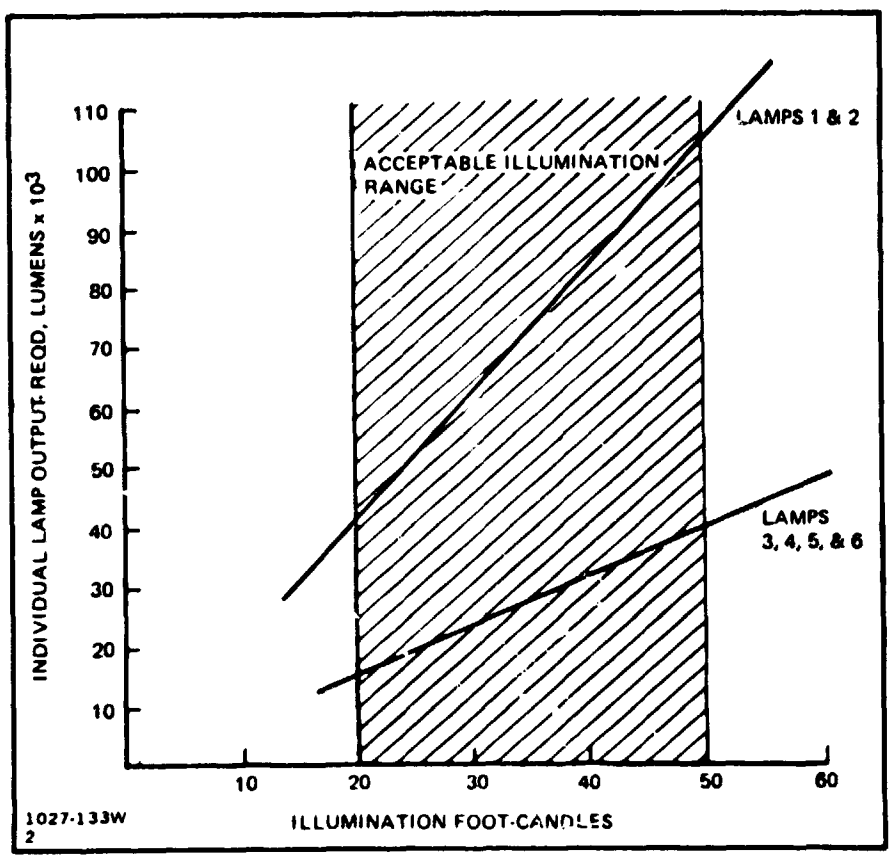

Fig. 6-31 Individual Lamp Output Required vs Illumination Levels

2

LAMPS	20 FOOT-CANDLES		30 FOOT-CANDLES		40 FOOT-CANDLES		50 FOOT-CANDLES	
	OUTPUT REQD, LUMENS	LAMP REQD, WATTS	OUTPUT REQD, LUMENS	LAMP REQD, WATTS	OUTPUT REQD, LUMENS	LAMP REQD, WATTS	OUTPUT REQD, LUMENS	LAMP REQD, WATTS
1 & 2	41,405	400	62,108		82,810		103,513	1,000
1A, 1B, 2A, 2B (SEE NOTE 2)			31,054	310	41,405	400		
3, 4, 5 & 6	16,000	200	24,000	250	32,000	310	40,000	400

NOTES: 1. LAMP SELECTION (WATTS REQUIRED) IS BASED ON USING A HIGH PRESSURE SODIUM, HIGH INTENSITY DISCHARGE TYPE. WATT LEVELS ARE COMMERCIALLY AVAILABLE.

2. FOR BOTH THE 30 AND 40 FOOT CANDLE LEVELS, LUMEN REQUIREMENTS ARE MORE EFFICIENTLY MET BY USING TWO SMALLER LAMPS AT EACH OF LOCATIONS 1 AND 2. THIS RESULTS FROM A LACK OF LAMP AVAILABILITY IN THE RANGE BETWEEN 400 AND 1000 WATTS.

1027-134W
2

Fig. 6-32 Lamp Power Requirements

AUXILIARY LIGHTING SYSTEM REQMTS	ILLUMINATION LEVELS, FOOT-CANDLES			
	20	30	40	50
POWER, kW	1.84	2.58	3.27	4.14
ENERGY, kWh	25.76	36.12	45.78	57.96

NOTE: POWER LEVELS INCLUDE A 15% ALLOWANCE FOR BALLAST WATTAGE.

1027-135W
2

Fig. 6-33 Auxiliary Lighting System Power & Energy Requirements

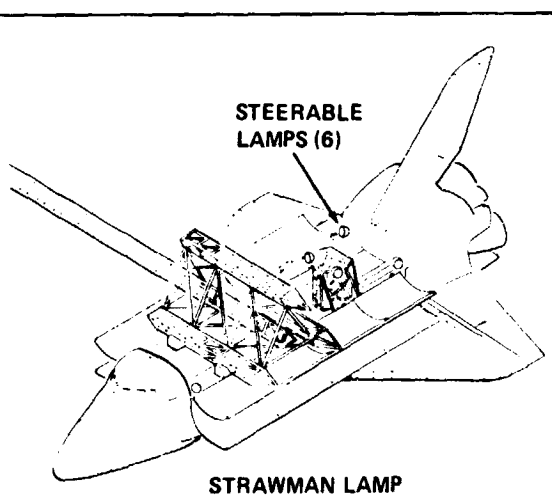

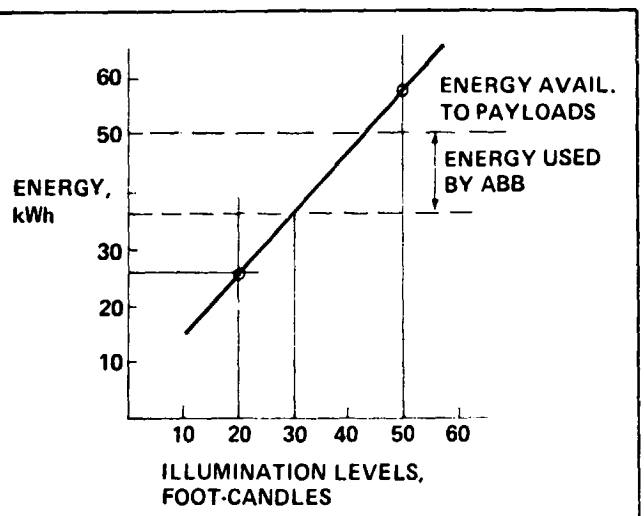

- ADDITIONAL ELECTRICAL ENERGY REQD FOR ILLUMINATION LEVELS > ≈ 30 FOOT-CANDLES
- LIGHTING SIMULATIONS NEEDED

1027-136W
2

Fig. 6-34 Auxiliary Lighting

information, the present flight plan assumes a 50 ft-candle illumination requirement, which subsequently requires an EPS kit for the LSS mission.

6.5.4 Comparison of Orbiter Capabilities and Mission Requirements

Figure 6-35 summarizes Orbiter capabilities and compares them to the LSS demonstration mission requirements. Capabilities inherent within the Orbiter and its crew of four are sufficient to accomplish the LSS mission with the addition of an OMS kit for the free-flier option. If lighting levels above 30 ft-candles are necessary, fuel cell consumables for an electric power kit (EPS) will also be needed.

	FREE FLIER		STRUCTURAL DEMO	
	REQD	AVAILABLE	REQD	AVAILABLE
POWER	5.8 kW(1)	7 kW (AVG)	5.8 kW(1)	7 kW (AVG)
ENERGY	72 kWh(1)	890 kWh(2)	63 kWh(1)	890 kWh(2)
RCS PROPELLANT (VERNIER)	< 300 kg	1814 kg	< 300 kg	1814 kg
RMS	1	2	1	2
PAYLOAD WGT UP	19093 kg	21000 kg	8037 kg	29490 kg
PAYLOAD WGT DOWN	7781 kg	14515 kg	8037 kg	14515 kg
CREW USAGE (BOTH EVA & NON-EVA MISSION ACTIVITIES)	245 MH(3)	268 MH	240 MH(3)	268 MH
EVA (CREW INVOLVED)	2	2	2	2

(1) REFERS TO ABB & LIGHTING ONLY
(2) ASSUMES USE OF ADDITIONAL ORBITER ELECTRIC POWER KIT FOR LIGHTING
(3) MAX EVA TIME IS 5:00 FOR THE FREE-FLIER AND 4:45 FOR THE STRUCTURAL DEMO OPTION

1027-137W
2

Fig. 6-35 Orbiter Services Required

Power and energy levels required for the LSS mission options reflect ABB and auxiliary lighting needs only, and assumes the need for 50 ft-candle lighting. Under these conditions, LSS mission energy requirements exceed that available from the Orbiter (50 kWh); thus the additional fuel cell consumables associated with the EPS kit have been included, which yield an available energy level of 890 kWh.

The "Crew Usage" item in Fig. 6-33 indicates how busy the crew will be on this 7-day flight. Assuming the crew of four are available for full work days during the flight (excluding launch, return, space acclimation, meals and sleep time) results in 268 man-hours available. This compares with an estimate of about 245 hours required for ABB testing and fabrication, assembly and checkout of the LSS Platform. Maximum EVA has been scheduled for 5 hr (6 hr permitted), thereby allowing a margin for contingencies.

2

6.6 CONCLUSIONS AND RECOMMENDATIONS

A test, fabrication, and assembly scenario has been developed which indicates that either the Structural Demonstrator or LSS Platform options can be completed in a seven-day flight. The test program, designed to produce the required LSS structural data, can be satisfied by either approach. Neutral buoyancy simulations should be conducted to substantiate the validity of assembly techniques and mission timelines. Additional simulation efforts are recommended to evaluate lighting requirements for dark-side construction/assembly operations and astroworker effectiveness in EVA operations. Both free-floating (tethered or MMU) and restrained (cherry picker/RMS) construction modes should be evaluated, together with the potential area vs task lighting needs associated with these candidate modes of astroworker construction. The results of these efforts will impact the program in the design and cost areas as well as mission planning.

2

7 - PROGRAMMATICS

7.1 PROGRAM LOGIC

To provide a basis for generating programmatic data (schedules and costs) for the LSS demonstration options, a program logic flow was developed. This logic flow, which identifies assumed inputs/outputs and major steps in the program's development, is shown in Fig. 7-1. Starting with an LSS study concept and a set of mission hardware requirements, a detailed LSS design is completed. Mission-supporting hardware is fabricated and assembled for ground development/qualification test and simulation. Included in the hardware developed are beam tripod end and node fittings, RMS end-effectors, and assembly fixtures.

The ground fabricated/assembled hardware as well as mission hardware and the ABB are delivered to the launch site. Following receiving inspection, checkout, and installation in the Shuttle payload bay, the payload is launched to the desired orbit.

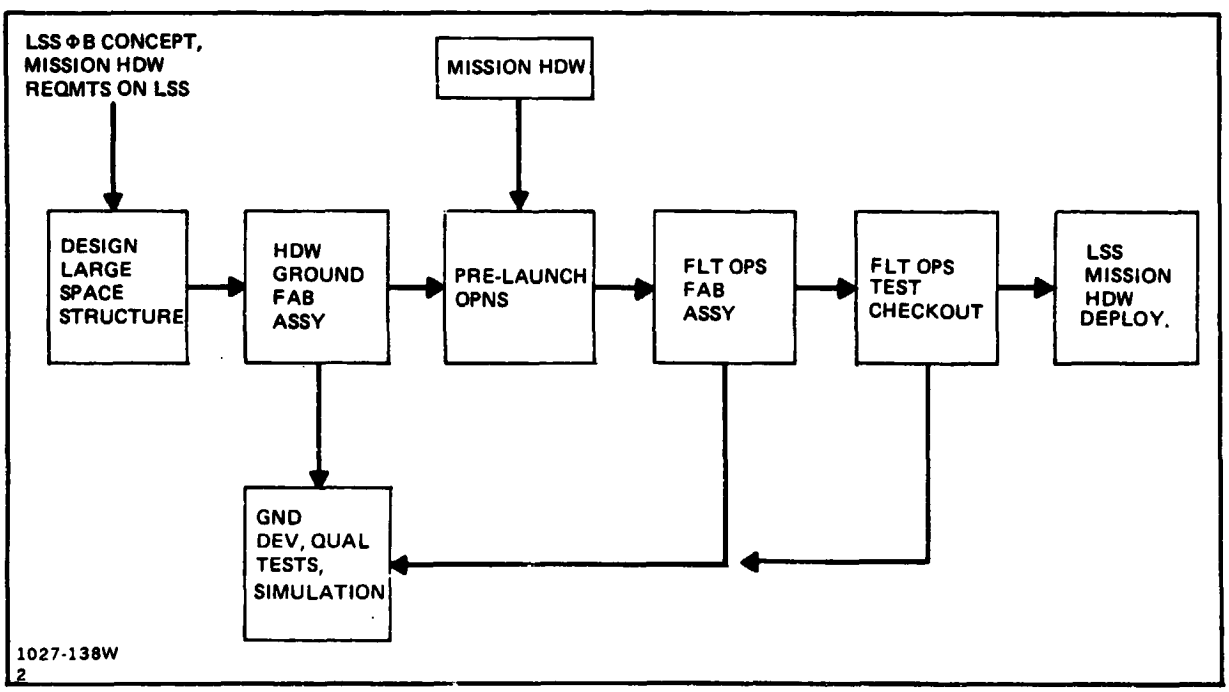

Fig. 7-1 Program Logic

In orbit, the LSS is fabricated by the ABB and assembled out of the Orbiter payload bay. Mission hardware and subsystems are installed on the LSS and checked out. Sample beams and the LSS, if not deployed, are returned to earth for further analyses and testing. This basic logic was used in developing the schedule and cost for each of the LSS options developed in this study.

7.2 PROGRAM SCHEDULES

Program schedules covering design, analysis, fabrication and test for both ground and flight activities were developed for each of the LSS program options. The free-flier option schedule is shown in Fig. 7-2, and the Structural Demonstrator in Fig. 7-3.

Each of the LSS option schedules are similar, and cover the time-span from contract award through post-flight testing of structural elements. Elapsed times are estimated to be about three years. The principal schedule drivers are:

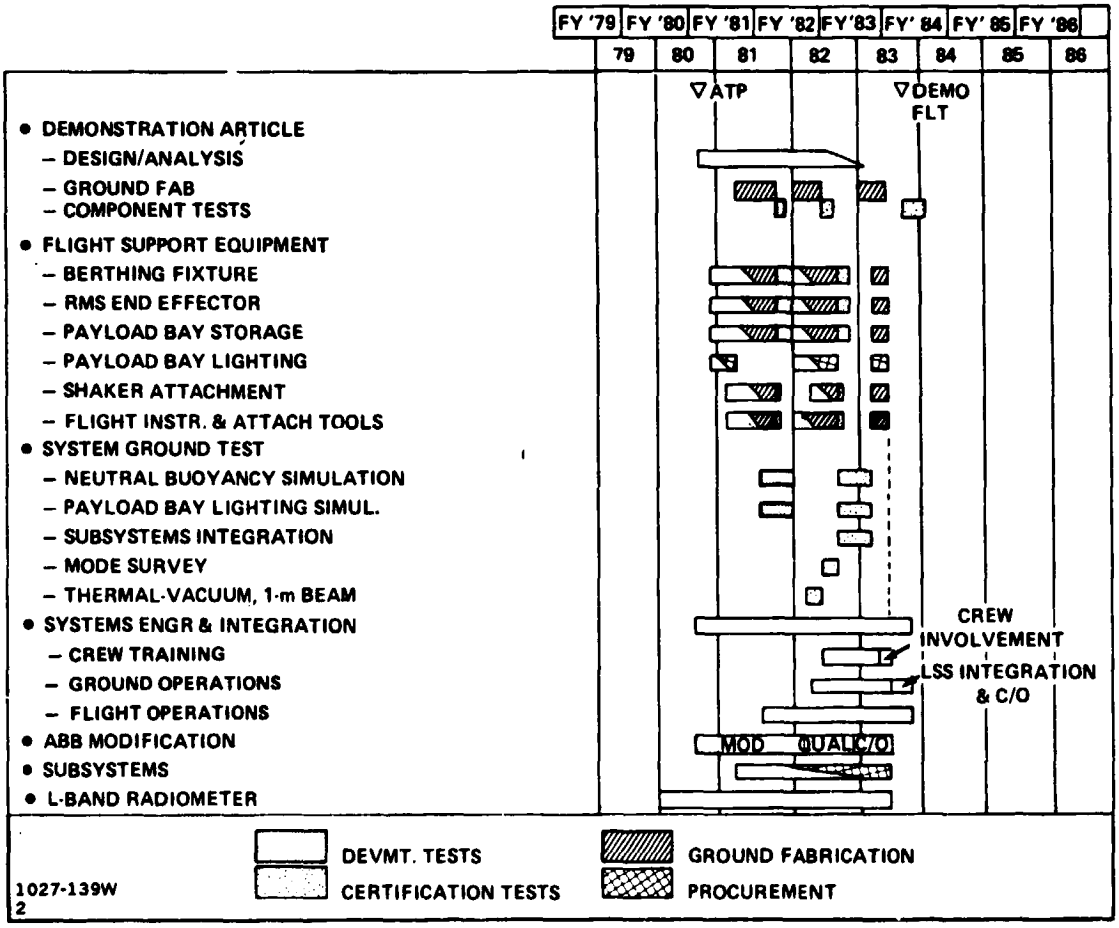

Fig. 7-2 Program Schedule – LSSD Free-Flier

- Modifying the ABB ground demonstration machine to flight status
- Systems Engineering/Integration
- Simulation and Crew Training.

One-meter beam hardware is needed for development testing and preflight qualifications. The ABB ground demonstration machine provides 1-meter beams for development testing and simulation to provide data/inputs to design/analysis efforts early in the program. Flight support equipment is developed concurrent with systems engineering, integration, and simulation efforts. All flight hardware is delivered at least three months before flight to allow for Shuttle integration.

Post-flight testing is scheduled to take place in a three-month period following the flight. These tests are intended to verify the structural integrity and quality of the beam fabricated in space and returned to Earth. Test data will be compared to similar tests of 1-meter beams made on the ground by the ABB after modification to flight status.

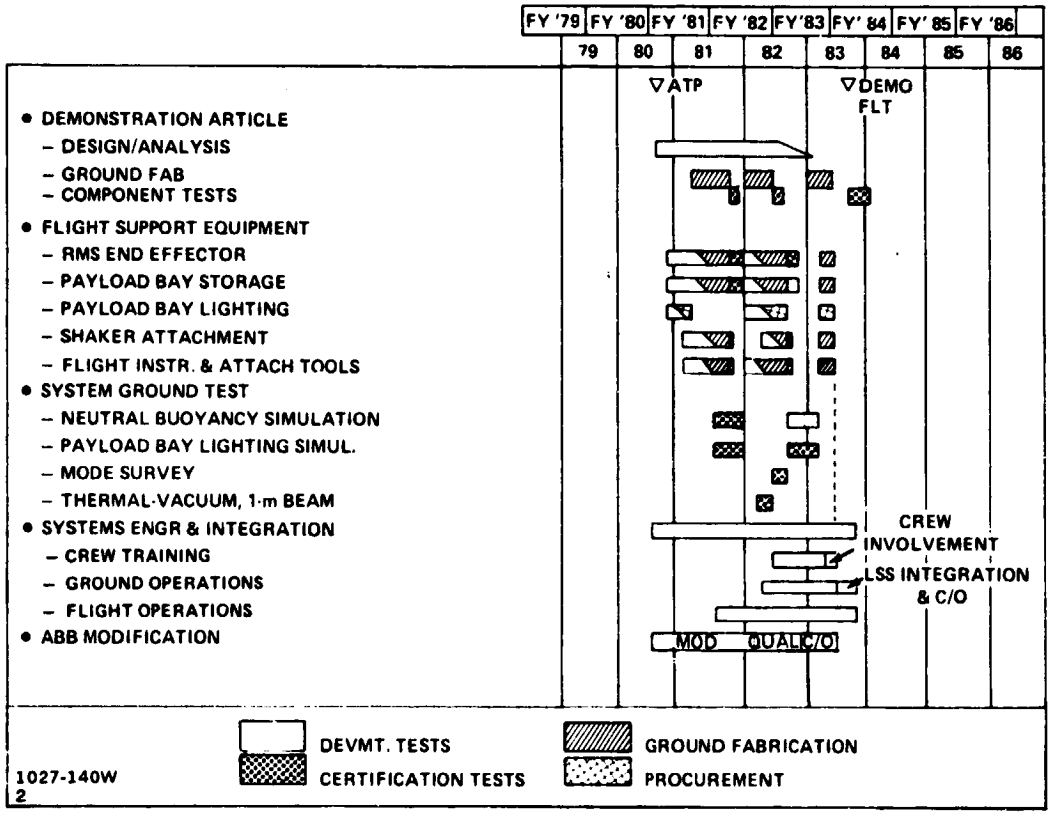

Fig. 7-3 Program Schedule – Structural Demonstrator Option

2

7.3 COSTING APPROACH

The approach used for costing LSS program options is described in this section. Included herein are the WBS, additional programmatic groundrules, and the costing methodology.

7.3.1 Work Breakdown Structure (WBS)

The WBS for the LSS demonstration program options is shown in block diagram form in Fig. 7-4. The Level 3 WBS is divided into the three major categories of Large Space Structure (LSS), program support, and mission hardware. A summation of costs at this level, all of which is considered DDT&E, constitutes the total program cost.

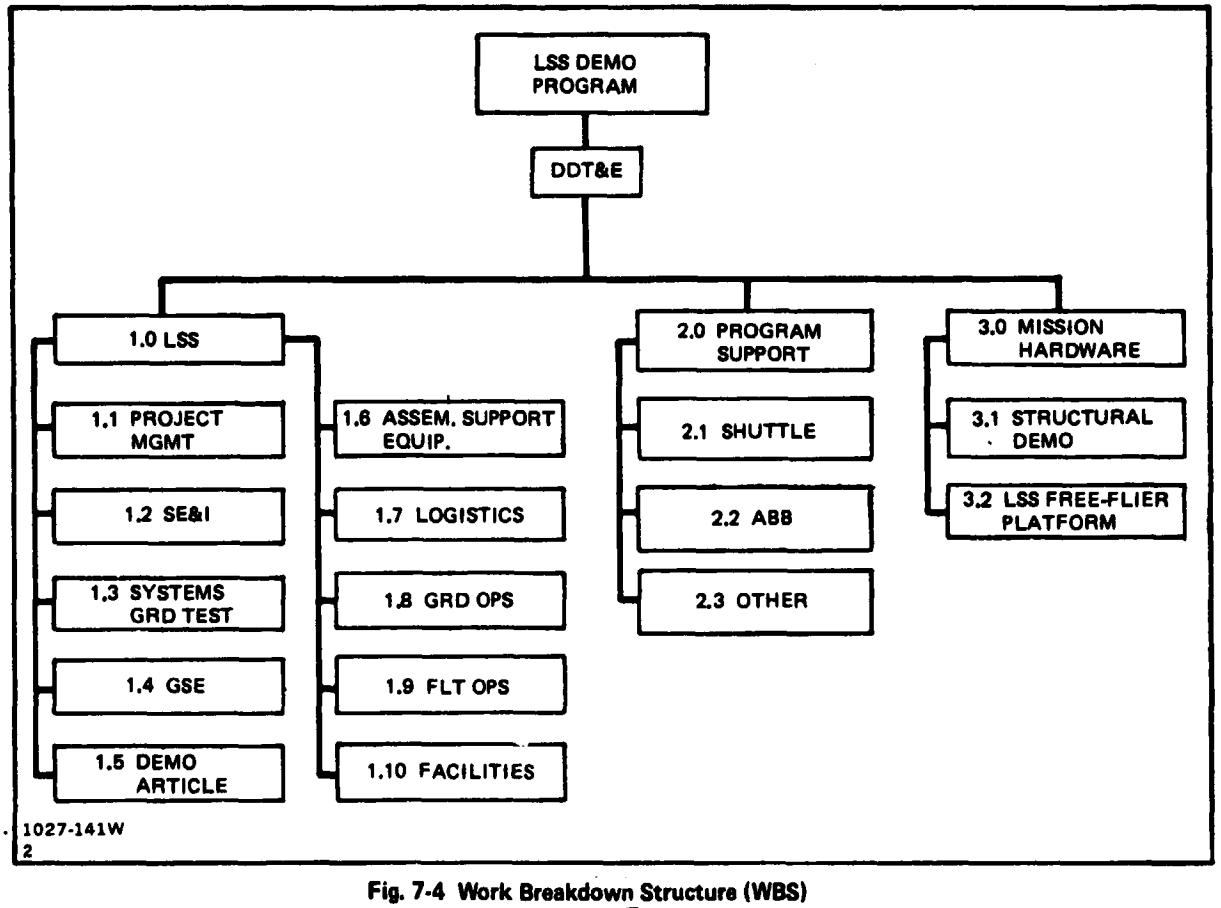

Fig. 7-4 Work Breakdown Structure (WBS)

For both options, WBS 1.0 (LSS) contains the costs associated with developing and producing a 1-m beam LSS demonstration unit. Costs related to integration of Program Support (WBS 2.0) and Mission Hardware (WBS 3.0) items into the LSS are also included in WBS 1.0.

Program support elements, collected under WBS 2.0, include Shuttle support costs and ABB modification costs related to upgrading the machine from a ground demonstrator to one suitable for flight.

WBS 3.0 (Mission Hardware) contains all hardware and supporting subsystems that are added to the LSS to accomplish mission requirements over and above those involved with the structural demonstration. The Structural Demonstrator has no additional mission hardware or subsystems. The free-flier option has a radiometer and experiments that are Government Furnished Equipment (GFE), and appropriate subsystems required to support this capability.

The WBS dictionary is presented in Appendix A of Volume 3, Programmatics, dated July 1978 which was prepared during the initial phase of this study.

7.3.2 Additional Programmatic Groundrules

A summary of the groundrules imposed upon the various LSS demonstration options are shown in matrix form in Fig. 7-5. These groundrules are both programmatic and cost-related. Additional costing groundrules applicable to this study effort include:

- Cost estimates in 1979 dollars
- Funding schedules by calendar year
- No inclusion of SR&T and NASA institutional costs
- Shuttle cost from "STS Reimbursement Guide".

GROUNDRULE	STRUCTURAL DEMO	LSS PLATFORM
1. ABB FLIGHT EVALUATION & FAB/ASSY OF AN LSS DEMO ARTICLE WILL OCCUR ON THE SAME SHUTTLE FLIGHT	•	•
2. THE FLIGHT WILL BE SCHEDULED FOR THE 1983-84 TIME-PERIOD	•	•
3. THE MISSION WILL BE ACCOMPLISHED WITHIN 7 DAYS	•	•
4. THE ABB USED ON THIS FLIGHT IS A MODIFIED VERSION OF THE GROUND DEMONSTRATOR MACHINE	•	•
5. THE LSS DEMO ARTICLE WILL PERFORM A USEFUL FREE-FLIGHT MISSION		•

1027-142W

Fig. 7-5 Program Groundrules

7.3.3 Costing Methodology

The development of WBS element costs utilized a number of data/information sources, as shown in Fig. 7-6. The parametric cost methodology determines cost as a function of physical parameters such as weight, square meters, etc. The in-house estimate refers to a "grass roots" type approach wherein costs for a given WBS element are derived from analyses of similar work efforts on a number of completed programs. MMS data relates to the use of projected hardware productions costs for selected satellite equipments, and NASA data relates to established costs for Shuttle Flights, or portions thereof. These cost data sources were used to generate the cost estimates presented in Subsection 7.4.

WBS ELEMENT \ COSTING METHODOLOGY	PARAMETRIC	IN-HOUSE ESTIMATE	HISTORIC DATA	MMS DATA	NASA DATA
1.1 PROJECT MGMT			●		
1.2 SE & I			●		
1.3 SYSTEMS GROUND TEST		●			
1.4 GSE			●		
1.5 DEMO ARTICLE		●			
1.6 FLT SUPPORT REQMT		●			
1.7 LOGISTICS			●		
1.8 GROUND OPS		●			
1.9 FLIGHT OPS		●			
2.1 SHUTTLE					●
2.2 AUTO BEAM BUILDER		●			
3.1 STR DEMO MISS. HDWR	NONE REQUIRED				
3.2 FREE-FLIER MISS. HDWR	●	●		●	

1027-143W
2

Fig. 7-6 Costing Methodology

2

7.4 COST DATA

This section contains a cost breakdown for each LSS option, funding schedules, and a cost comparison of the options. Cost data developed in this study should be considered preliminary in nature, reflecting the level of program definition to date.

7.4.1 Cost Estimates

Figure 7-7 shows a cost breakdown by WBS element for each program option in millions of 1979 dollars. A 25% contingency was added to estimates based on the current design level of development.

WBS	ITEM	STRUCT. DEMO	FREE-FLIER
1.1	PROJECT MANAGEMENT	0.68	0.85
1.2	SYSTEMS ENGINEERING & INTEGRATION	0.82	1.74
1.3	SYSTEMS TEST & EVALUATION		
1.3.1	MAJOR TEST ARTICLES	0.55	0.66
1.3.2	INSTRUMENTATION	0.38	0.44
1.3.3	SYSTEM TEST	0.31	0.37
1.4	GROUND SUPPORT EQUIPMENT	–	0.26
1.5	DEMONSTRATION ARTICLE		
1.5.1.1	GROUND FABRICATED STRUCTURE	0.19	0.27
1.5.1.2	GROUND FABRICATED MECHANISMS	0.20	0.28
1.5.2	SPACE FABRICATED STRUCTURE	0.18	0.18
1.5.3	INSTALL., ASSY & C/O	0.05	0.05
1.6	ASSEMBLY SUPPORT EQUIPMENT		
1.6.1	JIGS & FIXTURES	0.25	0.36
1.6.2	TOOLS	0.73	0.73
1.6.3	TEST INSTRUMENTATION	0.43	0.43
1.6.4	ALIGNING EQUIPMENT	0.25	0.25
1.7	LOGISTICS	0.20	0.23
1.8	GROUND OPERATIONS	0.12	0.17
1.9	FLIGHT OPERATIONS	0.23	0.28
1.10	FACILITIES		
	CONTINGENCY (25%)	1.39	1.89
	SUBTOTAL	6.96	9.44
2.1	SHUTTLE SUPPORT	23.9	24.22
2.2	AUTOMATED BEAM BUILDER	9.5	9.5
3.0	MISSION HARDWARE		
3.1	STRUCTURAL DEMO		
3.2	FREE-FLIER (SUBSYSTEMS/CONTINGENCY)		4.69
	PROGRAM TOTALS	40.36	47.85

1027-144
2

Fig. 7-7 Cost Breakdown (Millions of 1979 Dollars)

2

Costs for Ground Support Equipment (GSE), WBS 1.4, related to Large Space Structure (LSS), only appear for the free-flier option. LSS hardware for the Structural Demonstrator option was assumed not to require GSE because of its low complexity level. The LSS Free-Flier Platform contains required subsystems for the mission which is accounted for in WBS 3.0.

No facility costs were assumed to be required for any option.

Modification of the Automated Beam Builder (ABB) ground demonstration unit to flight status is included in WBS 2.2. The cost is constant for each option and was derived from the Space Fabrication Demonstration System (SFDS) Project (Ref NAS8-32472).

7.4.2 Funding Schedules

All funding schedules were determined mathematically by using Beta distributions. Figure 7-8 depicts a Beta distribution used when a symmetrical distribution is desired. A specific curve was selected for each Level 4 WBS line item. The selection was based on judgement about the characteristics of the given WBS item. For example, it was felt that building of the demonstration article would require spending 60% of its costs during the first half of its scheduled time. As a result, a Beta distribution curve was selected which is skewed to the left (long tail on the right side).

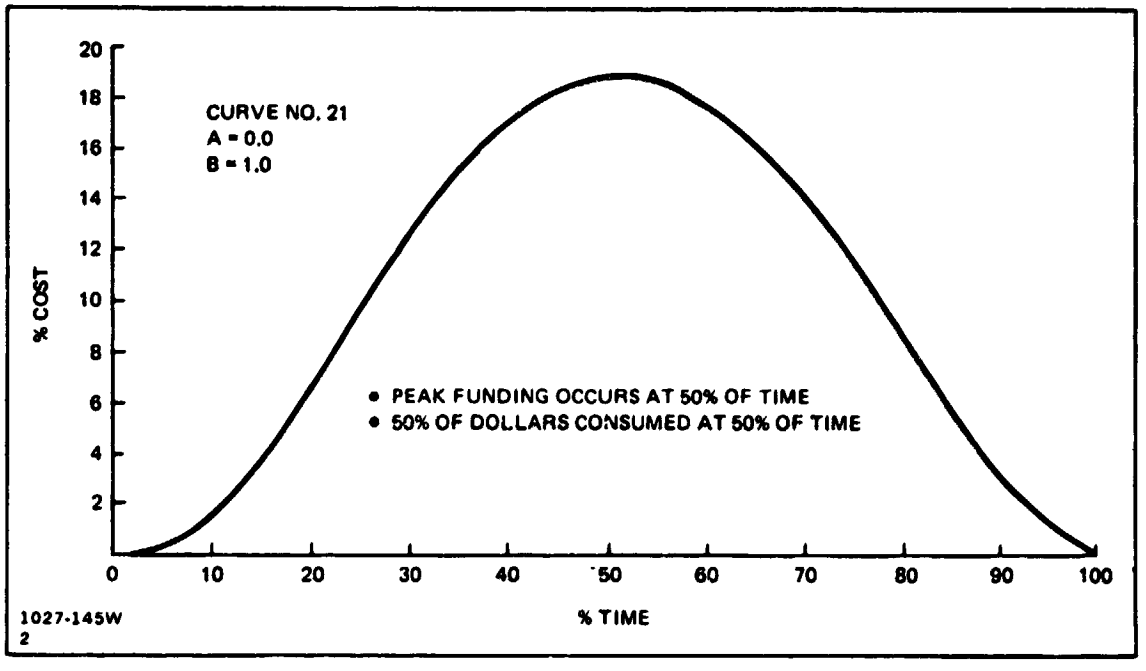

Fig. 7-8 Program Funding Schedule – Beta Distribution Curve

2

Figure 7-9 presents the funding schedule for the Structural Demonstrator Option. It indicates the funding requirements by quarter rather than year because of the relatively short duration of the overall program. Total DDT&E cost and the peak annual funding (PAF) requirements are noted. The funding requirements exclude costs for space transportation and the ABB modification since they are known, discrete costs.

Figure 7-10 contains the individual WBS item quarterly funding requirements for the Structural Demonstrator Option. The totals match those plotted in Fig. 7-9. Again, the data are presented by quarter rather than year because of the relatively short duration of the overall program.

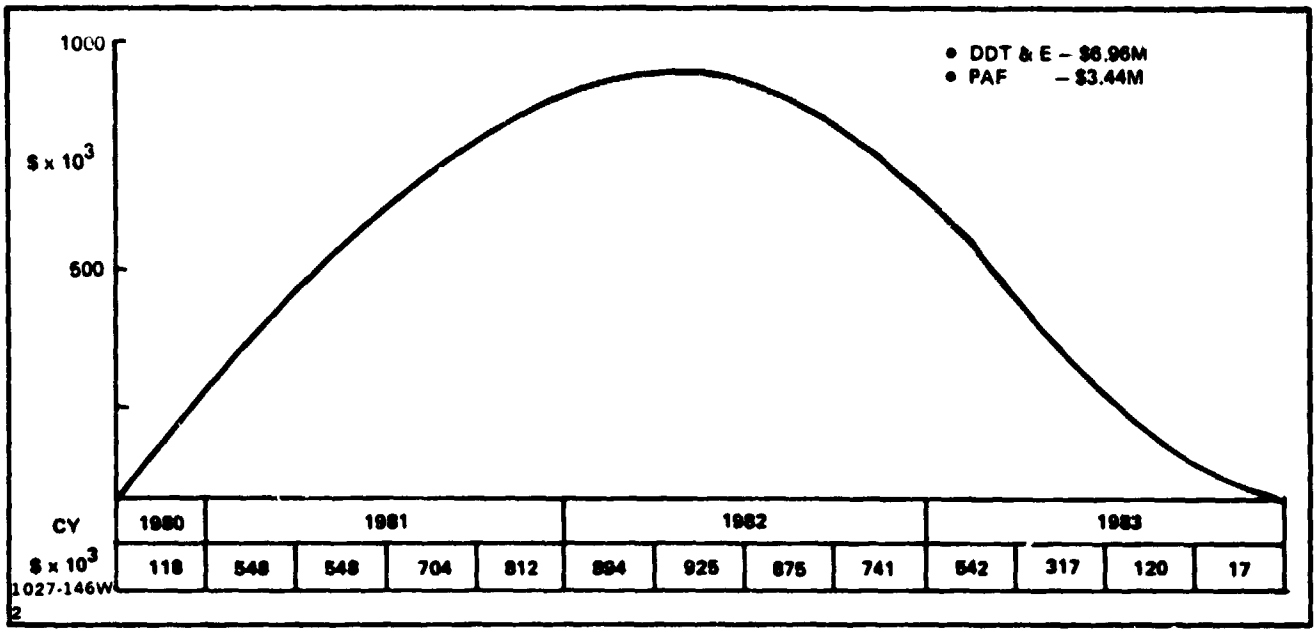

Fig. 7-9 Funding Schedule-Structural Demonstrator

CY	1980	1981				1982				1983			
QUARTER	4	1	2	3	4	1	2	3	4	1	2	3	4
PROJ. MGMT	16	47	74	95	108	113	109	97	79	58	35	15	2
SE & I	19	57	90	115	131	136	132	118	96	69	42	18	3
SYS GRND TEST	29	86	135	174	198	206	199	178	145	105	63	27	4
DEMO ARTICLE	15	43	68	87	99	103	100	89	72	52	32	13	2
ASSY SUPT EQUIP.	39	115	181	233	265	276	267	238	194	110	85	36	6
LOGISTICS & OPS	–	–	–	–	11	60	118	155	155	118	60	11	–
TOTAL	118	348	548	704	812	894	125	875	741	542	317	120	17

1027-147W
2

Fig. 7-10 Funding Schedule – Structural Demo Option Costs (Thousands of 1979 Dollars)

2

The funding schedules for the Free-Flier Option were developed in the same manner as the Structural Demonstrator and are presented in Fig. 7-11 and 7-12. The impact of the free-flier subsystems on total cost and PAF can readily be seen in Fig. 7-11.

7.4.3 Cost Comparisons

A cost comparison of the two LSS Options, developed during this follow-on phase of the study, is shown in Fig. 7-13. This comparison shows option costs broken down

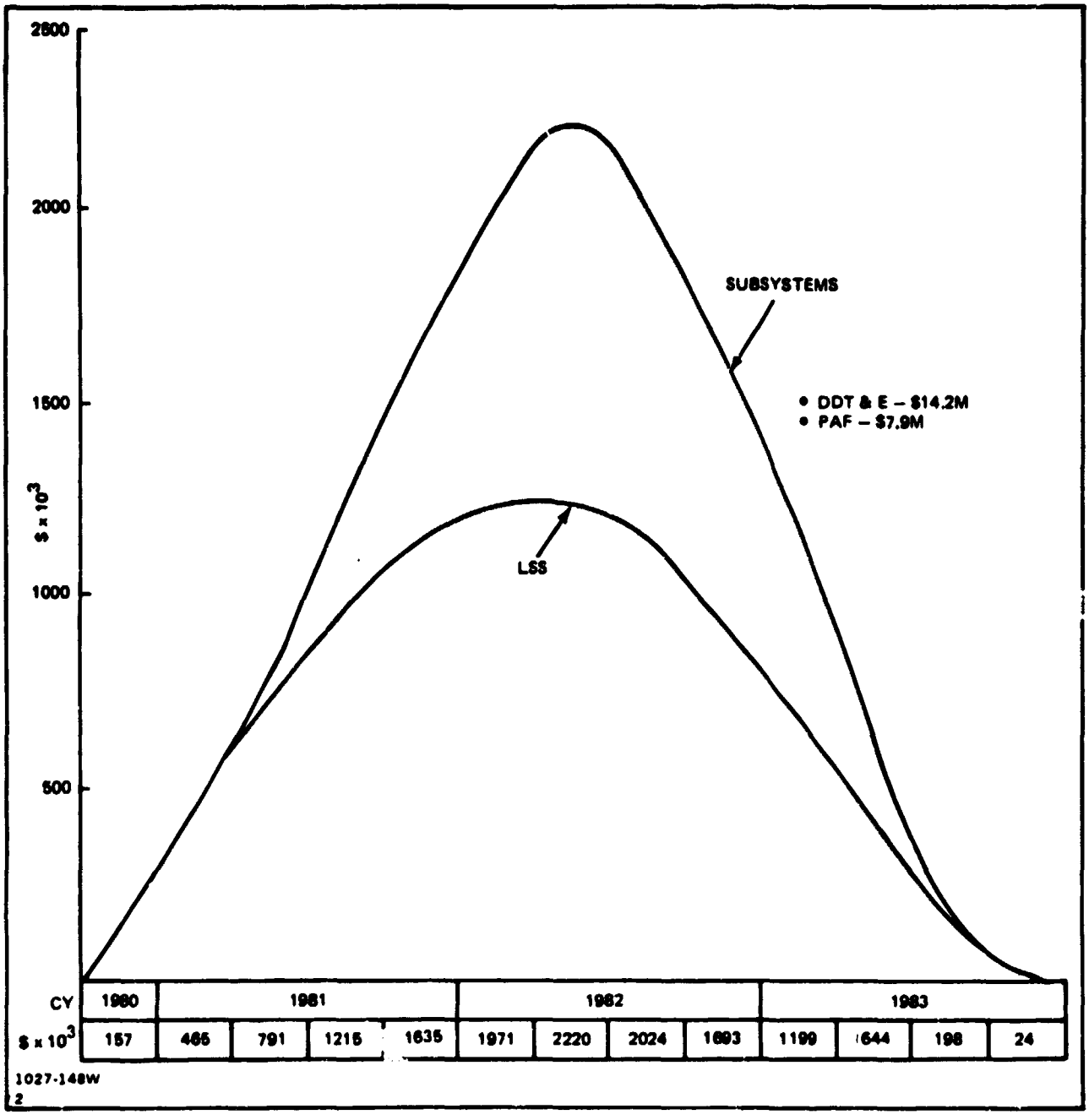

Fig. 7-11 Funding Schedule – Free-Flier

into WBS 1.0, 2.0 and 3.0 categories. The difference in WBS 2.0 costs reflects additional kits required for Shuttle support in the Free-Flier Option (OMS and EPS). As was previously noted, WBS 3.0 costs for the Structural Demonstrator are zero since it has no subsystems or payload.

CY	1980		1981			1982				1983			
QUARTER	4	1	2	3	4	1	2	3	4	1	2	3	4
PROJ. MGMT	20	59	93	119	136	141	137	122	99	72	43	18	3
SE & I	42	122	191	245	279	290	280	250	204	148	90	39	7
SYS GRND TEST	35	102	161	206	234	245	236	211	182	134	75	32	5
DEMO ARTICLE	18	54	85	109	124	150	125	112	91	66	40	17	3
ASSY SUPT EQUIP.	42	123	193	248	282	294	284	254	201	150	90	38	6
LOGISTICS & OPS	–	–	–	–	14	74	146	191	191	146	74	14	–
GSE	–	5	28	56	73	73	56	28	5	–	–	–	–
SUBTOTAL	157	465	751	983	1142	1247	1264	1168	969	706	412	158	24
SUBSYSTEMS	–	–	40	232	493	724	856	856	724	493	232	40	–
TOTAL	157	465	791	1215	1635	1971	2220	2024	1693	1199	644	198	24

1027-149W
2

Fig. 7-12 Funding Schedule – Free-Flier Option Costs (Thousands of 1979 Dollars)

OPTION	WBS 1.0 LSS	WBS 2.0 PROGRAM SUPPORT	WBS 3.0 MISSION HDWR	PROGRAM COST
STRUCTURAL DEMO	7.0	33.4	0	40.4
LSSD FREE FLIER	9.4	33.7	4.7	47.8

- COSTS ARE IN MILLIONS OF 1979 DOLLARS
- WBS 2.0 COSTS ARE MADE UP OF SHUTTLE (≈$24M) & ABB MODIFICATION ($9.5M)

1027-150W
2

Fig. 7-13 Option Cost Comparison

Figure 7-14 compares the Structural Demonstrator and free-flier Platform costs generated for the LSS concepts developed in both initial and follow-on study efforts. Structural Demonstrator costs are similar, whereas the more than $20M reduction in free-flier Platform costs reflects a considerable simplification in subsystems complexity for the presently-proposed LSS platform.

7.5 PROGRAMMATIC OBSERVATIONS AND RECOMMENDATIONS

An LSS space fabrication flight demonstration, utilizing an ABB, could be performed in the 1983-1984 time-period. Two options have been identified; a Structural Demonstrator and a free-flying LSS Platform. Both options provide low cost approaches for an early LSS demonstration mission.

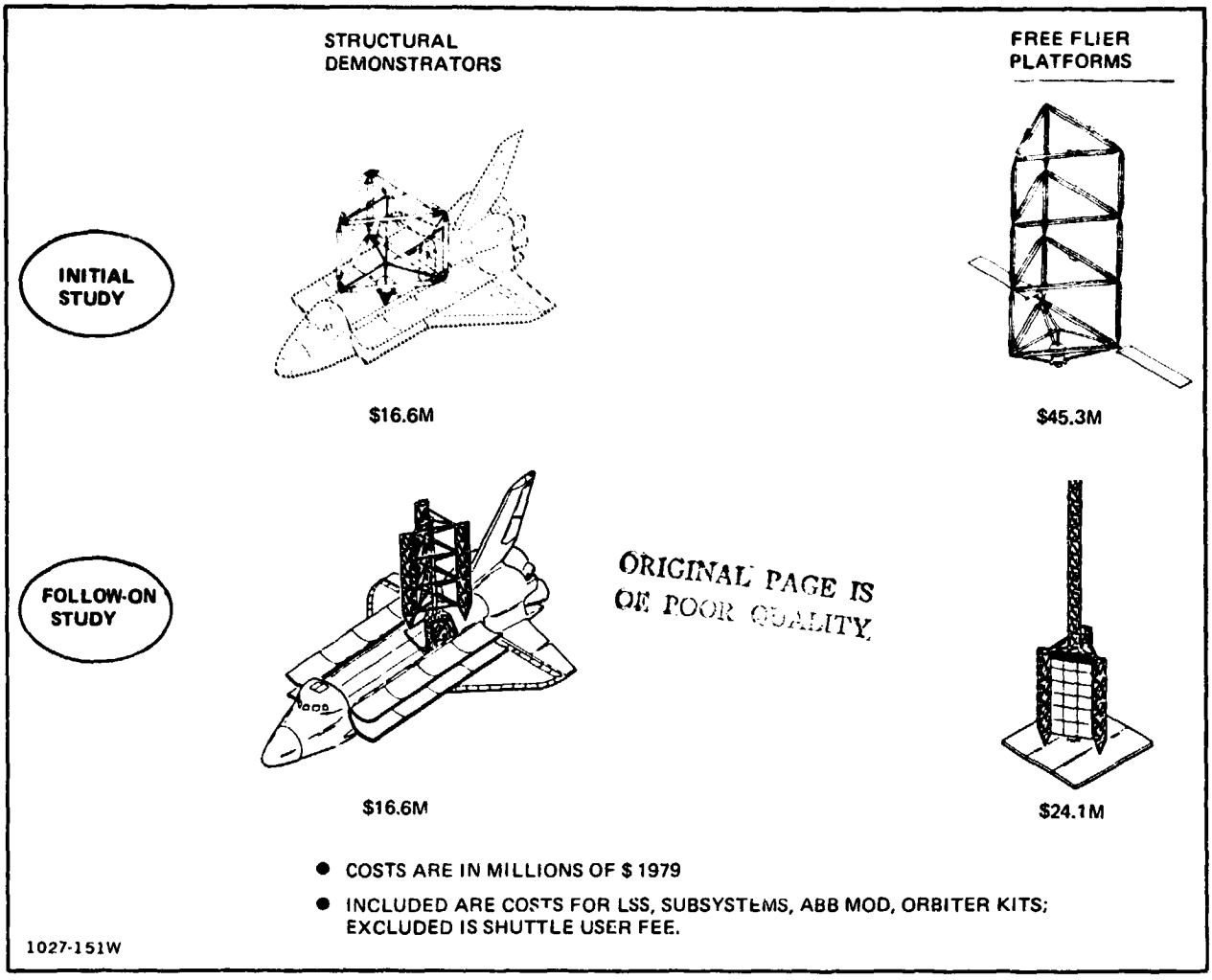

Fig. 7-14 LSS Concepts Cost Comparison

The simple LSS Platform concept should be further refined to extend its utility to potential near-term users. Simulation efforts are recommended to evaluate lighting needs for dark-side operations, and to establish relevant construction/assembly time-lines via neutral bouyancy simulation.

Our present LSS mission planning has baselined a flight adaptation of the ground demonstration ABB machine, with an estimated ROM cost of $9.5M to modify the ground demo machine to flight status. The reality, practicality, cost-effectiveness, and over-all merits of this "rehab" approach should be critically examined. An early appraisal addressing the issue of "what ABB to fly?" is urgently recommended.

2

8 - ALTERNATE LSS CONCEPTS EVALUATION

In the present study, attention has been focused on Large Space Structures with dimensions in the order of meters to hundreds of meters. Preliminary assessments of structures in the kilometer size-range have been performed for a:

- Pinhole Camera, and
- Gravity Wave Interferometer.

Figure 8-1 shows that the principal subject areas supporting these assessments are stabilization/control, dynamic analysis and, thermal analysis. Volume III of this report contains the results of work performed in the thermal analysis area, and Appendix A of this Technical Report the results of LSS structural dynamic analyses. These analyses form the underlying background for conducting these kilometer-size structural assessments. Although these missions are potentially further "down stream", a continuing awareness of Large Space Structure missions and user applicability is appropriate to reflect these future needs in LSS demonstration planning.

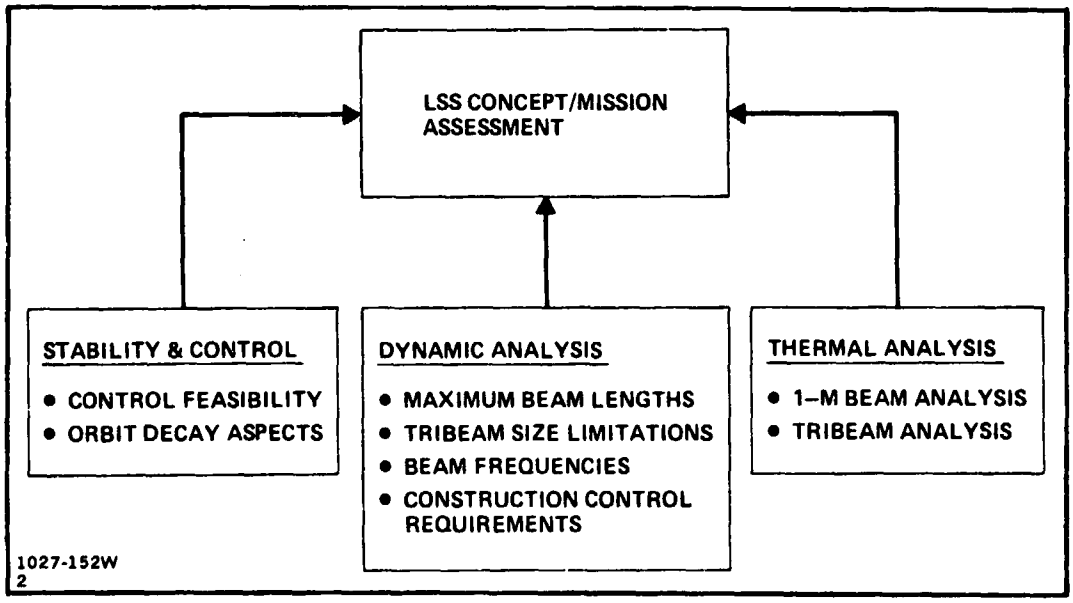

Fig. 8-1 Alternate LSS Concepts Evaluation

2

8.1 PINHOLE CAMERA

Preliminary studies by NASA have shown the mission and optical design feasibility of a pinhole camera to obtain:

- Hard-X-ray imaging of sources directly associated with chromospheric manifestations of flares and studies of the solar corona
- High spatial resolution observations of the corona
- Images of high energy astrophysical objects.

In a current NASA concept (Fig. 8-2), a lead shield with randomly distributed pinholes is mounted in the Orbiter and detector arrays are mounted on a free-flying satellite positioned 1 km away.

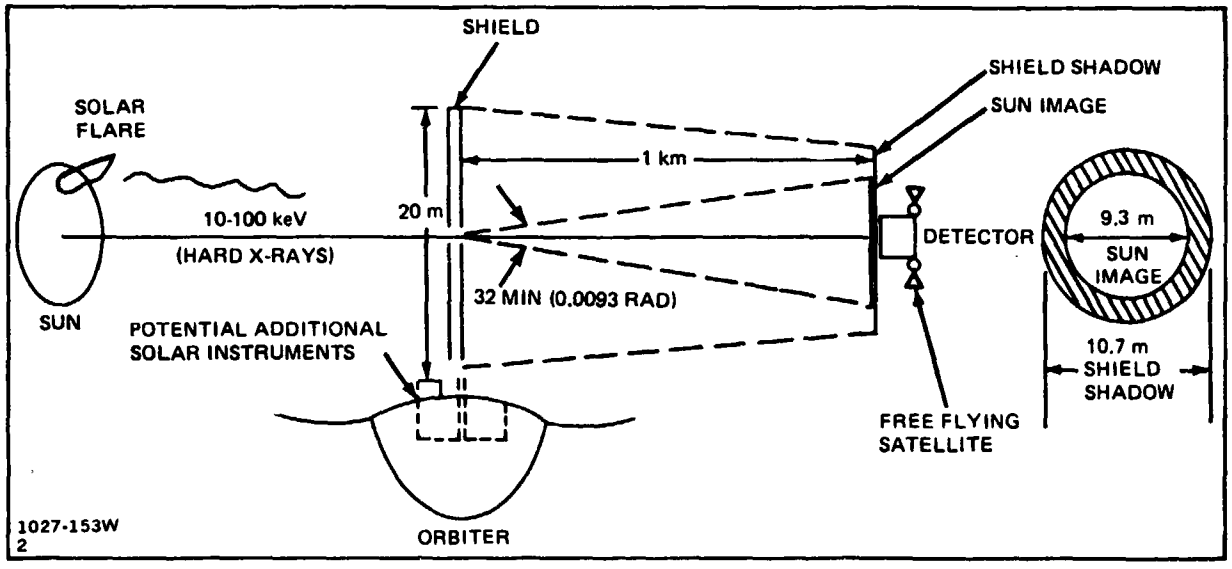

Fig. 8-2 System Configuration : Deployed Mask and Free Flying Detector Subsatellite

An investigation was made to determine the feasibility of using a large space structure to mount the shield and detector. The use of such a structure would avoid the constant maneuvering required of the free-flying elements to maintain proper separation distance. A separation distance of 1 kilometer between the shield and detector was chosen to obtain a representative length which also supplies adequate resolution (Fig. 8-3). Using the construction limitations information of Appendix A, a 10 to 20 m Tribeam of this length could be fabricated in low earth orbit by the Orbiter or a space construction platform. The 20 m Tribeam was chosen since it is compatible with mounting the 20 m diameter lead shield. A concept of the Pinhole Camera satellite is shown in Fig. 8-4. As shown in Fig. 8-5, the total satellite is estimated to weigh at least 20,000 kg.

2

SEPARATION, km	USE	PINHOLE DIAMETER, mm	N	FOV $\bar{s}$	RESOLUTION $\bar{s}$
1	X-RAYS	8	4×10^4	200	1
1	X-RAYS	10	10^4	200	2
1	γ, X-RAYS	10	10^2	200	20
N = NUMBER OF PICTURE ELEMENTS IN DETECTOR ARRAY					
1027-154W 2					

Fig. 8-3 Characteristics of FOV and Resolution for 1 m^2 Detector Array and Pinhole Camera

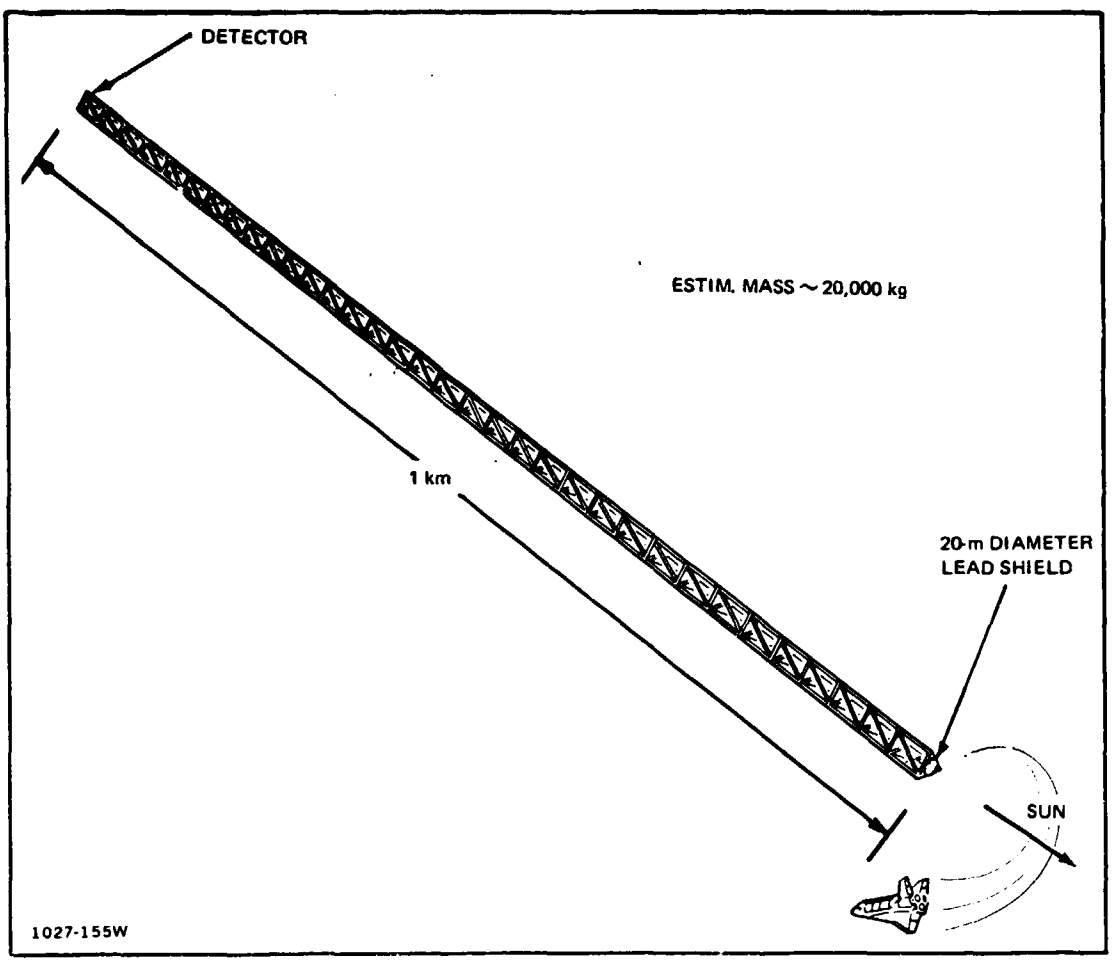

Fig. 8-4 Pinhole Camera

X-RAY PINHOLE SYSTEMS	WEIGHT, kg
SHIELD, FOCAL PLANE, INSTRUMT.,	8,500
20 m TRIBEAM (1,000-m Long)	11,700
TOTAL	20,200
1027-156W 2	

Fig. 8-5 Estimated Mass Characteristics

2

It would be desirable to fly the pinhole camera in a sun synchronous orbit. The satellite would be perpendicular to the orbital plane and continuously sun-pointing. Gravity-gradient torques would be minimal in this flight attitude. However, the total Orbiter payload to this orbit is limited to 13,000 kg at 200 n mi. Multiple Orbiter flights would thus be necessary to construct the satellite.

The satellite could also be placed in a low inclination orbit with a KSC launch. However, it would experience significant gravity-gradient torques (5700 ft-lb) in this orbit inclination, to maintain continuous sun-pointing. With the satellite mounted in the Orbiter, or during the process of construction, this torque could increase to 12,000 ft-lb, which would overpower the Orbiter's vernier control system. It would appear that construction from the Orbiter would have to be performed in a free-drift, earth-pointing orientation. In addition, it is expected that construction time would exceed 7 days and thus the Orbiter would require support from a power module, or the construction performed on an orbiting construction platform.

The pinhole camera will not be able to operate in Low Earth orbit. Because of its high drag to mass characteristics, it will experience a rapid orbital decay. Figure 8-6 shows that if the satellite is placed in a 450 km orbit (57° inclination) that the altitude will decay 100 km in 2 to 3 months with a nominal atmosphere.

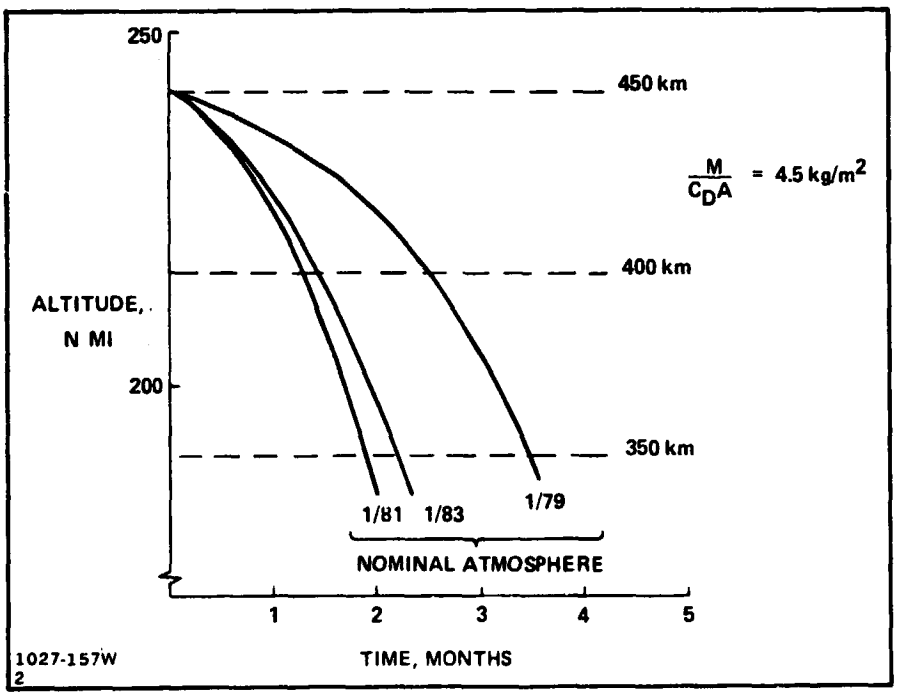

Fig. 8-6 Pinhole Camera — Orbital Decay

2

8.2 GRAVITY WAVE INTERFEROMETER

The existence of gravitational waves has long been predicted by leading members of the scientific community. At the present time, no gravity waves have been positively identified using laboratory techniques. It has been postulated that a large laser type interferometer placed in earth orbit with loosely suspended end masses could provide the sensitivity required to detect gravity waves. The successful detection will involve measurement of motions less than 10^{-8} cm for 1000 kg masses suspended on kilometer-length arms. Although laser technology might be applicable for this application, the amount of noise in the measurement is not well defined at this time. The question of whether the various noise sources will swamp the desired signal is crucial to the success of the detection concept. The major noise sources requiring analysis are:

- Laser amplitude fluctuations
- Laser phase fluctuations
- Laser radiation pressure fluctuations
- Thermal gradient noise
- Cosmic ray pulses
- Mechanical/thermal vibrations
- Gravity-gradient variations
- Electromagnetic field noise
- Solar wind variations
- Atmospheric pressure waves.

Once the noise levels from these sources are established, the required amount of isolation could then be defined.

Preliminary analyses indicate that the strongest noise appears to be cosmic ray pulses and structural vibrations. Although it is not possible to isolate the measuring mass from cosmic rays because the shielding mass required would affect the gravity wave measurement, techniques exist to measure this source. Thus, it may be possible to measure this stochastic force, rather than eliminate it. The structural requirement is for a homogeneous suspension, i.e., force independent of displacement, and this will require development of soft suspension techniques and control systems.

To detect gravity waves from a single spacial direction at least three masses oriented in space are required, with four masses symmetrically placed preferred. The masses should be "captured" by the structure when the interferometer is not in use, and would be released to be essentially free-flying when measurements are to be taken.

A preliminary analysis was conducted to determine whether a suitable large space structure could be constructed for this application. A cruciform configuration (Fig. 8-7) was considered and the structural characteristics examined were bending moments, deflections (Fig. 8-8), and natural bending frequency (Fig. 8-9). A "worst case" cruciform orientation, with its arms at 45 deg to the local vertical was examined to establish the magnitude of loads and deflections induced by gravity gradient loads, at an assumed 200 n mi altitude. Two beam depths were investigated: a one-meter beam as fabricated by the ABB, and a Tribeam of 14.3-m depth (16.5-m members), using the ABB one-meter members as structural caps. The equivalent stiffness of the Tri-beam selected was EI = 5.73×10^{11} lb-in.^{2}

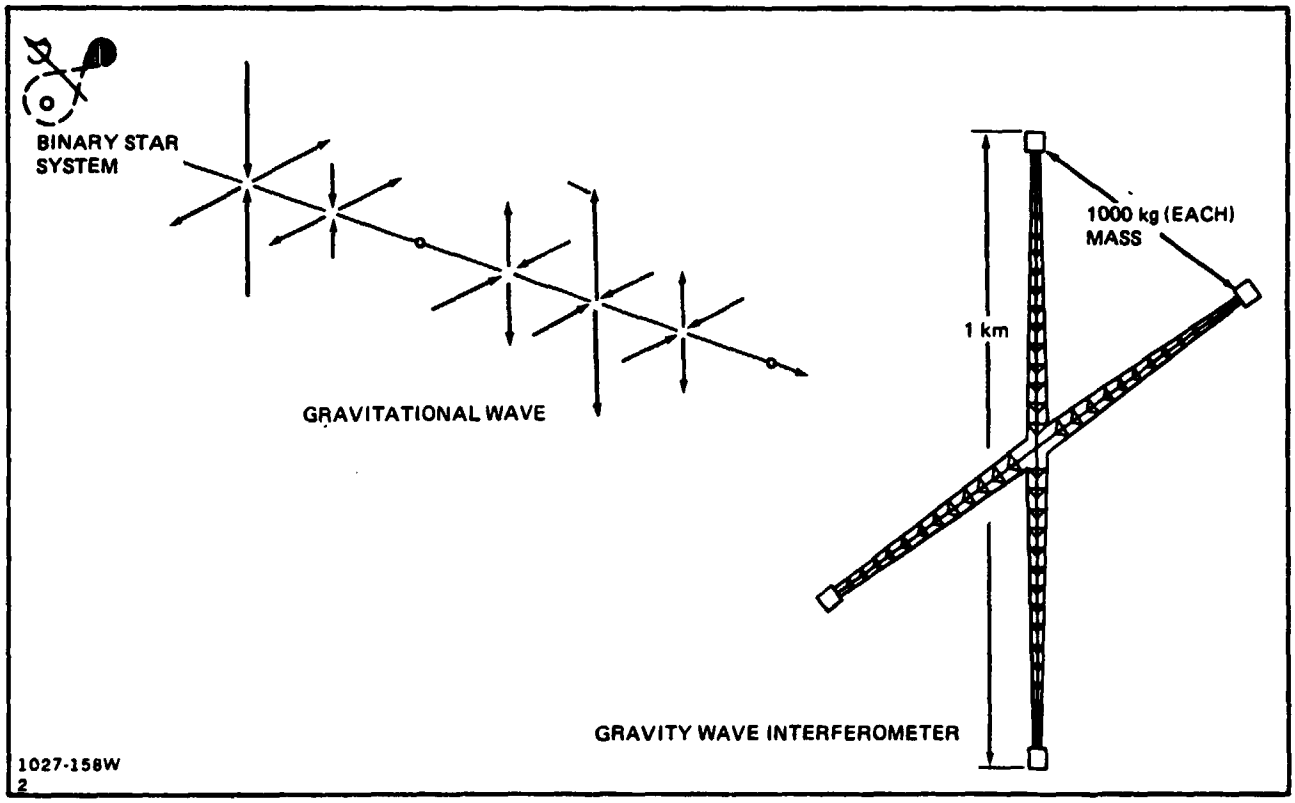

Fig. 8-7 Gravity Wave Interferometer Cruciform Configuration

2

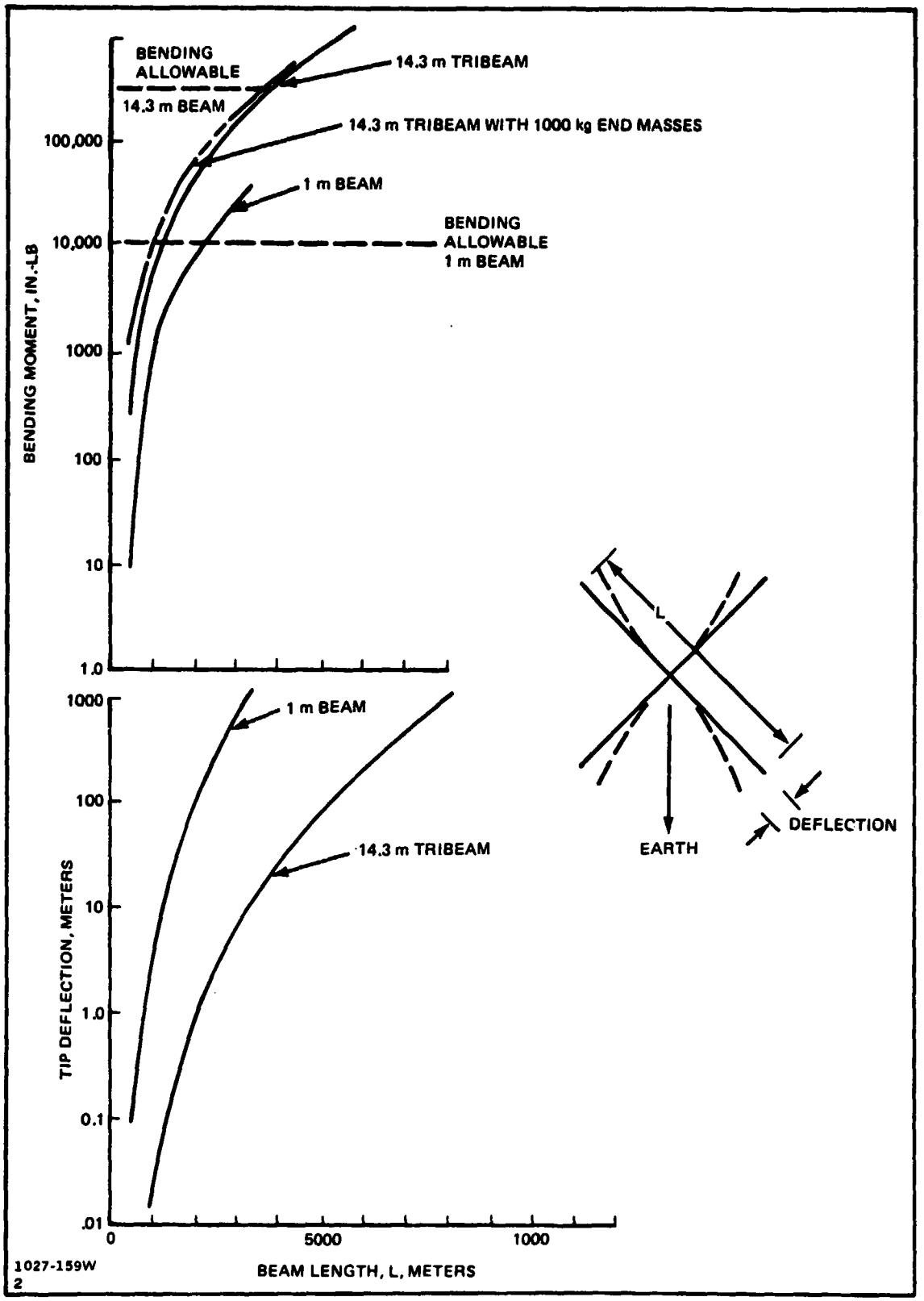

Fig. 8-8 LSS Gravity-Gradient Interferometer Cruciform Configuration Bending Moment and Deflection vs Beam Length

2

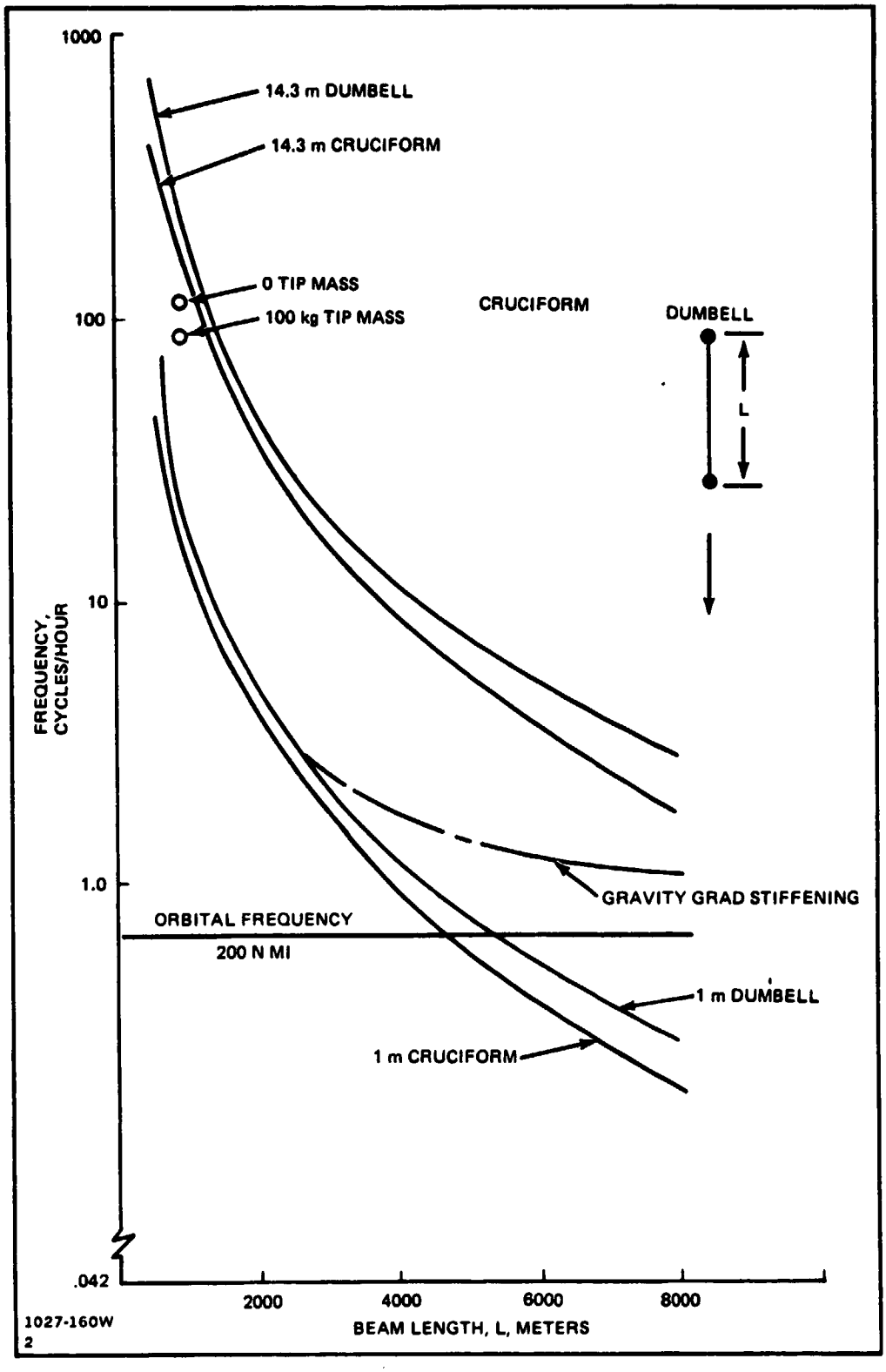

Fig. 8-9 Gravity-Gradient Stabilized Interferometer: Natural Bending Frequency (Free-Free) vs Beam Length Dumbell and Cruciform

Figure 8-8 plots the bending moment and deflection of a cruciform at 200 n mi altitude, 28-½° inclination. As shown, the maximum length of a 14.3-m Tribeam is limited by its structural strength to approximately 3750 m with the end masses released, and 3500 m with 1000 kg end masses captured. The point of interest on these curves is the 1000 m length where the curve indicates that the bending moment is well within allowable, and lateral tip deflection is about 1 cm for the Tribeam without end masses. Since the gravity-gradient torque producing this deflection (at 200 n mi altitude), will be greatly reduced by increasing its altitude of operation, the deflections induced by this effect should be considered minimal or negligible.

Figure 8-9 illustrates the natural bending frequency of the cruciform structure versus length. These frequencies were developed for a free-free beam and for 1000-meter lengths, and indicate that the structural frequencies are two orders of magnitude greater than the orbital frequency at LEO. The addition of 1000 kg end masses does not significantly affect these results since the frequency without tip masses (112 CPH) drops to only 88 CPH with the end masses. Since the rigid body rotation frequency due to gravity-gradient stabilization is $\sqrt{3}$ times the orbital frequency, structural coupling of the overall system should be minimal at any altitude of GWI operation. Figure 8-9 also shows the variation of frequency with length of a dumbell configuration (i.e., a long straight beam with tip masses). Although this configuration is not viable as a gravity wave interferometer, it serves to illustrate certain properties of the structure. For example, the figure shows the effects of gravity-gradient stiffening of the structure, which indicates that as length is increased, the tensile loads induced by gravity produce a stiffening effect on a beam oriented to the local vertical. In addition, since this configuration tends to align with the local vertical, bending moments and deflections are minimized. Figure 8-10 shows an interferometer configuration concept which could take advantage of these gravity-induced properties. The configuration is omnidirectional and minimizes the influence of gravity-gradient torques when the inertia about the earth pointing axis is four to six times that of the other axis. In addition, the extra masses allow gravity wave direction-finding without vehicle slewing.

The GWI configuration shown in Fig. 8-10 is estimated to weigh on the order of 80-100,000 kg. Drag characteristics of this configuration (M/CDA $\approx$ 12.3 kg/m^2) would also reflect a rapid decay in orbit altitude, as did the Pinhole Camera Satellite.

2

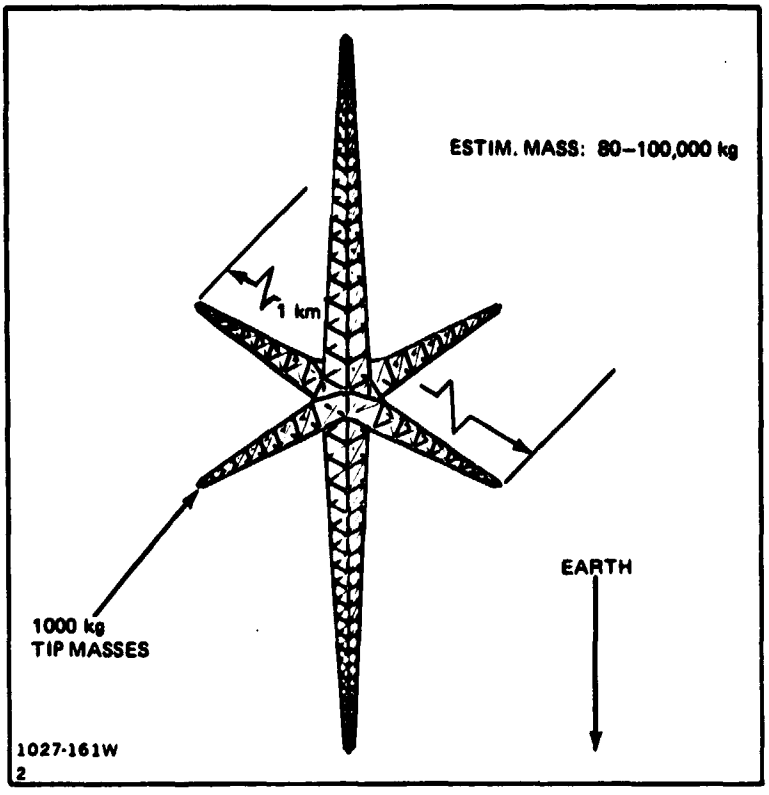

Fig. 8-10 Gravity Wave Interferometer: Gravity-Gradient Stabilized Configuration

8.3 CONCLUSIONS AND OBSERVATIONS

The high drag to mass ratios of the Gravity Wave Interferometer and Pinhole Camera Satellite concepts limit the practicality of their operation to high altitudes. LEO operation is not feasible. Analyses of structural deflections, induced at LEO altitudes by gravity-gradient torques, were found to be minimal. At higher altitudes these deflections are expected to be negligible.

As discussed in Volume III of this report, a large space structure operating in a LEO orbit, successively exposed to sunlight and darkness, will continuously distort (albeit minimally) under the influence of varying orbital conditions. From a structural point of view it would appear, therefore, that the GWI and Pinhole Camera's operations would be enhanced by maintaining an orientation fixed to the sun. In this regard, sun-synchronous or GEO orbits should be considered to minimize the structure's distortion in orbit.

2

9 - SUPPORTING RESEARCH AND TECHNOLOGY

9.1 INTRODUCTION

A summary of the Supporting Research and Technology (SR&T) efforts recommended in support of the LSS flight demonstration mission are presented in Fig. 9-1. The SR&T needs are categorized in terms of:

- Analysis and Testing
- Design Investigations
- Design and Development
- Ground Simulation Activity.

9.2 ANALYSIS AND TESTING

Three types of ground tests are recommended:

- Static Structural
- Structural Dynamic
- Thermal Vacuum.

Structural testing of the 1-meter beam is necessary to evaluate axial load, bending, shear and torsional capability, and combined loading effects. Since post-buckling characteristics of very thin gauge materials is a technology area presently not well understood, measurement of changes in beam stiffness, bending, and torsional capability should be evaluated by testing. Compression tests of the 1-meter beam have been conducted, for example, and during these tests, buckling in the cap member was observed to begin at about 25% of limit load. Thus, in other than lightly loaded situations, the beam caps will be in buckled condition.

In the absence of sufficient analytical tools, axial load, bending, shear and torsional tests should be conducted to establish appropriate design requirements for tripod/end fitting and Tribeam joint designs. In addition, the loading conditions induced within structural elements of a 1-meter beam during exposure to the thermal environment in orbit, should be assessed to determine if the beam's elements could be in a buckled state during an orbit transit. If so, a further refinement of the transient

thermal analysis of the 1-meter beam would be necessary to establish if the buckled condition of the beam's elements accentuate the induced loads and potential distortion of the beam.

Ground-based structural dynamic testing is recommended to identify the nodal frequency characteristics of 1-meter beams, individual Tribeams, and multiple Tribeam configurations (e.g., platforms). These tests can serve to verify analytic models presently being used, and also provide a means to evaluate the effects of fixity conditions imposed by alternative joint designs and structural attachment tech-

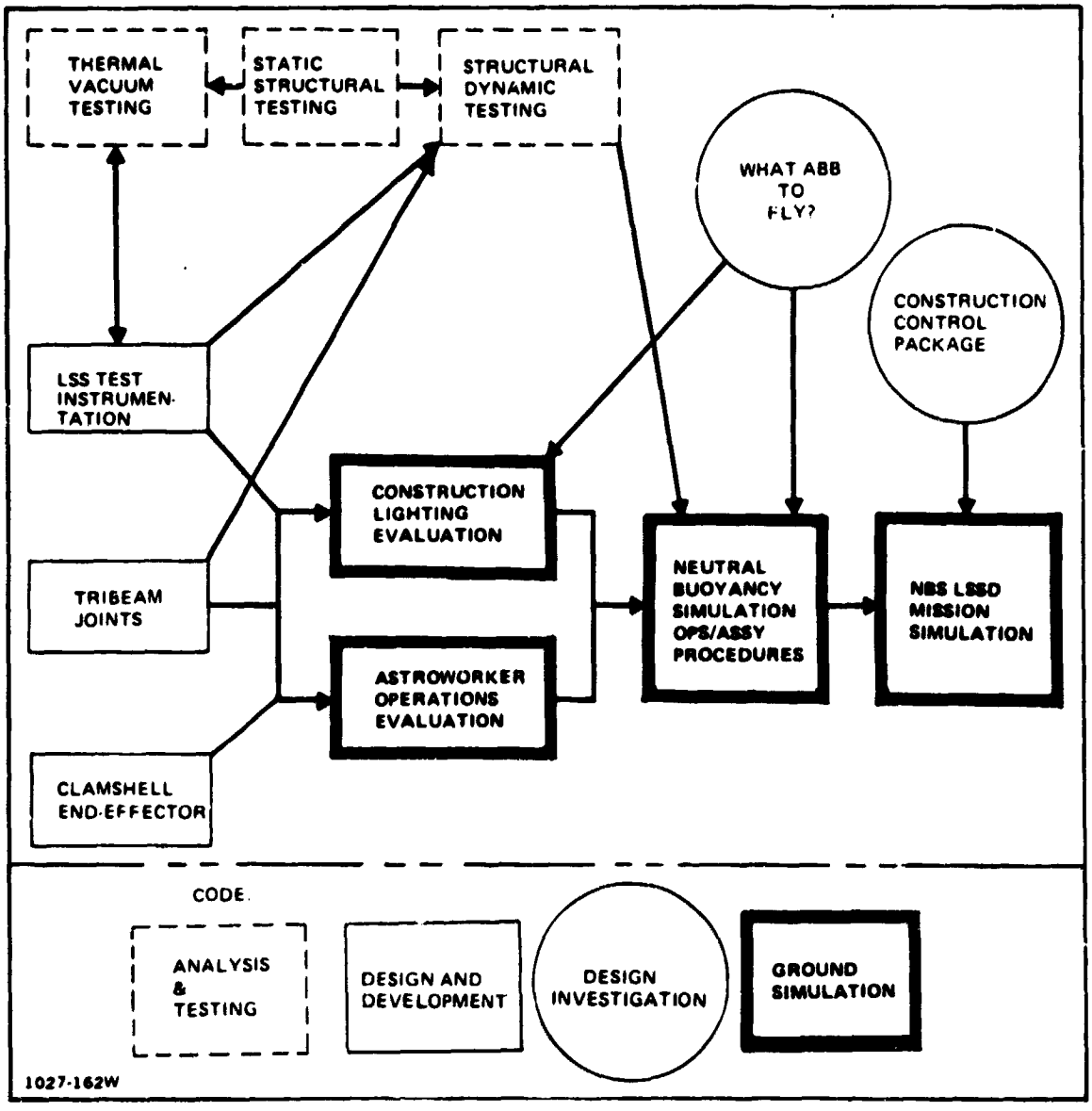

Fig. 9-1 Supporting Research and Technology Development

niques. In addition, the tests can provide the 1-g baseline information against which on-orbit dynamic characteristics may be compared, and could also serve to evaluate the effectiveness of proposed on-orbit test instrumentation.

A thermal vacuum test of the 1-meter beam should be performed in a solar simulator/vacuum test chamber to assess its thermal response to the simulated solar environment. The effects of alternate thermal coatings, member blockage, and thermal effects under local buckling conditions should be evaluated. These tests would serve to verify the validity of the analytical models being used in the transient thermal analysis (reference Volume 3 of this report), and also evaluations associated with predicting the structure's response (loading conditions and distortion) to thermal excitation.

9.3 DESIGN INVESTIGATIONS

Our present LSS mission planning has baselined a flight adaptation of the ground demonstration ABB machine. This flight version is estimated to weigh about 7250 kg (16,000 lb). Studies of flight weight ABB designs, reflecting ABB ground demonstration experience, are recommended to establish the necessary design characteristics of these machines and to provide appropriate weight "bogeys" for operational (versus demonstration) ABB hardware. Of critical importance to this LSS demonstration mission is a realistic appraisal of the practicality/cost-effectiveness of flying a modified ground demonstration ABB. This appraisal and its subsequent consequences represent the long-pole-in-the-tent vis-a-vis this LSS flight demonstration mission. An early appraisal, therefore, addressing the issue of "what ABB to fly" is urgently recommended. The low cost/low risk aspects of this proposed LSS mission offer considerable appeal.....thus the ABB issue must be resolved expeditiously.

An additional important area influencing the success of an LSS demonstration mission concerns the Orbiter's flight control system. In order to conduct meaningful and effective LSS flight demonstrations using the Orbiter as the construction platform, the general flight control characteristics exhibited by the Orbiter's Vernier RCS (VRCS) System were found desirable. It is our present understanding, however, that there is insufficient backup/redundancy in the VRCS System to allow its use as the primary flight control during an LSS flight demonstration mission. It is therefore recommended that a separate "construction control package" be investigated for adaptation to LSS construction missions from the Orbiter. This study has shown, for example (reference Appendix A), that limit cycle rates (ω_{LC}) of 0.001°/sec or less

and deadband angles of between 0.2 and 0.6 deg are desirable to allow on-orbit construction of large space structures, and to avoid undesirable frequency coupling conditions which could occur during both construction and Orbiter/LSS flight operations (e.g., deployment and retrieval of LSS spacecraft).

9.4 DESIGN AND DEVELOPMENT

As illustrated in Fig. 9-1, pacing SR&T items recommended for near-term design and development are:

- Joint designs
- LSS Test Instrumentation
- Clamshell End-Effector.

Design/development efforts in these areas will productively support the recommended test and simulation activities needed to bring the LSS demonstration mission to fruition.

The development of appropriate joint designs for the 1-meter beam are called for as it represents a fundamental need for this demonstration mission. One-meter beam tripod designs, nodal and lap joint designs, and Tribeam joint designs, should be developed and evaluated.

The data developed within this study (reference Volume 3), regarding the linear motions and distortions of the 1-meter beam exposed to the thermal environment in orbit, provides the basis for designing compatible joint designs. These structural response characteristics are fundamental design considerations which must be reflected in joint designs, construction/assembly procedures, and operation of an LSS built with 1-meter beams. Appropriate joint designs should now be developed to enable subsequent SR&T activities involving structural testing and simulation to proceed in timely fashion.

Just as joint design/development is a pacing item for subsequent LSS SR&T efforts, so is the development of appropriate LSS test instrumentation. Installation techniques and designs for accelerometers and thermocouples should be developed in support of the LSS demonstration mission, and their suitability subsequently validated in ground-based structural test and simulation efforts.

In addition, further study and development of the clamshell RMS end-effector is recommended. This device provides a means for handling "frangible" large space

structures, and also supports a fundamental LSS technology need. Its effectiveness could also be tested and evaluated in conjunction with subsequent ground simulation efforts.

9.5 GROUND SIMULATION ACTIVITY

Three types of ground simulation activities are recommended as precursors to an LSSD Mission simulation:

- Construction Lighting Evaluation
- Astroworker Operations Evaluation, and
- Neutral Buoyancy Simulation

Lighting requirements for darkside operations should be evaluated to establish the light levels which are suitable for construction and test phases of the LSS demonstration mission. The potential area vs task lighting needs, however, should be evaluated in conjunction with assessments of alternate Astroworker operational modes applicable to the LSSD mission. Our present mission planning assumes that all Astroworker EVA-related activity will be conducted in a tethered free-floating condition with suitable hand grips and foot restraints (TBD), provided where necessary. Two additional Astroworker operational modes should be evaluated: (1) a free-floating mode which uses a Remote Maneuvering Unit (RMU), and (2) a restrained mode which utilizes the RMS as a cherry-picker. The limitations and applicability of all of these potential Astroworker modes of operation should be established and appropriate guidelines developed for on-orbit construction operations and future mission planning.

The ability to conduct an LSS demonstration mission within a 7-day Orbiter flight limitation is critically dependent upon the extent of Astroworker EVA-time allowed. Therefore, simulation efforts are recommended to establish the maximum practical EVA time that can effectively be utilized for an Orbiter-based LSS mission. Although a 6-hour EVA limitation is presently believed to be acceptable, and has been used for mission planning purposes, the reality and effectiveness of this extended EVA duration remains to be verified. A neutral buoyancy simulation effort addressing this critical issue, in conjunction with evaluations of alternate Astroworker operating modes, is urgently recommended.

Neutral buoyancy simulation is also necessary to substantiate the validity of assembly techniques and mission timelines. Beam handling, joining techniques/tools, and alternate joint designs applicable to the LSS flight demonstration mission should

be evaluated to establish task suitability, timeline information, and LSS design practicality.

Reloading of ABB magazines/cannisters and ABB maintenance operations should also be simulated. An appropriate ABB mockup should be utilized to verify both design suitability and task times for these activities.

A - CONSTRUCTION LIMITATIONS ANALYSIS

During on-orbit construction, LSS elements will be subjected to natural environments (gravity-gradient, solar pressure, aerodynamic) and induced environments (control forces, handling loads). In addition to withstanding these loads, the structure must exhibit sufficient stiffness so that it may be controlled and/or handled. An earlier phase of this study indicated that control force and frequency requirements are a major driver in determining LSS structural dimensional limitations.

An investigation of construction limitations associated with LSS fabricated from the Orbiter, was conducted as part of Grumman's IRAD program. Length limitations due to control and dynamic considerations were determined for a 1-meter beam, and 4½, 10½ and 19½ meter Tribeams. The selection of Tribeam dimensions is related to dimensional considerations of the Orbiter payload bay.

Figure A-1 shows the member configurations. The aluminum 1-m beam is the basic member from which the various Tribeams are constructed. The 4.5-m Tribeam length (each 1-m beam member 4.5-m long) was selected as the largest Tribeam which could be supported within the width (15 ft) of the Orbiter payload bay. The 10.5-m Tribeam has the dimensions which are near the maximum that can be reached by the RMS when the Automated Beam Builder (ABB) is located in the rear of the payload bay. This Tribeam was the size investigated in the initial phase of this LSS study. The 19.5-m Tribeam is slightly larger than the length (60 ft) of the payload bay and is approximately the size of intermediate Tribeams that might be used in building-up a typical Solar Power Station (SPS).

A.1 BEAM AND TRIBEAM MASS AND STIFFNESS

The mass, stiffness and strength properties for the beam and Tribeams used in this investigation are summarized in Fig. A-2. The running weight of the 1-m beam has been calculated and measured experimentally. Tribeam running weights were determined by calculating the total weight of a 3-bay member and include weights of:

- 1-m beams
- Beam end fittings

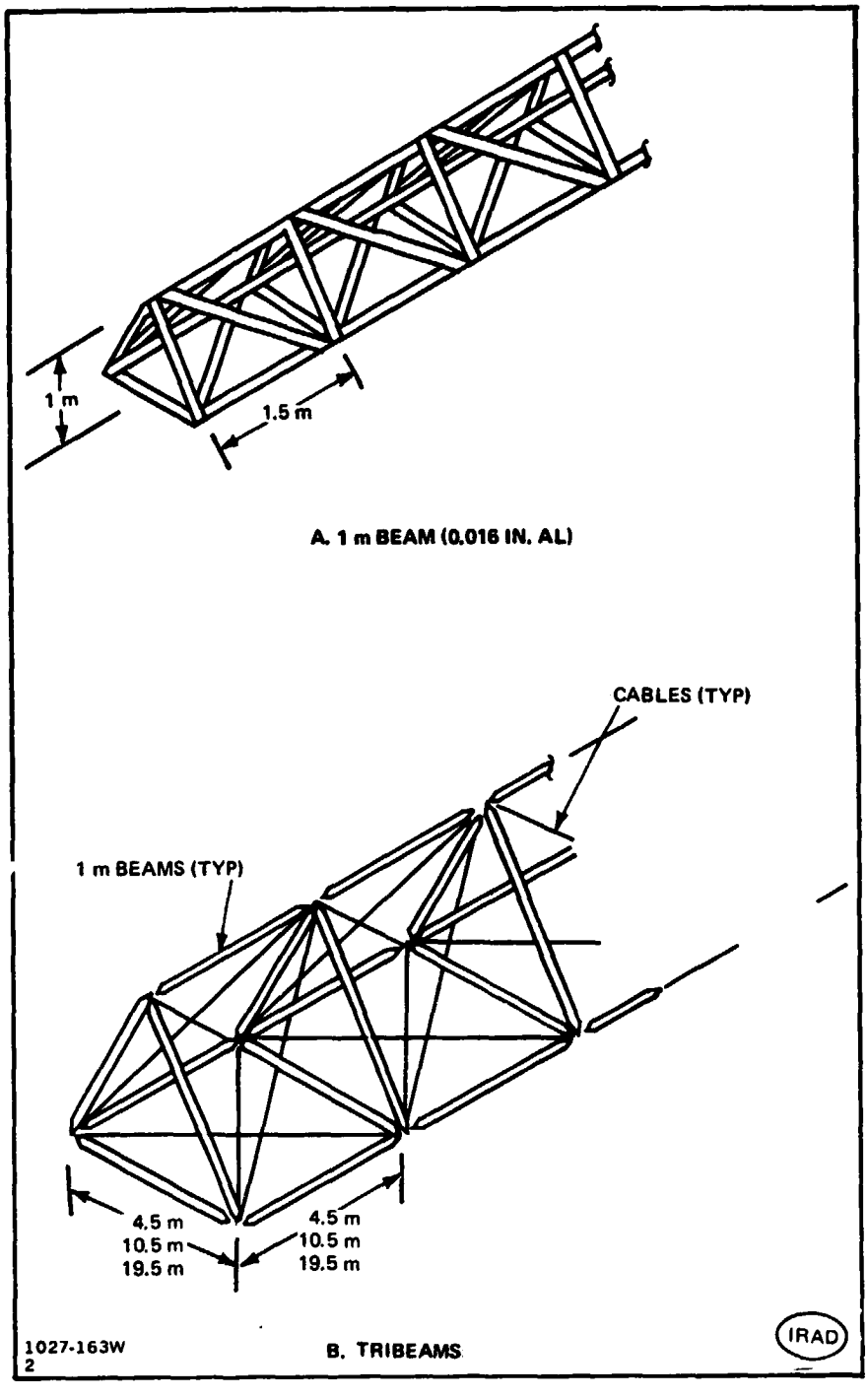

Fig. A-1 One-Meter Beam and Tribeam Geometry

2

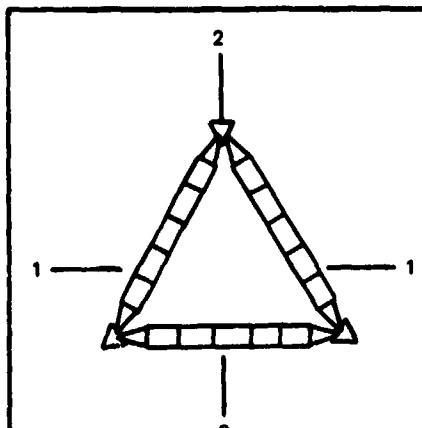

MEMBER	ρ LB/IN.	A IN.^{2}	I IN.^{4}	M LIMIT ALLOW., IN.-LB	
				1-1	2-2
1 m BEAM	0.0711	0.285	95	13,625	15,734
4-5 m TRIBEAM	1.244	0.855	4,473	165,046	190,578
10.5 m TRIBEAM	0.888	0.855	24,351	385,108	444,684
19.5 m TRIBEAM	0.766	0.855	83,988	715,200	825,842

IRAD

Fig. A-2 Member Properties

- Cable and end fittings
- 25% contingency.

Running weights were obtained by dividing the weight of a 3-bay Tribeam by its length. This running weight is approximately correct for the shorter Tribeam lengths and is conservative (10 to 12%) for lengths of 1000 m.

Stiffness properties of the 1-meter beam are determined by E - Modulus of Elasticity = 10.5 x 10^6 psi, and I - Area moment of Inertia = 95 in.^{4}. Tribeam inertias were determined by using the areas of the 1-m beam cap members (0.285 in.^{2}) and the appropriate separation distances for each Tribeam.

Tests on a 1-meter beam have shown that it can withstand an ultimate compression load of 1506 lb. Using an ultimate factor of safety of 1.4, limit allowable bending moments were derived. Note that the allowable bending moment varies depending on the direction of the applied bending moment.

A.2 LOAD CONSTRAINTS DUE TO RCS FIRING

Magnification (or attenuation) of rigid body loads depends on the magnitude and duration of the applied RCS torques and pulse firing frequency. For preliminary analysis, it was assumed that thruster torques could be applied for a duration long enough to produce a magnification of two times rigid body loads.

For short beam lengths, the bending moment due to roll or pitch excitation increases approximately as the length cubed. At longer lengths, however, the beam's inertia predominates over the Orbiter's inertia. Since the beam inertia increases as the length cubed (and the rotational acceleration decreases in a like manner), the resulting bending moment becomes independent of length.

As shown in Fig. A-3, considering bending moment limitations only, primary thruster torques limit the length of a 1-meter beam to 40 m while vernier thruster torques limit the length to 165 m. If the vernier thruster torque is reduced by approximately an order of magnitude, lengths of approximately 2000 m could be accommodated. The 4½ m, 10½ m, and 19½ m Tribeams are limited to 36 m, 55 m and 72 m in length respectively, due to primary RCS firing, while unconstrained in length by vernier RCS firing.

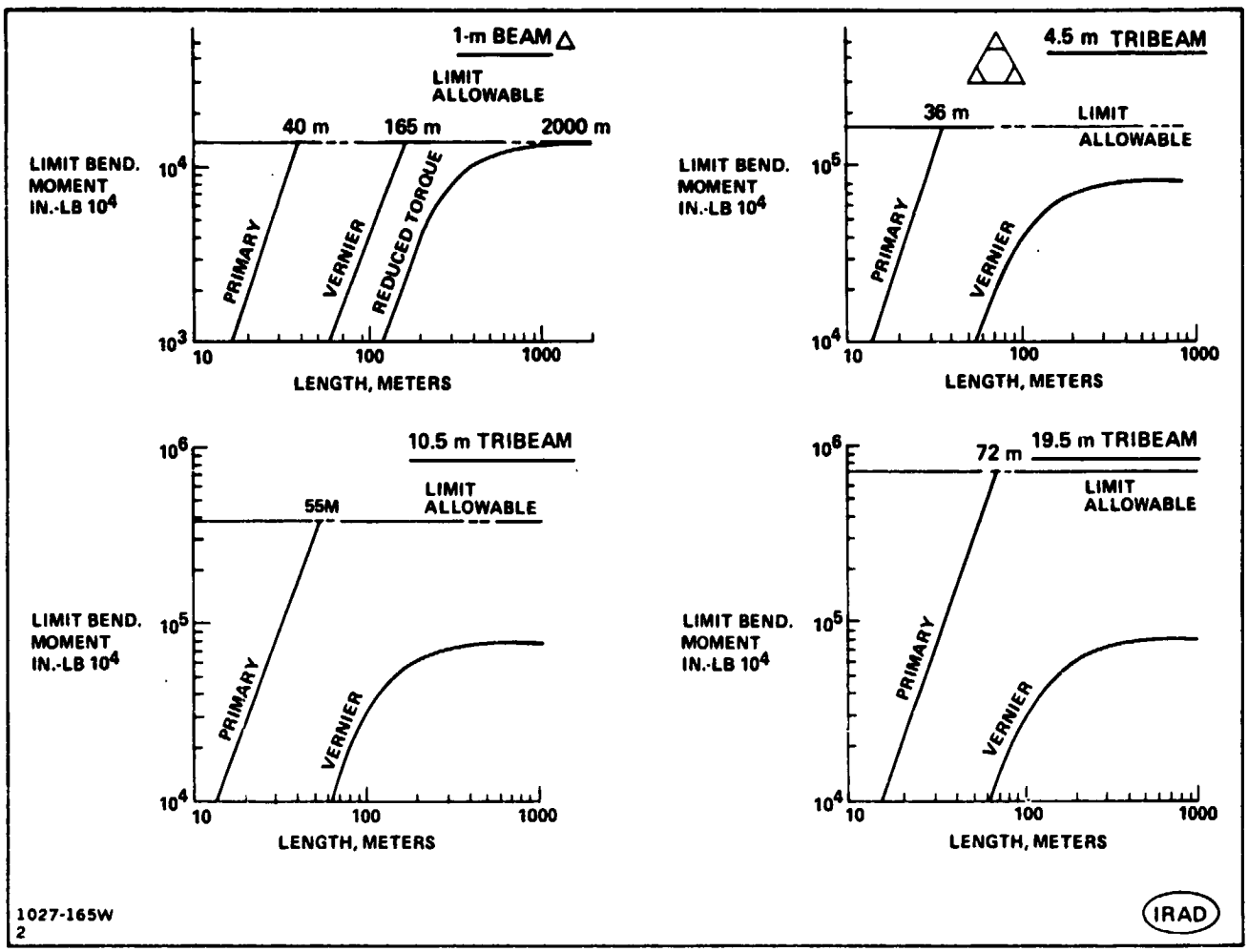

Fig. A-3 Limit Loads Due to RCS Firing

A.3 STRUCTURAL/CONTROL COUPLING CONSTRAINTS

A.3.1 Orbiter Control Characteristics

Although pulse time and firing frequency of the RCS will vary depending on the disturbance torque, the limit cycle frequency is approximately a function of deadband angle and altitude rate. The control frequency can be approximated by the following:

$$\text{Frequency} = \frac{1}{4\underbrace{\frac{(\text{Deadband Angle})}{\text{Altitude Rate}}}_{\text{Coast Time}} + 4\underbrace{\frac{(\text{Attitude Rate})}{\text{Torque Inertia}}}_{\text{Firing Time}}}$$

Rigid body control frequencies should be at least twice the forcing function (or disturbance) frequency; while structural frequencies should be 5 to 10 times greater than control frequencies.

Forcing function frequencies are typically related to orbital rate. Occultation, for example, could occur once per revolution while gravity-gradients could induce a disturbance at twice the orbital frequency, for spacecraft in inertially stabilized flight modes.

The above considerations are reflected on the frequency vs dead-band (as a function of limit cycle frequency) curve shown in Fig. A-4. An appropriate control frequency separation above LEO orbital frequency is shown, and the minimum control frequency range for LEO is indicated together with the corresponding minimum structural frequency range. As will be illustrated shortly, maximum length structures are achievable with construction platform control systems exhibiting limit cycle rates of 0.001°/sec or less. Thus, the basic control requirements for LEO construction platforms, building the largest possible structures, fall within the deadband range shown in Fig. A-4, for a limit cycle frequency of 0.001°/sec.

A.3.2 Structural Frequency Constraints

One-meter beam and Tribeam frequencies as a function of length are shown in Fig. A-5 and A-6. For short beam lengths, the frequency varies approximately as a cantilever, while for long beam lengths, the beam inertia predominates and only the Orbiter's mass is important. At the long beam lengths, the beam is expected to respond approximately as a "pin-free" beam. Specific Orbiter inertia characteristics are only important for the intermediate length beams. The data shown in Fig. A-5 and A-6 are therefore valid for typical construction bases as well as the Orbiter, in higher and lower beam length ranges.

For the Orbiter's nominal control parameters (deadband angle = 0.10°, primary attitude rate = 0.1°/sec, vernier attitude rate = 0.01°/sec), allowable beam lengths are considerably less than those imposed by load (bending moment) constraints. A reduction of the nominal vernier rate by an order of magnitude to 0.001°/sec, is used to illustrate a possible control software change which could allow longer beam lengths.

The control frequencies corresponding to the minimum control frequency range for LEO have also been superimposed on Figs. A-5 and A-6. A representative fixture flexibility (reflecting the fixture used to construct the LSS platform of the earlier phase of this study) has been assumed for purposes of illustration. Under nominal Orbiter vernier RCS limit cycle limitations, the influence of fixture flexibility reduces the maximum constructable length of a 10.5-m Tribeam to 36 m. By reducing the limit cycle rate to 0.001°/sec (an order of magnitude), the effect of fixture flexibility would appear negated.

By adapting a structural parameter reflecting beam stiffness and running weight $\sqrt{\frac{EI}{\rho g}}$ where:

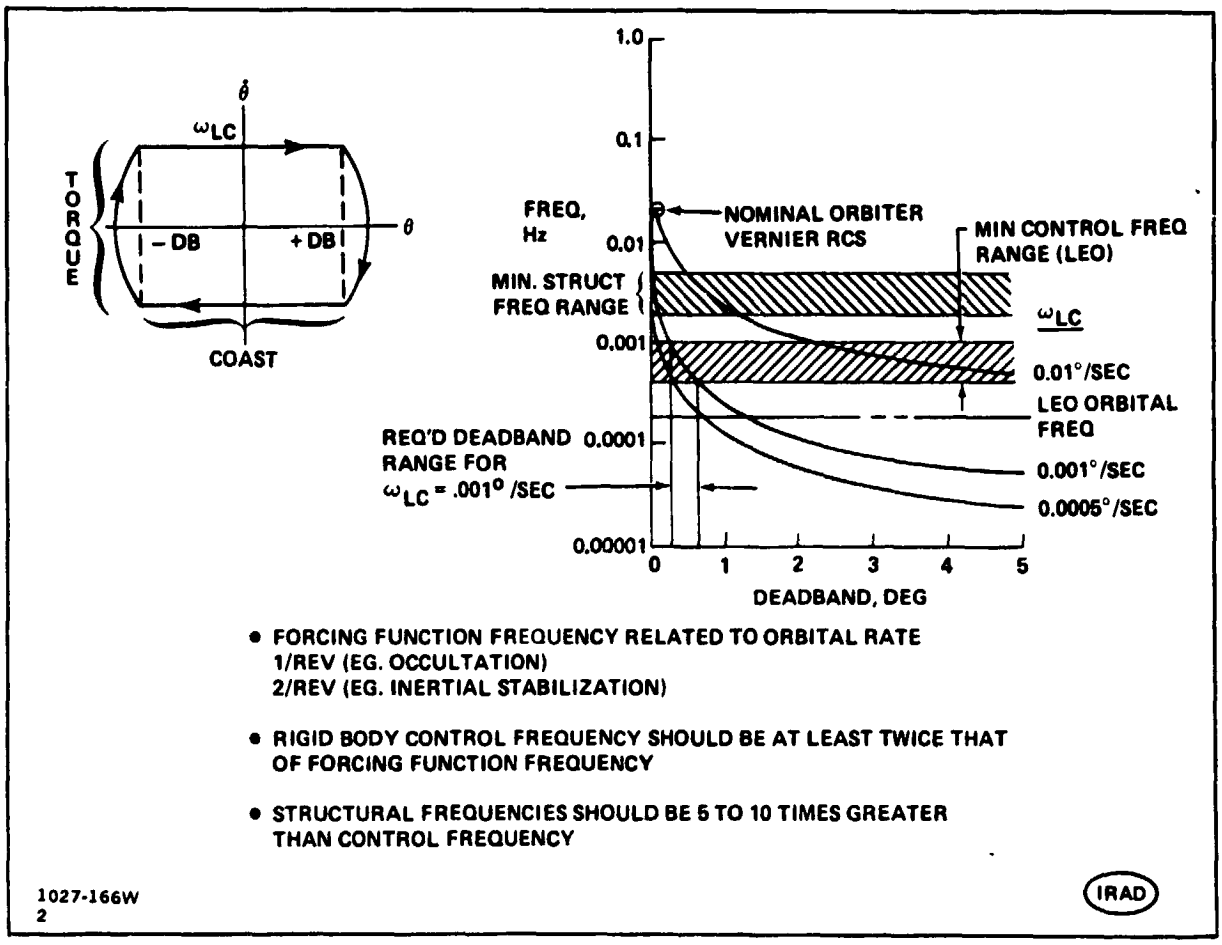

Fig. A-4 Orbiter Control Characteristics

E = Modulus of Elasticity, lb-in.^{2}

I = Beam Inertia, in.^{4}

ρ = Density, lb-in.

g = 386 in./sec^2

and using the previously identified beam length limitation data, the maximum beam lengths attainable in LEO can be determined. Figure A-7 reflects these data in terms of the control frequency factors discussed previously (e.g. a structural frequency representing a 10 or 20 times separation of LEO orbital frequency). The figure also indicates that a 20 - 30% increase in attainable beam lengths can be obtained for composite beams versus aluminum beams.

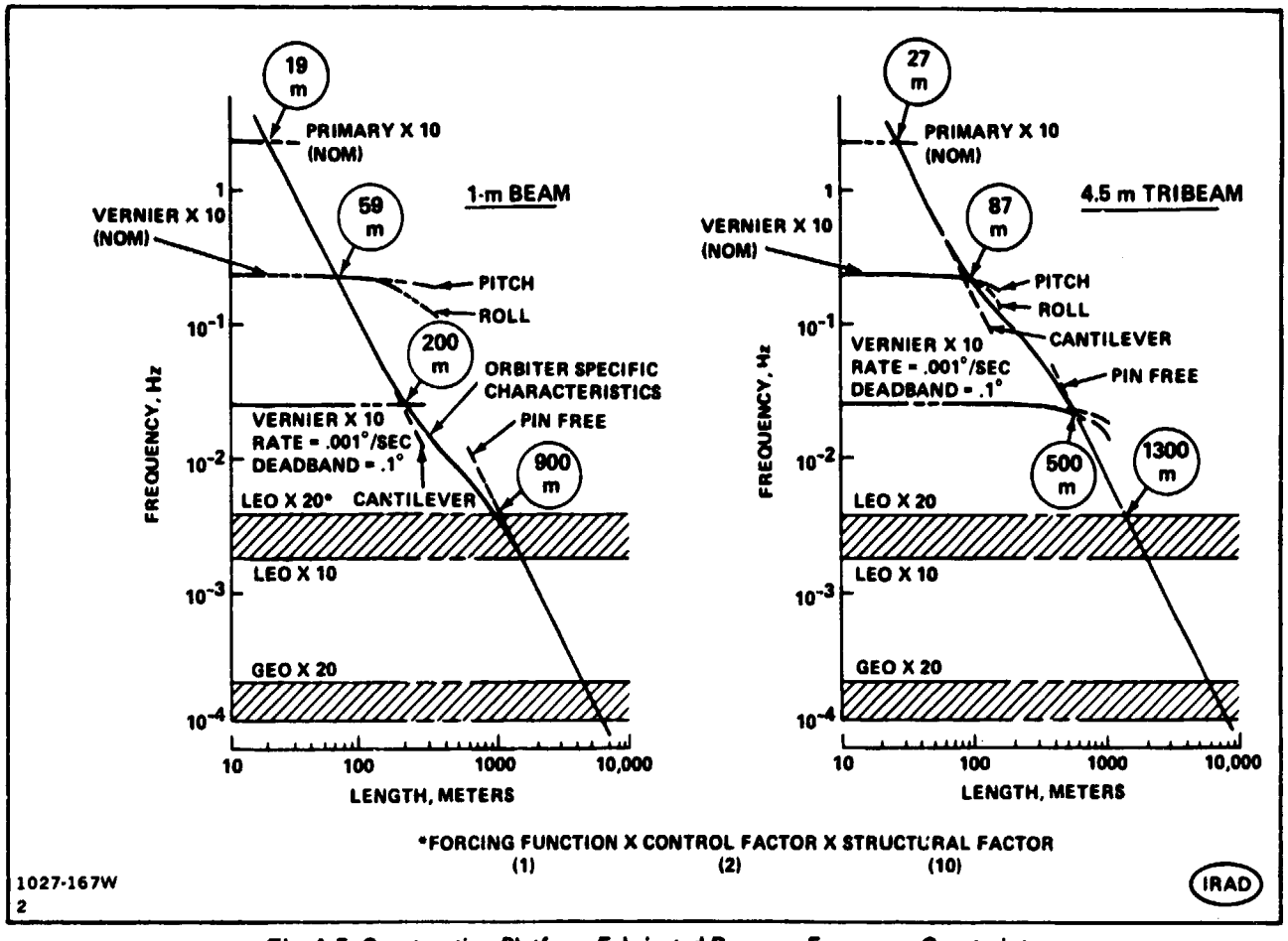

Fig. A-5 Construction Platform Fabricated Beams — Frequency Constraints

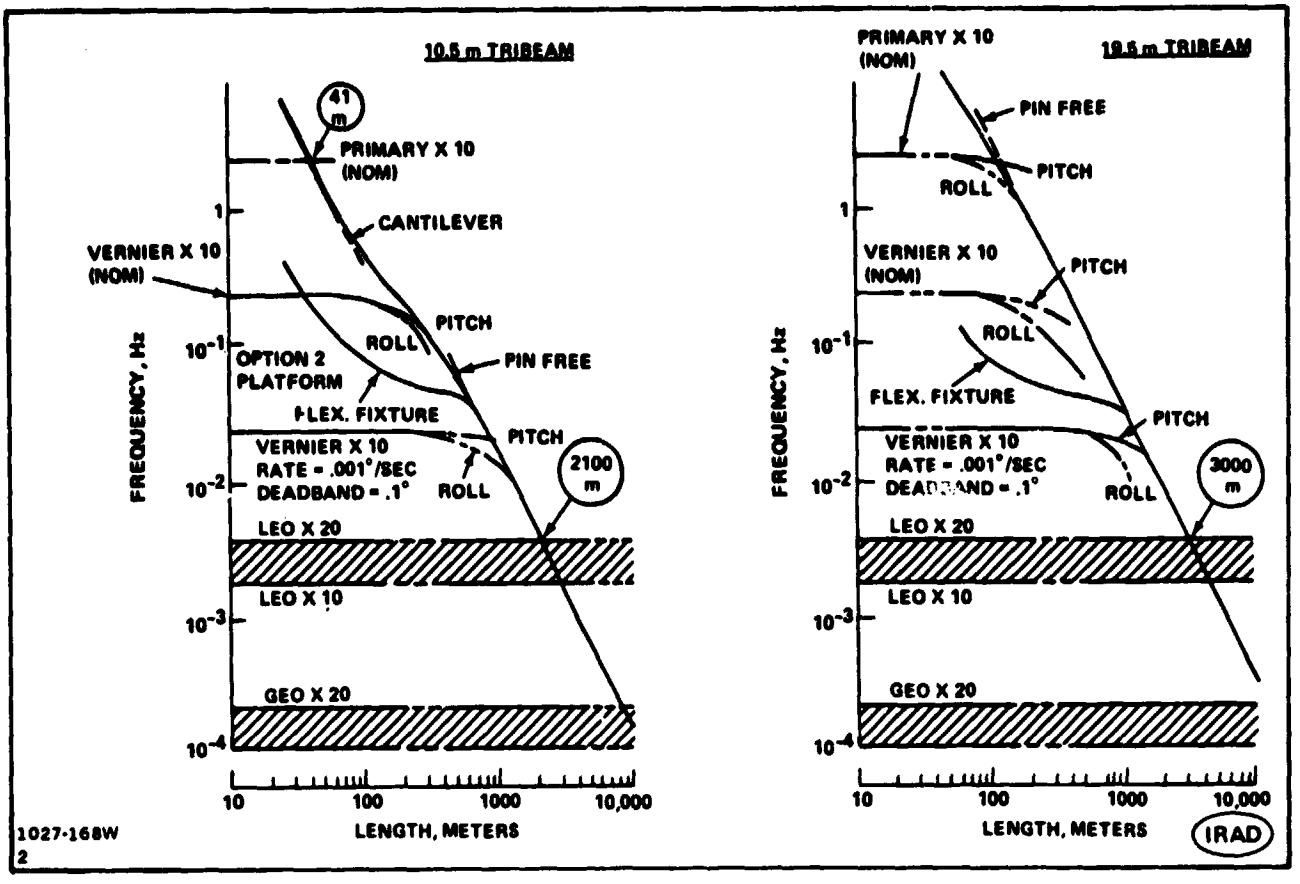

Fig. A-6 Construction Platform Fabricated Beams — Frequency Constraints

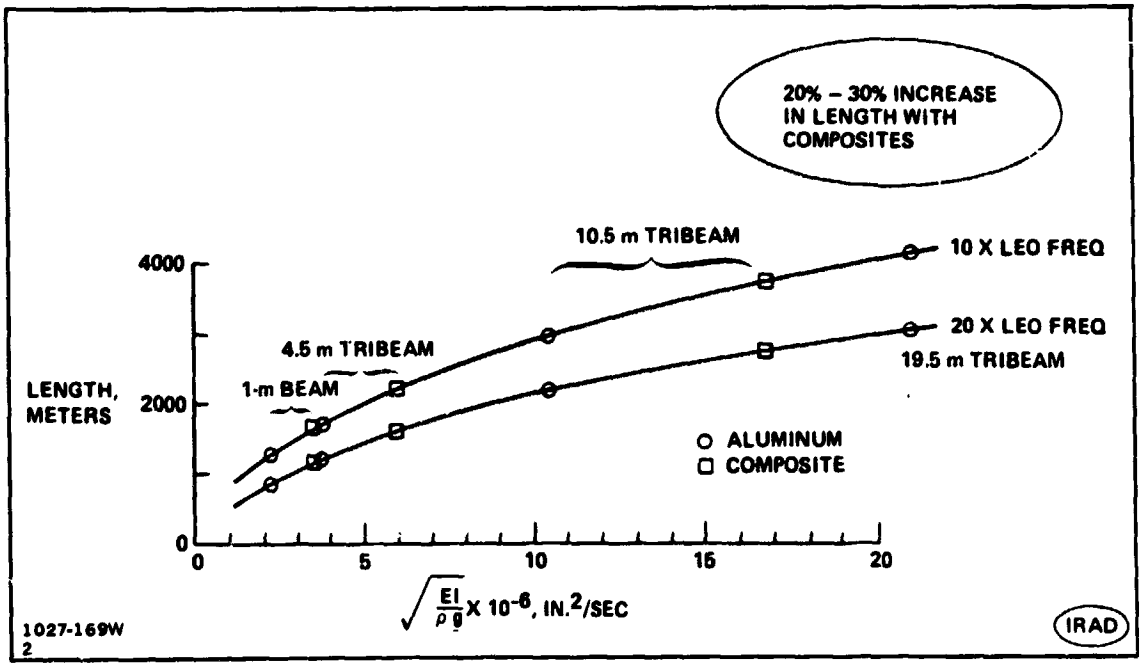

Fig. A-7 Maximum Beam Lengths in Leo-Frequency Criteria

A.4 OBSERVATIONS AND RECOMMENDATIONS

Key observations relating to this "construction limitations" effort are summarized in Fig. A-8. Analyses have shown that LSS lengths are limited primarily by frequency considerations rather than strength limitations. Variations in control parameters (deadband, limit cycle rate) however, can be employed to permit construction of longer LSS lengths. The maximum lengths are limited by orbital rate and appropriate frequency separation factors. Although for long beam lengths, fixture flexibility effects are no longer dominant, passage through this shorter length regime is necessary to attain these lengths. Finally, composites will allow slightly longer beam lengths to be constructed because of the resulting higher stiffness to mass ratio.

Further investigations should be conducted of handling and fabrication procedures/rates to determine if additional construction limitations exist. The present analysis should also be extended to determine the effects of tip masses and additional variations of fixture flexibility.

- LSS LENGTHS ARE PRIMARILY LIMITED BY FREQUENCY CONSIDERATIONS IN CONTRAST TO STRENGTH LIMITATIONS
- LONGER BEAM LENGTHS CAN BE ACCOMMODATED BY SUITABLE CONTROL PARAMETERS. DESIREABLE CONTROL FREQUENCIES SHOULD BE TWICE THOSE OF FORCING FUNCTIONS WHILE STRUCTURAL FREQUENCIES SHOULD BE 5 TO 10 TIMES GREATER THAN CONTROL FREQUENCIES
- FOR TRIBEAM LENGTHS GREATER THAN 1000 METERS FIXTURE FLEXIBILITY IS NO LONGER DOMINANT
- ORBIT RATE ESTABLISHES A FREQUENCY LIMIT WHICH INFLUENCES MAXIMUM LENGTHS OF LSS STRUCTURES. THIS LIMIT PERTAINS TO CONSTRUCTION BASES AS WELL AS AN ORBITER
- 20 – 30% INCREASES IN LENGTH COULD BE OBTAINED USING COMPOSITES BECAUSE OF THEIR HIGHER STIFFNESS TO MASS RATIO
- RECOMMENDED FUTURE EFFORTS
  - INVESTIGATE LIMITATIONS DUE TO HANDLING AND FABRICATION PROCEDURES/RATES
  - INFLUENCE OF TIP MASSES (E.G. GRAVITY WAVE INTERFEROMETER)
  - VARIATION OF FIXTURE FLEXIBILITY

1027-170W

IRAD

Fig. A-8 LSS Construction Limitations - Observations

Appendix B

PARAMETRIC DATA SHOWING VARIOUS ORBIT CONDITIONS WHICH PROVIDE REPEATING EARTH GROUND TRACKS

INTRODUCTION & BACKGROUND

An experiment package considered for application to the LSS flight demonstration is an L-Band microwave radiometer which would demonstrate the utility of the sensor to measure soil moisture for use in climatic modeling, crop yield estimating, and watershed runoff predictions. General requirements for this experiment call for orbital conditions which provided a ground track that revisits the ground it traversed every 3 or 4 days. Revisit intervals are desired to occur at about the same time of day.

The orbit altitudes which result in repeating ground tracks at approximately 3 and 4 day intervals for a range of orbit inclinations varying from 40 to 57 deg are presented herein.

DISCUSSION

Figures B-1 through B-5 present the orbital altitudes which provide repeating ground tracks at approximately 3 and 4 days for orbit inclinations of 40^{o}, 45^{o}, 50^{o}, 55^{o}, and 57^{o}. Shown are orbit altitude in nautical miles and kilometers, and the time after which the ground track is repeated. The time is shown in both hours and days. The data was computed considering earth rotation and orbit regression resulting from earth oblateness effects.

The time after which the ground track is repeated occurs at approximately 3 and 4 day intervals, not precisely at the same time of day. For example, from Figure B-4, it is noted that at an orbit inclination of 55^{o}, an orbit altitude of 213.453 n mi (395.313 km) provides an orbit which traverses over a previous ground track after 46 complete orbits, and after a duration of 70.887 hr. This occurs at a time of day of 1.113 hr earlier than the previous ground track. At an orbit inclination of 57^{o}, and an altitude of 215.071 n mi (398.309 km) the time of day in which the ground track is repeated is slightly closer, occurring 1.066 hr earlier. In general, for posigrade orbits, higher orbit inclinations and altitudes provide ground tracks that repeat closer to a

constant time of day. To achieve repeating orbits at precisely the same time of day requires retrograde orbits which were not considered in this analysis because of their unavailability to a shuttle launch.

It should be noted that this analysis has not considered orbital drag effects, which if uncompensated, will alter the ground track significantly. The orbit conditions summarized in Figures B-1 through B-5 would, therefore, have to be maintained through active spacecraft maneuvering. Since this would excessively complicate the mission, a high starting altitude minimizing drag effects and providing near-repeatability at the same time of day, is recommended.

NO. OF ORBITS	ALT, N MI	ALT, km	TIME, HR	TIME, DAYS		
44	316.687	586.500	70.696	2.946	APPX 3 DAYS	OVERFLIGHT INTERVAL
45	258.634	478.988	70.635	2.943		
46	202.609	375.229	70.572	2.940		
47	148.492	275.006	70.507	2.938		
48	96.177	178.119	70.440	2.935		
49	45.563	84.383	70.370	2.932		
NO. OF ORBITS	ALT, N MI	ALT, km	TIME, HR	TIME, DAYS		
57	392.297	726.529	94.359	3.932	APPX 4 DAYS	
58	346.512	641.737	94.300	3.929		
59	301.977	559.258	94.241	3.927		
60	258.634	478.988	94.179	3.924		
61	216.432	400.829	94.117	3.922		
62	175.319	324.689	94.052	3.919		
63	135.249	250.479	93.987	3.916		
64	96.177	178.119	93.919	3.913		
65	58.062	107.531	93.851	3.910		
66	20.865	38.642	93.780	3.908		

1027-171W
2

Fig. B-1 40° Orbit Inclination

2

NO. OF ORBITS	ALT, N MI	ALT, km	TIME, HR	TIME, DAYS	
44	319.769	592.209	70.782	2.949	APPX 3 DAYS
45	261.842	484.929	70.726	2.947	
46	205.945	381.408	70.668	2.945	
47	151.960	281.428	70.609	2.942	
48	99.779	184.789	70.547	2.939	
49	49.301	91.306	70.484	2.937	
NO. OF ORBITS	ALT, N MI	ALT, km	TIME, HR	TIME, DAYS	
57	395.226	731.953	94.467	3.936	APPX 4 DAYS
58	349.533	647.331	94.413	3.934	
59	305.090	565.024	94.358	3.932	
60	261.842	484.929	94.302	3.929	
61	219.736	406.948	94.244	3.927	
62	178.720	330.988	94.185	3.924	
63	138.750	256.963	94.125	3.922	
64	99.779	184.789	94.063	3.919	
65	61.766	114.390	93.999	3.917	
66	24.672	45.693	93.935	3.914	

OVERFLIGHT INTERVAL

1027-172W
2

Fig. B-2 45° Orbit Inclination

NO. OF ORBITS	ALT, N MI	ALT, km	TIME, HR	TIME, DAYS	
44	323.120	598.414	70.877	2.953	APPX 3 DAYS
45	265.329	491.386	70.826	2.951	
46	209.570	388.122	70.774	2.949	
47	155.727	288.404	70.720	2.947	
48	103.690	192.033	70.664	2.944	
49	53.360	98.822	70.606	2.942	
NO. OF ORBITS	ALT, N MI	ALT, km	TIME, HR	TIME, DAYS	
57	398.410	737.851	94.584	3.941	APPX 4 DAYS
58	352.816	653.412	94.536	3.939	
59	308.475	571.292	94.486	3.937	
60	265.329	491.386	94.435	3.935	
61	223.326	413.597	94.383	3.933	
62	182.416	337.833	94.329	3.930	
63	142.552	264.005	94.274	3.928	
64	103.690	192.033	94.218	3.926	
65	65.788	121.838	94.161	3.923	
66	28.806	53.348	94.103	3.921	

OVERFLIGHT INTERVAL

1027-173W
2

Fig. B-3 50° Orbit Inclination

C-3

2

NO. OF ORBITS	ALT, N MI	ALT, km	TIME, HR	TIME, DAYS	
44	326.710	605.064	70.978	2.957	APPX 3 DAYS
45	269.064	498.304	70.933	2.956	
46	213.453	395.313	70.887	2.954	
47	159.760	295.874	70.839	2.952	
48	107.877	199.786	70.789	2.950	
49	57.703	106.866	70.738	2.947	
NO. OF ORBITS	ALT, N MI	ALT, km	TIME, HR	TIME, DAYS	
57	401.824	744.173	94.710	3.946	APPX 4 DAYS
58	356.335	659.929	94.667	3.944	
59	312.101	578.008	94.623	3.943	
60	269.064	498.304	94.578	3.941	
61	227.172	420.719	94.531	3.939	
62	186.374	345.162	94.484	3.937	
63	146.623	271.545	94.435	3.935	
64	107.877	199.786	94.385	3.933	
65	70.091	129.809	94.334	3.931	
66	33.228	61.539	94.283	3.928	

OVERFLIGHT INTERVAL

1027-174W
2

Fig. B-4 55° Orbit Inclination

NO. OF ORBITS	ALT, N MI	ALT, km	TIME, HR	TIME, DAYS	
44	328.207	607.835	71.021	2.959	APPX 3 DAYS
45	270.621	501.187	70.978	2.957	
46	215.071	398.309	70.934	2.956	
47	161.440	298.985	70.888	2.954	
48	109.620	203.016	70.841	2.952	
49	59.512	110.215	70.793	2.950	
NO. OF ORBITS	ALT, N MI	ALT, km	TIME, HR	TIME, DAYS	
57	403.247	746.809	94.763	3.948	APPX 4 DAYS
58	357.802	662.646	94.722	3.947	
59	313.612	580.807	94.680	3.945	
60	270.621	501.187	94.637	3.943	
61	228.774	423.687	94.593	3.941	
62	188.023	348.216	94.548	3.940	
63	148.319	274.686	94.502	3.938	
64	109.620	203.016	94.455	3.936	
65	71.884	133.128	94.407	3.934	
66	35.070	64.949	94.357	3.932	

OVERFLIGHT INTERVAL

1027-175W
2

Fig. B-5 57° Orbit Inclination

2

Appendix C

SATSIM PROGRAM DESCRIPTION

INTRODUCTION

SATSIM is a three-axis, time-history digital computer program, developed within Grumman's IRAD program, to simulate the performance of Attitude Control Subsystems (ACS) during various phases of a mission (e.g., separation from the Orbiter). The program is written in the IBM CSMP III language with a great deal of flexibility incorporated in order to evaluate performance characteristics of different ACS designs and vehicle configurations.

DISCUSSION

The structure of SATSIM is described by the functional flow chart and I/O diagram of Figs. C-1 and C-2. As Fig. C-1 shows, the simulation is broken into blocks with the following functions:

1) Spacecraft Dynamics, Orbital Kinematics
   Momentum Equations, Euler Rotations

2) Attitude Determination

   a) Gyros
   b) Horizon Sensor
   c) Gyrocompass Estimator
   d) Star Scanner
   e) Magnetometer
   f) Sensor Noise Characteristics

3) Attitude Control Laws

   a) Error Correction Criteria
   b) Error Signal Weighing
   c) Control Command Signals

4) Momentum Unloading Logic

   Momentum Error Calculations
   Unloading Commands

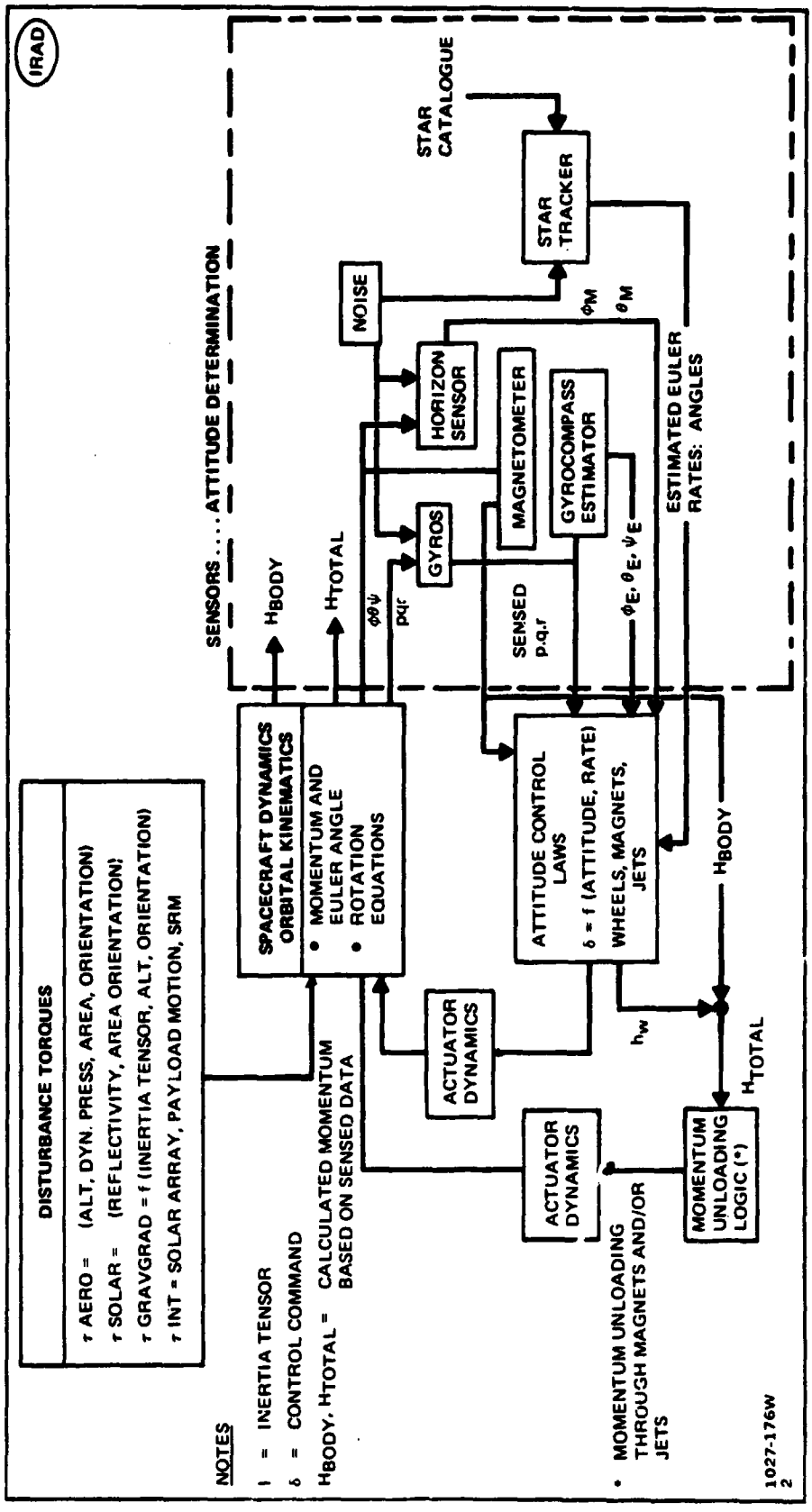

Fig. C-1 SATSIM Functional Block Diagram

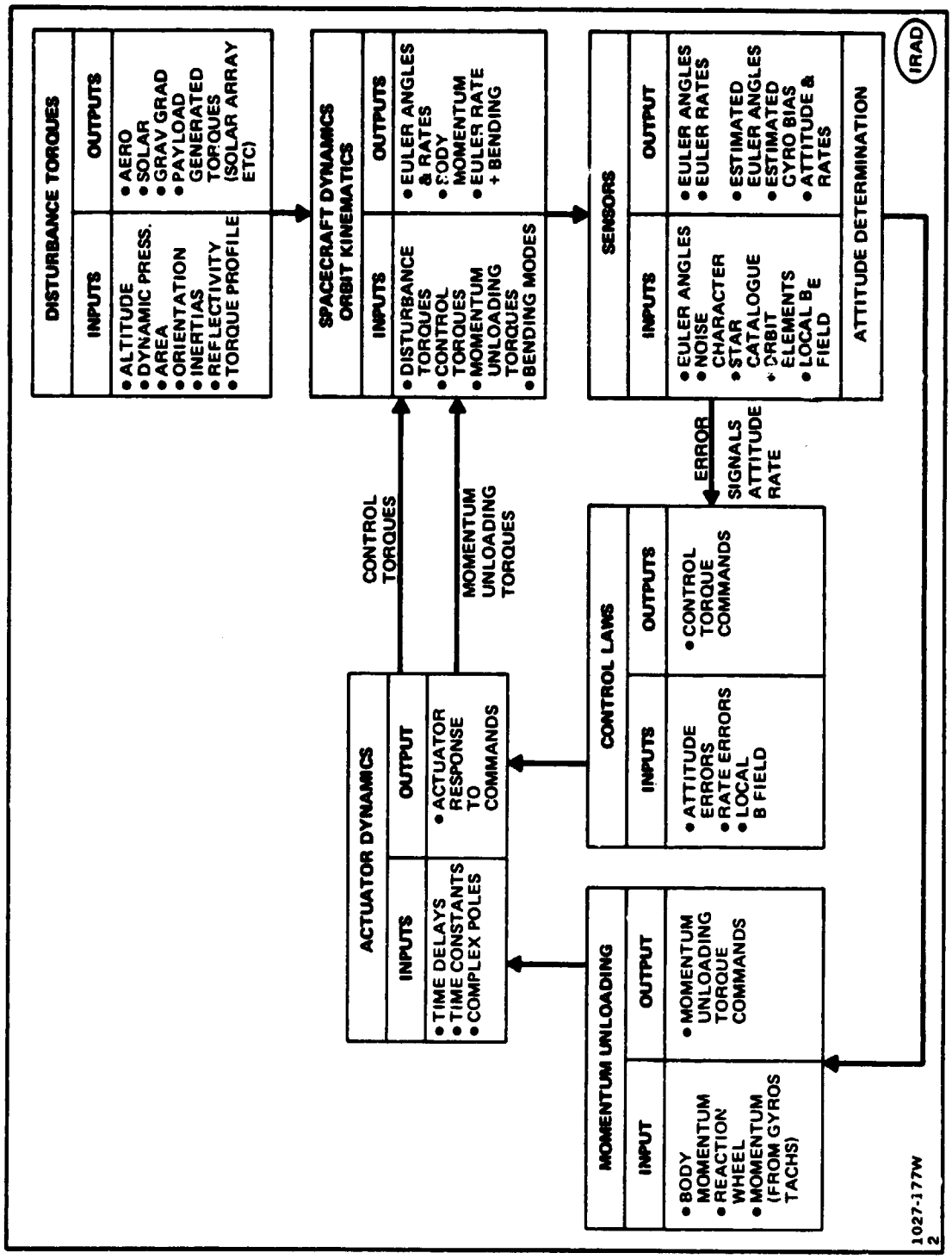

Fig. C-2 SATSIM I/O Diagram

5) Actuator Dynamics

Time Delays, Time Constants, Drag, Losses, etc.

6) Disturbance Torques

Aero Torque
Solar Pressure } CALCULATED
Gravity Gradient

Simulated - Payload & Machinery torque profiles

Figure C-2 shows the inputs and outputs of each functional block.

CAPABILITIES OF SATSIM

Figure C-3 presents a diagram of the Spacecraft coordinate system used in SATSIM relative to a local vertical orbital coordinate system. The nominal orientation of the spacecraft is shown with the +X body axis (roll axis) in the direction of the orbital velocity vector, the +Y body axis (pitch axis) is orbit normal and opposite to the direction of the orbital angular momentum vector, and the +Z body axis (roll axis) is along the local vertical, directed towards the earth.

SATSIM has been programmed to simulate a wide variety of ACS actuator and sensor components. The following is a brief description of each:

Reaction Wheels

Four reaction wheels (RW) are included, two oriented with their spin axes along the Y-axis (pitch), one along the X-axis (roll) and one along the Z-axis (yaw). Each wheel has torque and momentum storage limits and can be run with or without friction and motor cogging in the simulation.

Magnetic Torques

Three magnetic torquer bars, oriented one along each of the orthogonal body axes, are included in the simulation. They are designed to interact with the earth's magnetic field and are torque limited to simulate magnetic saturation. Algorithms are included to perform magnetic unloading of the RW against the earth's field.

RCS Jets

On-Off jet torques about each of the orthogonal axes can be commanded for either momentum unloading of the RW's or for attitude control using jets only. Jet logic includes dead zone plus hysteresis.

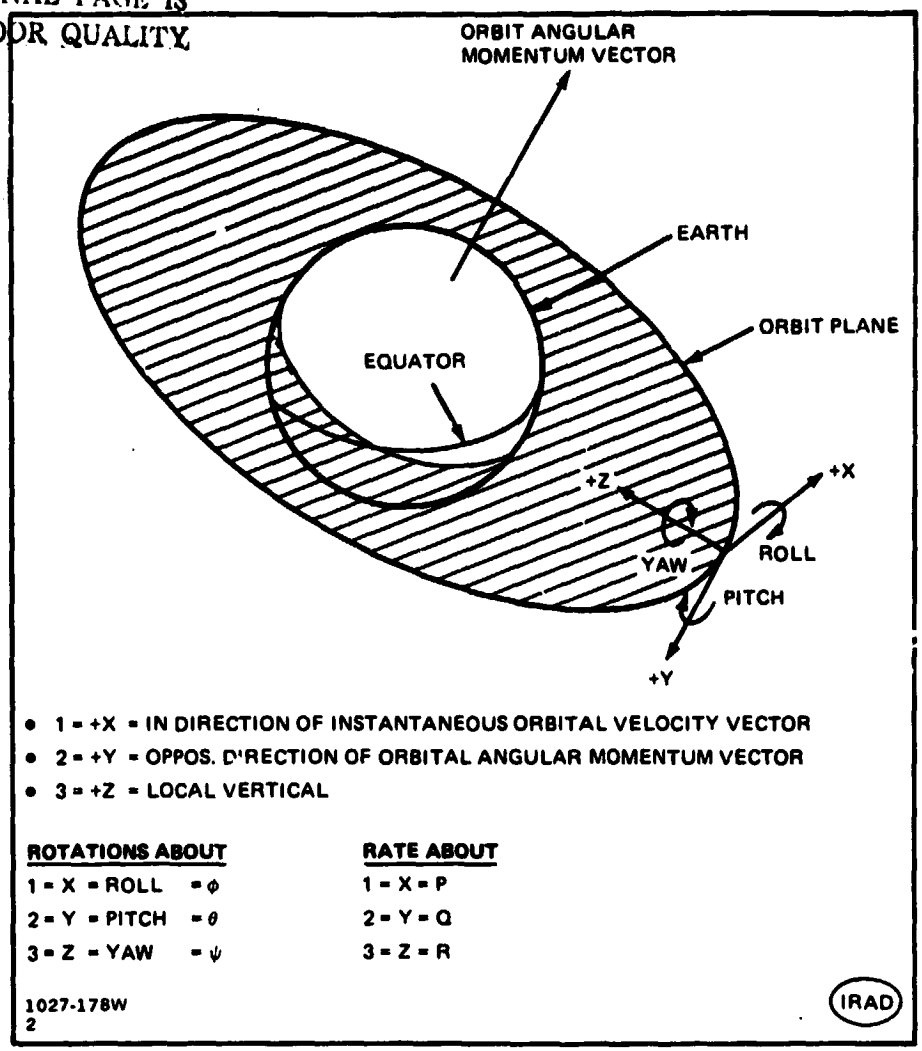

Fig. C-3 References Axes for SATSIM - Earth Pointing Satellite Simulation

Rate Gyros

Rate sensing gyros along the three body axes are included in the simulation. Gyro noise, is included about each of the measured body rates (P, Q, R). Steady-state gyro bias levels are included separately.

Horizon Sensor

Horizon sensor characteristics include linear outputs up to a desired pitch and roll angle and a flat output beyond these levels. Sensor noise is included about each of the measured body angles (roll, pitch and yaw).

Yaw Estimator

Yaw is measured in one of two ways: by a small-angle gyrocompass yaw estimator using gyro and horizon sensor information, or a large-angle gyrocompass estimator also using gyro and horizon sensor information. The large-angle gyrocompass estimator is, of course, more accurate for feeding back yaw information.

Magnetometer

Measurement of the earth's magnetic field is made available about each of the three-body axes. The earth's field is calculated on the basis of orbital altitude, inclination and orbit rate.

The simulated vehicle dynamics in SATSIM include the following effects:

- Inertia crossproduct terms
- Cross coupling of vehicle body momentum and reaction wheel momentum vectors with orbital momentum vector
- Environmental disturbance torques include:
  - gravitational torques, programmed as a function of orbital altitude and euler angles
  - aerodynamic torque, programmed as a function or orbital altitude and a user-specified function of time
  - solar torques, programmed as a function of a user-specified function of time
  - impulse torque disturbance programmed to occur at a specified time for a specified time-period.
- Structural bending modes about each of the three body axes.

The SATSIM program is written in the IBM Continuous System Modeling Program III (CSMP III) language which is described in detail in Reference C-1 and is therefore not discussed here. Asterisks in Column 1 indicate comment statements which are used liberally throughout the program to make it as self-explanatory as possible.

- - - - - - - -

C-1 "Continuous System Modeling Program III (CSMPIII), Program Reference Manual," IBM, SH19-7001-2, September 1972.

2

All significant parameter data values are inputted in the Spacecraft Input Data area. Figure C-4 defines these parameters. The Mode Control Parameters are defined separately in Figure C-5, along with the values necessary to achieve the defined effect.

All integrations and calculations of critical program variables are performed using a variable-time-step Runge-Kutta integration routine.

PARAMETER SYMBOL	DEFINITION	UNITS
IXX, IYY, IZZ	SPACECRAFT MOMENTS OF INERTIA	FT-LB-SEC^2
IXY, IXZ, IYZ	SPACECRAFT CROSSPRODUCT OF INERTIAS	FT-LB-SEC^2
WC	CONTROL SYSTEM BANDPASS FREQUENCY	RAD/SEC
ZETA	CONTROL SYSTEM DAMPING COEFFICIENT	
KM1, KM2, KM3	GAINS IN X, Y, AND Z MAGNETIC UNLOADING SYSTEM	(GAUSS^2-SEC)$^{-1}$
DP, DQ, DR	GYRO BIAS DRIFT ABOUT X, Y AND Z AXES	RAD/SEC
K11, K22	GYRO COMPASS ESTIMATOR GAIN SETTING	1/SEC
THETC, PHIC, PSIC	STEADY-STATE OFFSET EULER ANGLE COMMANDS (θ_C, φ_C, ψ_C)	RAD
HALT	ORBITAL ALTITUDE	N MI
INC	ORBITAL INCLINATION	DEG
CD	AERODYNAMIC DRAG COEFFICIENT	
CP1, CP2, CP3	DISTANCE BETWEEN CP AND CG ABOUT X, Y AND Z AXES	FT
AR1, AR2, AR3	PROJECTED SURFACE AREA ALONG X, Y AND Z AXES	FT^2
FO1, FO2, FO3	JET NOZZLE FORCE LEVELS ABOUT X, Y AND Z AXES	FT^2
LO1, LO2, LO3	JET NOZZLE MOMENT ARM ABOUT X, Y AND Z AXES	FT
PIC, QIC, RIC	INITIAL VALUE ON BODY RATES P, Q AND R	RAD/SEC
IW1, IW21, IW22, IW3	REACTION WHEEL INERTIAS	FT-LB-SEC^2
WN1, WN2, WN3	STRUCTURAL BENDING FREQUENCIES ABOUT X, Y, Z AXES	RAD/SEC
INF1, INF2, INF3	INFLUENCE COEFFICIENT OF STRUCTURAL BENDING MODES	RAD-SLUG/FT-LB
MV1, MV2, MV3	NORMALIZED MASS	SLUG
DB1, DB2, DB3	LIMIT CYCLE DEADBAND	DEG
WLC1, WLC2, WLC3	LIMIT CYCLE RATE	DEG/SEC
ISP	SPECIFIC IMPULSE	SEC
1027-179W 2		IRAD

Fig. C-4 Parameter Definitions

2

MODE CONTROL PARAMETER	VALUE	MODE SITUATION
KJET	-1	JET UNLOADING OF REACTION WHEELS (RW)
	+1	ACS USING JETS
XTIME	-1	RW, RCS AND MAGNETIC CONTROL IN ALL TIME
	+1	RW, RCS AND MAGNETIC CONTROL OUT PART TIME
KALM	-1	PHIPR = PHIE (ESTIMATED ROLL ANGLE FROM GYRO COMPASS)
	0	PHIPR = PHIM (MEASURED ROLL ANGLE)
GYRCTP	+1	USE SMALL ANGLE GYRO COMPASS ROLL ANGLE ESTIMATOR
	-1	USE LARGE ANGLE GYRO COMPASS ROLL ANGLE ESTIMATOR
KWHL	+1	REACTION WHEEL CONTROL IS IN
	0	REACTION WHEEL CONTROL IS OUT
KMAG	+1	MAGNETIC CONTROL IS IN
	0	MAGNETIC CONTROL IS OUT
KCTYP	-1	CONTROL ON GYROS AND HORIZON SENSOR
	+1	CONTROL ON GYROS ONLY
KWFRIC	+1	REACTION WHEEL FRICTION IS IN
	0	REACTION WHEEL FRICTION IS OUT
KIMPLS	-1	ENVIRONMENTAL DISTURBANCES IN ONLY
	+1	ENVIRONMENTAL PLUS IMPULSE DISTURBANCE IN
KBEND	+1	FLEXIBLE BODY BENDING IS IN
	0	FLEXIBLE BODY BENDING IS OUT
KGRAV	+1	GRAVITY GRADIENT DISTURBANCE IS IN
	0	GRAVITY GRADIENT DISTURBANCE IS OUT
KAERO	+1	AERO DISTURBANCES ARE IN
	0	AERO DISTURBANCES ARE OUT
KSOLAR	+1	SOLAR DISTURBANCES ARE IN
	0	SOLAR DISTURBANCES ARE OUT

1027-180W
2

IRAD

Fig. C-5 Definition of Mode Control Parameters

Appendix D

STRUCTURAL FLIGHT TEST REQUIREMENTS

D.1 ONE METER BEAM STRUCTURAL DYNAMIC FLIGHT TEST REQUIREMENTS

Preliminary Structural Dynamic Flight Test requirements for a 1-meter beam are provided herein. These tests should be performed while the one-meter beam is mounted in the Automated Beam Builder (ABB). The tests are;

1. Modal Survey
2. Response to RCS firing

Requirements for these tests are discussed herein.

D.1.1 Test No. 1: On-Orbit Modal Survey of One-Meter Beam Mounted in ABB

Purpose

Determine modal properties: frequencies, mode shapes, damping, of the one-meter beam mounted in the Automated Beam Builder (ABB) while exposed to zero-g and thermal on-orbit environments.

Background

The one-meter beam will be ground tested in the earth environment to determine its modal properties for comparison with on-orbit values. The effects on stiffness and damping due to zero-g, particularly from ABB mounting, will be determined from the on-orbit test.

Thermal-vacuum effects on stiffness and damping can partially be verified by ground test, but only for short beam lengths. The on-orbit tests will be used to verify extrapolations of ground test results to longer beam lengths.

The mode survey can also be used to partially verify that the beam machine (ABB) produces a sound structural member after exposure to the shuttle launch and on-orbit environments.

D.1.1.1 Test Description

Baseline

The ABB shall produce a 39-m long beam. This length is near the maximum which can safely withstand Orbiter primary RCS firing. A small shaker (2-5 lb force) mounted on the remote manipulator (RMS) will be used to excite the beam (Fig. D-1). A sinusoidal sweep will be made(0.1 Hz to 10 Hz) to determine resonant response peaks. Modal displacements will be measured during dwells at each resonant frequency and damping will be determined from response decays after shaker cutoff.

Tests will be performed under two thermal conditions:

- Nominal sunlight
- Occulted

The Orbiter should be in a drift mode or using vernier RCS to minimize thruster inputs during the times when data is recorded.

Alternate 1 - To minimize test time, a broadband random excitation will be applied for approximately 2 minutes. Modal properties will be obtained using Fast Fourier Transform Techniques. Ground development testing is required to determine if this technique is feasible in the frequency range of interest.

Alternate 2 - To minimize test time and eliminate the requirement for an on-orbit shaker attachment, a burst from the Orbiter RCS will be applied for approximately 10 sec. Modal properties will be obtained using Fast Fourier Transform Techniques. Again, ground testing is required to determine the feasibility of this technique. Control analysis is required to determine if the Orbiter can supply and recover from such an input.

Alternate 3- An initial deflection will be imparted to the beam by statically pulling on the beam with the RMS or a cable attached to the Orbiter. Using a quick release device the beam will be set in motion and modal data will be obtained using Fast Fourier Transforms. Feasibility testing is again required.

D.1.1.2 Test Instrumentation

Baseline - In the frequency range of interest (0.1 to 10 Hz) measurements will be made of the first 3 beam bending modes and torsion. Twenty-five accelerometers mounted on the beam will be required. A candidate accelerometer for this purpose is:

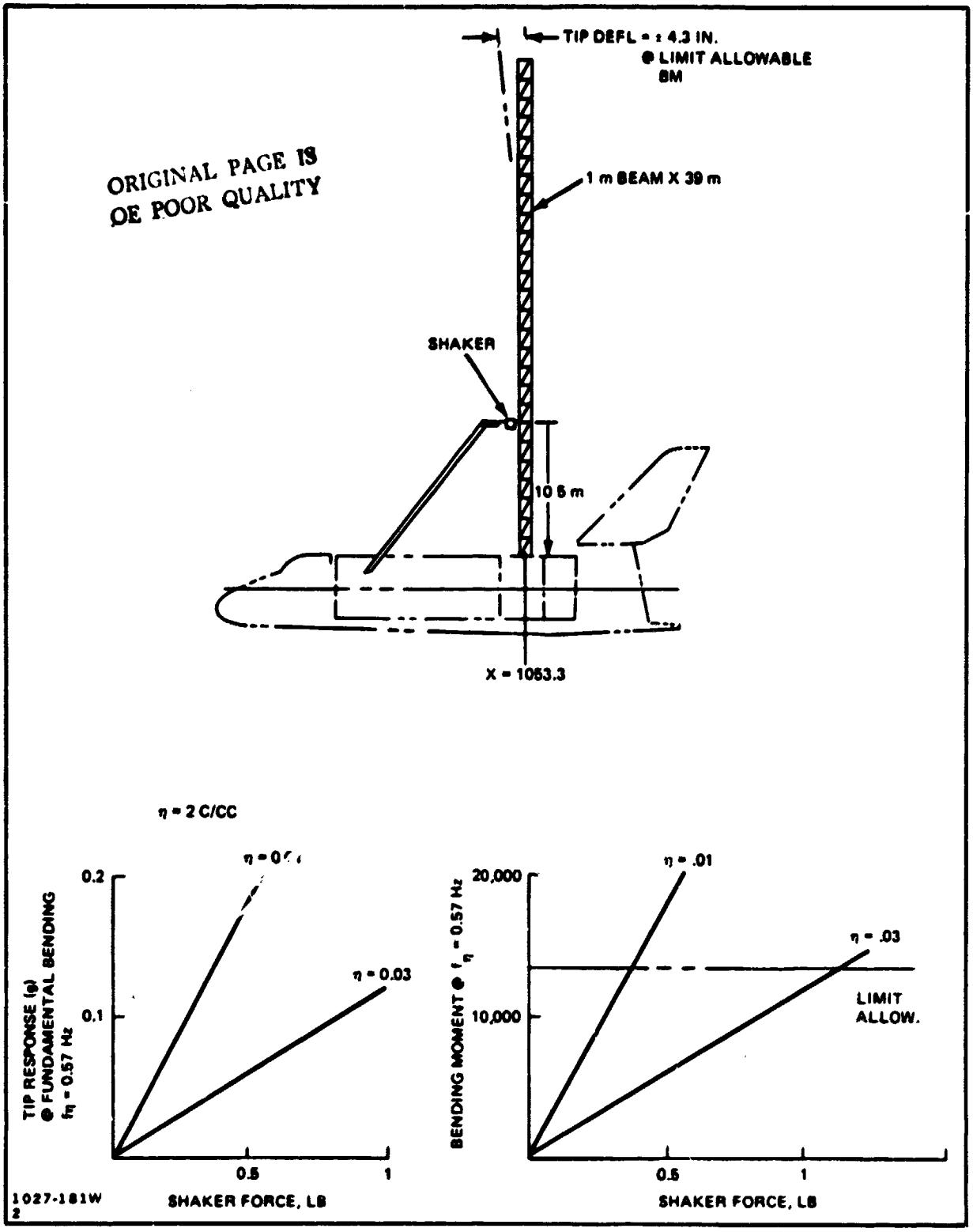

Fig. D-1 Shaker Force and Location Requirements

- PCB - Model Number 302-A02
- Weight = 18 gm
- Frequency Range = 0.05 - 5000 Hz
- Dimensions (approx) = 5/8-in. dia x 5/8-in. high

The method of attachment of accelerometers and wires is a further development item. At present, it appears that accelerometer attachments should be made manually by astronauts using clips and adhesive.

Alternate 1 - Deflection measurements will be made using laser beams. Targets must be mounted on the structure. Development testing is required to determine the feasibility of this approach.

D.1.2 Test No. 2: Response of One-Meter Beam to Orbiter RCS Firing

Purpose - Measure response of one-meter beam to Vernier and Primary RCS firing. Response data will be correlated with analyses.

Background - The one-meter beam mounted in the ABB will be subjected to a modal survey prior to response testing. The accelerometers mounted for the modal testing will also be used for RCS response measurements. The beam length shall be 39 m.

Static ground tests will be made to determine one-meter beam structural allowables for axial, bending, torsion and combined load cases.

D.1.2.1 Test Description - This test will utilize a one-meter beam mounted in the ABB. The Orbiter will operate normally for an orbit under VRCS control. Quick-look response data will be generated on board with the majority of data stored on magnetic tape for later ground reduction. The vernier engines will then be commanded to produce individually;

- X,Y, and Z translation
- Pitch, roll, and yaw rotations

The excitation should be applied for approximately 2 sec to produce a step input.

Upon completion of the testing with the vernier engine, the same test sequence (i.e., one typical orbit, pure translation and pure rotation) shall be performed using the primary engines. Reduction of nominal Orbiter control parameters (deadband angle and attitude rate) may be required to avoid structural coupling.

2

D.2 TRIBEAM STRUCTURAL/THERMAL FLIGHT TEST REQUIREMENTS

Preliminary structural-thermal flight test requirements for a Tribeam Platform are provided herein. The following tests are recommended to verify the thermodynamic math model, determine relative rotations and displacements of equipment mounting interfaces, to determine thermally induced load levels in the one-meter beams, and loads due to torsional and bending end fixity at the nodal joints:

1. Verification of analytic thermal data
2. Effects of beam end restraints

Figure D-2 shows three Tribeam orientations during an orbit. All orbits are LEO (400 km). Orbit orientations (A) and (B) are solar orientations; Orbit (C) is earth pointing.

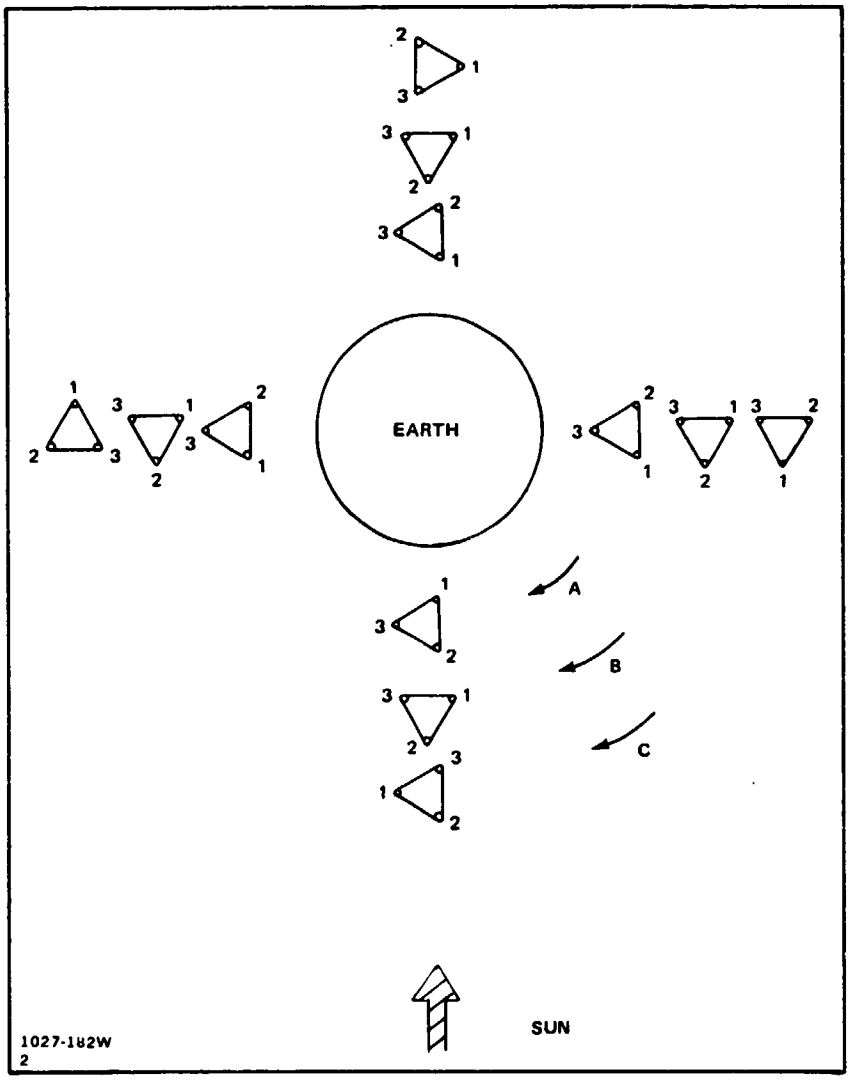

Fig. D-2 One-Meter Beam Thermal Test Orientations

Orbit A produces the orientation which results in a maximum beam to beam thermal gradient and therefore the maximum Tribeam rotation and mounting surface displacement. In addition, occultation of beam 1 by beam 2 occurs.

The Orbit B orientation produces minimum occultation between Tribeam elements and between elements of the one-meter beam.

Orbit C produces the transient occultations which result in high one-meter beam cap thermal gradients.

D.2.1 Test No. 1: Verification of Analytical Thermal Data

Purpose - To determine the thermal response of the one-meter beam(s), in an LSS assembly, to on-orbit thermal environments.

Background- A detailed mathematical thermal model will be used to obtain analytical thermal data for the one-meter beam. This model will be verified by testing in a solar simulator thermal vacuum chamber for two to three bay sections of the one-meter beam. However, the effects of partial occultation of one beam by another can only be confirmed with on-orbit testing due to size limitations on ground testing. In addition, the effect of Orbiter shading and the transient effects of earth occultation entry and emergence must be determined on orbit.

D.2.1.1 Test Description

Temperatures at various (TBD) correlatable locations on each one-meter beam of the Tribeam will be monitored during the Tribeam assembly sequence, and during the on-orbit duration of the Orbiter mission. Data will be recorded during nominal mission orientations, but in order to obtain "worst case" data, the Orbiter may be required to maintain predetermined orientations while thermal data is recorded (e.g., Orbit A, Fig. D-2). During this testing axial loading in the Tribeam verticals/diagonals and in the one-meter beam caps will be determined, and relative displacements and rotations monitored.

D.2.1.2 Test Instrumentation

Temperature sensors will be attached to the Tribeam structural members. A typical device is shown in Fig. D-3.

Electro-optical sensors will be used to obtain deflection and rotation data, (1) between a support fixture at the Orbiter mounting plane and its attachments to the Tribeam and, (2) between the fixture at the Orbiter mounting plane and the furthest location of the Tribeam from the Orbiter.

2

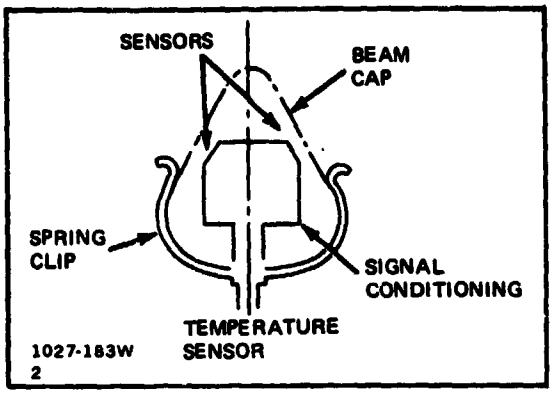

Fig. D-3 One-Meter Beam Instrumentation Installation Technique

D.2.2 Test No. 2: Effects of Beam End Restraint

Purpose - To determine the magnitude of thermally-induced stress levels resulting from torsional and moment end restraint.

Background - In order to accomplish the mounting of equipments, etc. projected for the Tribeam, some degree of torsional and bending restraint must be provided to the one-meter beams, either through the end attachments or through inter-costal structural members. Full moment restraint could result in significant compressive cap loads at the expected ΔT, therefore the magnitude of this end restraint must be carefully evaluated to determine the useable structural capability of the one-meter beam in an LSS. It is not practicable to simulate these effects in ground testing since the size limitation of a solar simulator thermal vacuum chamber would not accommodate a sufficiently complex structure to provide definitive data.

D.2.2.1 Test Description - Cap and diagonal member strains will be monitored during the nominal mission solar orientations and also during pre-determined worst case orientations wherein the maximum one-meter beam cap ΔT will be achieved.

D.2.2.2 Test Instrumentation - The one-meter test beam, which could be prefabricated and instrumented on the ground, will require a minimum of 18 strain gages on the cap members and 12 on the diagonals. The data obtained from these gages will be correlated with ground test data to determine the magnitude of the loading induced.

D.3 TRIBEAM STRUCTURAL DYNAMIC FLIGHT TEST REQUIREMENTS

Preliminary structural dynamic flight test requirements for a Tribeam Platform are provided herein. The following is a recommended test sequence, as it provides a progressive installation of required instrumentation:

- Astronaut Beam Transport and Placement Tests
- RMS Beam Transport and Placement Tests
- Indexing Tests
- Modal Survey
- Response of Tribeam Platform to Orbiter RCS Firing Tests
- Deployment and Capture Tests

Requirements for the first three and last test are discussed under the heading of Construction and Handling tests. Modal survey and RCS Response test requirements are separately identified.

D.3.1 Test No. 1: Tribeam Platform Construction and Handling Loads

Purpose - Determine applied loads induced during construction of the Tribeam Platform for the following:

- Astronaut beam transport and placement
- RMS beam transport and placement
- Platform indexing
- Platform deployment and capture

Background - Ground simulation will be needed to investigate construction methods and procedures. Facilities such as the:

- Neutral Buoyancy Tank
- RMS simulators,

are proposed for this purpose. Estimates of construction loads and movement rates will be obtained from these simulations.

Since the ground simulations are necessarily limited due to gravity and/or drag effects, flight testing is needed to verify the magnitudes of applied loads. This data is required to validate analytical models and to predict response of future larger structures.

D.3.1.1 Test Description

Astronaut Beam Transport and Placement - Two astronauts flying Manned Maneuvering Units (MMU) will be required. Initially, one astronaut will pick up a 1-meter beam near

its center and transport the beam to the assembly site. In addition, the following maneuvers shall be performed:

- Pure Translation (0.3 ± 0.05 ft/sec^2)
- Pure Rotation (10.3 ± 3 deg/sec^2)
- Hover (60 sec)

The astronaut will then attach the beam to the assembly fixture.

Using two astronauts, one at each end of a beam, the above sequence of events shall be repeated.

RMS Beam Transport and Placement - The Remote Manipulator Systems (RMS) with an appropriate end effector will capture a 10.5 m-long beam near its center and transport the beam to the erection jig. A series of transports shall also be performed in both the coarse and vernier RMS translation and rotation modes, at minimum, nominal, and maximum rates:

- Pure translation (0-2.0 ft/sec-coarse)
  (0-0.2 ft/sec-vernier)
- Pure rotation (0-4.76 deg/sec-coarse)
  (0-0.476 deg/sec-vernier)

During one transport, the RMS will be stopped and held in an intermediate position. The vernier RCS will be fired to produce pure roll, pitch and yaw.

The RMS will translate the beam to the erection fixture for astronaut installation.

Indexing - During the construction sequence of a Tribeam Platform where a vertical indexing (slide) of a fixture is required after completion of some construction activity, the indexing shall be accomplished in two ways:

- Astronaut indexing
- RMS indexing

An astronaut shall manually extend the fixture element(s) after a portion of the Tribeam configuration is constructed. Following this, the RMS shall be used to perform a fixture indexing task. It is expected that comprehensive ground testing will be performed to verify detailed procedures and movement rates for this operation.

Deployment and Capture - The completed Tribeam Platform shall be captured by the RMS, undocked and moved to its deployment position at a rate TBD fps. In this position,

- Solar arrays will be deployed, if necessary
- On-Orbit thrusters will be check fired

The Platform will then be released. The Orbiter will standoff for TBD min., and then rendezvous with the Platform, capture it with the RMS, and transfer the vehicle into a berthing position.

D.3.1.2 Test Instrumentation

Astronaut Beam Transport and Placement - The 1-meter test beam, which could be prefabricated and instrumented on the ground, will require a minimum of 6 accelerometers capable of measuring acceleration in a response range from 0 to 2 Hz. It may also be desirable to let the astronaut operate in a free flying (untethered) mode to avoid tangling situations with support hoses. In this case, the data recording devices must be self contained on the 1-meter beam (or MMU) or hardware for telemetering data to the Orbiter must be supplied. A power supply is also required. The MMU's must also be instrumented to obtain a 6-degree-of-freedom acceleration response. Load cells between the MMU and beam will also be necessary.

The one-meter test beam should also be instrumented with strain gages on the caps (18) and diagonals (12) to determine the magnitude of the loads induced in the beam during astronaut and RMS beam transport and placement. This data would be correlated with ground test data to determine the actual induced loads. This instrumentation could be attached to a selected length of 1-meter beam, prefabricated and instrumented on the ground.

If a fixture is utilized in the assembly process, it must be instrumented to determine placement and attachment loads. Load cells (6) at the attachment nodes as well as strain gages(16) at the base should be available to measure the applied loads and resulting bending and torsion loads.

RMS Beam Transport and Placement - The 1-meter beam previously discussed can also be used for RMS testing. The requirement for self contained recording could be relaxed, however, since wiring can be run along the RMS. Fixture instrumentation is the same as for the astronaut test.

Indexing - Six accelerometers are required to measure low frequency response (the beam instrumented for previous tests can be used). Accelerometers required for the modal survey (Ref: Test No. 2 Modal Survey of Tribeam Platform) could also be installed on the structure, during construction, to measure high frequency response.

Deployment and Capture - The low and high frequency accelerometers installed for indexing tests and the modal survey can also be used to measure deployment and capture test response. A disconnect for instrumentation wiring required on the RMS or a telemetering package must be supplied.

D.3.2 Test No. 2: On-Orbit Modal Survey of Tribeam Platform

Purpose - Determine modal properties:

- Frequencies
- Mode Shapes
- Damping

of the Tribeam Platform mounted in the Orbiter while exposed to zero-g and thermal on-orbit environments.

Background- The Tribeam Platform will be ground tested to determine its modal properties for comparison with on-orbit values. The effects of zero-g and thermal environment on stiffness and damping will be determined from the orbit test.

Thermal-vacuum effects on stiffness and damping, on joints in particular, can be partially verified by ground test, but for smaller structural assemblies only. The on-orbit tests will be used to verify extrapolations of ground test results to larger structures.

The results of the flight test will be used to verify that mathematical models can be correlated to predict the response of large space structures. In addition, zero-g damping data, which can only be gathered experimentally will be obtained.

D.3.2.1 Test Description

Baseline - A complete Tribeam structure will be assembled while in orbit. A small shaker (2-5 lb force) mounted on the remote manipulator (RMS) will be used to excite the Tribeam while mounted to the Orbiter. A sinusoidal sweep will be made (0.05 to 10 Hz) to determine resonant response peaks. Modal displacements will be measured during dwells at each resonant frequency and damping will be determined from response decays after shaker cutoff.

Tests will be performed under two thermal conditions:

- Nominal sunlight
- Occulted

The Orbiter should be in a free-drift mode to eliminate thruster inputs during the times when data is recorded.

Alternate 1 - To minimize test time, a broadband random excitation will be applied to the shaker for approximately 2 to 4 min. Modal properties will be obtained using Fast Fourier Transform Techniques. Ground development testing is necessary to determine if this technique is feasible in the frequency range of interest.

Alternate 2 - To minimize test time and to eliminate the requirement for an on-orbit shaker attachment, a burst from the Orbiter Venier RCS should be applied for approximately 20 sec. Modal properties will be obtained using Fast Fourier Transform Techniques. Again, ground testing is needed to determine the feasibility of this technique. Control analysis is required to determine if the Orbiter can supply and recover from such an input.

Alternate 3 - An initial deflection could be imparted to the Tribeam by statically pulling on the beam with the RMS or a cable attached to the Orbiter. Using a quick release device, the Tribeam will be set in motion and modal data can be obtained using Fast Fourier Transforms. Feasibility testing is again required.

D.3.2.2 Test Instrumentation

Baseline - In the frequency range of interest (0.05 to 10 Hz) measurements will be made using 15 tri-axial accelerometers. They will be located at appropriate nodal locations and at the mid-span point of each 1-meter beam at the end of the platform. A candidate accelerometer for this purpose is:

- PCB - Model Number 302-A02
- Weight = 18 gm
- Frequency Range = 0.05 - 500 Hz
- Dimensions (approx) = 5/3-in. dia x 5/8-in. high

The method of attachment of accelerometers and wires is a further development item. At present, it would appear that on-orbit accelerometer attachments should be made manually by astrcnauts using clips and adhesive.

Alternate 1 - In place of the acceleration measurements for the baseline information technique, deflection measurements are proposed using optical techniques. Targets must be mounted on the structure at each accelerometer location. Development testing is required to determine the feasibility of this approach.

D.3.3 Test No. 3: Response of Tribeam Platform to Orbiter RCS Firing

Purpose - Measure response of Tribeam Platform to Vernier RCS firing. Response data will be correlated with analyses.

Background - The Tribeam mounted in the Orbiter will be subjected to a modal survey prior to response testing. The accelerometers mounted for the modal testing will also be used for RCS response measurements.

D.3.3.1 Test Description - This test will utilize the Tribeam Platform mounted in its construction fixture or equivalent. The Orbiter will operate normally for an orbit under VRCS control. Quick-look response data will be generated on-board with the majority of data stored on magnetic tape for later ground reduction. The vernier engines will then be commanded to produce individually:

- X, Y, and Z translation
- Pitch, roll, and yaw rotations

The excitations should be applied for approximately 2 seconds to produce a step input.

D.3.3.2 Test Instrumentation - In addition to the transducers mounted for the mode survey, low frequency accelerometers and fixture strain gages required for handling tests will be monitored.

2

Appendix E

SPACECRAFT TIME IN SUNLIGHT FOR VARIOUS ORBITAL CONDITIONS

The percentage of time a spacecraft is in Earth shadow, over a calendar year, at orbit altitudes of 200 and 300 n mi is presented. Figure E-1 shows the percentage of time in shadow at 200 n mi and at an inclination of 28.5 deg. In this case, the orbit ascending node is assumed co-incident with the Vernal Equinox. Figure E-2 shows the data for the same conditions, with the exception that the ascending node is 90 deg from the Vernal Equinox. It is apparent from these figures that the total time a spacecraft is in Earth's shadow over a calendar year is insensitive to the position of the orbit ascending node relative to the Vernal Equinox, the only difference being day-to-day variations. Figure E-3 shows information for an orbit altitude of 300 n mi.

Figures E-4, E-5 and E-6 show data for an orbit inclination of 57 deg, at orbit altitudes of 200 and 300 n mi. Once again it is observed that the position at the ascending node relative to the Vernal Equinox is not influential to the time in Earth's shadow.

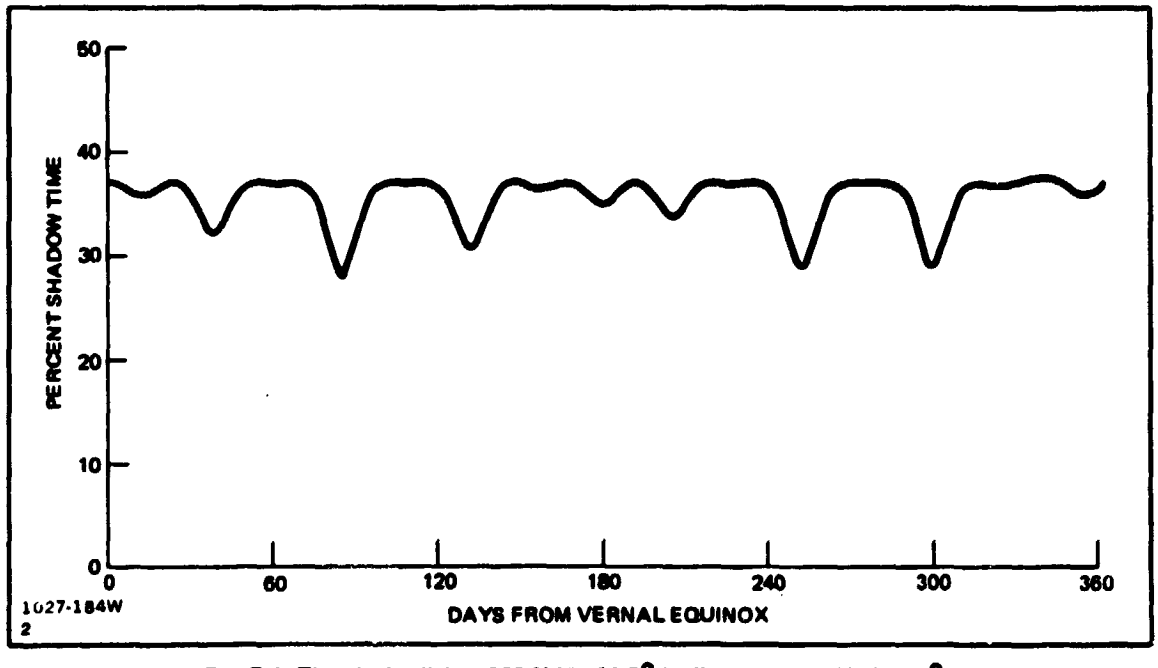

Fig. E-1 Time in Sunlight - 200 N Mi; 28.5° Inclination; Asc. Node = 0°

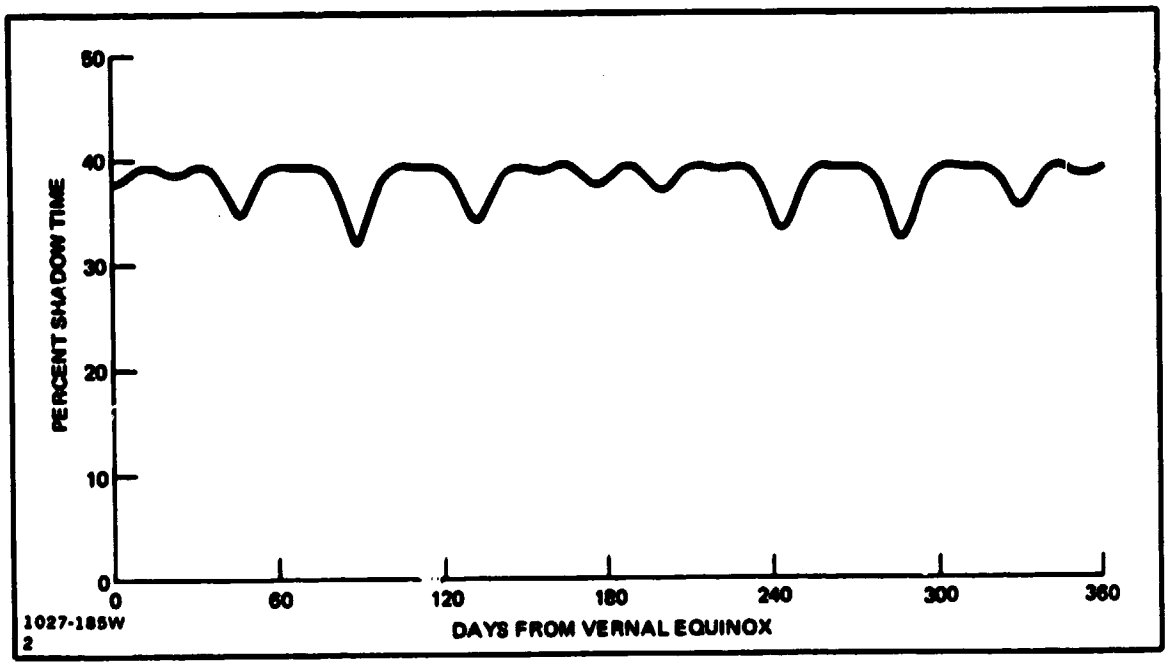

Fig. E-2 Time in Sunlight - 200 N Mi; 28.5° Inclination; Asc. Node = 90°

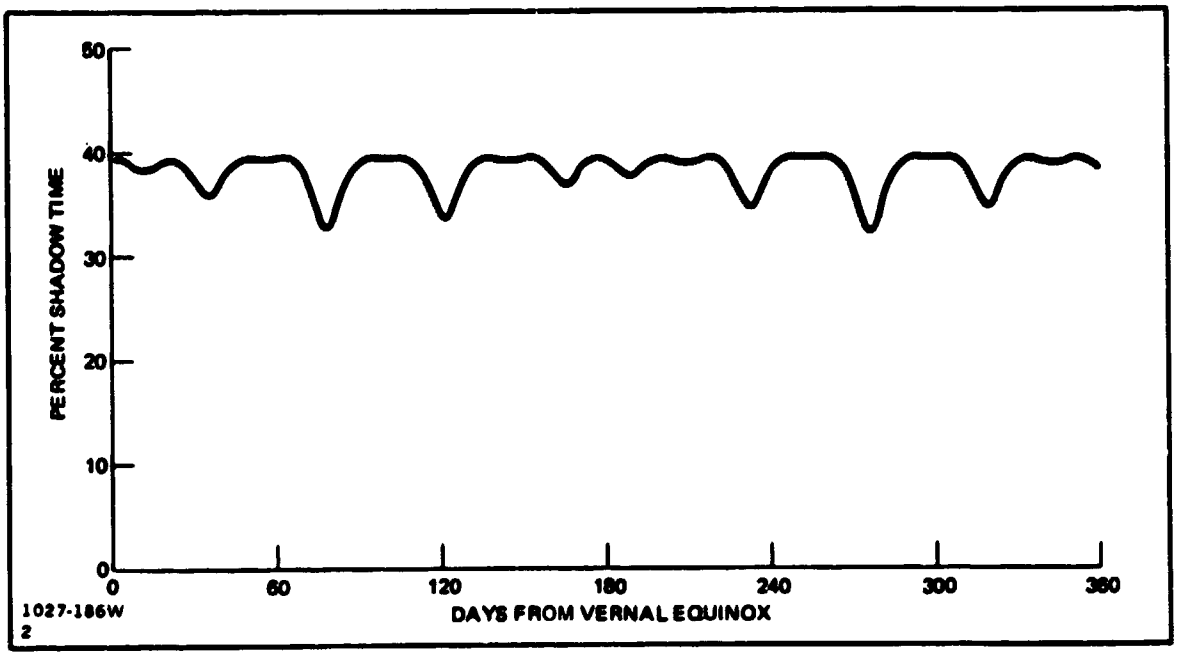

Fig. E-3 Time in Sunlight - 300 N Mi; 28.5° Inclination; Asc. Node = 0°

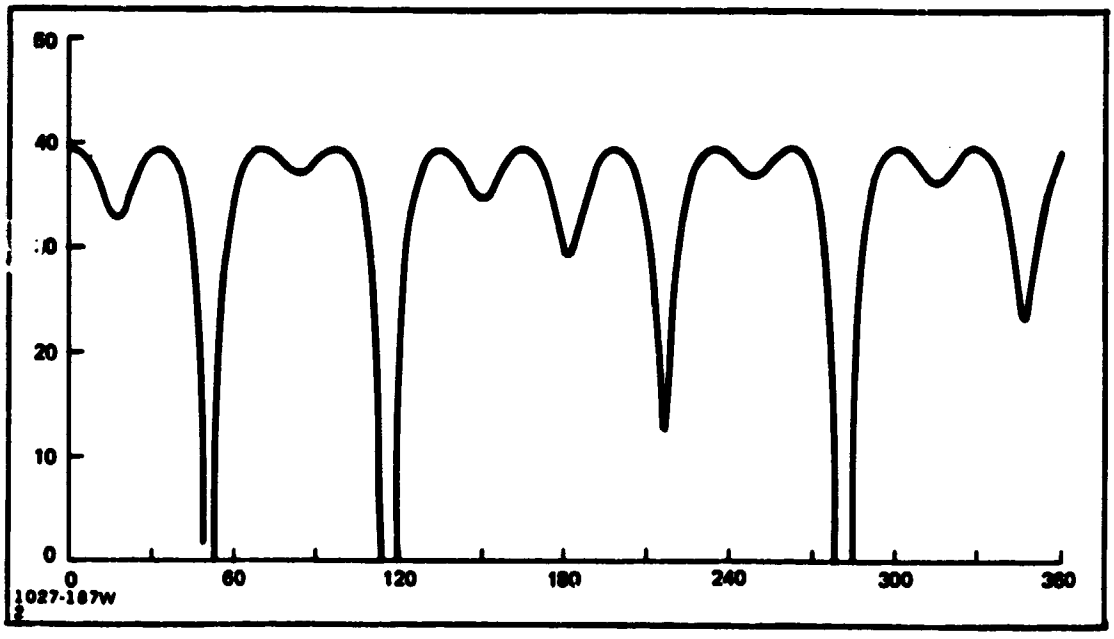

Fig. E-4 Time in Sunlight - 200 N Mi; 57° Inclination; Asc. Node = 0°

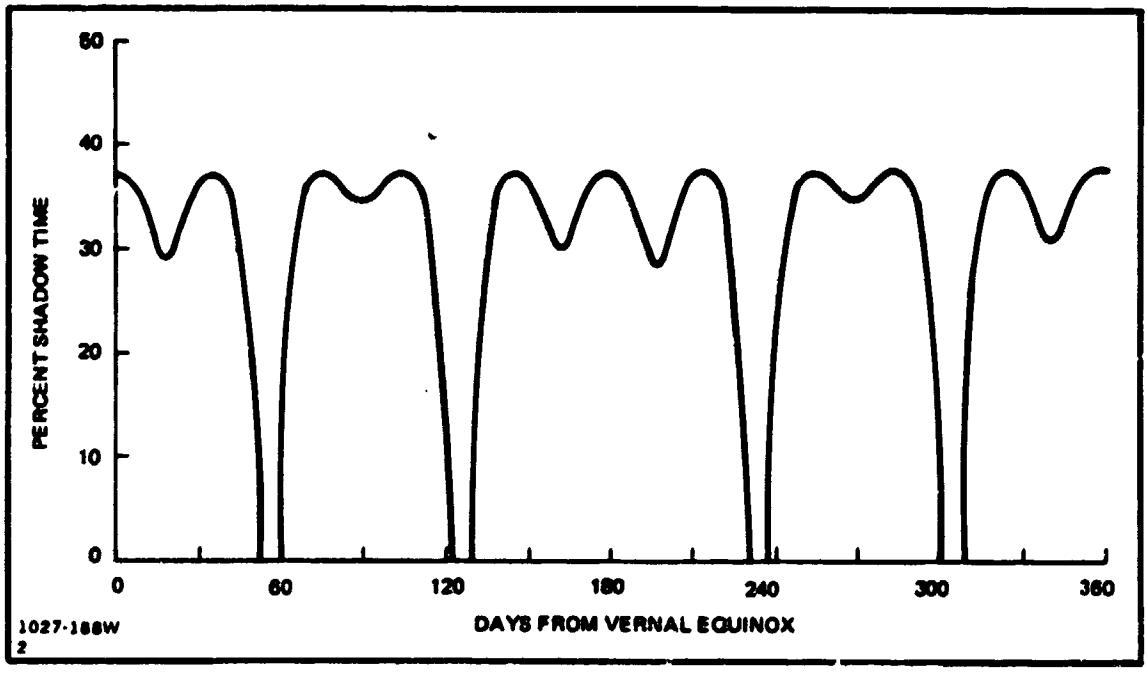

Fig. E-5 Time in Sunlight - 300 N Mi; 57° Inclination; Asc. Node = 0°

2

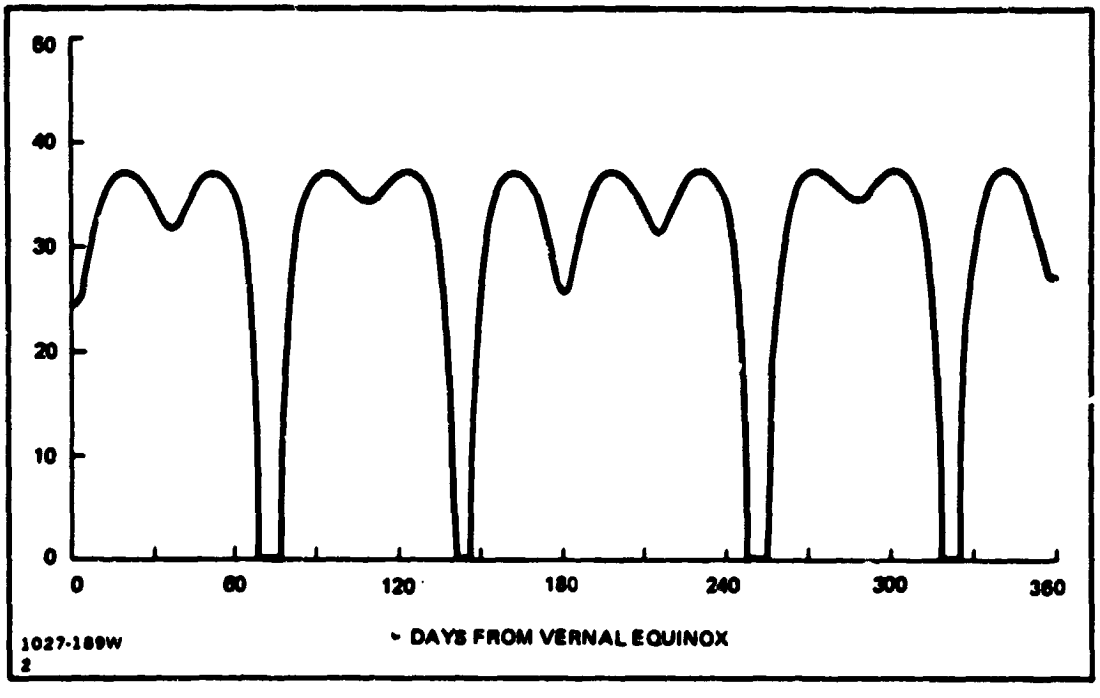

Fig. E-6 Time in Sunlight - 300 N Mi; 57° Inclination; Asc. Node = 90°